Chromatin Remodelling in light signalling

Submitted by

Alex Fisher

for the degree of Doctor of Philosophy

of the University of Leicester

2010

ProQuest LLC
789 East Eisenhower Parkway
P.O. Box 1346
Ann Arbor, MI 48106-1346

Acknowledgements

Thank you to everyone who has helped me with my work over the last four years. Some have helped me directly with my work and some, more importantly, have just helped me.

I would like to thank my supervisor Kerry for all of her support throughout my PhD. I would also like to thank Garry, whom I wish I had had the opportunity to have known longer.

As for the rest, well...in no particular order I would like to thank Ceinwen, Judy, Jean, Lisa, Joe, Tom, Trudie, Jon, Helen, Cat, Mike, Said and Tony. Mark for encouraging me and providing me with inspirational quotes. Pepper, again for his inspirational quotes – how is the arm by the way? Andrew for being a cowboy and for his eternal struggle for FEBS letters. Most importantly, I want to thank Abbie and my Dad for everything.

Abstract

Plants selectively deplete incident light of red (R) wavelength, relative to far-red (FR) wavelength light. Consequently, the relative proportions of R and FR (R:FR ratio) act as an indicator of surrounding vegetation and plants, via the phytochrome photoreceptors, are capable of detecting this. Low R:FR ratio is interpreted as surrounding competition and results in plants eliciting, what is known as, the shade avoidance response. This involves a host of both phenotypic and molecular changes, including increased hypocotyl growth, earlier flowering time and changes in gene expression. The fundamental mechanisms underlying R:FR-mediated changes in gene expression are not fully characterised. Given that increasing evidence in *Arabidopsis* suggests that the structure of chromatin is integral in the regulation of gene expression in response to environmental stimuli, it was investigated to see if this was the case in R:FR ratio signalling. Here, DNaseI sensitivity assays demonstrate that the shade avoidance genes *ATHB2, PIL1* and *XTH15* all undergo gross changes in chromatin structure in plants grown in light/dark cycles and treated with low R:FR ratio. These low R:FR induced changes in DNaseI sensitivity are conspicuously absent when plants are grown in continuous light, suggesting an involvement of the circadian clock. Complementary to this, the use of ChIP has identified the coding region of *PIL1* to show increased association with hyper-acetylated H3K9 and possibly H3K14 in response to low R:FR ratio. Together, this work demonstrates that changes in R:FR ratio induce changes in gene expression that are correlated with changes in chromatin structure and histone modifications and that these changes could be regulated by the circadian clock. In addition, the identification and construction of multiple mutant and transgenic lines expressing altered levels of chromatin modifying protein was attempted.

Abbreviations

AMV	Avian Myeloblastosis Virus Reverse Transcriptase
APD	Active Phytochrome binding Domain
APR6	Actin Related Protein 6
ATHB2	ARABIDOSPSIS THALIANA HOMEOBOX PROTEIN
B	Blue light
$CaCl_2$	Calcium Chloride
$Ca(NO_3)_2$	Calcium Nitrate
CBF	C Repeat Binding Factor
cDNA	Complimentary Deoxyribonucleic Acid
ChIP	Chromatin Immunoprecipitation
cm	Centimetre
$CoCl_2$	Cobalt Chloride
Col	Columbia
COP1	CONSITUTIVE PHOTOMORPHOGENESIS 1
Cry	cryptochrome
Ct	Cycle Time
$CuSO_4$	Copper Sulfate
DET1	DE-ETIOLATED1
dH_2O	Water
DNA	Deoxyribonucleic Acid
dNTPs	Deoxynucleotide Triphosphate
DMSO	Dimethyl Sulfoxide
EDTA	Ethylenediaminetetraacetic Acid

EOD	End of Day
ER	electromagnetic radiation
FLC	FLOWERING LOCUS C
FR	Far-Red light
g	Gram
GA	Gibberellin
GCN5	GENERAL CONTROL NON REPRESSIBLE
GFP	Green Fluorescent Protein
H	Histone
h	Hours
HAT	Histone Acetyl Transferase
H_3BO_3	Boric Acid
HCl	Hydrochloric Acid
HD1	Histone Deacetylase 1
HDAC	Histone Deacetylase
HF	High Fidelity
HFR1	LONG HYPOCOTYL IN FAR-RED 1
HIR	High Irradiance Response
HMT	Histone Methyl Transferase
Hsp70	Heat Shock Protein
HY5	ELONGATED HYPCOTYL 5
$KH2PO_4$	Potassium Dihydrogen Phosphate
KNO_3	Potassium Nitrate
LB	Lennox Broth
LA	Lennox Broth Agar

LFR	Low Fluence Response
La-*er*	Landsberg *erecta*
K	Lysine
LD	Long Days
LM	Lehle
LiCl	Lithium Chloride
m	metre
ml	Millilitre
min	Minutes
mol	Mole
$MgCl_2$	Magnesium Chloride
$MgSO_4$	Magnesium Sulfate
$MnCl_2$	Manganese Chloride
mRNA	Messenger Ribonucleic Acid
NaCl	Sodium Chloride
$NaMoO_4$	Sodium Molybdate
NaOAc	Sodium Oxaloacetate
NaOH	Sodium Hydroxide
NLS	nuclear localisation signal
Nph	nonphototropic hypocotyl
NURD	Nucleosome Remodelling and Deacetylase
PCR	Polymerase Chain Reaction
PetE	Plastocyanin
Pfr	Biologically Active Phytochrome
PHD	Plant Homeo Domain

Phy	Phytochrome
PIC	Pre-initiation Complex
PIF	PHYTOCHROME INTERACTIN FACTOR
PIL1	PIF3-LIKE 1
Pr	Biologically Inactive Phytochrome
qPCR	Quantitative Polymerase Chain Reaction
R	Arginine
R	Red light
RNA pol II	RNA polymerase II
RNA	Ribonucleic Acid
rpm	Rotations Per Minute
RT	Reverse Transcription
TAE	Tris Acetate EDTA
S	Serine
SAGA	Spt-Ada-Gcn5-Acetyltransferase
SAP	Shrimp Alkaline Phosphatase
SD	Short Days
SDS	Sodium Dodecyl Sulfate
SHL	SHORT LIFE
SWI/SNF	Mating Type Switching Sucrose Fermentation
VLFR	Very Low Fluence Response
W	White light
Ws	Wassilewskija
WT	Wild-Type
XTH15	XYLOGLUCAN ENDOTRANSGLYCOSYLASE

$ZnSO_4$	Zinc Sulfate
^oC	Centigrade
s	Seconds

Contents

Chapter 4

The effect of low R:FR on the association of shade avoidance genes with modified histones

Chapter 5

SHL, GCN5 and HD1

Chapter 1

Introduction

1.1 Light

Plants, like all organisms, are adapted to detect and respond to stimuli from their surrounding environment. In the absence of motility, plants have retained a high level of developmental plasticity to respond to changes in environmental conditions. One particularly important external stimulus for plants is light. Light is essential for the development, growth and ultimately, survival of plants. In order for plants to maximise their utilisation of the available light energy, they have evolved to monitor the quantity, quality, periodicity and direction of light and respond accordingly. By monitoring and integrating these four aspects of the light environment with other environmental stimuli, plants are able to intricately optimise their development through from seed germination to the timing of flowering.

The clear dichotomy of developmental responses in light and dark grown seedlings demonstrates the range of effects light elicits upon the development of plants. Dark-grown, etiolated seedlings display long hypocotyls, small, closed cotyledons and the formation of etioplasts from proplastids. This is in contrast to light grown seedlings, which typically exhibit short hypocotyls, large, expanded cotyledons and differentiated chloroplasts (Chen *et al.,* 2004). Furthermore, integration of information from the surrounding light environment with the endogenous circadian clock allows plants to anticipate seasonal environmental changes and temporally optimise their developmental responses to maximise productivity.

Higher plants have three families of characterised photoreceptors which are responsible for detecting light. These are the UV-A/blue (B) light absorbing cryptochromes and phototropins; and the red (R) /far-red (FR) light-absorbing phytochromes (Franklin and Quail, 2010).

1.2 Plant photoreceptors

1.2.1 Phytochromes

Observations had suggested that many components of plant development were regulated by a pigment which underwent a reversible photo-conversion between two distinct forms, with each form occupying distinct action maxima in either the R or FR region. This pigment, termed phytochrome, was first successfully isolated from plant tissue and studied *in vitro* over fifty years ago (Butler *et al.,* 1959).

Experiments analysing *Sinapsis alba L.* and its responses to combinational light treatments led to the suggestion that there were multiple phytochromes (Beggs *et al.,* 1980). Subsequently, a screen of a cDNA library of the model plant species *Arabidopsis thaliana* identified the possibility of five phytochromes, with the initial identification of three: phyA, phyB and phyC (Sharrock and Quail, 1989). Using the sequence information from these phytochromes, two further *Arabidopsis* phytochromes were isolated: phyD and phyE (Clack and Sharrock, 1994).

Early research suggested that each phytochrome forms homodimers; however, recent research has suggested that phyC and phyE exist only as heterodimers with either phyB or phyD making up the other half of the heterodimer (Clack *et al.,* 2009). Each phytochrome monomer is covalently and auto catalytically linked to a light absorbing chromophore (Lagarias and Lagarias, 1989). Experiments involving chimera proteins which fused the N terminal domain of oat PHYA to the C terminal domain of rice PHYB, and vice versa, demonstrated that the N terminal region acts as the chromophore

attachment and photosensory domain, determining the light specificity of the phytochrome molecule; whereas, the C terminal domain contains regulatory regions and is responsible for signal output and dimerization (Wagner *et al.*, 2006; Matsushita *et al.*, 2003; Deforce *et al.*, 1991).

Phytochromes exist as an equilibrium of two interchangeable isoforms: the biologically active form (Pfr), and the biologically inactive form (Pr). Phytochrome is synthesised in the dark in the Pr form and in the presence of light can be converted to the Pfr form. This reaction is optimised at R wavelengths. Pfr can be converted back to Pr by the absorption of FR wavelengths. Phytochromes were initially classified into type I and type II phytochromes, which are distinguished by their stability in response to light. PHYA is a type I, light-labile phytochrome and is degraded rapidly upon exposure to light and accumulates to high levels in the dark. PHYB – E are type II phytochromes and are more stable in the light. Phytochrome responses have been divided into the very low fluence response (VLFR), low fluence response (LFR) and the high irradiance response (HIR). The very low fluence response is not reversible and is saturated at low levels of Pfr, which can be induced by light pulses or continuous irradiation. The HIR is dependent on fluence rate and is caused by either continuous radiation or frequent light pulses. The LFRs are reversible R/FR responses that are induced by R and reversed by FR (Casal *et al.*, 2000; Chen *et al.*, 2004; Nagy and Schäfer, 2002).

The *Arabidopsis phyA* mutant was identified from a screen looking for mutant seedlings exhibiting abnormal phenotypes when grown in FR; similarly, the *phyB* mutant was identified by its long hypocotyl phenotype when grown in white (W) light (Whitelam *et al.*, 1993; Nagatani *et al.*, 1993; Parks and Quail, 1993; Reed *et al.*, 1994). Abnormal

flowering and internode elongation phenotypes in mutagenized *phyAphyB* double mutants were the basis of the isolation of *phyE* mutation (Devlin *et al.*, 1998). The *phyD* mutant was isolated as a naturally occurring mutation in the Wassileweskija (Ws) accession of *Arabidopsis* (Aukerman *et al.*, 1997). Finally, screens of T-DNA mutant collections and a fast neutron deletion approach led to the identification mutants deficient in phyC (Franklin *et al.*, 2003; Monte *et al.*, 2003).

1.2.1.1 Phytochrome functions

The five phytochromes in *Arabidopsis* have a diverse array of functions, covering the whole life span of the plant, from the germination of seeds, the development of seedlings and adult plants through to flowering.

In regards to seed germination, PHYA plays an important role in germination in response to FR (Johnson and Whitelam 1994). A dominant role for PHYB exists in germination in response to R, with an ancillary role for PHYD. Although not yet fully characterized, PHYE also appears to be involved in germination in continuous FR (Hennig *et al.*, 2002). The phytochromes are essential for proper seedling de-etiolation responses to R and FR light. PHYA is important in eliciting this response in FR light conditions, with the *phyA* mutant, when grown in FR light, resembling wild-type (WT) plants grown in the dark (Whitelam *et al.*, 1993; Nagatani *et al.*, 1993; Parks and Quail, 1993). De-etiolation in R and W is controlled primarily by PHYB with *phyB* mutants exhibiting longer hypocotyls and reduced cotyledon expansion. Conversely, seedlings over-expressing phyB have been shown to display shorter hypocotyls compared to WT plants (Somers *et al.*, 1991; Wagner *et al.*, 1991). A minor role also exists for PHYD in seedling de-etiolation, with mutants exhibiting slightly elongated hypocotyls in R light. Furthermore, a synergism between PHYB and PHYD exists in seedling de-etiolation as demonstrated by the fact the *phyBphyD* double mutant demonstrates greater hypocotyl elongation than either single mutant (Aukerman *et al.*, 1997). The *phyC* single mutant has been shown to display elongated hypocotyls compared to WT in R. Analyses of *phyBphyC* and *phyB* single mutants have demonstrated that this function of PHYC operates through modulation of PHYB function (Monte *et al.*, 20003; Franklin *et al.*,

2003). PHYE has also been shown to exhibit a small, redundant role in cotyledon expansion in R (Franklin *et al.*, 2003).

The phytochromes are also important in regulating adult plant architecture. The *Arabidopsis phyB* mutant exhibits increased petiole elongation, reduced leaf area, reduced branching, increased apical dominance and increased roots hairs (Nagatani *et al.*, 1991; Reed *et al.*, 1993). PHYC has been shown to be involved in suppressing petiole elongation (Franklin *et al.*, 2003; Monte *et al.*, 2003). Maintenance of a compact rosette structure is maintained redundantly by PHYA, PHYB and PHYE, with all three having to be mutated before an elongated internode phenotype is observed (Devlin *et al.*, 1998).

Control of flowering time is also an important function of the phytochromes. PHYA for example, has a role in sensing day length extensions (Johnson and Whitelam, 1994). In both short and long days (SD and LD) the *phyB* mutant has been shown to display early flowering (Somers *et al.*, 1991). PHYC is involved in a PHYB dependent manner in sensing SD. By contrast, PHYC operates redundantly with PHYA in sensing LD (Monte *et al.*, 2003). The *phyD* mutation, when combined in the *phyBphyD* double mutant, resulted in a greater reduction in the number of leaves at flowering compared to the *phyB* single mutant (Aukerman *et al.*, 2003). This observation suggests that PHYD acts with PHYB to repress flowering.

Arabidopsis plants have been generated which are mutated in all 5 phytochromes and these plants are known as quintuple mutants. The quintuple mutant displays very low levels of germination in response to W, B, R and FR light treatments, suggesting that

the phytochromes are required for normal germination, regardless of light treatment. The quintuple seedling was responsive to B in regards to hypocotyl elongation, but was completely unresponsive to R. Interestingly, quintuple mutant seedlings were still capable of synthesising some chlorophyll in response to a R pulse. As the synthesis of chlorophyll is a light dependent response it suggests that the quintuple mutant retains some ability to detect R. All adult quintuple mutants eventually became developmentally arrested when grown in R (Strasser *et al.,* 2010).

Experiments in other species have demonstrated the importance of phytochromes in a variety of plants. Despite the paucity of data in other species, the available information from species such as tomato, pea, maize and tobacco suggests that although the number of phytochromes may differ between species the presence and function of phyA and phyB are well conserved (Matthews 2010). A study by Boylan and Quail elegantly highlighted the phenotypic effects of aberrant phytochrome expression whilst demonstrating the functional homology of phytochromes between monocotyledons and dicotyledons, whilst also demonstrating the conserved nature of post-transcriptional modifications and chromophore attachment in phytochrome processing. Transgenic tomato plants were engineered to express an oat phytochrome. These transgenic tomato plants displayed phenotypic abnormalities spanning the developmental, vegetative and reproductive phases and exhibited a dwarfed height, green foliage and green fruit compared to WT plants (Boylan and Quail, 1989). Similar experiments were performed when transgenic tobacco plants were made to express oat phytochrome. Transgenic plants from this experiment demonstrated reduced apical dominance, reduced internode elongation and increased green pigmentation (Keller *et al.,* 1989).

1.2.2 Cryptochromes

Cryptochromes were initially characterised in *Arabidopsis*, although they are present in drosophila and mammals. Cryptochromes sense blue and UV-A light and the first crytochrome, cry1, was isolated by the mutants aberrant response to blue (B) light (Cashmore *et al.*, 1999). A second cryptochrome, cry2, was discovered using the cry1 sequence as a template to probe the *Arabidopsis* genome (Lin *et al.*, 1998).

Both CRY1 and CRY2 are important in plant photomorphogeneis in response to B light as demonstrated by the fact that cry1 and cry2 over-expressing plants have larger cotyledons and shorter hypocotyls than WT plants when grown in B and UV-A light. Conversely, *cry1* and *cry2* mutants have longer hypocotyls than WT plants when grown in B light. The relative impact of the *cry1* and *cry2* mutations on hypocotyl and cotyledon growth is dependent on light quantity (Lin *et al.*, 1998; Mazzella *et al.*, 2001). CRY1 and CRY2 differ in their responses to fluence, with CRY2 operating at lower fluences than CRY1 (Lin *et al.*, 1998) CRY1 and CRY2 are both involved in flowering, with CRY2 exhibiting a more prominent role. The *cry1cry2* double mutant has been shown to flower earlier than either single mutant in B light (Guo *et al.*, 1998; Mockler *et al.*, 1999)

1.2.3 Phototropins

The mutant, *nph1 (nonphototropic hypocotyl 1)*, was isolated by the fact that it is deficient in directed growth in response to light: phototropism. NPH1, which later became known as phototropin 1 (phot1), was found to be phosphorylated after B light irradiation. Also, NPH1 appeared to bind to flavin, which is a light harvesting chromophore. Taken together, these data led to the suggestion that PHOT1 was a B light photoreceptor (Christie *et al.*, 1998). Based on sequence similarity to phot1, a second phototropin, phot2, was identified (Briggs *et al.*, 2001).

PHOT1 and PHOT2 are both important in plant photropism, although they exhibit different properties at different fluences. Phototropins are important in maximising photosynthetic efficiency and this is highlighted by their roles in regulating leaf flattening, stomatal opening and chloroplast movement in a light-intensity dependent manner, which acts to prevent damage to chloroplasts at high light intensities (Christie *et al.*, 2007).

1.3 Shade avoidance

As a fundamental component of photosynthesis, light is vital in providing an energy source for plants; consequently, plants have adapted to maximise their utilisation of this resource. This is exemplified by the fact that plants not only use light as an energy source but also as a signal which provides spatial information of surrounding competitors. The chlorophyll and carotenoid pigments are the light absorbing components of the photosynthetic machinery and capable of absorbing specific wavelengths of electromagnetic radiation (ER), with red and blue wavelengths being preferentially absorbed and green and far-red (FR) light preferentially passing through or being reflected. This means that the presence of vegetation results in a change in the spectrum of solar radiation. The phytochromes and cryptochromes are predominantly responsible for detecting these variations in the surrounding radiation, with the phytochromes responsible for detecting R and FR radiation. As mentioned above, FR light is transmitted and reflected by vegetation; whereas, R light is absorbed. This creates a lower R:FR in light that has passed through or reflected away from vegetation as opposed to the R:FR in normal daylight. The ratio of R:FR radiation can more specifically be defined as:

$$\text{R:FR ratio} = \frac{\text{photon irradiance between 655 and 665 nm}}{\text{photon irradiance between 725 and 735 nm}}$$

The R:FR ratio of daylight remains a fairly consistent 1.15, and is independent of time of year and weather (Smith 1982; Franklin and Whitelam, 2005). In contrast, the detected R:FR ratio of light underneath canopies of vegetation are in the range 0.05 –

0.07; thus demonstrating a stark contrast between the R:FR of incident and reflected/transmitted radiation (Smith 1982; Franklin and Whitelam, 2005).

The relative concentrations of the two phytochrome forms: Pr and Pfr, are determined by the ratio of R:FR and can be used by the plants at the molecular level to communicate their vegetational surroundings. In the presence of reduced relative concentrations of Pfr, which is a consequence of low R:FR, which in turn is indicative of surrounding vegetation, plants respond by implementing alternative developmental pathways. Typically, they exhibit an increase in stem and petiole elongation rate, elevated leaf angles (leaf hyponasty) and a concomitant reduction in leaf thickness and chlorophyll levels. This response is termed the shade avoidance response and is thought to allow better access to daylight. However, if the reduced relative concentrations of Pfr are maintained for a prolonged period the plant initiates the flowering developmental pathway, ostensibly to try maximise the probability of seed production in unfavourable conditions (Smith and Whitelam, 1997).

Among the phytochromes, PHYB is the main mediator of developmental responses to low R:FR ratio. Unlike WT plants, low R:FR and End Of Day (EOD-FR) treatment had little effect on hypocotyl elongation and petiole extension in *phyB* mutants, which display constitutive shade avoidance (Robson *et al.*, 1993; Nagatani *et al.*, 1991). EOD-FR is a short FR treatment which is applied prior to darkness. This results in a low Pfr:Pr ratio throughout the dark period and phenotypically mimics growth in low R:FR ratio. The *phyB* mutant still exhibits some response to low R:FR, suggesting the participation of other phytochromes in shade avoidance. These included: accelerated flowering, reduced leaf area and a decrease in specific stem weight (weight to length

ratio) when compared to plants grown in high R:FR (Robson *et al.*, 1993). A role for PHYD in mediating *Arabidopsis* responses to low R:FR ratio was demonstrated in the *phyBphyD* double mutant, with the double mutant being less responsive to EOD - FR mediated hypocotyl growth and petiole extension than either the *phyB* or *phyD* single mutants. The effect of the *phyD* mutation is minimal in the *phyD* single mutant and is only really evident in the *phyBphyD* double mutant, highlighting the redundancy of PHYD in these responses (Aukerman *et al.*, 1997). PHYE also appears to play a minor, redundant role in shade avoidance. The *phyAphyB* double mutant and *phyAphyBphyE* triple mutant were treated with or without an EOD-FR treatment. The *phyAphyB* double mutant displayed elongated internodes and early flowering with EOD - FR. The *phyAphyBphyE* triple mutant, however, flowered early and exhibited internode elongation in both light treatments. This finding suggests that PHYE plays a redundant role in flowering and internode elongation (Devlin *et al.*, 1998). WT and *phyA* mutant seedlings grown in high R:FR have the same length hypocotyls, but in low R:FR the *phyA* mutants have longer hypocotyls than WT. Furthermore, when grown in low R:FR, *phyAphyB* double mutants have been shown to display longer hypocotyls than the *phyB* mutant. Together, these observations suggest a role for PHYA in limiting hypocotyl length in low R:FR, thereby suppressing shade avoidance and excessive elongation growth (Johnson *et al.*, 1994; Salter *et al.*, 2003)

1.4 Light and gene regulation

1.4.1 Phytochrome cellular localisation

Changes in R:FR ratio and altered abundance of phytochromes has not only been shown to regulate plant development at the phenotypic level but also at the transcriptional level. As early as 1993, changes in R:FR ratio were known to have reversible effects on the expression of genes, specifically the transcription factor ARABIDOPSIS *THALIANA HOMEOBOX PROTEIN 2 (ATHB2)* (Carabelli *et al.*, 1993). Microarray studies confirmed these initial findings and expanded the cohort of genes identified as being regulated by R:FR ratio (Devlin *et al.*, 2003; Salter *et al.*, 2003; Sessa *et al.*, 2005). These included the basic Helix Loop Helix (bHLH) transcription factor *PIF3-LIKE 1* (*PIL1*) and the xyloglucanendotransglycosylase *XTH15*. Furthermore, these low R:FR ratio regulated genes have been shown to be aberrantly regulated in phytochrome – deficient mutants (Devlin *et al.*, 2003; Salter *et al.*, 2003).

Phytochromes are important in the regulation of R:FR regulated genes and a mechanism by which different light treatments can achieve this is through differential localisation of phytochromes. Fluorescent microscopy was used to examine *Arabidopsis* seedlings transformed with *PHYA-GFP*. PHYA was absent from the nucleus of dark grown seedlings; however, short treatments of W, R, FR or B and longer treatments of continuous B or FR resulted in nuclear localisation of the protein fusion construct. This is in contrast to prolonged periods of continuous W or R, which resulted in no detectable GFP fluorescence in the cell. In addition to this, if dark grown seedlings were treated with 24 hours of R immediately prior to 24 hours of FR, there was no GFP

fluorescence in the cell (Kim *et al.*, 2000; Kircher and Nagy 2002). These observations are consistent with the light-labile nature of PHYA and suggest that after prolonged irradiation with certain wavelengths of light PHYA becomes degraded.

Similar experiments were performed using *PHYB-GFP* constructs. Again, dark grown seedlings exhibited cytosolic staining; whereas, W treatment resulted in translocation of PHYB:GFP into the nuclei (Kircher and Nagy 2002). A separate study using transgenic tobacco seedlings transformed with a GFP-PHYB construct supported these results. Seedlings were exposed to pulses or continuous R, B or FR. R induced the formation of nuclear speckles. In contrast, up to 3 hours of FR induced no nuclear speckles and 3 hours of B induced only minimal nuclear speckles. Transfer back to dark resulted in immediate decline in all nuclear speckles. Gil and colleagues investigated the effect of pulses of R and FR. Seedlings were irradiated with R, FR or R followed by FR. It was found that the R pulse was sufficient to cause formation of nuclear speckles, FR did not induce speckles and the FR pulse after the R pulse completely reversed the R pulses effects (Gil *et al.*, 2000). Experiments using *PHYC:*, *PHYD:* and *PHYE: GFP* constructs, found that these protein fusions are cytosolic in the dark. Exposure to W resulted in the formation of nuclear speckles of PHYC and PHYE and to a lesser extent PHYD (Kircher and Nagy 2002). These data taken together suggest that phytochrome, in the form of Pfr, enters the nucleus and forms nuclear speckles. Downstream of the phytochromes is the ELONGATED HYPOCOTYL 5 (HY5) basic domain/leucine zipper (bZIP) transcription factor, which promotes photo-morphogenesis. In all light conditions, the *hy5* mutant exhibits aberrant hypocotyl elongation, demonstrating that HY5 operates downstream of the phytochromes. HY5 constitutively localises to the nucleus where it binds to the promoters of many light regulated genes (Lee *et al.*, 2007).

HY5 expression is regulated by the E3 ubiquitin protein ligase, CONSITUTIVE PHOTOMORPHOGENESIS 1 (COP1) and when COP1 localises to the nucleus it degrades HY5. In the dark, COP1 localises to the nucleus, whereas, in the light it is excluded from the nucleus (Osterlund *et al.,* 2000).

1.4.2 PIFs

Yeast two hybrid screens were used to try and determine the interacting partners of the phytochromes. The C terminal regions of PHYB and PHYA were used as bait in a screen. The bHLH transcription factor, *Phytochrome Interacting Factor 3 (PIF3)* was identified as a potential binding partner of both PHYA and PHYB and this interaction was confirmed *in vitro* by pull down assays. PIF3 contains a region of similarity to a PAS domain and a putative bipartite NLS motif. Constitutive localisation to the nucleus is observed irrespective of light treatment (Ni *et al.*, 1998).

Following on from these initial findings, the nature of the phytochrome – PIF3 interaction was further characterised. The interaction between PHYB and PIF3 is dependent on PHYB being in the Pfr form. Treatment with FR results in dissociation of PIF3 from PHYB, indicating that if PHYB is converted back to its inactive form it will dissociate from PIF3 even if it was previously bound to PIF3. PIF3 was observed not to bind at all to the phyB apoprotein (Ni *et al.,* 1999). A further study confirmed that both PHYB and PHYA bound to PIF3 when in the Pfr form, with regions at both the N-terminus and C-terminus of PHYB involved in binding (Zhu *et al.*, 2000). Bauer and colleagues showed that the phytochromes A, B and D are involved in the degradation of PIF3 (Bauer *et al.*, 2004). A subsequent study by Al-sady *et al* showed that R treatment results in PIF3 exhibiting a gel shift. Treatment with a proteasome inhibitor and alakaline phosphatase prevented PIF3 degradation and the gel shift, respectively. Furthermore, if *phyA* and *phyB* mutant constructs, which are incapable of binding PIF3, were transformed into a *phyA/phyB* double mutant background then R no longer caused

degradation and a gel shift of PIF3. Together, these data suggest that it is the interaction of A and PHYB with PIF3 which mediates its degradation (Al-sady *et al.* 2006).

An *in vitro* co-immunoprecipitation assay was used to test for interactions between the other members of the PIF3 sub-family of bHLH containing proteins and PHYB. The Pfr form of phyB was shown to interact with PIF3, PIF4, PIF5 and PIF6. A conserved motif, termed the active phytochrome binding motif (APB) was found in most of the bHLH proteins that interact with PHYB and is important for binding. Despite their close similarity to PIF3, PIL1 and LONG HYPOCOTYL IN FAR-RED 1 (HFR1) exhibited no detectable binding to PHYB (Khanna *et al.*, 2004).

PIF3 was examined to see if it was capable of binding to DNA. The bHLH domain typically consists of approximately 60 amino acids, with the 15 amino acids at the N terminal involved in DNA binding and the C terminal end operating as a dimerization domain. Proteins containing this motif frequently form hetero or homodimers. The recognition sequence of bHLH domains is the E box sequence, CANNTG, although the context of the sequence can influence binding (Toledo-oritz *et al.*, 2003). *In vitro* studies found that the DNA sequence CACGTG, is a target of PIF3. This sequence is known as the G box motif. It was further suggested that PIF3 binds directly to G box containing promoters of certain light regulated genes (Martinez-Garcia *et al.*, 2000).

Although PIF3 performs a dominant role in de-etiolation, alternate members of the PIF3 family, namely PIF4 and PIF5, appear to be important in shade avoidance. Analysis of PIF5 and PIF4 proteins found that they accumulate in the dark and are degraded in a proteasome-dependent manner in response to R, but not FR. If the R pulse is followed

by a FR pulse, however, there is no decrease in PIF4 and PIF5. This is indicative of a LFR and provides evidence that the degradation of these proteins is phytochrome mediated. This notion is further supported by experiments showing that when the APB domain of PIF4 and PIF5 is deleted, R mediated degradation is reduced. Phytochromes A, B and D were subsequently found to redundantly regulate the degradation of PIF5 (Huq and Quail 2002; Shen *et al.*, 2007).

Transgenic plants over-expressing *PIF4* and *PIF5* have been shown to exhibit a 'constitutive shade avoidance phenotype'; whereas, *pif*4 and *pif*5 mutants exhibit a light hypersensitive phenotype (Fujimori *et al.*, 2004; Huq and Quail, 2002; Lorrain *et al.*, 2008). Mutants deficient in PIF4 displayed reduced hypocotyl elongation in response to low R:FR compared to WT controls. The *pif4/pif5* double mutant displayed greater reduction of low R:FR mediated elongation growth than the *pif4* single mutant, suggesting a redundant role for PIF5. In terms of R:FR - mediated petiole elongation, PIF5 exhibits a significant role, with *PIF5* over-expressing lines displaying considerably elongated petioles when compared with WT plants (Lorrain *et al.,* 2008). Following physiological analyses, mutant and over-expressing plants were investigated at the transcriptional level. *PIL1*, *HFR1* and *ATHB2* are three factors whose expression increases in response to low R:FR. In *pif4*, *pif5* and the *pif4/pif5* mutants these three shade avoidance marker genes were still increased in expression in response to low R:FR, but to a lesser extent than WT. In contrast, *PIF5* over-expressing plants had higher levels of the three marker genes in high R:FR and the levels increased further in response to low R:FR (Lorrain *et al.*, 2008). The *phyBpif4pif5* triple mutant suppressed the phenotype of the *phyB* mutant, in regards to shade avoidance marker genes and hypocotyl elongation. This provides evidence that PIF4 and PIF5 operate downstream

of PHYB. Some residual shade avoidance responses were present in the *pif4pif5* double mutant, suggesting other pathways, not involving PIF4 and PIF5, are also important (Lorrain *et al.*, 2008).

1.4.3 GA and DELLAs

Gibberellin (GA) is a hormone that regulates the growth and development of plants, with GA-deficient mutant plants exhibiting a severe dwarf phenotype (Harberd *et al.*, 2009). GA results in proteasome mediated degradation of the growth-repressing DELLA proteins. *Arabidopsis* contains five DELLA proteins: RGA, GAI, RGL1, RGL2 and RGL3 (Feng *et al.*, 2008). The hypocotyls of dark-grown seedlings contain high levels of GA and this results in destruction of the DELLAs. In light grown seedlings GA levels are low, leading to an accumulation of DELLA proteins and growth restraint (Achard *et al.*, 2007). Experimentally, this can be demonstrated by growing seedlings on supplemented media. Seedlings on media supplemented with GA have longer hypocotyls than controls and those grown on media containing a GA inhibitor have shorter hypocotyls than controls. Light can therefore control hypocotyl length via changes in GA abundance.

The DELLAs regulate several genes that respond to GA. Studies have, however, suggested that DELLAs do not directly regulate these GA responsive genes (Feng *et al.*, 2008). One proposed mechanism by which the DELLAs could regulate these GA responsive genes is via the PIFs. Two separate yeast two hybrid screens have identified an interaction between the PIFs and the DELLAs. Interactions were confirmed by co-immunoprecipitation and bimolecular fluorescence complementation (BiFC) (Feng *et al.*, 2008; de Lucas *et al.*, 2008). These studies demonstrated that the interaction of DELLA proteins with both PIF3 and PIF4 prevented DNA binding, thereby suppressing their transcriptional activity.

ChIP and PCR analyses determined that an increasing abundance of DELLAs resulted in a reduction of PIFs binding to their target genes and correspondingly when GA is increased (and thereby DELLAs destroyed), the binding of PIFs to their target genes is increased. Therefore, PIFs and DELLAs function antagonistically with respect to the expression on PIF target genes (Feng et al., 2008). Furthermore, these studies demonstrated that RGA, which could not bind PIF4, could no longer inhibit PIF4 transcription. *In vivo*, a GA inhibitor was found to disrupt binding of PIF4 to DNA and PIF4 DNA binding was amplified by GA application (de Lucas *et al.*, 2008).

The role of GA and DELLAs in shade avoidance has been investigated by Djakovic-Petrovic and colleagues (2007). They demonstrated, using *GFP:RGA*, that in low R:FR ratio, the levels of the fusion protein decreased compared to high R:FR controls. The presence of a GA inhibitor abrogated this effect and RGA fusion protein levels were maintained at the same levels in high and low R:FR ratio, confirming that levels of DELLA proteins in response to changes in R:FR ratio are regulated via GA (Djakovic-Petrovic *et al.*, 2007). Furthermore, this research showed that low R:FR responses were reduced in plants expressing a mutated GAI protein which is resistant to degradation by GA. Analysis of a DELLA quadruple mutant demonstrated a role for low R:FR mediated DELLA degradation in hypocotyl, but not petiole, elongation. A summary of the roles of phytochromes, DELLAs and PIFs in shade avoidance is shown in Figure 1.1.

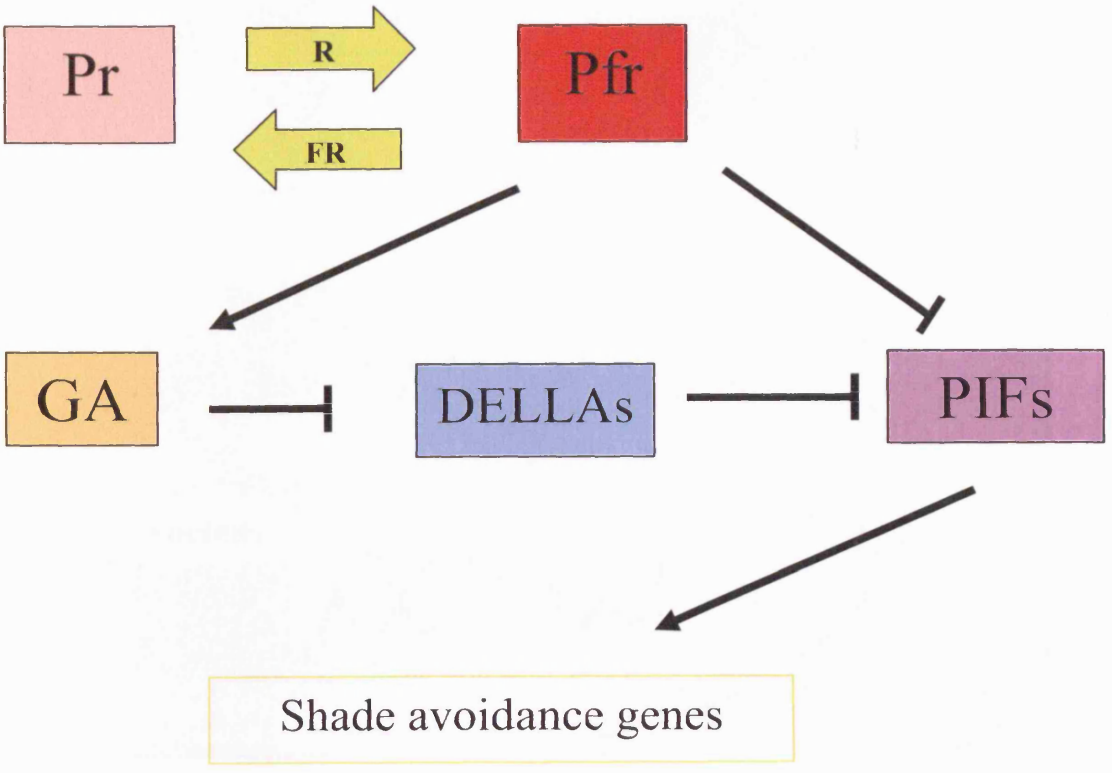

Figure 1.1a: The key factors known to be involved in the shade avoidance response and there basic relationships.

High R:FR

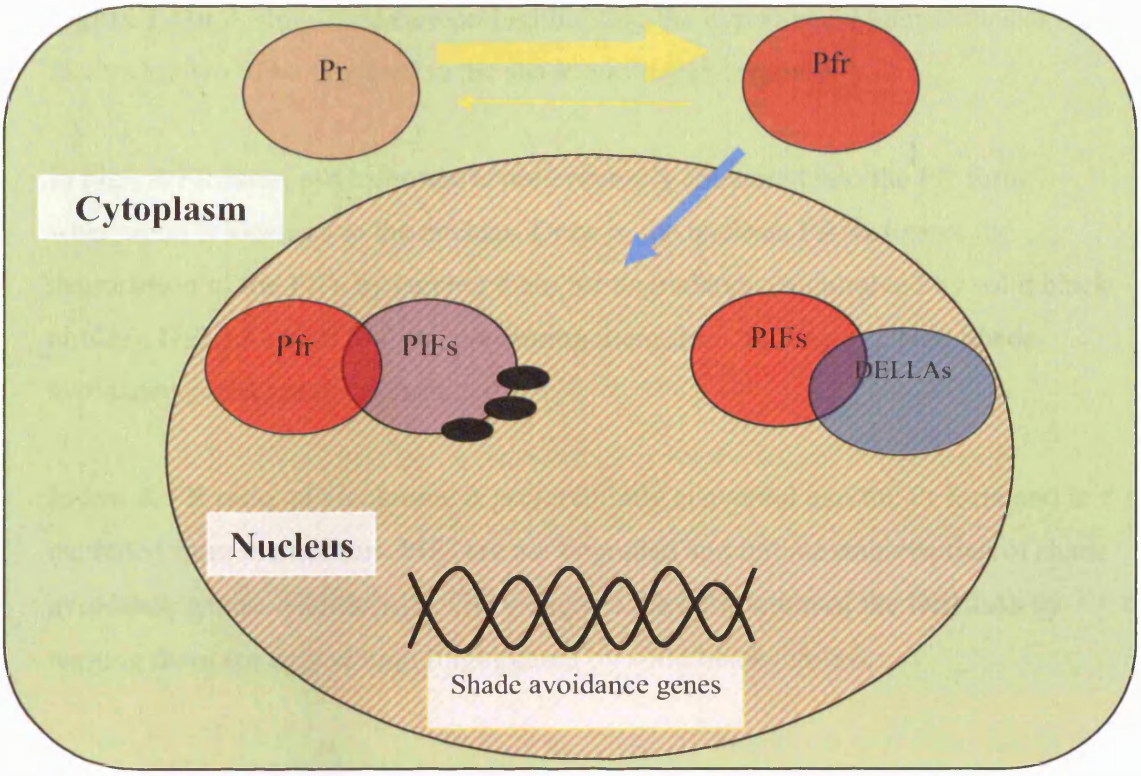

Low R:FR

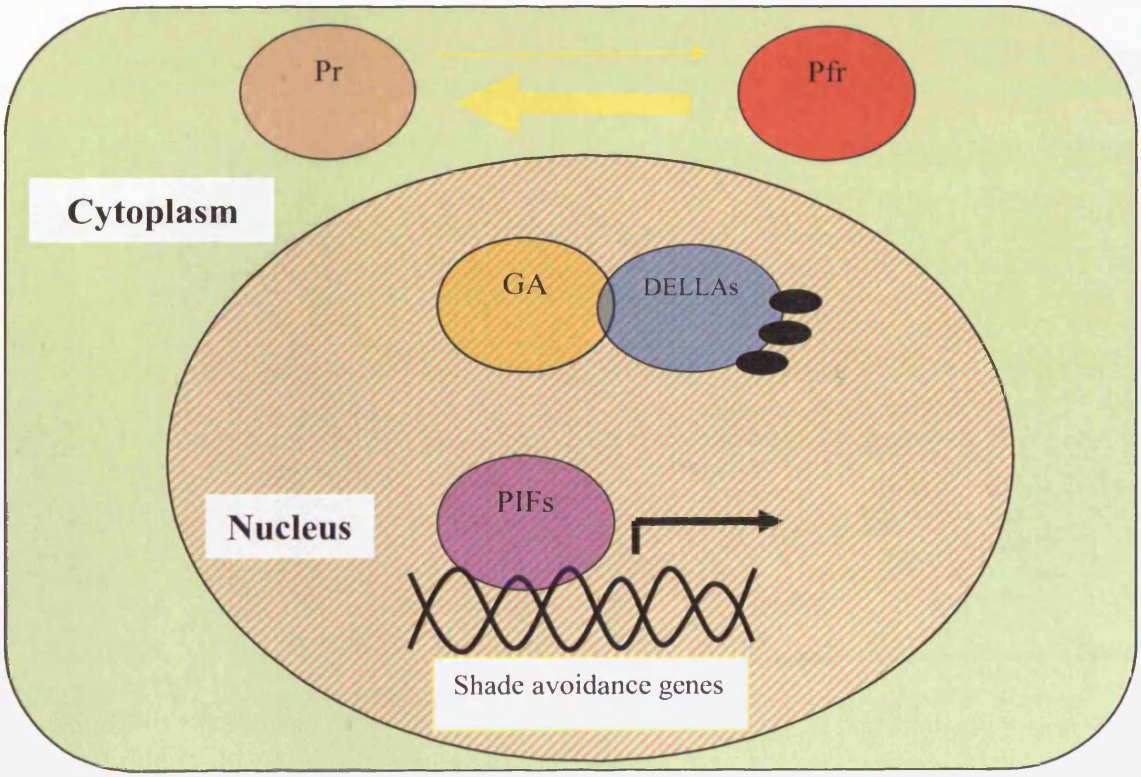

Figure 1.1b: A simplified cartoon highlighting the hypothetical interactions of the factors known to be involved in the shade avoidance response.

In high R:FR ratio, phytochrome is preferentially converted into the Pfr form, whereupon it localises to the nucleus. Once in the nucleus, Pfr instigates the degradation of the PIFs by tagging them for degradation (highlighted by solid black circles). DELLAs bind to PIFs, preventing them from binding to DNA. Shade avoidance genes are not transcribed.

In low R:FR ratio, phytochrome is preferentially converted into the Pr form and is excluded from the nucleus. PIFs are not degraded and initiate transcription of shade avoidance genes. Additionally, GA instigates the destruction of the DELLAs by tagging them for degradation (highlighted by solid black circles).

1.5 Chromatin

Eukaryotic chromatin is composed of DNA and closely associated proteins, termed histones. Histone proteins consist of the core histones: H2A, H2B, H3 and H4; and the linker histone H1. The core histones assemble to form a protein octamer, which typically consists of a H3-H4 tetramer, to which two H2A-H2B heterodimers bind (Eickbush and Moudrianakis 1978). In certain situations, these canonical core histones are replaced with variant histones, such as H3.3 in and H2A.Z, replacing H3 and H2A respectively. Whilst similar to their traditional counterparts, these variant histones frequently confer different properties upon the core histone particle and are favoured in certain contexts (Sarma and Reinberg 2005). Wrapped around this central histone octamer is~145bp of DNA. This forms the fundamental unit of eukaryotic chromosomes: the nucleosome. Between the histones and DNA, in a single nucleosome, there are 14 contact points, which generates a very stable DNA-protein interaction (Luger *et al.*, 1997). Adjacent nucleosomes are linked to one another by approximately 50 bp of DNA, creating what is known as the 10 nm fibre, or, 'beads on a string' model. With the help of histone H1, this 10 nm fibre can be compacted further into the 30 nm fibre (Luger *et al.*, 1997). Experiments in which H1 was deleted revealed that it is not necessary for cellular survival, but its deletion resulted in diffuse, uncondensed chromosomes (Shen *et al.*, 1995). The structural hierarchy of chromatin is represented in figure 1.2

All four core histones have N-terminal tails, and H2A has a C-terminal tail (Wolffe and Hayes 1999). Histone tails can undergo a number of posttranslational modifications such as acetylation and methylation (Loidl, 2004). Histone tails have been shown to be

important in the formation of condensed, higher-order chromatin. Removal of histone tails has been shown to result in an inability of linker DNA to bend thereby preventing the formation of higher-order chromatin structures (Garcia-Ramirez *et al.*, 1992). Visualization with electron microscopy has further confirmed the necessity of the histone tails in forming higher-order structures, with the removal of the histone tails resulting in the absence of the 30 nm solenoid fibre (Allan *et al.*, 1982). Another investigation used differences in sedimentation profiles of *in vitro* reconstructed nucleosomes to show that when the N terminal 19 amino acids of H4 was deleted the nucleosomes could not form the 30 nm fibre. Furthermore, they found that nucleosomes that were constitutively acetylated at lysine residue 16 (H4K16) did not form the 30 nm fibre, thereby suggesting a link between nucleosome modification and chromatin structure. They further confirmed these results by examining HeLA ell extracts and finding that H4K16 acetylation is correlated with an absence of the 30 nm fibre (Shogren-knaak *et al.*, 2006). In fact, it has been known for over 40 years that modifications of histones, specifically acetylation, can result in a relaxation in the inhibition of transcription from the nucleosome-DNA template (Allfrey *et al.*, 1964).

It is now well established that chromatin is a dynamic structure and through a multitude of interactions and modifications chromatin can go from a closed, higher-order, compact structure through to an open, dynamic system of mobile nucleosomes on DNA. One investigation using nucleosomes bound to DNA and run on a polyacrylamide gel showed that histone octamers are not rigidly fixed to the DNA to which they are associated. Incubation of this nucleosome-DNA complex with linker histone, however, resulted in restriction of octamer mobility. Incubation with H1 also resulted in decreased transcription and decreased accessibility of micrococcal nuclease to linker

DNA. A corollary of these findings is that there may be a direct link between histone packaging and mobility, and transcription of DNA (Ura *et al.*, 1995). Ultimately, this ability of chromatin, and consequently DNA, to adopt an exposed, open conformation or a concealed, closed arrangement, does have implications at the transcriptional level. An *in vitro* system, in which plasmid DNA was combined with nucleosomes, found that saturation of nucleosome binding to DNA resulted in an inhibition of transcription and that transcription was not initiated from the plasmid until nucleosomes were depleted below 2/3 of saturation. These data indicate that the presence of nucleosomes on DNA is inhibitory to transcription (Knezetic and Luse 1986).

1.6 Histone modifications

There are many different types of histone modifications: acetylation, methylation (lysines and arginines) phosphorylation, ubiquitylation, sumoylation, ADP riobsylation, deimination and proline isomerisation. So far, at least 60 histone residues in eukaryotes have been found to be modified. Lysines and arginines can be methylated; this methylation can be mono, di or tri on lysine residues and can be mono or di on arginine residues, with this mono or di being asymmetric or symmetric. The majority of histone modifications are generally considered to be reversible (Kouzarides 2007).

Evidence suggests that individual histone marks do not necessarily act in isolation or in a reciprocal manner, which results in a complex interplay between histone marks and demonstrates that the dynamics of histone modifications are dependent on context. Reas and colleagues (2000) using an *in vitro* approach highlighted the importance of the surrounding template. In this work they found that in response to H3 serine 10 (H3S10) phosphorylation or H3K14 methylation, H3K9 on the same template could be methylated by a Histone Methyl Transferase (HMT) enzyme. In contrast, acetylation of H3K9 prevented the methylation of H3K9 by the same HMT enzyme (Rea *et al.*, 2000). Another study investigating the HMT, Set9, which has specificity for H3K4, found that Set9 methylation of a H3 substrate inhibited binding of the Nucleosome Remodelling and Deacetylase (NURD) HDAC complex; whereas, methylation of H3K9 did not affect binding of NURD. They additionally found that methylation of K4 inhibited the ability of the enzyme Suv39 to methylate H3K9 (Nishioka *et al.*, 2002, Zegerman *et al.*, 2002).

The modification of histone tails is thought to be the principal means by which histone-DNA interactions of chromatin are remodelled. There are two mechanisms by which histone tail modifications are proposed to elicit remodelling. Firstly, the modification of histone tails ostensibly directly affects the conformation of chromatin by altering the electrostatic interactions both between DNA and histones of individual nucleosomes and the interactions between nucleosomes. Affinity chromatography has be used to show that the nucleosomes of actively transcribed genes undergo conformational changes, exposing chemical groups that are concealed in nucleosomes associated with transcriptionally inactive genes (Walker *et al.*, 1990; Sterner *et al.,* 1987). Hong and colleagues examined the interaction of the N terminal 23 amino acids of H4 with purified DNA and they found that when this 23 amino acid fragment was acetylated it exhibited a reduced affinity for purified DNA than an unacetylated fragment (Hong *et al.*, 1993). Additional investigations found that the N terminal tail of H4 can interact with an acidic region of the H2A/H2B dimer of a neighbouring nucleosome; therefore, disruption of the electrostatic properties of this interaction could destabilize the higher order formation of chromatin (Luger *et al.*, 1997). It has also been reported in yeast that acetylation of K5, K8 and K12 each contribute equally to the electrostatic de-stabilization of the 30nm fibre by influencing the interaction of the H4 tail with the H2A/H2B dimer of surrounding nucleosomes (Dion *et al.*, 2005). Disruption of the electrostatic properties of histone tails can affect histone stabilization within the same core particle e.g. hyperacetylated as opposed to hypoacetylated H4 resulted in a decrease in the stabilisation forces in a nucleosome core particle (Oliva *et al.*, 1990).

The second mechanism by which histone modifications can result in chromatin remodelling is by means of histone modifications behaving as signals which can be

interpreted by the cell. This is where distinct combinations of modifications of histone tails are interpreted by machinery of the cell, resulting in direct outputs. This is often referred to as the 'histone code' hypothesis. There are four lysine residues of H4 which can be modified *in vivo*: K5, K8, K12 and K16. Experiments in yeast found that, in the case of many genes, acetylation of K16 is a unique, specific modification which is interpreted by the cellular machinery; however, acetylation of K5, K8 and K12 are not specific and are redundant, with the absolute number of these modifications being the important factor (Dion *et al.*, 2005).

1.6.1 Function of histone modifications

Evidence suggests that histone modifications are involved in a range of vital cellular processes (Lee *et al.*, 1993). These include DNA replication. For example in the protozoan Tetrahymena, if S10 of histone H3 is mutated then aberrant chromosomal segregation occurs at mitosis. If H3 dephosphorylation is prevented, then condensed chromosomes are maintained and exit from mitosis is inhibited. Indeed, H3 at S10 is phosphorylated in many organisms during mitosis and meiosis (Hsu *et al.*, 2000). Histone modifications have also been shown to be associated with apoptosis in a number of organisms. Budding yeast exposed to hydrogen peroxide were found to undergo phosphorylation of S10 H2B prior to apoptosis. If this residue was mutated then cells became resistant to hydrogen peroxide induced apoptosis (Ahn *et al.*, 2005). DNA repair, in particular double strand break repair, has been also shown to involve histone modifications. Exposure of mice to ionizing radiation that induced double strand breaks resulted in phosphorylation of S139 on H2A (Rogakou *et al.*, 1998). Work in mouse embryonic stem cells has further implicated the histone variant H2AX in the normal process of dealing with double strand breaks. When the H2AX variant was deleted it resulted in an increase in cancer incidence due to an increased sensitivity to double strand breaks. This study also found evidence for modifications of H2B, H3 and H4 being important in detecting and flagging up regions of DNA damage and co-ordinating in cell cycle arrest (van Attikum and Gasser, 2005). In addition, a major role exists for histone modifications and chromatin remodelling in regulating transcription.

1.7 Chromatin and transcription

An axiom of chromatin biology is that nucleosomes provide a means of regulating gene expression by physically restricting the access of the transcriptional apparatus to the DNA and a corollary of this is that among all the cellular processes, histone modifications have been the most extensively researched in regards to their role in transcription. Eukaryotes utilise a number of different classes of RNA polymerases, each responsible for replicating different templates. The RNA polymerase responsible for transcribing DNA into mRNA is RNA polymerase II (RNA pol II). RNA pol II transcription is performed by panoply of factors, collectively termed the general transcription factors, which include: RNA polymerase II and associated factors: TFIIA, TFIIB, TFIID, TFIIE, TFIIF and TFIIH. These factors co-ordinate the formation of RNA pol II at the transcriptional start site in the promoter (Green, 2005; Roeder, 2005). Many studies have identified nucleosomes as a hindrance to transcription. One study found that the presence of a nucleosome downstream on a DNA template caused RNA pol II to pause more frequently and for a greater duration during transcription, resulting in an increased frequency of transcriptional termination (Hodges *et al.,* 2009). Frequently, when RNA pol II pauses it undergoes backtracking, which is where RNA pol II moves upstream on the DNA template, resulting in the 3' DNA no longer being at the RNA pol II active site. Backtracked RNA pol II can terminate or re-initiate transcription. The option favoured is largely determined by the force exerted upon RNA pol, the greater the force the greater the likelihood of termination of transcription. Nucleosomes are believed to increase the force RNA pol II is under and hence are thought to decrease the probability of re-initiation of transcription after backtracked events. Force, however, does not seem to be important (unless at very high forces) for

the initiation of pauses of RNA pol II, which is supported by the fact that RNA pol II appears to pause at the same sequences regardless of whether the template is naked DNA or DNA is bound to nucleosomes (Hodges *et al.,* 2009). The factor, TFIIS was found to increase the necessary force required to permanently arrest backtracked RNA pol II, hence TFIIS can promote transcription under higher forces. It has therefore been suggested that TFIIS can help transcription through nucleosomes. In eukaryotes the binding of TFIIS to RNA pol II can be regulated by a number of factors (Galburt *et al.,* 2007). Even in active genes, the nucleosomes frequently remain bound to DNA in the coding region of genes. The protein complex, FACT, a heterodimer of Spt16 and SSPR1 can, *in vitro*, make nucleosomal DNA more accessible to RNA pol II. Elongator, which contains the HAT subunit Elp3, is another complex which can aid RNA pol II transcription through nucleosomes. FACT and elongator are proposed to interact with other chromatin factors and the basal transcription machinery (Kireeva *et al.*, 2005)

The general transcription factors are sufficient for transcription but typically they are assisted by activator proteins. In fact, RNA pol II transcription is typically initiated by the binding of DNA sequence specific activator proteins. Activator proteins contain a DNA binding domain (to localise the factor to a specific location) and a separate activation domain (to promote transcription). Activators function in a number of ways: they can stimulate preinitiaion complex (PIC) assembly, promote initiation, elongation and reintiation of pol II. They can also facilitate the binding of co-activator or co-repressor factors (Green, 2005; Roeder, 2005). Co-activators and co-repressors can be seen as intermediaries (which probably is why they have also been termed mediators), between activators and the general transcription factors. Furthermore, the absence of

DNA binding capabilities of co-activators and co-repressors implies a degree of flexibility is important for their functioning (Utley *et al.*, 1998; Berger 2002). Co-activators and co-repressors are generally large multi-subunit protein complexes that consist of catalytic and non-catalytic subunits. Importantly, they typically exhibit chromatin modifying and/or chromatin remodelling activities. Studies in budding yeast have found co-ordinated efforts of these chromatin activities with genes that undergo chromatin modification also undergoing chromatin remodelling, thus indicating a functional link between these two processes. In addition, the same activators can be responsible for the localisation of modification and remodelling complexes (Berger, 2002).

The association of particular histone modifications with transcriptionally active or inactive regions has been studied for many genes in multiple organisms. Although there is no hard and fast rule, some general trends have been observed: methylation of K4, K9 acetylation, K14 acetylation, Arginine 17 (R17) methylation, K18 acetylation and K23 acetylation have been associated with activation of transcription; whereas, K9 methylation and K29 methylation have been associated with gene silencing (Guo *et al.*, 2008). In *Arabidopsis*, genome-wide screens have been performed to give a general indication of the prevalence of modifications of H3. It has been shown that some histones were not modified but the majority were modified, frequently acetylated or methylated on at least one of their residues (Johnson *et al.*, 2004). A similar study in yeast yielded complementary results, with nearly all H4 acetylated at least once on residues 4-17 (Smith *et al.*, 2003). Together these studies demonstrate the prevalence of histone modifications of H3 and H4.

A characteristic chromatin modifying complex originally, identified in yeast, is the multi-subunit complex SAGA (Spt-Ada-Gcn5-Acetyltransferease). Gcn5, the enzymatic subunit of SAGA is capable of acetylating histones and this is potentiated by its histone acetyltransferase (HAT) domain. Experiments found that Gcn5 can modify free histones but is incapable of modifying histones when they are associated with chromatin. Further investigation of the SAGA complex revealed that another subunit, Ada2, and also maybe the subunits Spt3 and Spt20, interact with the activator protein TBP, thereby demonstrating a means by which the complex is recruited to certain genes (Grant *et al.*, 1997). Additional studies have also found evidence for an interaction between the SAGA subunit Spt20 and TBP. A functional interaction has been suggested by the fact that certain mutations in the TBP gene result in similar phenotypes as null SAGA mutations (Roberts and Winston, 1997).

1.8 Nucleosome Remodelling

An archetypical eukaryotic chromatin remodelling complex is the highly conserved SWI/SNF complex. This complex was identified by analysis of yeast strains which exhibited defects in mating type switching (SWI) and sucrose fermentation (SNF). SWI/SNF is recruited to chromatin by activators and studies have suggested that SWI/SNF can remain retained on chromatin upon dissociation of the activator proteins. The retention of SWI/SNF is, however, contingent on the acetylation state of the localised histones. When HAT proteins were prevented from binding to the localised chromatin the SWI/SNF complexes were not retained (Hassan *et al.*, 2001). A variety of evidence, including a reduction in the relative mass of DNA associated with nucleosomes, reduced super coiling of DNA per nucleosome and reduced nucleosome stability, indicate that remodelling by SWI/SNF results in unwrapping of DNA from the nucleosome (Peterson and Workman, 2000). SWI/SNF has also been demonstrated to regulate superhelical torsion of the DNA; therefore providing a potential means by which it could affect higher-order chromatin structure (Havas *et al.*, 2000)

A characteristic of chromatin remodelling complexes is the utilisation of energy from ATP hydrolysis to physically move localised nucleosomes, which can result in either activation or repression of transcription. Typically, movement of nucleosomes so that they are equally spaced is associated with transcriptionally silenced genes; whereas, regions of DNaseI sensitivity (which indicates regions of DNA where histones have been disrupted and are subsequently more susceptible to restriction by DNaseI) are frequently present at certain regions of promoters and enhancers during, or immediately prior to, transcription (Weintraub and Groudine 1976). A number of studies have been

performed to try and determine the specifics of ATP dependent nucleosome remodelling. Among those examined is the Drosophila ATP dependent chromatin remodelling complex NURF. The authors employed the heat shock protein 70 (hsp70) promoter as a DNA template to examine NURF mediated remodelling. It was discovered that NURF maintains the overall structure of the histone octamers while moving them in small increments (a few bp) at a time in a cis manner, with the whole process taking a very short time (minutes or less). It was also discovered that the histone octamers were remodelled to specific locations on the DNA, suggesting that the locations occupied by histone octamers are dependent on the underlying DNA template. When alternative DNA templates were examined in otherwise identical experimental conditions, remodelling did not occur, again highlighting the importance of the DNA structure in nucleosome remodelling (Hamiche *et al.*, 1999). Somewhat conflicting evidence was found in a separate study which showed that the yeast ATP chromatin remodelling complex, RSC, moved histone octamers in trans. The means by which chromatin remodelling factors remodel nucleosomes could therefore be dependent on multiple factors (Lorch *et al.,* 1999).

ATP-dependent nucleosome remodelling is also employed when histones, which exist in variant forms, are swapped (van Attikum and Gasser 2005). The SWR1 complex, which is part of the SWI/SNF family, is a multi-subunit complex that is responsible for the replacement of the histone variant H2A with H2AZ. The use of alternative histones is important in a number of processes, including regulating transcription (Mizuguchi *et al.,* 2004). Studies in mammals have found three H3 variants: H3.1, H3.2 and H3.3; differing by only a few amino acids. These variants differ in their cellular expression profile, with an increase in relative abundance of H3.3 found in differentiated cells.

Using tagged variants, immunoprecipitation and mass spectrometry, the variants have been found to interact with different proteins (Tagami *et al.*, 2004). Variant forms of H2A have also been found in mice (West and Bonner 1980). In *Arabidopsis*, variants of H3: H3.1 and the more prevalent H3.2; have been identified. The H3.2 variant has been shown to be generally more highly acetylated than the H3.1 variant (Waterborg 1992). When the relative abundance of the two forms were compared to genome size in a number of plant species, an inverse correlation was discovered. This finding may be explained by observations that smaller genomes typically have a larger fraction of transcriptionally active DNA (Waterborg, 1992).

1.9 Common domains of chromatin associated proteins

A number of domains are conserved across many chromosomal modifying proteins and are necessary for their recruitment to, and modification of, chromatin. These domains include the bromodomain (which can bind to acetylated histone residues), chromodomain (which can bind methylated histone residues), Plant Homeo Domain (PHD) finger domain, the SANT domain (which is capable of binding to DNA and proteins) and the PWWP domain (which is necessary for the localisation of DNA methyl-transferaeases to chromatin) (Qian *et al.*, 2005).

Mitotic chromosome

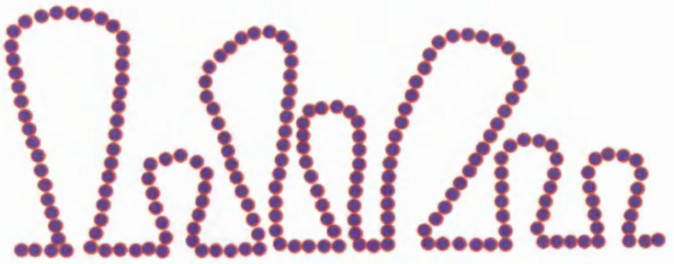

Extended chromosome

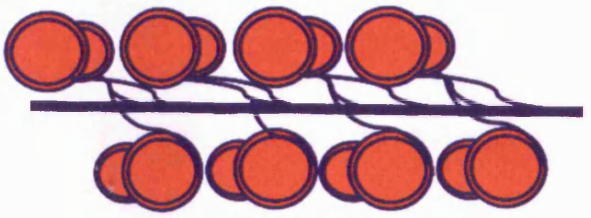

30nm solenoid

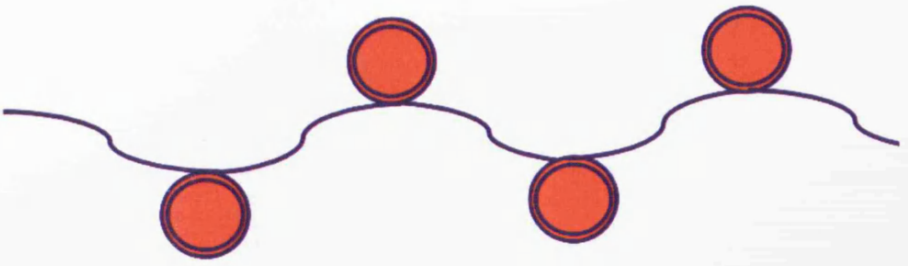

Beads on a string

HAT

HDAC

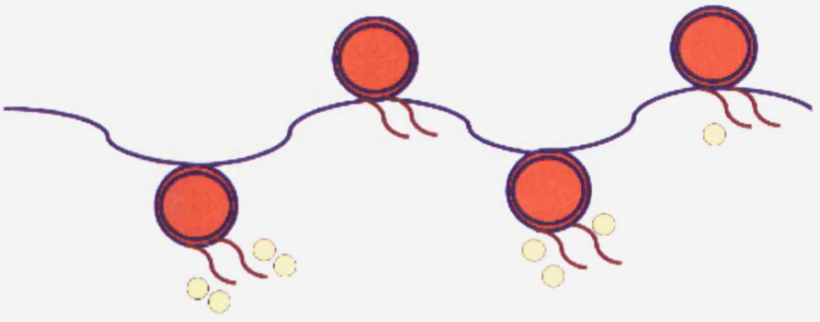

Acetylated histones

Figure 1.2: Structural hierarchy of chromatin. Diagram shows the levels of packaging present within the chromosome. Orange circles represent nucleosomes and Blue lines represent DNA. At the bottom of the diagram the acetylation of histones is represented by yellow circles.

1.10 Chromatin remodelling in plant environmental signalling

In regard to plants, chromatin remodelling has been extensively studied in the regulation of flowering by low temperature, termed vernalization (Henderson and Dean 2004). Vernalization functions by down-regulation of the floral repressor, *FLOWERING LOCUS C (FLC)*. The down regulation of *FLC* correlated with an enrichment of H3K9 and H3K27 methylation around the *FLC* locus (Bastow *et al.*, 2004). Wigge and colleagues have recently provided further evidence for a role of chromatin remodelling in plant temperature signalling. Using an *Arabidopsis* screen, the authors identified a role for ACTIN RELATED PROTEIN 6 (APR6) in regulating the ambient temperature transcriptome. Previously, APR6 had been identified as a subunit of the SWR1 complex, which functions in incorporating the alternative H2A histone, H2A.Z, into nucleosomes. Upon temperature increase, the nucleosome at the transcriptional start site of these temperature regulated genes showed a decrease in enrichment for H2A.Z and an increase in enrichment of H2A. As H2A.Z associates with DNA more strongly than H2A, incorporation of H2A relaxes the nucleosome-DNA interaction and is more permissive to transcription (Kumar and Wigge, 2010).

The role of chromatin remodelling in plant light signalling was first convincingly demonstrated in 2001. Plastocyanin (PetE) is a protein involved in the photosynthetic electron transfer chain. Its expression is light dependent with green shoots expressing high levels of PetE, etiolated shoots expressing low levels and roots expressing none. A ChIP approach was used to show that the enhancer, promoter and part of the transcribed region of PetE were associated with hyperacetylated H3 and H4. Conversely, in non-photosynthetic tissues these regions were hypoacetylated. DNaseI and micrococcal

nuclease accessibility assays also showed that the promoter and enhancer regions of PetE in photosynthetic shoots had a more open structure than those in etiolated shoots and (Chua *et al.*, 2001). Subsequent experiments in tomato suggested another link between chromatin remodelling and plant light signalling. This work demonstrated that the photosynthetic regulator, DE-ETIOLATED (DET1), preferentially bound to chromatin containing unacetylated H2B (Benvenuto *et al.*, 2002).

Recently, the expression of a number of light-regulated genes has been associated with histone modifications during seedling de-etiolation. Six light regulated genes were analysed and 5 of the 6 genes exhibited an increase in association with H3K4me3 and H3K9ac as their transcription increased. Four of the six genes demonstrated an increase in association with H3K9me2 and H3K27me3 as their transcript decreased. A role for the phytochromes was demonstrated in this process, with the *phyB/phyD/phyE* triple mutant demonstrating aberrant formation of these modifications. Mutants deficient in the putative chromatin remodelling factor HISTONE DEACETYLASE 1 (HD1) exhibited elevated H3K9ac at all 6 genes, suggesting that HD1 is important in removing this mark (Guo *et al.*, 2008). A positive correlation between H3K9ac and H3K27ac levels and gene expression was observed with the strongest correlation for regions approximately 100 bp downstream of the transcriptional start site (TSS). Furthermore, genes associated with histones carrying both modifications exhibited higher transcription than those associated with histones carrying a single modification. In particular, the key photomorphogenic regulator HY5 and its homologue HYH, displayed enriched association of their coding regions with H3K9ac when transferred from dark to light. Downstream targets of HY5 and HYH also displayed increased association with H3K9ac following the same treatment (Charron *et al.*, 2009).

Analysis of natural genetic variation in 21 *Arabidopsis* accessions has also recently identified PHYB as a potential positive regulator of chromatin compaction during reductions in light quantity by spectrally neutral shading. Data from this study suggests that PHYB and potentially R:FR ratio, could be involved in chromatin folding, by regulating areas of the genome that form chromocenters, which are highly condensed, heterochromatic, inaccessible regions of the genome. This interesting development suggests that light quality, in the form of R:FR ratio could affect chromatin folding, but whether this has any implications for the shade avoidance response in terms of gene expression and phenotypic response, has not been investigated (Tessadori *et al.*, 2009).

1.11 Factors involved in plant chromatin remodelling

1.11.1 GCN5 and HD1

Arabidopsis thaliana has four types of histone acetyltransfereases (HATs) which are grouped according to their homology to yeast and mammalian HATs. The four classes of *Arabidopsis* HATs are; GNAT, MYST, CBP and TAF1. *Arabidopsis* histone deacetylases (HDACs) are also grouped into four classes. These are: RDP3, HDA1 and SIR2, all three of which are classed according to their homology to yeast HDACs. The fourth class of *Arabidopsis* HDACs is HD2 and this class is specific to plants. The RDP3 class of HDACs are the major group of HDACs in yeast and mammals. HDA19/HD1 belongs to the RDP3 group of HDACs (Benhamed *et al.,* 2006). *Arabidopsis* mutants deficient in the HDAC, HD1, and HAT, GCN5, have been shown to display aberrant light signalling phenotypes in multiple studies (Benhamed *et al.,* 2006; Guo *et al.*, 2008).

In *Arabidopsis*, HD1 is a constitutively expressed protein of 501 amino acids, with approximately 55% amino acid sequence identity to its mammalian and yeast homologues (Tian and Chen 2001). Analyses of null mutants revealed lower chlorophyll levels and twisted leaves in *hd1* plants. Additionally, *hd1* plants exhibited abnormal flowers which had fewer petals, split flowers and partial sterility. Except for slightly shorter siliques, heterozygotes displayed a WT phenotype (Tian *et al.*, 2003). Homozygous *hd1* lines had hyperacetylated H4K12; whereas, the heterozygote had levels of acetylation of histone H4 that were the same as WT (Tian *et al.*, 2003).

The *Arabidopsis* protein, GENERAL CONTROL NON-REPRESSSIBLE (GCN5), displays a high degree of similarity to homologues in other organisms. In yeast, it forms a component of the complexes SAGA and ADA, which regulate transcription (Stockinger *et al.*, 2001). Mutation of GCN5 in yeast results in aberrant expression of 4% of genes and mutation of the homolog in mice results in embryonic defects (Bertrand *et al.*, 2003). In *Arabidopsis*, homozygous *gcn5* plants have been shown to display pleiotropic abnormalities. These include: elongated petioles, reduced leaf expansion, mild leaf serration and reduced chlorophyll. Abnormal inflorescence structure and reduced numbers of misshapen siliques were also recorded, leading to reduced fertility. The acetylation levels of histone H3 in *gcn5* lines was lower than WT (Bertrand *et al.*, 2003; Vlachonasios *et al.*, 2003). Interestingly, yeast two hybrid studies revealed that *Arabidopsis* GCN5 bound to the transcriptional regulator C repeat Binding Factor 1 (CBF1). The CBFs are induced during cold acclimation and initiate the transcription of a suite of genes (the CBF regulon) involved in enhancing plant freezing tolerance (Stockinger *et al.*, 2001; Vlachonasios *et al.*, 2003; Thomashow 1999; Franklin and Whitelam, 2007). These observations provide further support for the role of histone acetylation and deacetylation in plant environmental signalling.

Under W, R, FR and B the *gcn5* mutant exhibited longer hypocotyls and the *hd1* mutant shorter hypocotyls than WT. These phenotypes were particularly pronounced in FR light. Interestingly, the *gcn5/hd1* double mutant had hypocotyls similar to WT. Differential expression of a number of light-regulated genes was observed between the mutants and WT. ChIP experiments additionally revealed H3 acetylation at the core promoter regions of a number of light regulated genes to be decreased in the *gcn5* mutant compared to WT. Mutation of *HD1* resulted in increased acetylation of histone

H3 and H4 on the core promoter region of these same light regulated genes (Benhamed *et al.*, 2006).

1.11.2 SHL

SHORT LIFE (SHL) is a 228 amino acid protein containing a PHD domain, a BAH (bromo-adjacent homology) domain and a nuclear localization signal (NLS). The *Arabidopsis* genome contains two homologues of SHL: At4g22140 and At4g04260. There are closely related proteins present in tomato, barley and wheat. No related proteins have been found in fungi or animals (Mussig *et al.*, 2000).

Over-expression of SHL was shown to result in reduced growth, early flowering and reduced seed production. Plants expressing antisense *SHL* constructs displayed smaller, darker leaves, more compact rosette, later flowering and reduced seeds. Transgenic plants with the lowest levels of *SHL* did not flower at all (Mussig *et al.*, 2000). Microarray analyses of plants expressing sense and antisense *SHL* constructs revealed aberrant expression of the low R:FR regulated genes *DIN2* (At3g60140), *PUTATIVE ENDOCHITINASE* (At2g43570), *COR78* (At5g52310) and *COR15a* (At2g42540), suggesting a potential link between SHL and chromatin remodelling events in plant light signalling (Mussig and Altmann, 2003).

1.12 Techniques available to study chromatin

There are a number of different techniques available to study the structure of chromatin and which to use depends on what is being investigated. At one end of the scale, the broad arrangements of chromatin domains can be studied. A variety of stains, such as Giemsa, can be used to distinguish between highly condensed and uncondensed regions of chromosomes. This can be combined with fluorescent in situ hybridization (FISH), which involves hybridization of fluorescently labelled DNA probes to chromosomes. With the utilization of these two techniques it becomes possible to determine the broad structure of chromosomes, and hence chromatin, and also whether certain DNA sequences are associated with them. Additionally, antibodies against histones modifications can be used and this can identify associations between histone modifications and general chromatin structure (Jasencakova *et al.*, 2000). This technique allows a broad characterisation of the structure of chromatin but it does not produce data of high resolution.

Chromatin can be analysed in more detail with the use of foot-printing/nuclease accessibility assays. This technique allows the spatial identification of protein-DNA interactions. In the analysis of chromatin structure it can be used to identify where nucleosomes are bound to DNA. The procedure involves the treatment of chromatin with endonucleases, such as micrococcal nuclease or DNaseI, which cut the DNA in particular regions not bound to nucleosomes. The DNA can then be analysed by either PCR or fluorescently labelled probes. The signal from PCR, or the banding pattern of the fluorescently labelled gel, gives an indication of whether that region is bound by a nucleosome or not (Chua *et al.*, 2001). This allows identification of nucleosome-DNA

interactions, but it does not provide information histone modifications and some prior knowledge must be known about which genes to analyse.

Chromatin modifications can also be analysed in detail with a technique known as chromatin immunoprecipitation (ChIP). ChIP can be used to determine if there is an interaction between a protein of interest, in this case histones, and DNA. It frequently involves the use of formaldehyde treatment in vivo to form chemical cross-links between DNA and histones, thus preserving the arrangement of these molecules. Antibodies directed against histones can then be used to isolate histone-DNA complexes. The DNA can be removed from the histones and studied by PCR to determine enrichment of DNA sequences relative to control immunoprecipitations (Solomon *et al.,* 1988). ChIP allows the association of histone modifications with particular DNA sequences to be characterised. One downside of ChIP is that some prior knowledge of which DNA sequences are expected to be associated with a particular modification needs to be known before the experiment can be performed.

ChIP and nuclease accessibility have been expanded upon to allow for greater through-put and to analyse changes on a genome-wide scale (Ozsolaki *et al.,* 2007). By combining these techniques with microarray and sequencing technology, whole genomes can be analysed and regions can be identified without previous knowledge of their potential involvement. For example, ChIP on chip combines microarray and ChIP technology. In this technique, instead of analysing the DNA using PCR, it is labelled with a fluorescent tag and a separate sample which has not been enriched by immunoprecipitation, is also tagged with a different fluorescent tag. These two samples are then hybridized to the same microarray. If a particular probe on the microarray is

particularly associated with one off these probes then this suggests that this region of DNA is associated or not associated with the histone modification used in the immunoprecipitation (Ren *et al.,* 2000). ChIP-seq is a technique which replaces microarrays with sequencing. Instead of hybridizing to a microarray, the DNA is amplified by high-throughput sequencing reactions (Johnson *et al.,* 2007). These techniques offer the opportunity to identify more targets and analyse entire genomes. They are, however, expensive and ChIP and nuclease accessibility experiments must first be optimised before they can ne implemented.

1.13 Project aims

The aim of the project is to investigate the role of chromatin structure in *Arabidopsis* shade avoidance signalling. A number of studies (1.10 Chromatin remodelling in plant environmental signalling) have suggested that environmental factors, including temperature (Bastow *et al.*, 2004; Kumar and Wigge, 2010), light (Benvenuto *et al.*, 2002; Chua *et al.*, 2001; Guo *et al.*, 2008) and perhaps even R:FR ratio (Tessadori et al., 2009), can regulate the structure of chromatin. Furthermore, light and temperature have been shown to co-ordinately regulate chromatin structure and transcriptional regulation of genes (Guo *et al.*, 2008; Bastow et al., 2004; Kumar and Wigge, 2010). However, there has been no research to establish whether R:FR ratio can regulate chromatin structure and shade avoidance signalling.

Given the wealth of data demonstrating the importance of environmental signals in regulating chromatin and transcription in *Arabidopsis*, it was hypothesised that R:FR induced changes in gene expression would be associated with changes in chromatin structure. Additional evidence in support of this hypothesis was the fact that aberrant expression of the factor SHL, which exhibits domains frequently associated with chromatin remodelling proteins, disrupts expression of a number of R:FR regulated genes. To investigate this hypothesis, changes in chromatin structure will be analysed around shade avoidance marker genes, such as athb2 and pil1, using nuclease accessibility assays and ChIP. Additionally, mutants and over-expressing lines of putative chromatin remodelling proteins HD1, GCN5 and SHL, will be obtained. Physiological analyses of these lines should enable their putative roles in shade avoidance signalling to be ascertained.

Chapter 2

Materials and Methods

2.1 Materials

2.1.1 Plant material

In all experiments, the *Arabidopsis thaliana* ecotypes used were either Columbia (Col), Landsberg *erecta* (La-*er*) or Wassilewskija (Ws). These, and all T-DNA-containing Salk lines were obtained from the Nottingham *Arabidopsis* Stock Centre (NASC, UK, http://arabidopsis.info/).

2.1.2 Plant growth media

Seeds used in all experiments were either grown on media or soil. Lehle (LM) was the sole media used for the growth of seedlings. LE was prepared by combining 2 ml 1 M $MgSO_4$, 5 ml 1 M KNO_3, 2.5 ml 1 M KH_2PO_4 pH 5.6, 2 ml 1 M Ca $(NO_3)_2$, 1 ml micronutrient mix (70 mM $H3BO_3$, 14 mM $MnCl_2$, 0.5 mM $CuSO_4$, 1 mM $ZnSO_4$, 0.2 mM $NaMoO_4$, 10 mM NaCl, 0.01 mM $CoCl_2$), 2.5 ml of 1.8 % Sequestrene and 6 g of agar, made up to 1 l with dH_2O. All media was then autoclaved prior to use. If antibiotics were to be added to the LE they were added when the LE had cooled to about 50 °C. The soil used was Levingtons's (http://www.Monrosouth.co.uk) F2 + S (3 parts soil and 1 part sand) Seed and Modular compost.

2.1.3 Bacterial strains

The bacterial strains used for cloning were *Escherichia coli* (*E. coli*) α-select Silver Efficiency cells (genotype: F^- *deo*R *end*A1 *rec*A1 *rel*A1 *gyr*A96 *hsd*R17(r_k^-, m_k^+) *sup*E44 *thi*-1 *pho*A Δ(*lac*ZYA-*arg*F)U169 Φ80*lac*ZΔM15 λ^-) (Bioline (www.Bioline.com)).

The bacterial strains used for transformations were *Agrobacterium tumefaciens* (*A. tumefaciens*) strain GV3101, which contains the disarmed plasmid pMP90RK (Monsanto (http://www. Monsanto.com)).

2.1.4 Bacterial growth media

The bacterial strains used were grown in Lennox Broth (LB), which was prepared by combining 10 g tryptone, 5 g yeast extract and 10 g NaCl in 1 l of dH_2O, which was then autoclaved. LB agar (LA) was made in the same way except 12 g of agar was added prior to making up the volume to 1 l.

2.1.5 Plasmids

The plasmids used were pROK2 (Baulcombe *et al.*, 1986), pDONOR221, pB2GW7, pB7GWIWG2 (I) (Department of plant systems biology University of Gent, Belgium (http://www.psb.ugent.be/)) (Karimi *et al.*, 2002).

2.1.6 Oligonucleotides

All oligonucleotides were purchased from Sigma (http://www.sigmaaldrich.com/).

2.1.7 Sequencing

All sequencing was performed by the John Innes Centre, Norwich, UK (http://www.jicgenomelab.co.uk/).

2.2 Methods

2.2.1 Plant growth conditions

All seeds were sown at the required density (either sprinkled or individually spotted) on the appropriate medium and were stratified for 4 days at 4 °C in the dark. They were then light pulsed for 1 h and returned to the dark at room temperature for a further 24 h, to unify germination. Following this, they were transferred to the relevant growth conditions. All plants were grown at 22 °C. For adult plant experiments, uniformly-sized seedlings were transferred to 5 cm x 5 cm pots of soil at 7 days.

2.2.2 Light sources

White light was provided by fluorescent tubes at a photon irradiance of approximately 130 $\mu molm^{-2}s^{-1}$ and R:FR of 2.7. Low R:FR was produced by supplementary FR LEDs (λ_{max} 735 nm, Shinkoh Electronics; shinkoh-elecs.com) positioned overhead. In these experiments, the same photon irradiance of photosynthetically active radiation (PAR) was used, with a R:FR ratio of 0.1. R:FR ratio measurements were made using a Stellarnet EPP200O fiber optic spectrometer with a planar sensor (stellarnet-inc.com). Light quality measurements were made with a Li-COR Li-190 quantum sensor (http:/www.licor.com).

2.2.3 Bacterial growth and transformation

2.2.3.1 Transformation of *E. coli* cells

E.coli cells (see section 2.1.3 Bacterial Strains) were transformed with plasmids according to the manufacturer's instructions. All transformed bacterial cells were grown at 37 °C for 12 – 24 h.

2.2.3.2 Making competent *A. tumefaciens* cells

A 2 ml vial of LB was inoculated with a culture of *A. tumefaciens* and grown for 12 h at 28 °C. This culture was then transferred to a 250 ml conical flask and made up to 50 ml with LB and grown at 28 °C at 200 rpm until the OD_{600} was between 0.5 and 1. All solutions of LB used to culture *A. tumefaciens* were supplemented with 50 µg/ml of gentamycin and 50 µg/ml of rifampicin. The solution was then centrifuged for 5 min at 3000 g in a Beckman GPR centrifuge that had been pre-cooled to 4 °C (http://www.beckmancoulter.co.uk/). The supernatant was discarded and the pellet was re-suspended in 1 ml of 20 mM $CaCl_2$ that had been pre-cooled to 4 °C. The cells were separated into eppendorf tubes in 100 µl aliquots and frozen at – 80 °C.

2.2.3.3 Transforming *A. tumefaciens* cells

A 100 µl aliquot of competent *A. tumefaciens* cells was removed from – 80 °C and transferred to 4 °C, whereupon 1 µg of plasmid was added to the cells. The cells were then transferred to 37 °C for 150 s and the tube flicked to mix the contents. Cells were then returned to 37 °C for a further 150 s. One ml of LB was added to cells prior to incubation at 28 °C at 200 rpm for 2 – 4 h. The solution was then pipetted onto 9 cm petri dishes containing LA supplemented with the appropriate antibiotic and spread evenly over the plate using a sterilized spreader. The plates were incubated at 28 °C for 2 -3 days.

2.2.4 Harvesting seeds

Seeds were harvested from individual, dry plants. Seeds were deposited from the plants onto clean sheets of paper, dried plant debris removed and stored in eppendorf tubes.

2.2.5 Sterilizing seeds

Harvested seeds were transferred to a 50 ml Falcon tube and washed for 5 min in 40 ml of 50 % bleach and 0.05 % tween 20 in dH_2O by inversion. The seeds were allowed to settle and the solution removed by decanting. The seeds were then washed 1 min in 40 ml dH_2O by inversion and the seeds were allowed to settle before the solution was decanted this was repeated a further 5 times. The seeds were then transferred to filter paper and left to dry in the flow hood. Once dry, the seeds were transferred to eppendorf tubes.

2.2.6 Plant transformation

A 5 ml vial of LB was supplemented with the relative antibiotics, inoculated with a colony a of *A. tumefaciens* transformed with the appropriate construct and incubated for 1 – 2 days at 28 °C at 200 rpm. Of this culture, 2 ml was transferred to a 1 l conical flask containing 400ml of LB supplemented with the appropriate antibiotics and this was incubated at 28°C at 200rpm for 16 h. The culture was then centrifuged in a Sorval centrifuge for 20 min at 4000 rpm at 20 °C (http://www.sorvallcentrifuge.co.uk/). The supernatant was decanted and the pellet re-suspended in 100 ml of 5 % sucrose. A further 900 ml of 5 % sucrose solution was added to take the volume to 1 l and 50 µl of Silwett (Lehle seeds (http://www.Arabidopsis.com)) solution was added. The solution was decanted into a glass beaker and the aerial parts of the plants were submerged in the solution for 10 s (the plant used were ones that had just started to produce flowers). Plants were removed and placed on tissue paper to remove excess solution and then covered and kept out of direct sunlight for 12 h. The plants were then returned to the growth room. Seeds were ready to harvest after about 4 weeks.

2.2.7 Analysis of SALK T-DNA mutants

Tissue was taken from individual SALK T-DNA mutants and WT plants of the same ecotype and DNA was extracted (2.2.8.1) and was used as a template in a PCR reaction with primers recommended by the SALK website (2.2.8.2) and the reaction was run on a gel (2.2.8.3). Tissue was taken from plants that were deemed homozygotes by PCR testing and RNA was extracted from the tissue (2.2.9.1) and cDNA was synthesised from this tissue and used in a qPCR reaction (2.2.9.3) to test for mRNA expression of gene of interest. Plants without expression of mRNA were grown on.

2.2.8 DNA analysis

2.2.8.1 DNA extraction from plant tissue

Plant tissue was harvested into 1.5 ml eppendorf tubes and frozen in liquid nitrogen before storage at – 80 °C. Samples were removed from liquid nitrogen and ground in eppendorf tubes for 20 s using a plastic pestle. A 400 µl aliquot of PCR extraction buffer (200 mM Tris-HCl, pH 7.5, 250 mM NaCl, 25 mM EDTA) was then added to each before further grinding for 10 s. Samples were vortexed for 10 s and then centrifuged in a 5415R eppendorf at 13000 rpm for 1 min (http://www.eppendorf.com). A total of 300 µl of supernatant was transferred to a fresh eppendorf tube and the pellet discarded. To the supernatant, 300 µl of isopropanol was added. The sample was inverted several times and then stored at – 80 °C for at least 10 min. Following a 10 min centrifugation supernatants were discarded and the pellets re-suspended in 500 µl of 70 % ethanol. A final 10 min centrifugation was performed, supernatants removed and pellets re-suspended in 100 µl dH_2O and stored at – 20 °C.

2.2.8.2 Polymerase chain reaction (PCR)

PCR reactions were all set up in 0.2 ml 8 strip tubes and performed on a Biometra T3 Thermocycler (http://www.biometra.de/). In general, a 10 µl reaction was performed, which comprised: 1 µl of template DNA, 0.5 µl of 10 µM forward primer, 0.5 µl of 10 µM reverse primer, 5 µl of Taq PCR mastermix (Qiagen (http://www.qiagen.com)) and 2 µl dH_2O. A typical PCR program would constitute a 5 min denaturation step at 94 °C, followed by 35 repeats of 94 °C for 30 s (denaturing), 55 °C for 30 s (annealing) and 72°C for 1 min (polymerization). This would be finished off with a single cycle of 5 min at 72 °C and then 10 min at 4 °C.

If the purpose of the PCR reaction was to generate DNA for cloning then an alternative PCR reaction was performed. The Phusion DNA polymerase kit (Finnzymes (http://www.finnzymes.com)) was used for all cloning reactions but the constituents of the reaction, their relative ratios and the PCR program utilised varied according to the template DNA: HF (high-fidelity) or GC (GC rich) buffer was used and the $MgCl_2$ concentrations were varied.

2.2.8.3 Agarose gel electrophoresis

Flowgen (Flowgen bioscience (http://www.flowgen.co.uk)) tanks and trays and bio-rad (Bio-rad Laboratories (http://www.bio-rad.com)) power packs were used in all agarose gel electrophoresis experiments. Agarose gels were prepared by melting 0.8 – 1.5 % agarose (Melford (http://www.melford.co.uk)) in the appropriate amount of 1 x Tris Acetate EDTA (TAE) (40 mM Tris-acetate, 1mM EDTA) by boiling in a microwave. A total of 1.5 µl of 10 mg/ml of ethidium bromide (sigma) was added per 100 ml of TAE-agarose solution. Prior to loading DNA samples were mixed with 10 x loading buffer (4 g sucrose, 0.025 g bromophenol blue and 10 ml dH_2O). 3 – 5 µl of DNA hyperladder I was run along with the DNA samples. Electrophoresis took place in 1 x TAE running buffer at 100 V. Gels were visualized on a Syngene transilluminator and UVP camera (Syngene (http://www.syngene.com)).

2.2.8.4 Purification of DNA

2.2.8.4.1 Gel extraction of DNA

DNA was purified from an agarose gel by excision with a scalpel and purification with a Gel extraction kit (Qiagen) according to the manufacturer's instructions (http://www.qiagen.com)).

2.2.8.4.2 Plasmid extraction

Plasmids were extracted from bacterial cells using a Plasmid mini prep kit (Sigma) according to the manufacturer's instructions (http://sigmaaldrich.com).

2.2.8.5 Modification of DNA

2.2.8.5.1 DNA treatment with shrimp alkaline phosphatase (SAP)

Phosphatase reactions were typically 10 µl reactions consisting of: 1 µl SAP buffer (promega (http://www.promega.com)), 1 µl SAP, the relevant volume of vector and dH_2O. The reaction was incubated at 37 °C for 15 min and then at 65 °C for 20 min.

2.2.8.5.2 DNA treatment with ligase

Ligation reactions were all set up in 0.2ml, 8 strip tubes and incubated in a Biometra T3 thermocycler. In general, a 10µl reaction was performed, consisting of: 1µl ligase buffer (NEB (http://www.NEB.com)), 1µl ligase, and the relevant volumes of insert, vector and dH_2O to make a final volume of 10µl. Reactions were incubated overnight at 16 °C.

2.2.8.5.3 Restriction of DNA

Restriction enzyme reactions were typically 10 µl reactions consisting of: 0.5 µl of restriction enzyme, 1 µl of buffer and the relevant volume of vector and dH_2O. If necessary and buffer permitting, double digests were performed, otherwise single digests were performed and the DNA purified and digested with the second enzyme. Reactions were incubated for temperature and duration according to the manufacturer's recommendation for the enzyme. All restriction enzymes and buffers were ordered from NEB.

2.2.9 RNA analysis

2.2.9.1 RNA extraction

Plant tissue was harvested, frozen in liquid nitrogen and stored at – 80 °C. A mortar was pre-cooled with liquid nitrogen and the frozen material transferred to the mortar. Tissue was ground in the mortar with a pestle until the liquid nitrogen had evaporated, whereupon fresh liquid nitrogen was re-applied. Tissue was again ground with the pestle and the process was repeated until the tissue was a fine, white/green powder. Ground tissue was scraped from the mortar using a pre-cooled metallic spatula and transferred to an eppendorf tube which was then frozen in liquid nitrogen. Total RNA was extracted from the plant tissue using a Sigma Spectrum extraction kit, following the manufacturer's instructions. The isolated RNA was then treated with the Sigma Amplification Grade DNaseI kit to remove any contaminating DNA. For each 10 µl of RNA 1 µl of DNase and 1 µl of DNase buffer was added and the sample was incubated at 22 °C for 15 min. Following DNase treatment, 1 µl of stop solution per 10 µl of starting sample was added and it was incubated at 70 °C for 10 min. RNA was quantified using a spectrophotometer (Ultrospec 4300 pro Amersham biosciences (http://www.amersham.com)) set to 260 nm. 1 µl of RNA was added to 199 µl of RNase free water and RNA concentration was quantified in the spectrophotometer. Readings were performed using quartz cuvettes with a 1 cm path-length. The extinction coefficient for single stranded RNA in dH_2O was taken as 40 µg/ml/cm and this was used to calculate the quantity of RNA in the samples. For example, using this calculation, a sample with an optical density (OD) of 1 would have 40 µg of RNA per ml.

2.2.9.2 cDNA synthesis

cDNA synthesis was performed on DNase-treated RNA samples using the Promega AMV (Avian Myleoblastosis Virus Reverse Transcriptase) Reverse Transcription (RT) system according to the manufacturer's instructions (http://www.promega.com). RNA samples were diluted in RNase free dH_2O to a total volume of 9.5 µl. The majority of reactions were performed with 1 µg RNA. When lower yields of RNA were obtained, 0.5 µg was used. Appropriate volumes of AMV RT, AMV RT buffer, RNase inhibitor (RNasin), $MgCl_2$, dNTPs and random primers were added to a total volume of 20 µl. A 'no-RT' control sample was additionally made up which did not contain AMV RT. Samples were left at room temperature for 10 min to enhance primer annealing before incubation at 42 °C for 1 h. cDNA synthesis reactions were stopped by incubation at 95 °C for 5 min and samples transferred to ice. Working stocks of cDNA were prepared by the addition of 80 µl of RNase free dH_2O to each sample. These were stored at - 80°C.

2.2.9.3 Quantitative PCR (qPCR)

qQCR reactions were set up using a Corbett CAS-1200 liquid handling robot (Corbett Life Science (http://corbettlifescience.com)) and performed using a MJ Research PTC-200 qPCR machine (MJ research (http://bio-rad.com)). Reactions were set up on ice in 96 well plates with optically transparent lids (Abgene (http://www.abgene.com)). A typical reaction would consist of the following: 10 µl Sybr Green (Sigma), 8.5 µl dH_2O, 0.25 µl of 5 µM forward primer, 0.25 µl of 5 µM reverse primer and 1 µl of cDNA (described above). A typical qPCR reaction would consist of: 30 s at 95 °C and then the following cycle was repeated 42 times: 30 s at 95 °C, 30 seconds at 60°C, 30 seconds at 72 °C. *ACTIN2* primers were used in each experiment to provide template quantity controls. A threshold value was set for each experiment which coincided with the initiation of the PCR exponential phase of the samples.

Relative transcript abundance was calculated by first subtracting *ACTIN2* cycle values from sample cycle values (dCt). Individual sample values were then normalised to a control sample through subtraction of this value (ddCt). Fold increases in transcript abundance (relative to the control sample) were obtained though calculation of 2^(-ddCt).

The efficiency of all primer combinations was tested through the qPCR analysis of dilution series and inefficient combinations discarded. Melting curves were analysed at the end of each experiment to check that single PCR products had been produced.

2.2.10 Gateway cloning

The Gateway Cloning system was employed for the majority of cloning reactions performed and for this a specific protocol was followed. All reactions were performed in 0.2 ml, 8 strip tubes on a Biometra T3 Thermocycler. The Gateway cloning procedure is a two step reaction. An initial 25 µl PCR reaction was set up with the following constituents: 14.2 µl dH_2O, 5.0 µl 5 x buffer (either HF or GC), 0.5 µl of 10 mM dNTPs (Thermo scientific), 1 µl of 5 mM $MgCl_2$, 1.5 µl of 5 µM of forward primer, 1.5 µl of 5 µM of reverse primer, 1 µl of DNA template and 0.3 µl of Phusion DNA polymerase. The amount of individual constituents was varied if the reaction did not work, particularly the amount of $MgCl_2$ (between a range of 0 µl and 3 µl per reaction). HF buffer was used initially and if this was not successful in amplifying the sequence then the GC buffer was used. The PCR program for this reaction was as follows: 98 °C for 1 min then 10 repeats of the following: 98 °C 20 s, 52 °C for 30 s and 72 °C for 1 min. This was followed by a single repeat of 3 min at 72 °C and then 10 min at 4 °C. A second PCR was then performed using some of the first PCR as template DNA. The second PCR contained the following: 15.4 µl dH_2O, 10 µl of 5 x buffer (HF or GC), 1 µl of 10 mM dNTPs, 2 µl of 5 mM $MgCl_2$, 8 µl of 5 µM of forward adaptor primer, 8 µl of 5 µM of reverse adaptor primer, 5 µl of DNA template (first PCR) and 0.6 µl Phusion DNA polymerase. Again, the amount of individual constituents and buffer was varied if the reaction did not work. A range of between 0 µl – 6 µl $MgCl_2$ was used in these reactions. The PCR for this was: 1 min at 98 °C, followed by 10 repeats of the following: 20 s at 98 °C, 30 s at 45 °C and 1 min at 72 °C. This was followed by 20 repeats of: 20 s at 98 °C, 30 s at 55 °C and 1 min at 72 °C. This was finished off with a single repeat of: 10 min at 72 °C and 10 min at 4 °C. The second

PCR reaction was run on an agarose gel (2.2.8.3 Agarose Gel electgrophoresis) and the band of appropriate size excised and purified (2.2.8.4.1 Gel Extraction of DNA). A 2 µl sample of the purified PCR product and 2 µl of pDONOR was run on an agarose gel (2.2.4.3 Agarose Gel electrophoresis) and visually quantified. A reaction was then set up to integrate the PCR product in the pDONOR vector. The following reaction was set up to achieve this: 125 ng of PCR product, 75 ng of pDONOR, 1µl of BP Clonase II (invitrogen (invitrogen.com)) and this was made up to a total volume of 5 µl with TE. The reaction was incubated at 25 °C for 12 h whereupon 0.5 µl of proteinase K (invitrogen) was added. It was then transferred to 37 °C for 10 min. Half of this reaction, 2.5µl, was transformed into E. coli cells (2.2.3.1 Transformation of *E. coli* cells). Colonies were removed and transferred to vials containing 5 ml of LB supplemented with the appropriate antibiotic and incubated for 12 h at 37 °C 200 rpm. The plasmid was extracted from the bacterial culture (2.2.8.4.2 Plasmid extraction) and sent off for sequencing (2.1.7 Sequencing). If the sequencing revealed the sequence to be correctly amplified, the pDONOR plasmid was combined with the appropriate destination vector as outlined in the LR clonase II (Invitrogen (http://www.invitrogen.com)) procedure guide.

2.2.11 DNaseI sensitivity assay

2.2.11.1 Isolation of nuclei

All steps were carried out at 4 °C and all centrifugation for10 min at 1000 g in a Beckman GPR centrifuge. A liquid nitrogen pre-cooled pestle and mortar was used to grind 5 g of tissue. Liquid nitrogen was added and grinding maintained until the tissue was a fine, green/white powder. The tissue was then transferred to a fresh pestle and mortar and 20 ml of Hamilton buffer (10 mM Tris-HCL pH 7.6, 1.14 M sucrose, 5 mM $MgCl_2$, 5mM β-mercaptoethanol) was added before further grinding in the buffer. The solution was transferred to a magnetic stirrer and gently stirred for 1 h. Nylon mesh was used to filter the solution and it was then centrifuged. Supernatant was discarded and the pellet was resuspended in 10 ml of Hamilton buffer containing 0.15 % Triton and incubated for 30 min at 4°C. Following incubation the solution was centrifuged. The supernatant was discarded and the pellet again resuspended in 10 ml of Hamilton buffer containing 0.15 % Triton and centrifuged. The supernatant was removed and the pellet resuspended in 10 ml nuclease digestion buffer (50 mM Tris-HCL pH 8.0, 0.3 M Sucrose, 5 mM $MgCl_2$, 1.5 mM NaCl, 0.1 mM $CaCl_2$, 5 mM β-mercaptoethanol) and centrifuged. The supernatant was discarded and the pellet resuspended in 2 ml nuclease digestion buffer.

2.2.11.2a DNaseI treatment in Southern blotting approach

The 2 ml of suspension was aliquoted into 6 x 200 µl samples. To 5 of the 6 aliquots 5 U of DNaseI and the appropriate volume of DNaseI 10 x buffer (New England Biolabs (http://www.neb.com)) was added. To one of the DNaseI – treated samples, 40 µl of stop solution (0.5 M EDTA) was added, and the sample labelled 0. All samples were then incubated at 37 °C. At 5, 10, 20 and 30 min time-points, one of the DNase I – containing samples was removed and 40 µl stop buffer added before incubation at 4 °C. The aliquot with no DNaseI was removed at 30 min and 40 µl stop buffer added. This untreated samples was labelled U 30.

2.2.11.2b DNase I treatment in the qPCR approach

The 2 ml of suspension was aliquoted into 10 x 200 µl samples. To 9 of the 10 aliquots, 5 U of DNaseI and the appropriate volume of DNaseI 10 x buffer (New England Biolabs) was added. To one of the DNaseI – treated samples, 40 µl of stop solution (0.5 M EDTA) was added and labelled 0. All samples were then incubated at 37 °C. At 2, 4, 6, 8, 10, 15, 20 and 30 min time-points, one of the DNaseI – containing samples was removed and 40 µl stop buffer was added before incubation at 4 °C. The aliquot with no DNaseI was removed at 30 min and 40 µl stop buffer added. The untreated sample was labelled U 30.

2.2.11.3 DNA extraction and digestion

To each of the ten samples from the DNaseI treatment 120 µl dH_2O and 40 µl 10 % SDS was added. Samples were then incubated at 50 °C for 15 min. After this incubation, 132 µl of 5 M potassium acetate was applied to each sample. Tubes were then mixed by inversion and incubated on ice for 15 min. Samples were centrifuged for 15 min at 4 °C at 13000 rpm. A 500 µl aliquot of phenol chloroform (Sigma) was added to each sample. These were mixed and centrifuged for a further 15 min. The supernatant from each sample was removed to a new tube. A 1 ml aliquot of 96 % ethanol and 10 µg of yeast tRNA were added before incubation for 1 h at – 20 °C. Following a 15 min centrifugation, supernatants were removed and tubes centrifuged for a further 1 min. The residual supernatant in each tube was aspirated. Tubes were then left open at room temperature for a further 20 min. Each pellet was resuspended in 50 µl dH_2O and digested with NcoI. To each sample, 1µl of NcoI and 5 µl of NcoI buffer (New England Biolabs) was added. Tubes were incubated at 37 °C for 2 h. Digestion was stopped by incubation at 65 °C for 20 min.

2.2.11.4a Running gel and Southern blotting

Samples were run on a 0.7 % agarose gel (2.2.8.3 Agarose Gel electrophoresis) for approximately 1 h, or until the fragments were deemed to be sufficiently separated. The gel was then photographed and the marker lane removed. Following this, the gel was incubated at room temperature in ten gel volumes of 0.25 M HCl with gentle agitation for 15 min and then rinsed with dH_2O. For 45 min the gel was then soaked in ten gel volumes of denaturation solution (1.5 M NaCl, 0.5 M NaOH) at room temperature under gentle agitation. Following rinsing in dH_2O, the gel was soaked for 30 min at room temperature under gentle agitation in ten gel volumes of neutralisation buffer (1 M Tris-HCl pH 7.4, 1.5 M NaCl). This process was then repeated. As outlined by Southern, the apparatus was assembled to transfer the DNA. Hybond XL (Amersham biosciences (http://gelifesciences.com)) nylon membrane was used for the transfer and 10 x SSC solution (20 x SSC was prepared by adding 175.3 g NaCl and 88.2 g sodium citrate to 800 ml of dH_2O, the pH was adjusted to pH 7.0 with HCl and the volume was made up to 1 l with dH_2O) was used as the transfer buffer and the transfer was left to proceed for 12 h. The membrane was removed and DNA crosslinked using a UV sratalinker set to 1200 (Stratagene (http://www.genomics.agilent.com/)). Church buffer (1 % w/v bovine serum albumin, 1 mM EDTA 7 % w/v SDS, 0.5 M phosphate buffer) was prepared and incubated at 65 °C. The membrane was then incubated in 40 ml of church buffer in a pre-heated bottle, with rotation, for 4 h at 65 °C. The DNA probe for hybridisation was made by amplifying the region of interest via PCR, using genomic DNA as a template (2.2.8.1 DNA extraction from plant tissue, 2.2.8.2 PCR). Following gel electrophoresis, DNA fragments were extracted as described previously (2.2.8.3 Agarose Gel electrophoresis, 2.2.8.4.1 Gel Extraction of DNA). The DNA probe was

then quantified using a spectrophotometer (Ultrospec 4300 pro Amersham biosciences) and 10 ng labelled with ^{32}P using the Rediprime II random primer labelling kit (GE healthcare (http://gehealthcare.com)). The membrane was incubated in 15 ml of fresh church buffer and radio-labelled probe for 24 h at 65 °C, with rotation. Following incubation, the membrane was washed in 30 ml 3 x SSC, 0.1 % SDS at 65 °C for 15 min. This was repeated before washing the membrane in 1 x SSC 0.1 % SDS in the same conditions. The membrane was then monitored for radioactivity with a Geiger counter and if the radiation level was approximately 10 – 30 counts per min then it was developed. If the radiation level was higher than this the membrane was washed again. Washed membranes were transferred to a phosphor plate (GE Healthcare) and left for 12 h before analysis using Image Quant Software (http://www.gelifesciences.com).

2.2.11.4b qPCR of DNaseI treated material

Alternatively to the Southern blotting method, a qPCR based method was used. Following NcoI digestion, DNA was quantified using a Qubit fluorometer (invitrogen), in accordance with the manufacturer's instructions. Samples containing 0.1µg of DNA were made up to 100 µl and used as a template for qPCR reactions (2.2.9.3 qPCR).

2.2.12 Chromatin Immunoprecipitation (ChIP)

2.2.12.1 Cross-linking

A total of 1.5 – 4 g of plant tissue was harvested for each treatment and placed in a 50 ml Falcon tube. Seedlings were then rinsed twice with dH_2O, whilst trying to ensure as much soil as possible had been removed from the plant tissue. Any remaining dH_2O was removed and 37 ml of 1 % formaldehyde was added. Nylon mesh was placed in the tube above the seedlings and small holes cut in the lid. Falcon tubes containing plant tissue were then placed in an exsiccator for 0 – 10 min to draw formaldehyde into the cells. Following this process, 2.5 ml of 2 M glycine was added and each tube returned to the exsiccator for 5 min. Liquid was then removed and the seedlings rinsed twice in 40 ml of dH_2O. At this stage, the plant tissue was removed from the falcon tube and excess water removed using blue kitchen roll. Fixed material was frozen in liquid nitrogen and stored at - 80 °C.

2.2.12.2 Isolation of chromatin-DNA complexes

Liquid nitrogen was poured into a mortar and the cross-linked plant material added. Tissue was ground with a pestle until a fine green/white powder. This was then transferred to a pre-cooled mortar, 30 ml of extraction buffer 1 (0.4 M sucrose, 10 mM Tris-HCl pH 8.0, 10 mM $MgCl_2$, 5 mM β-mercaptoethanol, 1 protease inhibitor tablet (Roche (http://www.roche.com)) per 10ml of buffer) was added before further grinding. Samples were twice filtered into a Falcon tube using a nylon mesh. These were then centrifuged for 20 min at 4000 rpm at 4 °C. Supernatants were decanted and pellets resuspended in 1 ml of extraction buffer 2 (0.25 M sucrose, 10 mM Tris-HCl pH 8.0, 10 mM $MgCl_2$, 5 mM β-mercaptoethanol, 1 complete mini protease inhibitor cocktail tablet per 10 ml of buffer). Following centrifugation (10 min, 1300 rpm, 4°C), supernatants were removed and the pellets resuspended in 300 µl of extraction buffer 2. To a separate, fresh, eppendorf tube, 300 µl of extraction buffer 3 (1.7 M sucrose, 10 mM Tris-HCl pH 8.0, 2 mM $MgCl_2$, 0.15 % Triton X-100, 5 mM β-mercaptoethanol, 1 protease inhibitor tablet per 10 ml of buffer) was added and the resuspended pellet slowly and carefully pipette layered on the top. This was then centrifuged for 1 h at 13000 rpm at 4°C. Following centrifugation, supernatants were removed and pellets resuspended in 500 µl of nuclei lysis buffer (50 mM Tris-HCl pH 8.0, 10 mM EDTA, 1 % SDS, 1 protease inhibitor tablet per 10 ml of solution) pre-cooled to 4 °C.

2.2.12.2a Sonication using Soniprep 150 MSE

A 10 µl aliquot chromatin solution was removed. This was labelled un-sonicated and stored at – 20 °C. The remaining solution was sonicated on wet ice using a Soniprep 150 MSE (http://wolflabs.co.uk) for the appropriate time (10 s), amplitude and frequency (6 pulses). Samples were then centrifuged for 10 min at 13000 rpm at 4 °C and the supernatants transferred to a fresh tube. The supernatant were then centrifuged again for 10 min at 13000 rpm at 4 °C and supernatants collected. A 10 µl sample was removed from the supernatant and labelled sonicated. The un-sonicated and sonicated samples were run on a 1.5 % agarose gel for analysis (2.2.8.3 Agarose Gel electrophoresis).

2.2.12.2b Sonication using Bioruptor

A 10 µl aliquot of chromatin solution was first removed. This was labelled un-sonicated and stored at – 20 °C. The remaining solution was transferred to a Birouptor tube and stored on wet ice before sonication in a Diagenode Bioruptor (http//www.diagenode.com) at medium setting for 30 s. Each sonication treatment was followed by 30 s rest. The number of cycles varied between experiments but was approximately 12. The samples were centrifuged for 10 min at 13000 rpm at 4 °C and the supernatant removed to a fresh eppendorf tube. These were labelled isolated chromatin. Following further centrifugation, residual supernatants were removed and added to the isolated chromatin tubes and pellets discarded. A 10 µl sample was removed from each supernatant and labelled sonicated. The un-sonicated and sonicated samples were run on a 1.5 % agarose gel for analysis (2.2.8.3 Agarose Gel electrophoresis).

2.2.12.3 Immunoprecipitation

2.2.12.3.1 Bead preparation

An aliquot of 50 µl of protein A or G, agarose or magnetic beads, were transferred to fresh eppendorf tubes. A 1 ml sample of ChIP dilution buffer (1.1 % Triton X-100, 1.2 mM EDTA, 16.7 mM Tris-HCl pH 8.0, 167 mM NaCl) was added to each aliquot of beads and tubes placed on a moving platform for 5 min at room temperature. For agarose beads, tubes were centrifuged for 30 s at 4000 rpm at 4 °C. Supernatants were removed carefully to ensure no bead contamination. For magnetic beads, tubes were placed in a magnetic rack and left for 1 min before the supernatant was removed. This washing process was repeated a further 2 times. The beads were then resuspended in 100 µl of ChIP dilution buffer.

2.2.12.3.2 Pre-clearing

Sonicated chromatin was diluted with ChIP dilution buffer to make a 10 x dilution. Each of these aliquots were added to a separate tube of pre-cleared beads (2.2.8.3.1 Bead preparation). These were incubated with and rotated at 4 °C for 1 h. Samples containing agarose beads were centrifuged for 30 s at 4000 rpm at 4 °C. Samples containing magnetic beads were transferred to a magnetic rack and left for 1 min. Supernatants were carefully transferred to a fresh tube.

2.2.12.3.3 Formation of immune complexes

A chromatin sample from (2.2.12.3.2 Preclearing) was stored at – 20 °C as the input control. For each desired antibody immunoprecipitation (IP) reaction, the appropriate quantity of antibody was added (2.2.12.3.5 Details of antibodies used). The tubes were incubated and rotated at 4 °C for 12 h.

2.2.12.3.4 Formation of bead-immune complexes

Fresh beads were prepared as outlined in 2.2.12.3.1. To each of the aliquots of prepared beads an IP reaction from 2.2.12.3.3 was added. These were rotated and incubated for the appropriate time (1 h) at 4 °C.

2.2.12.3.5 Details of antibodies used

Name	Lot Number	Type	Company	Dilution Used	Beads Used
Anti-acetyl-Histone H3	DAM1513997	Rabbit Polyclonal	Millipore	1:30	Magnetic A (Invitrogen)
Anti-Histone H3	DAM1581033	Rabbit Polyclonal	Millipore	1:20	Magnetic A (Invitrogen)
Anti-dimetyl-Histone H3 (Lys4)	DAM1503382	Rabbit Polyclonal	Millipore	1:20	Magnetic A (Invitrogen)
Acetyl-Histone H3 (K9)	YE-12-17-01	Rabbit Monoclonal	Epitomics	1:40	Magnetic A (Invitrogen)

2.2.12.4 Washing

Tubes from 2.2.12.3.4 were centrifuged at 4000 rpm for 30 s at 4 °C (in the case of agarose beads) or were transferred to a magnetic rack (in the case of magnetic beads). Supernatants were aspirated and discarded (the agarose and magnetic beads were always prepared in this way in all of the following washes, prior to aspiration). Each IP pellet was resuspended in 1 ml of low salt wash buffer (150 mM NaCl, 0.1 % SDS, 1 % Triton X-100, 2 mM EDTA, 20 mM Tris-HCl pH 8.0) and incubated at 4 °C for 5 min with rotation. Supernatants were aspirated and the low salt wash repeated. This procedure was then repeated using high salt wash buffer (500 mM NaCl, 0.1 % SDS, 1 % Triton X-100, 2 mM EDTA, 20 mM Tris-HCl pH 8.0) twice. The beads were then washed in LiCl wash buffer (0.25 M LiCl, 1 % nonidet p-40, 1 % sodium deoxycholate, 1 mM EDTA, 10 mM Tris-HCl pH 8.0). This was finally repeated with TE buffer (10 mM Tris-HCl pH 8.0, 1 mM EDTA) twice.

2.2.12.5a DNA extraction using NaCl

A 250 µl sample of elution buffer (1 % SDS, 0.1 M $NaHCO_3$) was added to each IP. These were vortexed briefly and incubated at 65 °C for 15 min. Supernatants were removed and transferred to a fresh tube. Pellets were again washed in elution buffer and the supernatants from both washes pooled. At this stage, 480 µl of elution buffer was added to the input sample (20 µl). To each of the IPs and the input control sample, 20 µl of NaCl was added. Reactions were incubated at 65 °C for 12 h.

The following reagents were added to all IPs and the input control: 10 µl of 0.5 M EDTA, 20 µl 1 M Tris-HCl pH 6.5 and 1µl of 20 mg/ml poteinase K. All were then incubated for 1 h at 45 °C. A 500 µl of phenol-chloroform was then added before centrifugation at 13000 rpm for 15 min at 4 °C. The supernatant from each reaction was removed and transferred to a fresh eppendorf tube. A 1/10 volume of 3 M NaOAc pH 5.2, 3 volumes of absolute ethanol and 4 µl of glycogen was then added to each reaction and they were incubated for at least an hour at – 20 °C. DNA was precipitated by centrifugation at 13000 rpm for 15 min at 4 °C. Pellets were re-suspended in 1 ml of 70 % ethanol and centrifuged. Supernatants were discarded and pellets air-dried before re-suspension in 50 µl of 10 mM Tris-HCl pH 7.5. Samples were then analysed by qPCR reaction (2.2.9.3 qPCR) to determine if there was any enrichment of target sequences between treatments.

2.2.12.5b Chelex extraction

Residual TE was removed from IPs and 100µl of 10% Chelex (BioRad (http://bio-rad.com)) added to each sample. Chelex was added to bind ions and thus prevent ion-dependent enzymes from degrading the DNA. Samples were vortexed and incubated in a boiling water bath for 10 min. Samples were cooled and 1µl of 20 mg/ml proteinase K added before incubation at 50°C for 30 min. Samples were returned to the boiling water bath for a further 10 min before a 5 min centrifugation at room temperature at 13000 rpm. Supernatant were removed and a 100 µl aliquot of TE added to each sample tube. These were vortexed and centrifuged at 13000 rpm for 5 minutes. Supernatant were pooled and analysed by qPCR reaction (2.2.9.3 qPCR) to determine if there was any enrichment of target sequences between treatments.

2.2.13 TSA experiment

Seedlings were sown (2.2.1 Plant growth conditions) on LE (2.1.2 Plant growth media) plates and grown for 14 days in 16 h light/ 8 h dark cycles. On day 15 seedlings were removed from the plates and their roots excised for efficient chemical uptake. Half were placed in petri dishes (root side down) containing 10 μM Trichostatin A (TSA) (Sigma). TSA was purchased in a powder form and was dissolved in dimethyl sulfoxide (DMSO) diluted in 20 mM MES buffer. The other half were placed in petri dishes (root side down) containing 20 mM MES buffer-DMSO. Following a 1 hour incubation period, half of the seedlings were transferred to low R:FR conditions. Samples of the seedlings in both high and low R:FR were then removed at designated time points, excess solution removed with tissue paper, and frozen at – 80 °C. The RNA was extracted, converted to cDNA and analysed by qPCR (2.2.9)

2.2.14 Primer table

Primer Name	Sequence
ATHB2 promoter probe F	5' CACGACTCAACGATCTAACCAA
ATHB2 promoter probe R	5' GAGGAACGAAGAAAGCGATG
ATHB2 coding probe F	5' CACAGATCCACAAGGCTCAA
ATHB2 coding probe R	5' TTGTAGCCGACGGTTCTCTT
XTH15 promoter probe F	5' GCTCGAGGTATGATGGGTGT
XTH15 promoter probe R	5' AGAAGAACAGTCGCCACGAT
XTH15 coding probe F	5' TGGCGACTGTTCTTCTTGTG
XTH15 coding probe R	5' GAGCCTTGGACCAGTCAGTC
GAT SHL RNAi Central F	5' ACAAAAAAGCAGGCTGCCGATACGATTGAAGGAAA
GAT SHL RNAi Central R	5' ACAAGAAAGCTGGGTTCAGAACACTCCTCGCATTG
GAT SHL RNAi N F	5' ACAAAAAAGCAGGCTGCAAAAAGCTCCAAGGAAGC
GAT SHL RNAi N R	5' ACAAGAAAGCTGGGTAGGATGAAACCACTCAGAACACTC
GAT SHL RNAi C F	5' ACAAAAAAGCAGGCTCGTCGTACGTAGCGAGGGTA
GAT SHL RNAi C R	5' ACAAGAAAGCTGGGTTGTTCTTCGATTTAGTTACCTCCAG
GAT SHL OVER F	5' ACAAAAAAGCAGGCTATGCCCAAGCAAAAAGCTCC
GAT SHL OVER R	5' ACAAGAAAGCTGGGTTTAACCTGGTCGCTTAGTG
GAT GCN5 OVER F	5' ACAAAAAAGCAGGCTATGGACTCTCACTCTTCCCAA
GAT GCN5 OVER R	5' ACAAGAAAGCTGGGTCTATTGAGATTTAGCACCAG
GAT HD1 OVER F	5' ACAAAAAAGCAGGCTATGGATACTGGCGGCAATTC
GAT HD1 OVER R	5' ACAAGAAAGCTGGGTTTATGTTTTAGGAGGAAACG
GAT ADAPTOR F	5' GGGGACAAGTTTGTACAAAAAAGCAGGCT

GAT ADAPTOR R	5' GGGGACCACTTTGTACAAGAAAGCTGGGT
HD1 OVER F	5' GGCCCGGGATGGATACTGGCGGCAATTCG
HD1 OVER R	5' GCGGTACCTTATGTTTTAGGAGGAAACG
GCN5 OVER F	5'CGCCCGGGATGGACTCTCACTCTTCC
GCN5 OVER R	5'CGCCCGGGCTATTGAGATTTAGCACC
SHL OVER F	5' GGGGTACCATGCCCAAGCAAAAAGC
SHL OVER R	5'CGGAGCTC TTAACCTGGTCGTTAGTG
ATHB2 UPF1	5' TCAACATCCTCATTAACATCATCA
ATHB2 UPF2	5' AAGTGTGCAACAAGCGTGAC
ATHB2 UPR1	5' GGTCGACCGCATGAGTTTTA
ATHB2 UPR2	5' CATGAACAATTGCACATCCA
ATHB2 UPF3	5' GATGATACTCTCTCAACAT
ATHB2 UPR3	5' CGCATGGGTCGACCGCATGAG
ATHB2 F1	5' TGTTCTCGCCTTATGAATATCCT
CHIP ATHB2 F1	5' GTTCAACAGAAGATGATGTTCG
CHIP ATHB2 F2	5' ATGCAGTTCCAAACTCAGATTCG
CHIP ATHB2 F3	5' CAGATCCACAAGGCTCAAGAGG
CHIP ATHB2 F1.1	5' GCTAGTCACATACTCATGATTGC
ATHB2 R1	5' TGCTTCTTTGTCCCCCTCTA
CHIP ATHB2 R1	5' GAAGGAGTAACAGAAACAGATGG
CHIP ATHB2 R2	5' CTCTCGTTCCATGAAGATCTTCTG
CHIP ATHB2 R3	5' GGATTGAGAGTACTGTGATC
CHIP ATHB2 R1.1	5' GATAGAAGATGAGAAAGTAAAGG
ATHB2 INTERNAL F	5'CGGAGGTAGACTGCGAGTTC

ATHB2 INTERNAL R	5'GAAGGGCACATGGTCAAAGT
PIL1 UPF1	5'GGTCACAATTCGATATCAATCG
PIL1 UPF1.1	5'GCCTAATTGTGGGTCCCATT
PIL1 UPF2	5'CGTCTCTCTCGCATGTCACTC
PIL UPF3	5'GGAGCGGTGGAGAGTAGAGAAG
CHIP PIL1 F1	5'TGCCAATGGGTCATTACTCTC
CHIP PIL1 F2	5'GGACCAAAACAAATCCTCCATA
CHIP PIL1 F3	5'GCAACGTAGGCAATCTCTCC
CHIP PIL F1.1	5'CCTCCTGATGAGCAATCTGCAGC
CHIP PIL1 F2.1	5'CGTGCTTTGCAGGACCTACTACC
CHIP PIL1 F3.1	5' CCTTGATTCTTGGAACG
PIL1 UPR1	5' CCTCTGTGATTTGAGATCTC
PIL1 UPR1.1	5' CATGCGAGAGAGACGGGCAC
PIL1 UPR2	5' GCGTCCAACTGAACTTAC
PIL UPR3	5' GAAGCAAGATAATGTATGGG
CHIP PIL1 R1	5' AGCTTAGCATTTGTGGTGGTG
CHIP PIL1 R2	5' GATTCGGACTTCACACTTTGGT
CHIP PIL1 R3	5' TCACCGGAACAACTTGTGTG
CHIP PIL R1.1	5' GATCTCTCGAAGTTCCTCGAG
CHIP PIL1 R2.1	5' CCTCATCCAACAATGAAGCCT
CHIP PIL1 R3.1	5' GCAATTGCACGTCCTCTAC
XTH15 UPF1	5' TTCCATTACAATTTCCAAATG
XTH15 UPR1	5' ATTTGACATCCCCAAGATGC
ACTIN2 F	5' TCAGATGCCCAGAAGTCTTGTTCC

ACTIN2 R	5' CCGTACAGATCCTTCCTGATATCC
QPCR PIF3 F	5' AACAGAGACAGACGAAGTGTGCAG
QPCR PIF3 R	5' AGAGAAGAGAGTTGGAGCATGGTG

Chapter 3: Results

The effect of low R:FR on chromatin structure

3.1 The effect of low R:FR ratio on chromatin structure

A number of studies in plants have suggested that environmental signals, such as light and temperature, can regulate transcriptional profiles via changes in chromatin structure and histone modifications. Histone modifications around the *FLC* gene have been shown by multiple groups to be regulated by vernalization (eg. Bastow *et al.*, 2004). Furthermore, Kumar and Wigge (2010) have shown that changes in temperature can regulate which histone subtypes are present at temperature regulated genes. With regards to light signalling, Guo *et al* (2008) have shown that light can directly influence the presence of specific histone modifications on a number of genes during seedling de-etiolation. Moreover, the blue light photoreceptor cry2 has been shown to be involved in large scale chromatin compaction in rosette leaves during floral transition (Tessadori *et al.*, 2007). Analysis of natural genetic variation in 21 *Arabidopsis* accessions has also recently identified phyB as a potential positive regulator of chromatin compaction during reductions in light quantity by spectrally neutral shading (Tessadori *et al.*, 2009). There is currently, however, no information as to whether low R:FR signals can elicit changes in chromatin structure around specific genes. Chua and colleagues have previously observed differences in chromatin structure around the promoter of the pea platocyanion gene *PetE* in etiolated and de-etiolated photosynthetic tissues. DNaseI and micrococcal nuclease accessibility assays revealed differences in chromatin structure

and ChIP revealed differences in acetylation states of histones between tissue types (Chua *et al.*, 2001).

In attempt to determine whether R:FR ratio can regulate chromatin structure, in the form of chromatin remodelling, the DNaseI sensitivity of a number of shade avoidance genes in response to a low R:FR signal was investigated.

3.2 DNaseI sensitivity assays

3.2.1 Southern Blotting Approach

The aim of this part of the project was to determine if there are changes in chromatin structure around R:FR-regulated genes in response to changes in R:FR. The promoter and coding regions of *ATHB2* and *XTH15*, both known to be up-regulated in response to low R:FR, were used as probes to examine changes in chromatin structure around these two genes.

Briefly, the DNaseI sensitivity assay entailed grinding 5g of plant tissue for each light treatment. Nuclei were isolated, lysed and treated with DNaseI. The DNA was then purified from the proteins of the cells and run on an agarose gel. This was transferred to a membrane which was exposed to a radioactively labelled probe. It was hypothesised that alterations in chromatin structure would alter nuclease accessibility, thereby resulting in different banding patterns on Southern blots.

3.2.1.1 Making DNA probes

WT *Arabidopsis* plants of the accession Columbia (Col) were grown on soil for 4 weeks in long days (LD: 16 h W and 8 h dark) in high R:FR (2.7). DNA was extracted from the plant tissue and was used as a template to produce southern blotting probes. Using this DNA four sets of primers: *ATHB2* promoter probe F + *ATHB2* promoter probe R; *ATHB2* coding probe F + *ATHB2* coding probe R; *XTH15* promoter probe F + *XTH15* promoter probe R; and *XTH15* coding probe F + *XTH15* coding probe R (2.2.13, Primer table) were used in a PCR reaction to amplify the DNA fragments termed respectively: *ATHB2* promoter probe, *ATHB2* coding probe, *XTH15* promoter probe and *XTH15* coding probe (primers and genomic regions to which they are designed are shown in supplementary data, figures S1.1, for *ATHB2* and S1.2 for *XTH15*). The four PCR reactions were run on a 1 % agarose gel and the products visualised (Figure 3.1) to confirm their correct size before gel extraction. The extracted DNA was run on a 1 % agarose gel and visualised (Figure 3.2) to confirm successful extraction. The DNA was quantified using a spectrophotometer.

3.2.1.2 Plant growth conditions

Col plants were grown on soil for 3 weeks in continuous W in high R:FR. On the 20th day half of the plants were transferred to low R:FR (0.1) for 24 hours and the other half were maintained in high R:FR (2.7). The plant tissue was harvested, transferred to liquid nitrogen and stored at - 80°C. The results of the DNaseI sensitivity assays using the Southern blotting approach are shown in figures 3.3 – 3.6.

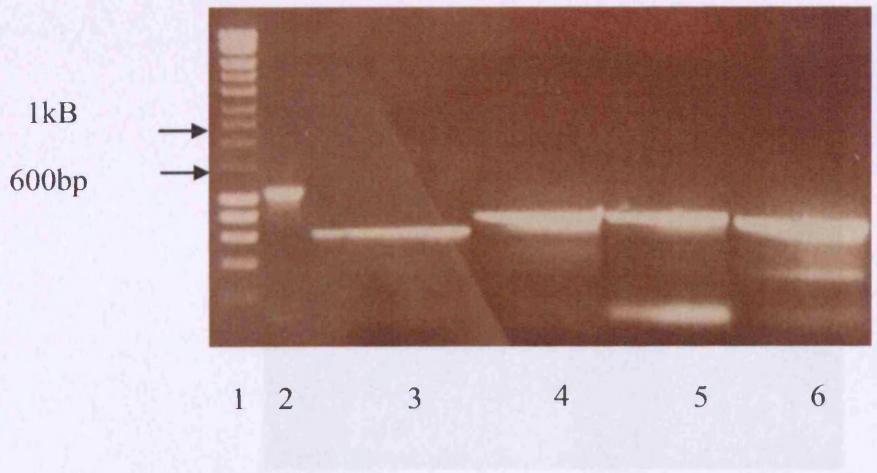

Figure 3.1: PCR reactions amplifying the four DNaseI probes run on an agarose gel. Lane 1 is Hyperladder I, lane 2 is a positive control, lane 3 is the *ATHB2* coding region, lane 4 is the *ATHB2* promoter region, lane 5 is the *XTH15* coding region and lane 6 is the *XTH15* promoter region. All bands are the appropriate size (for lanes 3–6, the top band in each well represents the correct band) (sizes shown in S1.1). The four probe lanes were gel extracted (2.2.8.4.1 Gel Extraction of DNA).

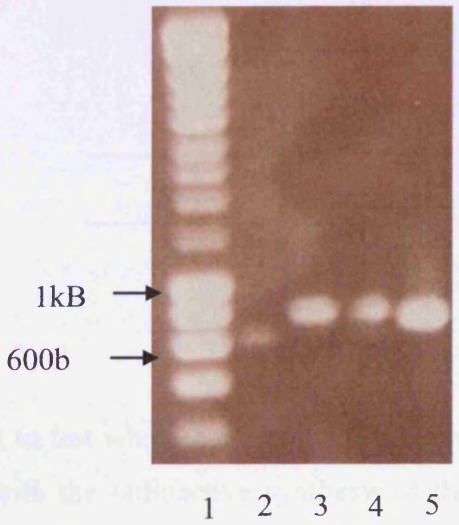

Figure 3.2: Samples of the gel extracted probes run on an agarose gel. Lane 1 is Hyperladder I, lane 2 is the *ATHB2* coding region, lane 3 is the *ATHB2* promoter region, lane 4 is the *XTH15* coding region and lane 5 is the *XTH15* promoter region.

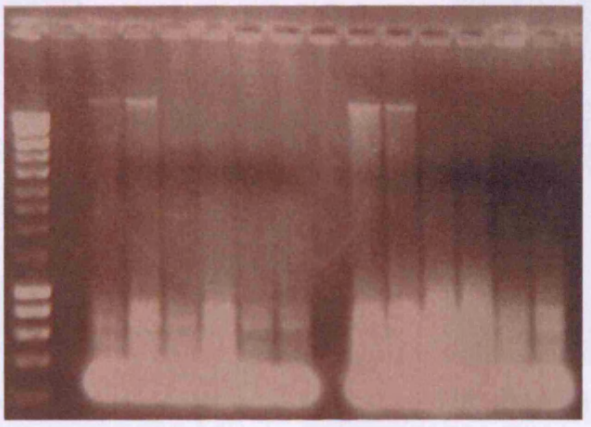

1 High Low

Figure 3.3: An example of DNaseI treated genomic DNA run on an agarose gel. Lane 1 is hyperladder 1. High indicates a high R:FR treatment and Low indicates a low R:FR treatment. Both the high and low treatments are made up of 6 lanes of DNA which represent from left to right: 0, untreated, 5, 10, 20 and 30; with the number representing length of DNaseI treatment (min).

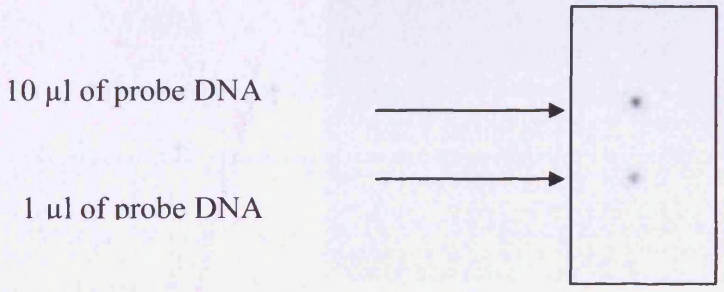

Figure 3.4: A dot blot to test whether the probe can hybridize to itself and to check that there is no problem with the radioactive synthesis of the probe. The probe DNA was spotted onto the membrane at various concentrations and then probed with the same radioactive probe. The dot blots were performed with the *ATHB2* coding and *XTH15* promoter probes on both old and new membranes. All of the four dot blots worked and produced spots. Shown is the dot blot for the *XTH15* promoter probe on the new membrane, probe DNA was at a concentration of 160 ng/µl

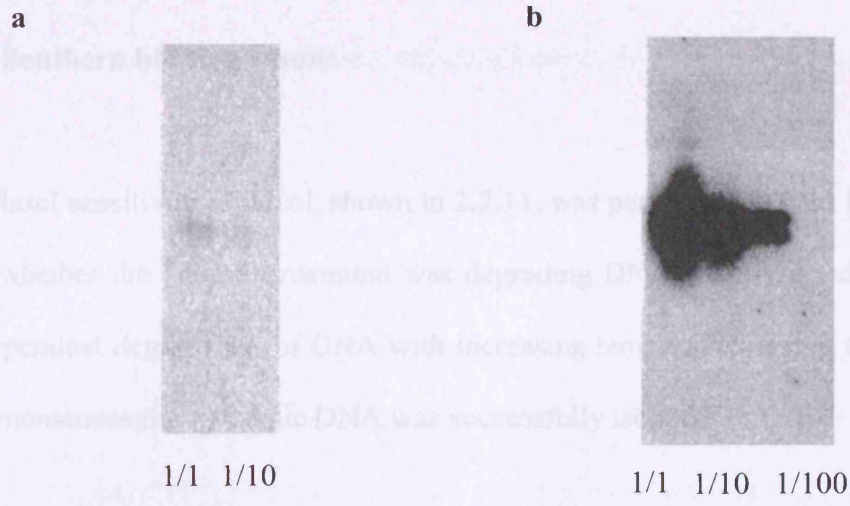

Figure 3.5: A blot to test whether there is any problem in transferring the DNA from the agarose gel to the membrane. Probe was run on an agarose gel in 10 fold dilutions and southern blotted to the membrane and then probed with a radioactive version of the same probe. **Figure 3a**: *XTH15* promoter probe. **Figure 3b**: *XTH15* coding probe.

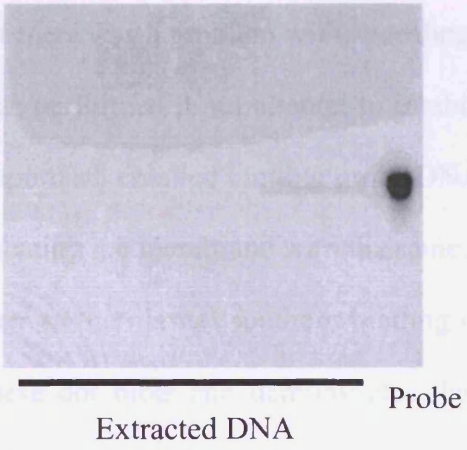

Figure 3.6: A DNaseI sensitivity assay to test whether sufficient DNA is being loaded onto the gel. Three times the amount of DNA from high and low R:FR ratio treated plants that was used in the original assay was used in this assay. A sample of the *XTH15* promoter probe was run as a control, labelled probe. The blot was probed with the *XTH15* promoter probe. The lane producing the band corresponds to where the *XTH15* promoter probe control was run

3.2.1.3 Southern blotting results

The DNaseI sensitivity protocol, shown in 2.2.11, was performed to gain familiarity and to test whether the DNaseI treatment was degrading DNA. Figure 3.3 demonstrates a time-dependent degradation of DNA with increasing temporal exposure to DNaseI and also demonstrates that genomic DNA was successfully isolated.

Following the confirmation of probe production and that DNaseI was degrading DNA in a time dependent manner, the complete southern blotting protocol was performed. Unfortunately, no bands were detected on the blot. All four probes were tested and no bands were produced on any of the blots.

One proposition was that there was a problem with annealing or radioactive labelling of the probe. A dot blot was performed in an attempt to establish whether the probe was the problem. A dot blot approach entailed blotting probe DNA directly onto the Hybond membrane and then incubating the membrane with the same, but radioactively labelled, probe in the same manner as the normal southern blotting protocol. Figure 3.4 shows the results of one of these dot blots and demonstrates that the probe is both being radioactively labelled and is annealing.

A further potential problem could be that the DNA was not being successfully transferred from the gel to the membrane. To test if this was the case, probe DNA was run on an agarose gel, as DNaseI-treated genomic DNA would be, and was Southern blotted and probed as in the normal protocol. This procedure produced a clear banding

pattern, shown in figure 3.5, which suggests that there is no problem in transferring DNA from the gel to the membrane.

The next proposal was that insufficient genomic DNA was transferring to the membrane. To test if this was the case, three times the amount of starting tissue outlined in 2.2.11 was used in the protocol. However, figure 3.6 demonstrates that no banding pattern was present.

It could still be that insufficient DNA was being transferred to the membrane; however, following the repeated failures of the Southern blotting approach, an alternative approach was sought.

3.2.2 qPCR approach

It was considered that a qPCR based approach could be used as an alternative to Southern blotting. This procedure would involve performing a time-course of genomic DNA degradation upon exposure to DNaseI and then utilizing qPCR to determine the degree of degradation of DNA. qPCR gives an accurate readout of the DNA template concentration of a given sample, in the form of a cycle time (Ct value). If primers are designed against a region which demonstrates differential sensitivity to DNaseI then a qPCR based approach can be used to detect for degradation of DNA by DNaseI. As DNA comprising the region of interest is progressively degraded by DNaseI there will be less template which can be amplified in the qPCR reaction and this will give a readout of less starting template (a higher Ct value). An important aspect of this procedure is that the total amount of genomic DNA is accurately quantified; otherwise, ascribing differences in Ct values to changes in DNaseI accessibility will be almost impossible. Two different strategies were employed to assess the quantity of DNA present. Firstly, a Qubit fluorometer was used to quantify the DNA and these values were used to load equal quantities of DNA onto the qPCR. Secondly, internal control primers were used. If primers designed against regions of genes thought not to be remodelled show the same Ct values for the same time points in both high and low R:FR treatments, then it will suggest that the DNA has been accurately quantified.

3.2.2.1 Plant growth conditions

Two different light treatments were used in the investigation, one with growth in light dark cycles (LD) and the other in continuous light. *Arabidopsis* Col seedlings were used in both light treatments Seedlings grown in LD cycles were grown at 22°C in high R:FR for 21 days and then at dawn of the 21st day, half were transferred to low R:FR and half maintained in high R:FR. Whole shoots were harvested four hours later. This treatment was designed to co-incide with maximum seedling gene expression response to low R:FR (Salter *et al.*, 2003; Lorrain *et al.*, 2008). Seedlings grown in continuous light were grown at 22°C in high R:FR for 20 days, whereupon half were transferred to low R:FR and half maintained in high R:FR. Whole shoots were harvested 24 h later. This treatment was designed to co-incide with high levels of shade avoidance gene expression in continuous light (Franklin and Whitelam 2007). All harvested plant material was transferred to liquid nitrogen and stored at - 80°C.

3.2.2.2 Primer design

Primers were designed against the R:FR-regulated genes *ATHB2*, *XTH15* and *PIL1*. Additionally, primers were designed against *PIF3*, which is light - regulated and closely related to *PIL1* (Toledo-Oritz *et al.,* 2003) but is not regulated by R:FR ratio, thereby providing a control (Salter *et al.*, 2003).

Chua *et al* (2001) found that light treatments regulated the expression of transcript of the pea plastocyanin gene (PetE) gene and that this difference in expression was associated with difference in DNaseI sensitivity. They found that regions upstream of the ATG were more susceptible to degradation by DNaseI and micrococcal nuclease when the transcript was more highly expressed; whereas, there was no difference in sensitivity to DNaseI and micrococcal nuclease in the coding region (Chua *et al.,* 2001). Taking this into consideration, primers were designed against coding regions and upstream/promoter regions of genes. Three R:FR regulated genes were focused upon: *ATHB2, PIL1* and *XTH15*. The promoter region of a gene is often not clearly defined or determined; however, a suitably sized region upstream of the start codon had to be selected to focus the primer design upon. A region comprising up to 2kb upstream of the start codon was considered a suitably large region to encompass a number, if not all of a genes promoter elements. The reasoning was that this region should represent docking sites for transcription factors, cofactors, or any other trans acting factor involved in gene transcription and binding of these factors may require or result in local remodelling of the chromatin. Once the light responsive elements had been identified, primer pairs were designed to encompass these elements. The design of primers was constrained by the AT rich nature of promoter elements and by the fact that pairs of

qPCR primers should optimally produce a product of approximately 70 – 200bp. All primers were designed by eye. All primers used in were tested to ensure that they produced a distinct, unique melting curve, with a single peak, thereby confirming that a single PCR product had been produced.

3.2.2.3 Confirming up-regulation of R:FR-regulated gene transcription

Before the DNaseI sensitivity experiments were conducted, a portion of the harvested tissue was removed and used to test the transcript levels of a number of R:FR regulated genes. The purpose of this experiment was to confirm that the R:FR treatment was resulting in a change in gene transcription of R:FR-regulated genes. If no change in transcript levels of these genes was observed, then a change in chromatin structure would not be expected.

3.2.2.4 Data representation

The qPCR approach produces a Ct for each sample. These Ct values represent the amount of DNA template present in each reaction. For each sample, data was normalised to sample time 0 of the high R:FR treatment. Data is therefore represented as relative amount of PCR product on the X axis of graphs and this is plotted against time of DNaseI treatment (min). The slope of each graph is a measure of the rate of DNaseI-mediated degradation of target sequences. The steeper the slope, the lower the amount of template and the faster the rate of target sequence degradation by DNaseI. It is hypothesised that if a sequence has a more open chromatin structure, it will show a faster rate of DNA degradation.

Low

High

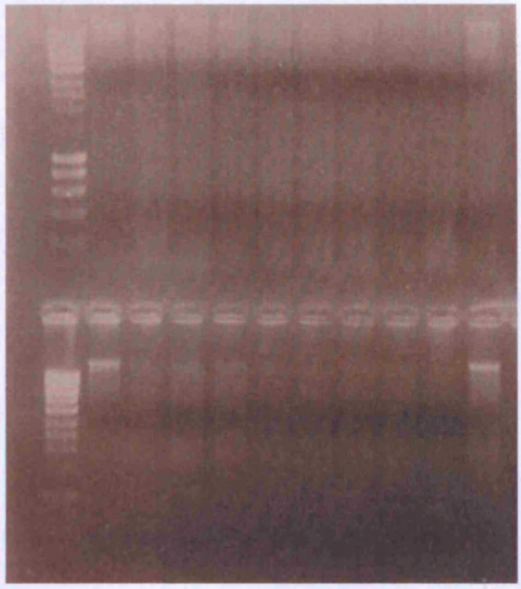

Figure 3.7: DNaseI-treated genomic DNA run on an agarose gel. Numbers represent the treatment time in minutes with DNaseI. U stands for untreated. Top is Low R:FR treatment, bottom is High R:FR treatment. From left to right the lane order is; hyperladder I. 0. 2. 4. 6. 8. 10. 15. 20. 30. U30.

Figure 3.7 shows the typical degradation pattern of the DNA samples after treatment with DNaseI. Samples were taken at slightly different intervals in the qPCR-based approach, compared to the southern blotting approach (figure 3.3). The reason for this was to provide more early time-points, which preliminary results suggested were important as the DNaseI reaction could proceed very quickly. The bands at the top of the gel indicate genomic DNA. This genomic band of genomic DNA can be seen to become progressively fainter as exposure to DNaseI increases, indicating that DNaseI is cutting the DNA.

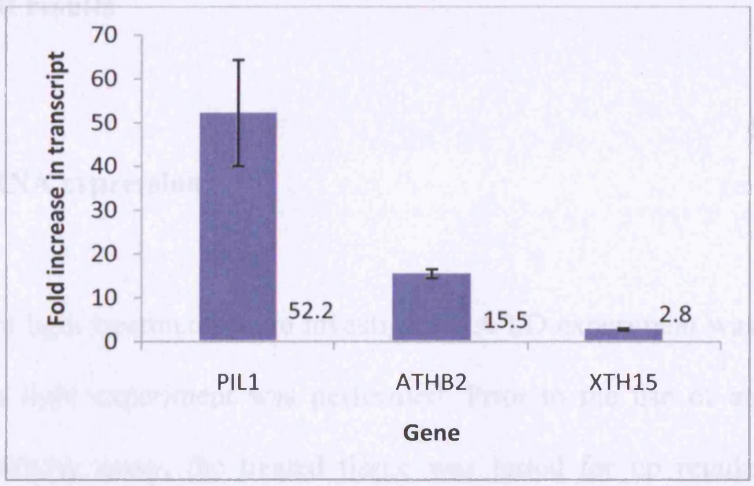

Figure 3.8: Fold increases in transcript abundance for *PIL1*, *ATHB2* and *XTH15* in response to a 4 h, low R:FR ratio treatment. Data are relative to high R:FR controls and are normalised to *ACTIN2*. Data represent mean values from three separate biological repeats. All plant tissue was grown in LD and harvested at 4 h after dawn.

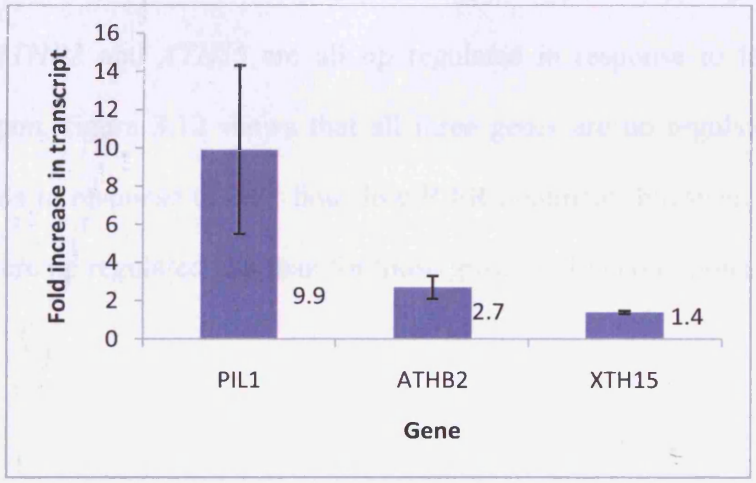

Figure 3.9: Fold increases in transcript abundance for *PIL1*, *ATHB2* and *XTH15* in response to a 24 h, low R:FR ratio treatment. Data are relative to high R:FR controls and are normalised to *ACTIN2*. Data represent mean values from two separate biological repeats. All plant tissue was grown in continuous light and harvested at 24 h after commencement of low R:FR ratio treatment.

3.2.2.5 qPCR results

3.2.2.5.1 mRNA expression

Two different light treatments were investigated. A LD experiment was performed and a continuous light experiment was performed. Prior to the use of any tissue in the DNaseI sensitivity assay, the treated tissue was tested for up regulation of mRNA expression of low R:FR regulated genes in response to the low R:FR ratio treatment. The rationale for this was that a restructuring of chromatin and hence a change in DNaseI sensitivity would not be expected without an increase in transcription. Figures 3.8 and 3.9 show the change in transcript of three R:FR regulated genes in response to low R:FR ratio for LD and constant light conditions respectively. Figure 3.11 shows that *PIL11, ATHB2* and *XTH15* are all up regulated in response to low R:FR ratio treatment. Again, figure 3.12 shows that all three genes are up regulated in constant light conditions in response to a 24 hour low R:FR treatment; however, *PIL1, ATHB2* and *XTH15* were up regulated less than for those grown in LD conditions.

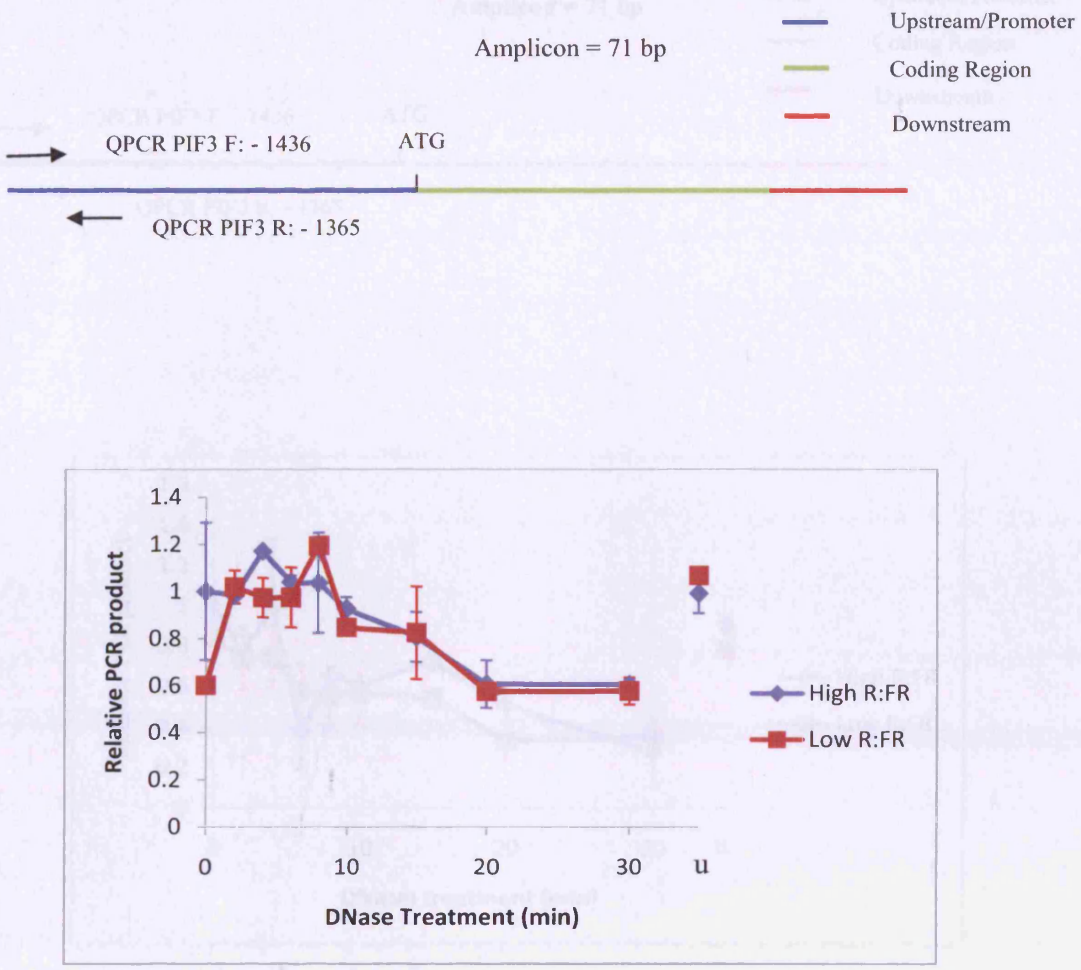

Figure 3.10: Relative amount of PCR product against duration of DNaseI treatment for a region of the *PIF3* promoter following 4 h, low R:FR treatment in LD. The primers used are shown in 2.14 and S1.3. All of the data points are joined up except for the data point labelled u (the far right of the graph), this represents the sample untreated with DNaseI. The data are from 3 separate biological repeats. Each experiment contains duplicate or triplicate qPCR repeats. Standard error bars are shown for each data point. All data are from plants grown in LD cycles. Above the graph is a cartoon displaying the particulars of the primer set used.

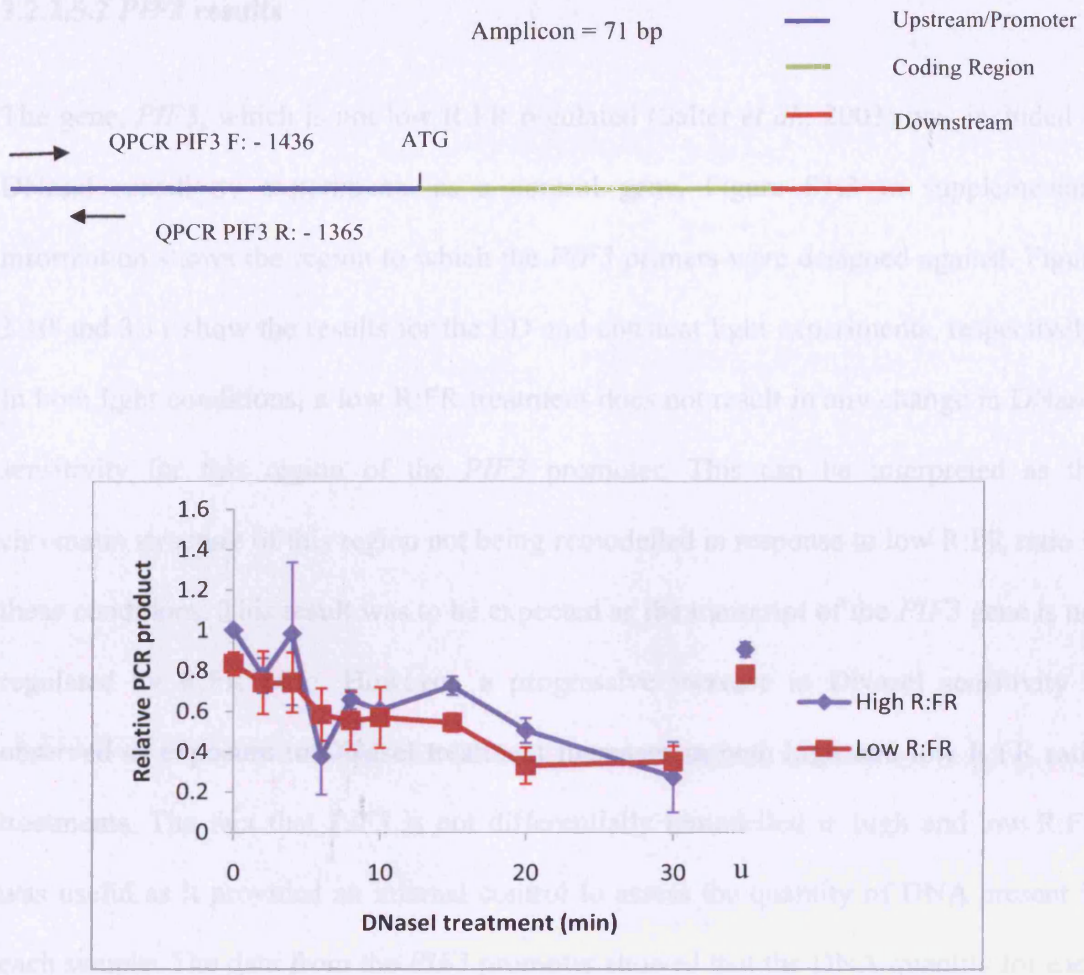

Figure 3.11: Relative amount of PCR product against duration of DNaseI treatment for a region of the *PIF3* promoter following 24 h low R:FR treatment in continuous light. The primers used are shown in 2.14 and S1.3. All of the data points are joined up except for the data point labelled u (the far right of the graph), this represents the sample untreated with DNaseI. The data are from 2 separate biological repeats. Each experiment contains duplicate or triplicate qPCR repeats. Range bars are shown for each data point. All data are from plants grown in continuous light. Above the graph is a cartoon displaying the particulars of the primer set used.

3.2.2.5.2 *PIF3* results

The gene, *PIF3*, which is not low R:FR regulated (Salter *et al.,* 2003) was included in DNaseI sensitivity experiments as a control gene. Figure S1.3 in supplementary information shows the region to which the *PIF3* primers were designed against. Figure 3.10 and 3.11 show the results for the LD and constant light experiments, respectively. In both light conditions, a low R:FR treatment does not result in any change in DNaseI sensitivity for this region of the *PIF3* promoter. This can be interpreted as the chromatin structure of this region not being remodelled in response to low R:FR ratio in these conditions. This result was to be expected as the transcript of the *PIF3* gene is not regulated by R:FR ratio. However, a progressive increase in DNaseI sensitivity is observed as exposure to DNaseI treatment increases in both high and low R:FR ratio treatments. The fact that *PIF3* is not differentially remodelled in high and low R:FR was useful as it provided an internal control to assess the quantity of DNA present in each sample. The data from the *PIF3* promoter showed that the DNA quantity for each time point to be very similar for low and high R:FR ratio treatments and this provides confidence that if a difference in sensitivity is seen for other regions then they are probably due to difference in DNaseI sensitivity as opposed to differences in quantity of DNA

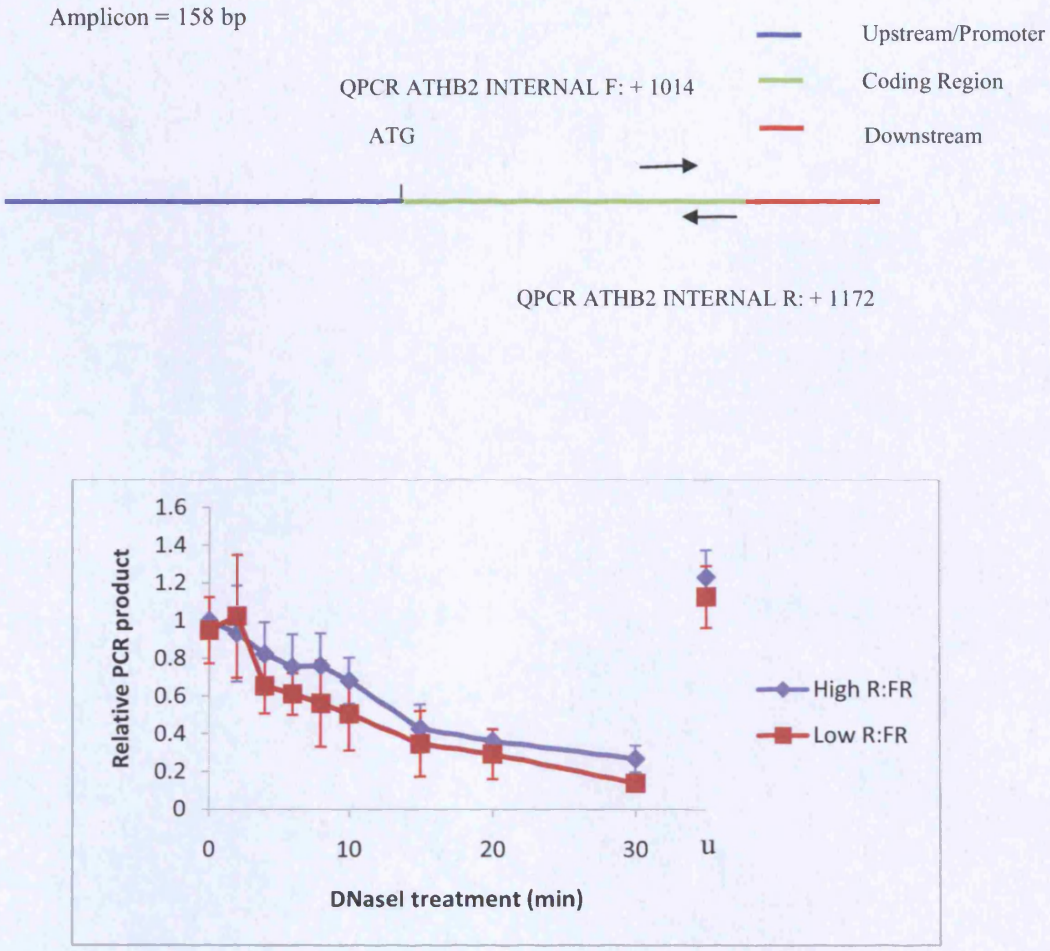

Figure 3.12: Relative amount of PCR product against duration of DNaseI treatment for a region of the *ATHB2* coding region following 4 h, low R:FR treatment in LD. The primers used are shown in 2.14 and S1.4, and they are: QPCR ATHB2 INTERNAL F and QPCR ATHB2 INTERNAL R All of the data points are joined up except for the data point labelled u (the far right of the graph), this represents the sample untreated with DNaseI. The data are from 3 separate biological repeats. Each experiment contains duplicate or triplicate qPCR repeats. Standard error bars are shown for each data point. All data are from plants grown in LD cycles. Above the graph is a cartoon displaying the particulars of the primer set used.

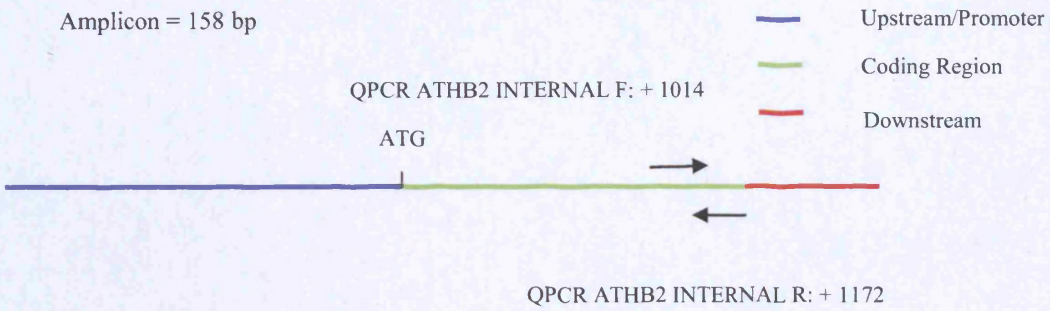

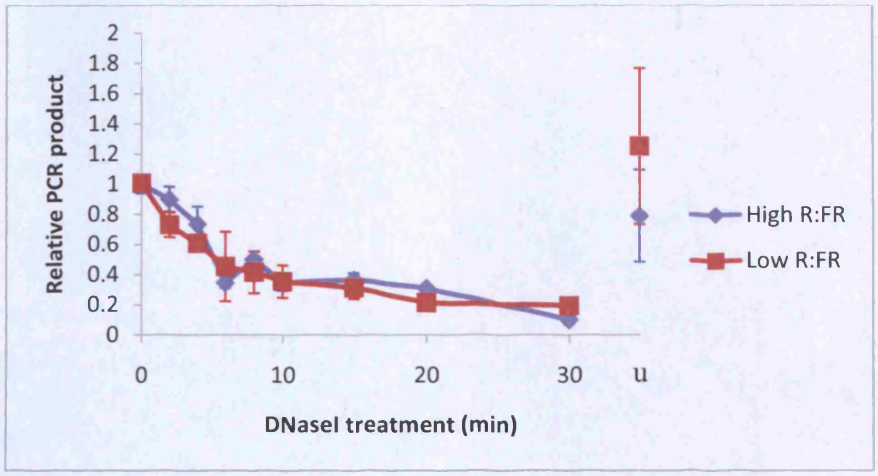

Figure 3.13: Relative amount of PCR product against duration of DNaseI treatment for a region of the *ATHB2* coding region following 24 h low R:FR treatment in continuous light. The primers used are shown in 2.14 and S1.4 and they are: QPCR ATHB2INTERNAL F1 and QPCR ATHB2INTERNAL R1. All of the data points are joined up except for the data point labelled u (the far right of the graph), this represents the sample untreated with DNaseI. The data are from 2 separate biological repeats. Each experiment contains duplicate or triplicate qPCR repeats. Range bars are shown for each data point. All data are from plants grown in continuous light. Above the graph is a cartoon displaying the particulars of the primer set used.

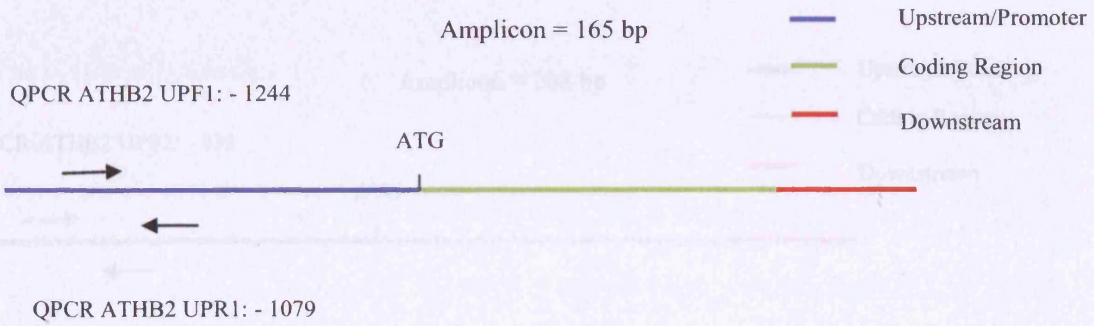

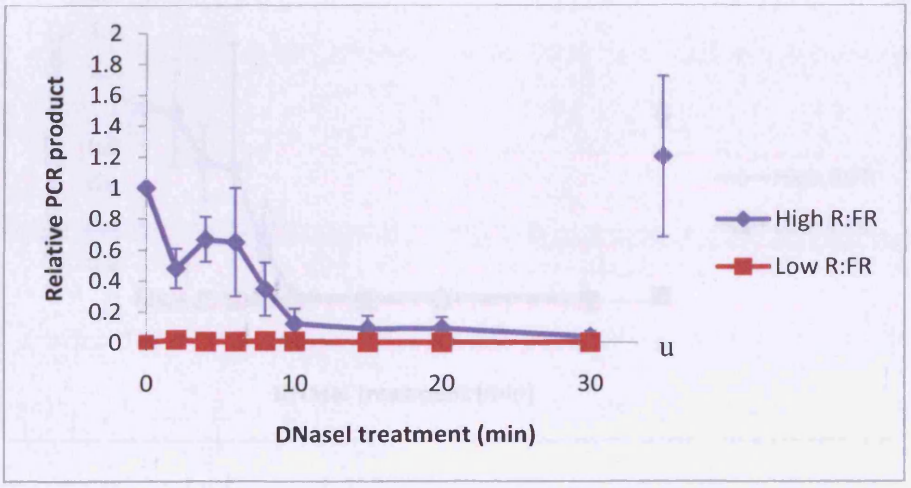

Figure 3.14: Relative amount of PCR product against duration of DNaseI treatment for a region of the *ATHB2* promoter region following 4 h, low R:FR treatment in LD. The primers used are shown in 2.14 and S1.4, and they are: QPCR ATHB2 UPF1 and QPCR ATHB2 UPR1. All of the data points are joined up except for the data point labelled u (the far right of the graph), this represents the sample untreated with DNaseI. The data are from 3 separate biological repeats. Each experiment contains duplicate or triplicate qPCR repeats. Standard error bars are shown for each data point. All data are from plants grown in LD cycles. Above the graph is a cartoon displaying the particulars of the primer set used.

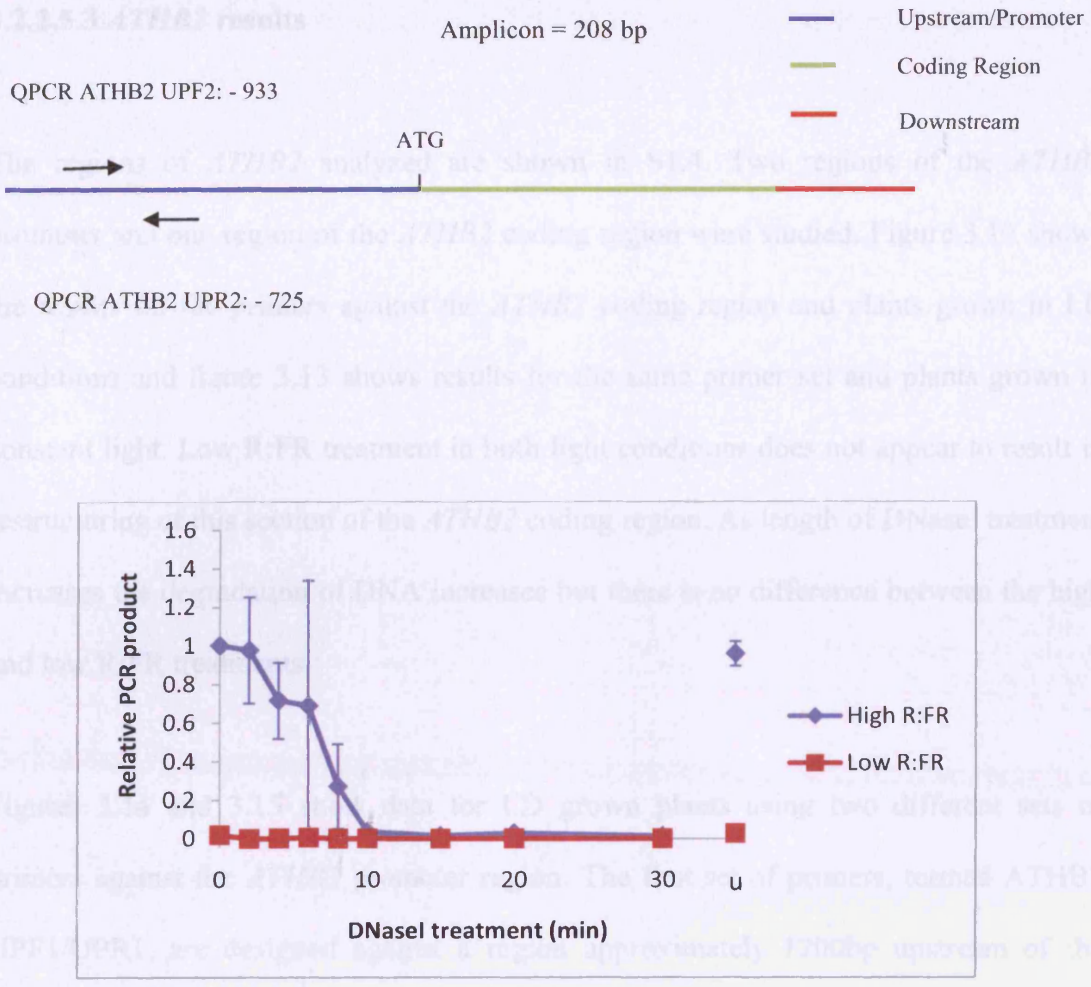

Figure 3.15: Relative amount of PCR product against duration of DNaseI treatment for a region of the *ATHB2* promoter region following 4 h, low R:FR treatment in LD. The primers used are shown in 2.14 and S1.4, and they are: QPCR ATHB2 UPF2 and QPCR ATHB2 UPR2. All of the data points are joined up except for the data point labelled u (the far right of the graph), this represents the sample untreated with DNaseI. The data are from 3 separate biological repeat. Each experiment contains duplicate or triplicate qPCR repeats. Standard error bars are shown for each data point. All data are from plants grown in LD cycles. Above the graph is a cartoon displaying the particulars of the primer set used.

3.2.2.5.3 *ATHB2* results

The regions of *ATHB2* analyzed are shown in S1.4. Two regions of the *ATHB2* promoter and one region of the *ATHB2* coding region were studied. Figure 3.12 shows the results for the primers against the *ATHB2* coding region and plants grown in LD conditions and figure 3.13 shows results for the same primer set and plants grown in constant light. Low R:FR treatment in both light conditions does not appear to result in restructuring of this section of the *ATHB2* coding region. As length of DNaseI treatment increases the degradation of DNA increases but there is no difference between the high and low R:FR treatments.

Figures 3.14 and 3.15 show data for LD grown plants using two different sets of primers against the *ATHB2* promoter region. The first set of primers, termed ATHB2 UPF1/UPR1, are designed against a region approximately 1200bp upstream of the ATG; the second set of primers, termed ATHB2 UPF2/UPR2, are designed against a region approximately 800bp upstream of the ATG. Both regions appear to have a more open chromatin structure in response to low R:FR ratio. For both regions, even after 10 minutes DNaseI treatment in tissue treated with high R:FR ratio there is negligible DNA remaining, indicating a relatively open chromatin structure in the absence of a low R:FR signal, which becomes even more open in response to a low R:FR treatment. The chromatin become so open in response to a low R:FR signal that even at the shortest time-points (0 minutes and untreated) there is negligible template present, indicating that when the cells are lysed in the extraction process, the endogenous factors present in the cells may be sufficient to degrade the DNA of these regions. This is in

contrast to the *ATHB2* coding region, which shows no change in template abundance in high and low R:FR, suggesting that these regions of sensitivity are sequence specific.

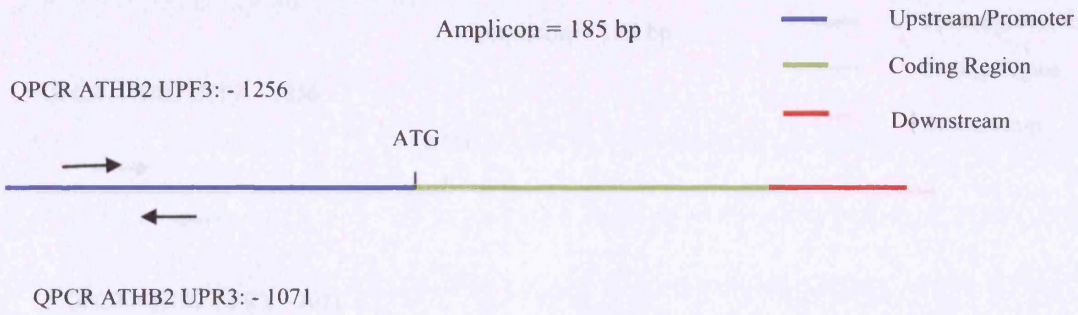

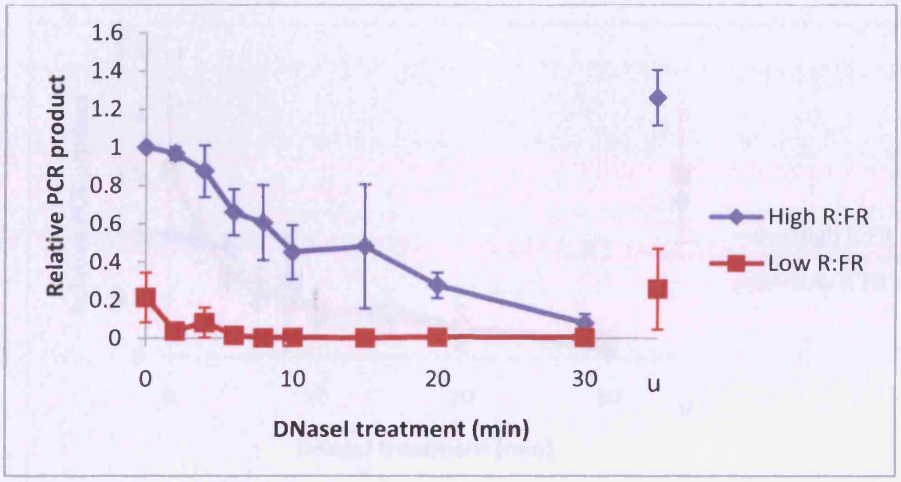

Figure 3.16: Relative amount of PCR product against duration of DNaseI treatment for a region of the *ATHB2* promoter region following 4 h, low R:FR treatment in LD. The primers used are shown in 2.14 and S1.4, and they are: ATHB2 UPF3 and QPCR ATHB2 UPR3. All of the data points are joined up except for the data point labelled u (the far right of the graph), this represents the sample untreated with DNaseI. The data are from 3 separate biological repeats. Each experiment contains duplicate or triplicate qPCR repeats. Standard error bars are shown for each data point. All data are from plants grown in LD cycles. Above the graph is a cartoon displaying the particulars of the primer set used.

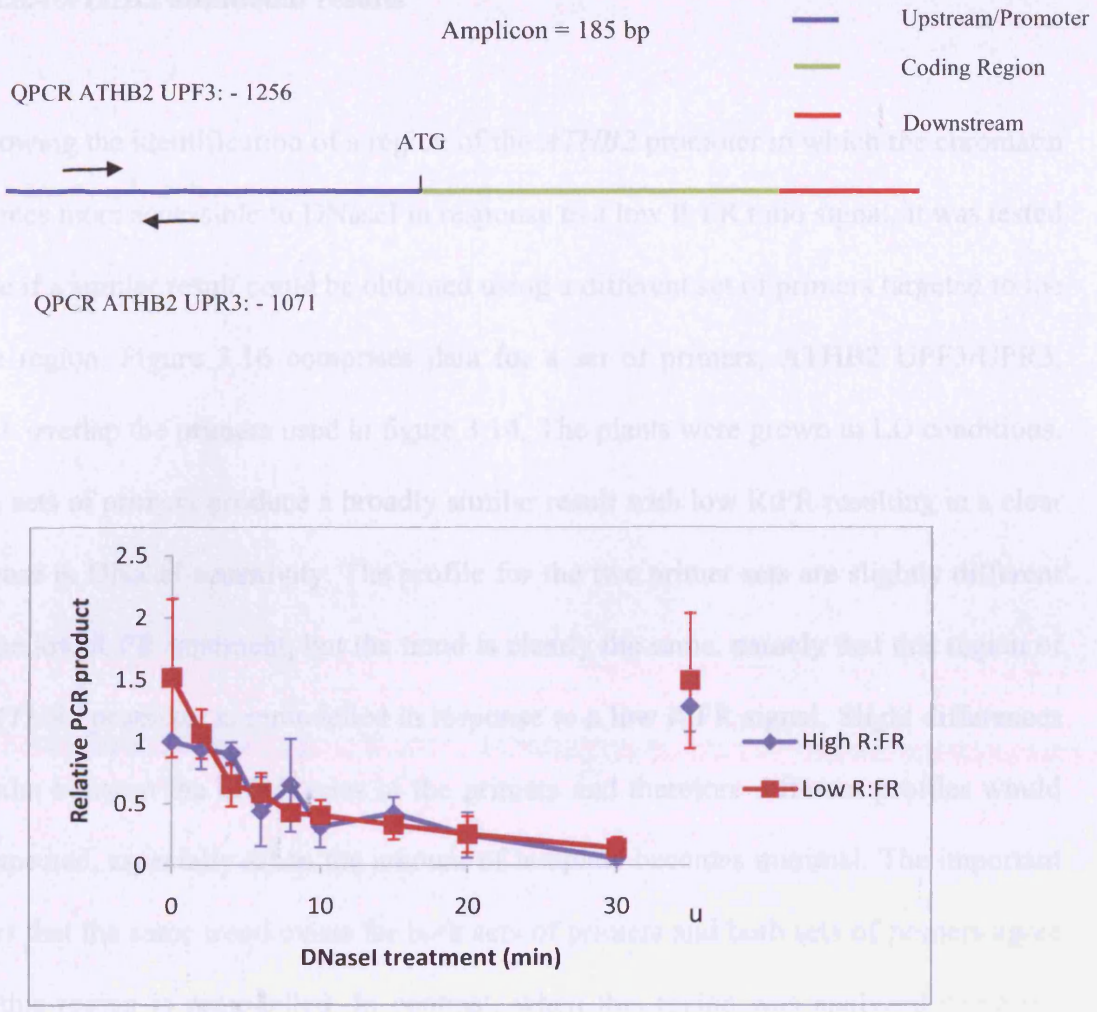

Figure 3.17: Relative amount of PCR product against duration of DNaseI treatment for a region of the *ATHB2* promoter region following 24 h low R:FR treatment in continuous light. The primers used are shown in 2.14 and S1.4 and they are: QPCR ATHB2 UPF3 and QPCR ATHB2 UPR3. All of the data points are joined up except for the data point labelled u (the far right of the graph), this represents the sample untreated with DNaseI. The data are from 2 separate biological repeats. Each experiment contains duplicate or triplicate qPCR repeats. Range bars are shown for each data point. All data are from plants grown in continuous light. Above the graph is a cartoon displaying the particulars of the primer set used.

3.2.2.5.4 *ATHB2* additional results

Following the identification of a region of the *ATHB2* promoter in which the chromatin becomes more accessible to DNaseI in response to a low R:FR ratio signal, it was tested to see if a similar result could be obtained using a different set of primers targeted to the same region. Figure 3.16 comprises data for a set of primers, ATHB2 UPF3/UPR3, which overlap the primers used in figure 3.14. The plants were grown in LD conditions. Both sets of primers produce a broadly similar result with low R:FR resulting in a clear increase in DNaseI sensitivity. The profile for the two primer sets are slightly different for the low R:FR treatment, but the trend is clearly the same, namely that this region of the *ATHB2* promoter is remodelled in response to a low R:FR signal. Slight differences do exist between the efficiencies of the primers and therefore different profiles would be expected, especially when the amount of template becomes minimal. The important fact is that the same trend exists for both sets of primers and both sets of primers agree that this region is remodelled. In contrast, when this region was analyzed using the ATHB2 UPF3/UPR3 primers and constant light conditions, as shown in figure 3.17, there is no remodelling in response to the low 24 h R:FR treatment at this time–point.

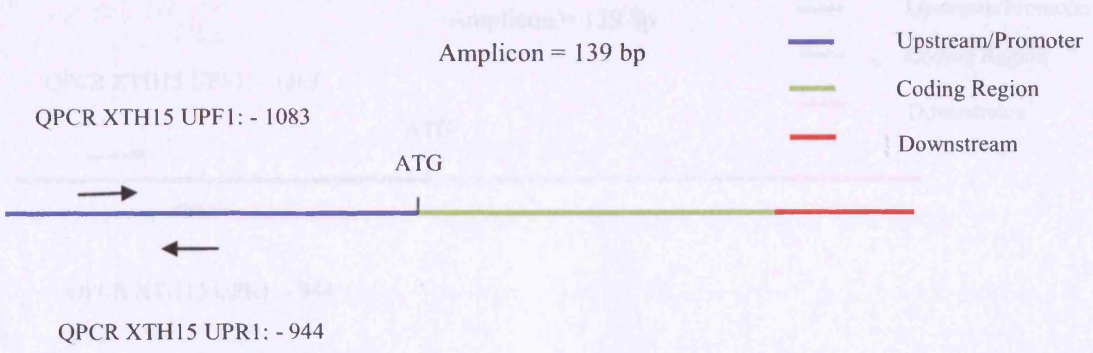

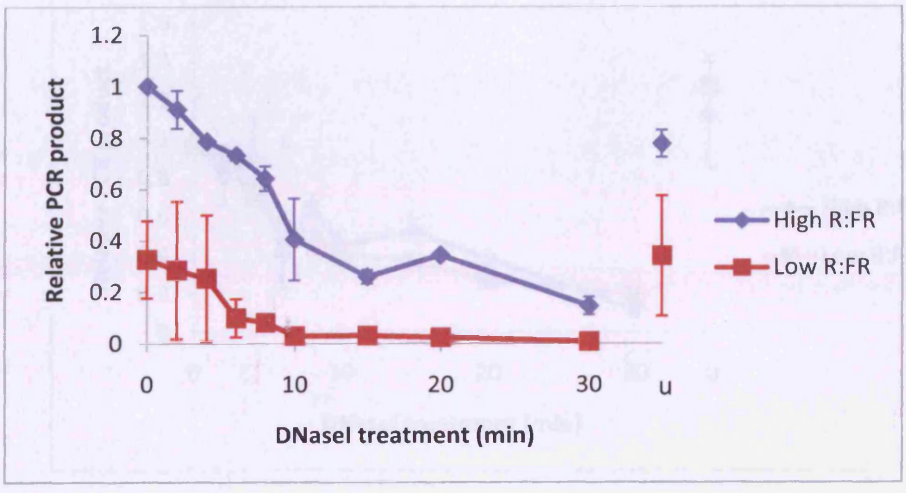

Figure 3.18: Relative amount of PCR product against duration of DNaseI treatment for a region of the *XTH15* promoter region following 4 h, low R:FR treatment in LD. The primers used are shown in 2.14 and S1.5. All of the data points are joined up except for the data point labelled u (the far right of the graph), this represents the sample untreated with DNaseI. The data are from 3 separate biological repeats. Each experiment contains duplicate or triplicate qPCR repeats. Standard error bars are shown for each data point. Above the graph is a cartoon displaying the particulars of the primer set used.
All data are from plants grown in LD cycles.

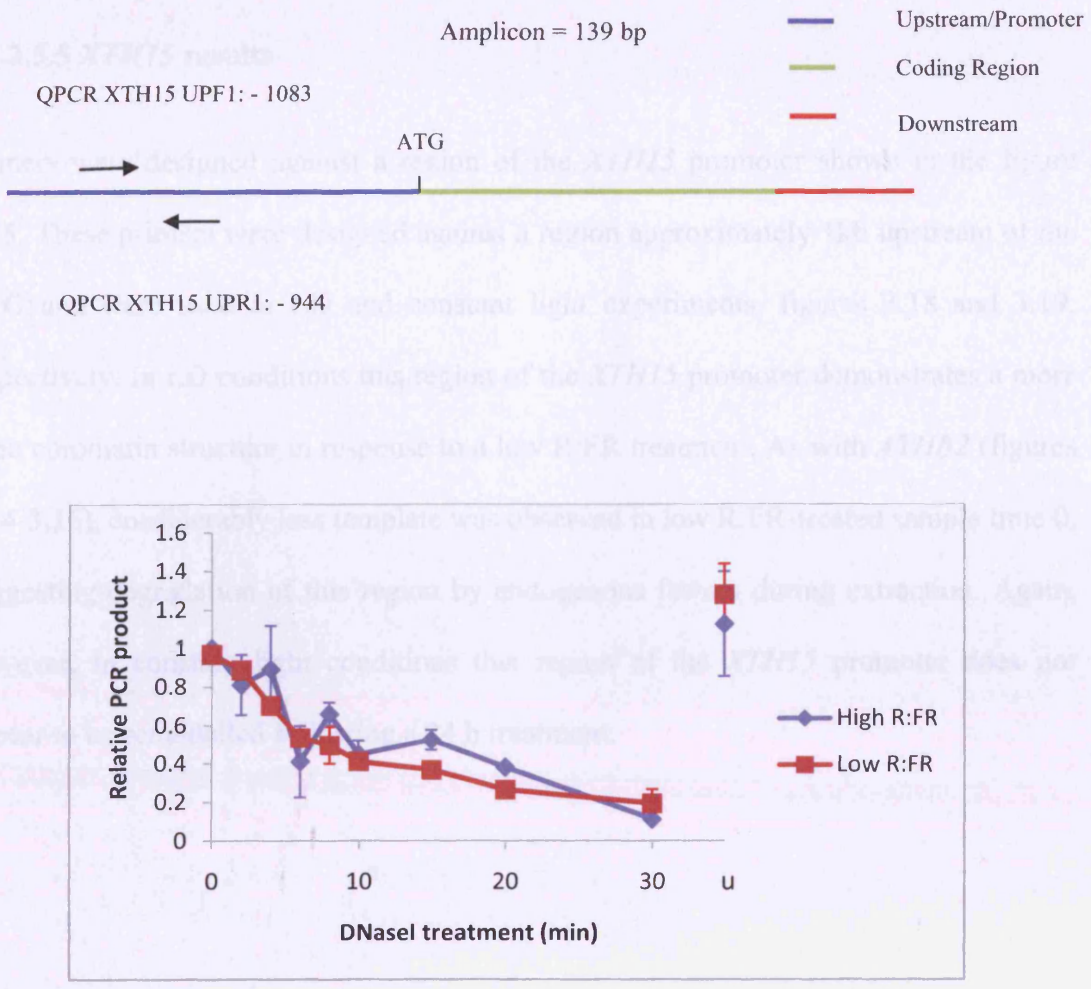

Figure 3.19: Relative amount of PCR product against duration of DNaseI treatment for a region of the *XTH15* promoter region following 24 h low R:FR treatment in continuous light. The primers used are shown in 2.14 and S1.5. All of the data points are joined up except for the data point labelled u (the far right of the graph), this represents the sample untreated with DNaseI. The data are from 2 separate biological repeats. Each experiment contains duplicate or triplicate qPCR repeats. Range bars are shown for each data point. All data are from plants grown in continuous light. Above the graph is a cartoon displaying the particulars of the primer set used.

3.2.2.5.5 *XTH15* results

Primers were designed against a region of the *XTH15* promoter shown in the figure S1.5. These primers were designed against a region approximately 1kb upstream of the ATG and were used in LD and constant light experiments, figures 3.18 and 3.19, respectively. In LD conditions this region of the *XTH15* promoter demonstrates a more open chromatin structure in response to a low R:FR treatment. As with *ATHB2* (figures 3.14-3.16), considerably less template was observed in low R:FR-treated sample time 0, suggesting degradation of this region by endogenous factors during extraction. Again, however, in constant light conditions this region of the *XTH15* promoter does not appear to be remodelled following a 24 h treatment.

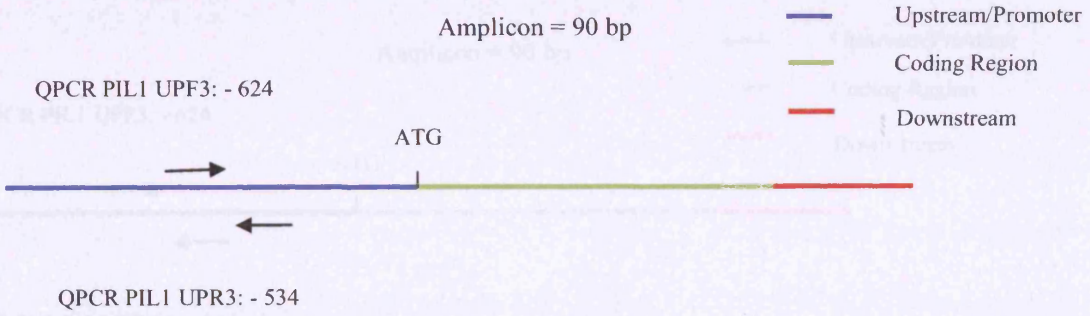

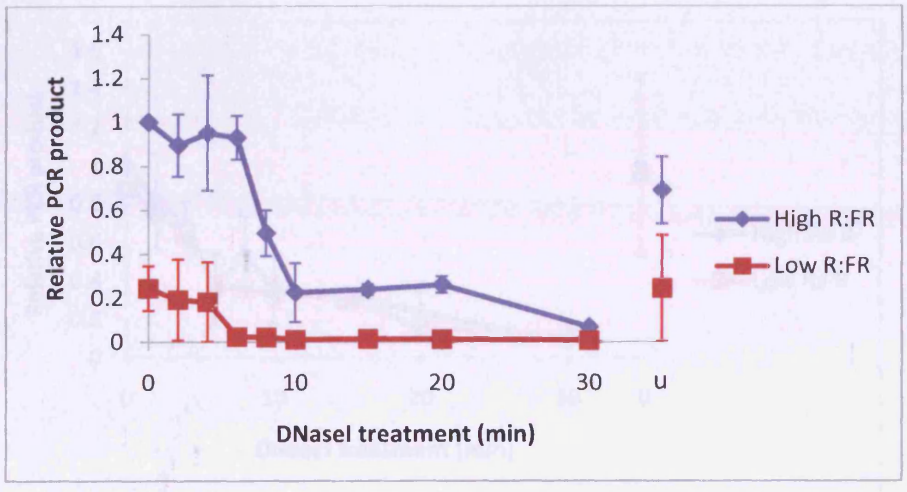

Figure 3.20: Relative amount of PCR product against duration of DNaseI treatment for a region of the *PIL1* promoter region following 4 h, low R:FR treatment in LD. The primers used are shown in 2.14 and S1.6. All of the data points are joined up except for the data point labelled u (the far right of the graph), this represents the sample untreated with DNaseI. The data are from 3 separate biological repeat. Each experiment contains duplicate or triplicate qPCR repeats. Standard error bars are shown for each data point. All data are from plants grown in LD cycles. Above the graph is a cartoon displaying the particulars of the primer set used.

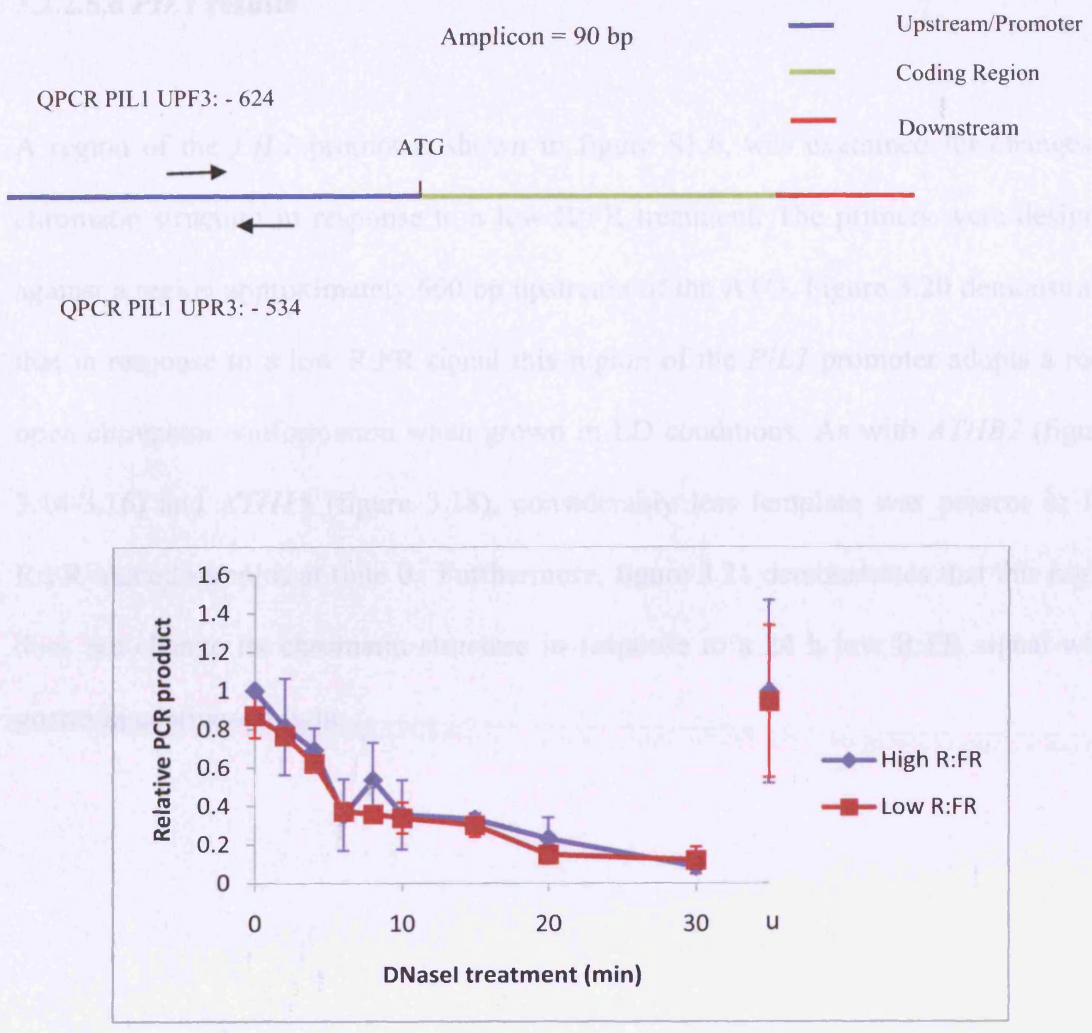

Figure 3.21: Relative amount of PCR product against duration of DNaseI treatment for a region of the *PIL1* promoter region following 24 h low R:FR treatment in continuous light. The primers used are shown in 2.14 and S1.6. All of the data points are joined up except for the data point labelled u (the far right of the graph), this represents the sample untreated with DNaseI. The data are from 2 separate biological repeats. Each experiment contains duplicate or triplicate qPCR repeats. Range bars are shown for each data point. All data are from plants grown in continuous light. Above the graph is a cartoon displaying the particulars of the primer set used.

3.2.2.5.6 *PIL1* results

A region of the *PIL1* promoter, shown in figure S1.6, was examined for changes in chromatin structure in response to a low R:FR treatment. The primers were designed against a region approximately 600 bp upstream of the ATG. Figure 3.20 demonstrated that in response to a low R:FR signal this region of the *PIL1* promoter adopts a more open chromatin conformation when grown in LD conditions. As with *ATHB2* (figures 3.14-3.16) and *XTH15* (figure 3.18), considerably less template was present in low R:FR-treated samples at time 0. Furthermore, figure 3.21 demonstrates that this region does not change its chromatin structure in response to a 24 h low R:FR signal when grown in continuous light.

3.2.3 DNaseI discussion

All data acquired from the qPCR are in the form of Ct value against length of DNaseI treatment. These data give a clear, unambiguous representation of the results, but it is not easily accessible and not immediately obvious what trends exist in the data. Data for each primer pair for each DNaseI assay was therefore normalized to that for the high R:FR ratio treatment of 0 minutes. These numbers were then represented in a line graph as relative PCR product against length of DNaseI treatment for both high and low R:FR treatments. This method was chosen over normalising both high and low R:FR data to their own 0 time-points because it was felt that this would only represent the overall trend within treatments and not between them.

Previous research in yeast has found that promoter regions of genes are typically depleted of histones (histone H3 was studied) compared to coding regions, with the level of depletion correlating with level of transcription. Genes not transcribed at all, or transcribed at very low levels, were found to exhibit a uniform H3 occupancy across the promoter and coding region, with even a slight suggestion of an increase in H3 occupancy at promoter regions compared to coding regions. However, when genes were highly expressed, the promoter regions were depleted in H3 to a greater extent than the coding regions. This is in agreement with the findings here that the promoter region becomes more open/depleted of histones as transcription increases but the coding region does not (Pokholok *et al.*, 2005)

It is interesting to speculate as to what the increase in DNaseI sensitivity actually represents at the chromatin level. There is some debate as to what DHS (DNaseI

hypersensitive sites) actually represent. There is debate as to whether they represent regions of altered nucleosome structure or regions which are entirely devoid of nucleosomes. It has been shown that DNaseI can cleave DNA which is associated with nucleosomes at multiple, periodic sites, with some sites remaining relatively protected, presumably because of certain histone – DNA interactions which protect these sites from cleavage. There is therefore no requirement for histones to be completely absent from the DNA (Simpson and Whitlock 1976). These observations are supported by a study which employed the human immunodeficiency virus (HIV-1) 5' long terminal repeat (LTR) model system, involving the *in vitro* assembly of HIV-1 LTR DNA (which contains binding sites for protein factors) to a nucleosome. In this system, nucleosomal DNA is still digested to some degree by DNaseI. If a factor binds to DNA that is associated with the nucleosome then the specific region of DNA which is bound becomes more protected from DNaseI. DNA regions directly flanking the factors binding site have increased sensitivity to DNaseI but the whole region of DNA associated with the nucleosome does not show a concomitant increase in DNaseI sensitivity. These results suggest, at least in this model system, the formation of ternary complexes (DNA, nucleosomes and DNA binding factors) and yet still the presence of DHS, meaning that DHS sites do not necessarily mean an absence of nucleosomes/histones (Steger and Workman 1997). These findings were complemented by another study which used UV lasers to produce crosslinks between the NH_2 tails of histones and DNA. They found that transcription factor binding did not affect the tail interactions with the DNA. However, if multiple transcription factors bound to the DNA then the tail – DNA interactions were disrupted. Furthermore, they found that addition of the SWI/SNF (1.8, nucleosome remodelling) complex changed the DHS profile of the nucleosome-DNA complex but the tail-DNA contacts remained the same,

demonstrating that DHS sites do not necessarily indicate an absence of nucleosomes (Angelov *et al.*, 2000).

In contrast to the above, other studies have found that DNA polymerases were incapable of initiating transcription when a nucleosome was bound to the promoter DNA. RNA polymerase can, however, transcribe through nucleosomes, as shown by the fact that templates which contain nucleosomes are capable of being transcribed Lorch *et al.,* 1987). Polymerases are thought to transcribe trough nucleosomes by transcribing up to them and then waiting for local fluctuations between nuclesomes and DNA to occur and then advancing to transcribe the DNA which has dissociated from the nucleosome. Forces then dictate whether the nucleosome is forced further downstream of the DNA template or is shifted upstream of the RNA polymerase, in a cis-looping DNA manner (Hodges *et al.,* 2009). All of these findings are reconcilable given the reasoning that DNA – nucleosome interactions periodically fluctuate, either stochastically or through enzymatic means, allowing protein factors to bind to the DNA. These nucleosome-DNA-protein complexes are permitted and can produce changes in the DHS of the region; however, if large proportions of the DNA associated with nucleosomes are required to dissociate, either for transcription, or for the binding of large protein complexes (as is the case for the RNA polymerase initiation complex), then nucleosomes will completely dissociate from that particular region of the DNA. As to whether the DHS generated in response to low R:FR ratio are regions devoid of nucleosomes or merely regions with altered DNA – nucleosomes interactions, it is not possible to tell.

The findings of the studies discussed above suggest that even when DNA is associated with nucleosomes they will still demonstrate some degree of DNaseI sensitivity, which is in agreement with the results of the *PIF3* promoter, which still demonstrates sensitivity even though it does not undergo remodelling.

Data from the DNaseI sensitivity assays suggest that there is an involvement of chromatin remodelling in the regulation of R:FR regulated genes. The data suggest that regions of the *ATHB2, PIL1* and *XTH15* promoter are all remodelled in response to a low R:FR signal. Importantly, this remodelling is only seen when plant are grown in LD treated with a 4 h low R:FR treatment conditions and is conspicuously absent when plants are grown in constant light conditions with a 24 h treatment. These data could reflect the different time-points used in both experiments or may suggest the involvement of the circadian clock in the regulation of the chromatin structure of these genes. Previously, it has been shown that the expression of shade avoidance markers genes in response to low R:FR is gated by the circadian clock and it could be that the mechanism by which this works is via rhythmic alterations of chromatin structure (Salter *et al.* 2003).

The circadian clock is an endogenous, molecular oscillator that is characterised by a number of transcriptional-translational feedback loops which are temporally calibrated by external environmental cues with the effect of regulating physiological processes (Grimaldi *et al.,* 2009). In *Arabidopsis*, several phenotypes including leaf movements, stomata opening and hypocotyl elongation exhibit rhythmic oscillations with a period of approximately 24 hours, indicative of circadian regulation (Dowson-Day and Millar, 1999). Rhythmic hypocotyl elongation in seedlings is regulated by circadian regulation

of the growth promoting bHLH transcription factors PIF4 and PIF5 (Nozue *et al.*, 2007). Mutations in clock genes can result in deregulation of this rhythm. For example, mutation of the clock gene, *TIMING OF CAB EXPRESSION1 (TOC1)*, results in a shortened period of hypocotyl elongation; whereas, mutation of the clock gene, *ELF3*, results in complete abolition of rhythmic hypocotyl elongation (Dowson-Day and Millar 1999).

Light is an important environmental input that entrains the clock. This process involves both phytochrome and cryptochrome photoreceptors (Devlin and Kay, 2000). The intimate association between the clock and the function of phytochromes is demonstrated by RNAi knock-down of *TOC1*, which results in deregulation of the circadian clock and decreased sensitivity to R and FR light, as measured by hypocotyl growth (Mas *et al.*, 2003). Furthermore, yeast two hybrid screens have identified an interaction between TOC1 and PIF3 and also between TOC1 and PIL1 (Makino *et al.*, 2002). All of this information taken together suggests a close association between components of the circadian clock and the molecular components of light signalling.

It is not a new idea that regulation of chromatin and the circadian clock are associated. Over ten years ago, it was shown that a light pulse during dark periods could phase shift components of the mammalian circadian clock and that this shift was associated with modifications to the H3 tails of these circadian clock genes (Crosio *et al.*, 2003) In *Arabidopsis*, Perales and Mas (2007) recently showed that *TOC1* demonstrates cyclical mRNA oscillations and that the periodic increase in transcript are temporally preceded by H3 acetylation of the *TOC1* promoter. The circadian clock component CIRCADIAN CLOCK ASSOCIATED 1(CCA1) was shown to bind the TOC1 promoter in antiphase of H3 acetylation and when CCA1 is over-expressed it resulted in constitutive

occupancy of the *TOC1* promoter by CCA1, background levels of TOC1 H3 acetylation and minimal TOC1 mRNA. This suggests that the clock component, CCA1, represses H3 acetylation of the *TOC1* promoter (Perales and Mas, 2007). Although CCA1 hasn't been shown to have direct histone modifying activity, another component of the murine circadian clock, CLOCK, has. CLOCK is a histone acetyl transferase (HAT) and if the HAT domain of CLOCK is mutated then the clock becomes deregulated. Furthermore, several components of the circadian clock have been shown to undergo histone modifications by CLOCK (Curtis *et al.,* 2004; Ripperger *et al.,* 2006) demonstrating that a chromatin modifying protein is both a central component of the clock and is important in the direct functioning of the clock (Doi *et al.,* 2006) Taken together, these studies suggest that the circadian clock is responsible for rhythmically establishing chromatin conformations permissive for transcription.

The fact that the three shade avoidance genes: *PIL1*, *ATHB2* and *XTH15* are still up regulated in continuous light suggests that chromatin remodelling is not essential for up regulation of transcription in response to a low R:FR signal; however, as the increase in transcription is less than that observed in plants grown in LD cycles, it may suggest that chromatin remodelling is required for maximal transcription.

Chapter 4: Results

The effect of low R:FR on the association of shade avoidance genes with modified histones

4.1 Chromatin Immunoprecipitation

The results shown in 3.1 demonstrated that in response to a R:FR signal, the genes *PIL1*, *ATHB2* and *XTH15* exhibit changes in chromatin structure. Importantly, these results were observed when the plants were grown in LD conditions but not when the plants were grown in constant light conditions. Following these results, it was postulated that these gross changes in chromatin structure could be correlated with circadian-regulated chromatin remodelling events. This process could involve rhythmic oscillations in the association of shade avoidance genes with modified histones. The purpose of the following analyses was to determine if this was the case, using Chromatin Immunoprecipitation (ChIP).

The ChIP procedure briefly comprised harvesting of 4 g of plant tissue, followed by cross-linking of histones to DNA to ensure that the histone-DNA associations at the time of harvest are maintained. The tissue was then ground and the nuclei isolated and lysed. The lysed nuclei were then sonicated to shear the DNA into smaller fragments. Beads were added to the sample in an attempt to remove the factors that would bind non-specifically. This was followed by removal of the beads and incubation with antibodies against histone modifications. Fresh beads were added that bind to the antibodies. The DNA-histone-bead complexes were washed and the DNA purified.

Isolated DNA was then used as a template in qPCR reaction to determine if enrichment was present.

4.1.1 Plant growth conditions

WT *Arabidopsis* Col plants were grown on soil for 21 days in LD at 22°C high R:FR. On the dawn of the 21st day, half the plants were transferred to low R:FR and half were maintained in high R:FR. Whole shoots were harvested 4 hours later.

4.1.2 Primer design

Figure 3.8 and 3.9 show that the genes *PIL1* and *ATHB2* increased their transcript to considerably higher levels, in response to a low R:FR ratio signal, compared to *XTH15*. Due to this, and time constraints, the search for histone modifications was focused upon *ATHB2* and *PIL1* and to a much lesser extent *XTH15*. Previous research (Guo *et al.*, 2008, Perales and Mas, 2007; Bastow *et al.*, 2004; Chua *et al.*, 2001) have found that in *Arabidopsis* histone marks can occur over a variety of positions (upstream, promoter and coding region) of a gene locus and for this reason it was decided that primers should be designed against the upstream, promoter and coding regions of *ATHB2* and *PIL1*. The light-regulated gene, *PIF3*, and the housekeeping gene, *ACTIN2*, were used as controls (Salter *et al.*, 2003). Figures S1.7 and S1.8 shows the regions to which primers were designed against *ATHB2* and *PIL1*, respectively. All primers were designed by eye and all primers used were tested to ensure they produced a discrete, unique melting curve with a single peak. A number of the primers shown in S1.7 and S1.8 did not produce a distinct melting curve and frequently did not return any product from a qPCR reaction when tested on ChIP material. This meant that only certain primers sets could be used in the ChIP experiments.

4.1.3 Antibodies used

Acetylation marks are typically associated with transcriptional activation (Grunstein, 1997; Eberharter and Becker, 2002). Because low R:FR results in an increase in transcription, antibodies were ordered against acetylated histones. It was unknown what acetylation marks to expect and it was therefore considered best to order as general antibodies as possible. Perales and Mas (2007) used an anti-acetylated histone 3 antibody (H3ac) and unmodified anti-histone 3 antibody (H3no) to study the role of histone acetylation in the regulation of *TOC1*. It was therefore decided that these would be good antibodies to begin the ChIP experiments with. These antibodies are polyclonal rabbit antibodies and were obtained from Millipore (http://www,millipore.com). The epitope they are raised against are amino acids 1 – 20 of Tetrahymena H3. The anti-acetylated H3 antibody was raised against an epitope acetylated at residues H3K9 and H3K14.

Work by Guo *et al* (2008) identified a number of histone H3 modifications which showed altered enrichment with light-regulated genes during seedling de-etiolation. One of the modifications they identified was H3K9 acetylation. The H3K9 antibody used in their investigations was a rabbit monoclonal antibody. Due to the fact it was a monoclonal antibody it was considered more reliable than polyclonal antibodies which can vary between lots. This antibody was ordered from Epitomics (http://www.epitomics.com) (Guo *et al.,* 2006).

The histone mark H3K4me2 has previously been associated with transcriptionally permissive chromatin (Wysocka *et al.,* 2005). Because of this, it was considered that

there would be a possibility of the mark being associated with the genes being investigated. A rabbit polyclonal H3K4me2 antibody was therefore obtained from Millipore.

4.1.4 Optimisation of ChIP

4.1.4.1 Optimisation of sonication

Prior to commencement of the full ChIP protocol the various components were optimized. Sonication was the first parameter of the ChIP protocol to be investigated because it was the most upstream part of the procedure in which a readout, in the form of a gel photo, could be obtained. Tissue for sonication was prepared as outlined in 2.2.12. Sonication was run as outlined in 2.2.12.2a. The aim of sonication is to break the DNA-chromatin complexes into fragments approximately 200bp – 1kb in size, making them amenable to efficient immunoprecipitation. It was unknown as to the settings required to achieve such sonicated fractions using the available sonicator (Soniprep MSE). A range of settings were therefore investigated. Pulses of 10 seconds duration, at medium power, were maintained as constants and the number of pulses was varied: 0 (un-sonicated), 3, 6, 9 and 12 pulses were performed. The DNA was extracted using the chelex method as outlined in 2.2.12.5b, but when the DNA was run on the gel no bands were present.

Following the failure with the chelex method, DNA was extracted using the NaCl method as outlined in 2.2.12.5a. Figure 4.1 shows that this method produced bands, with 12 pulses (lane 7) producing DNA of approximately the correct size

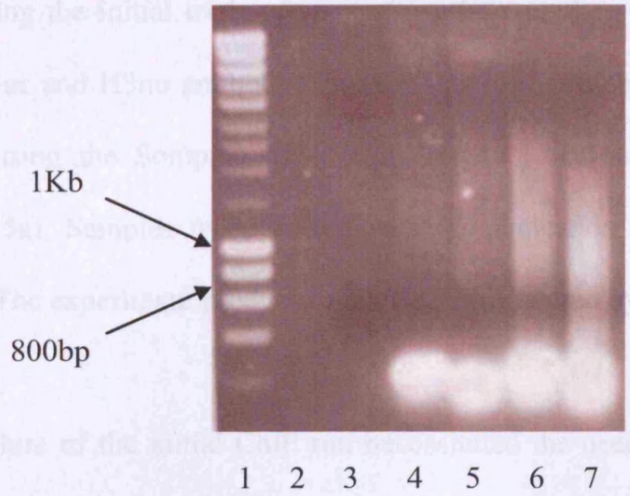

Figure 4.1: An example of sonication of DNA, with left to right representing increasing sonication pulses. Lane 1 is 3µl of hyperladder I, lane 2 is blank, lane 3 is un-sonicated DNA, lane 4 is DNA sonicated for 3 pulses, lane 5 is DNA sonicated for 6 pulses, lane 6 is DNA sonicated for 9 pulses and lane 7 is DNA sonicated for 12 pulses. Samples were not RNase treated.

Following the initial trials of sonication, the complete ChIP protocol was performed. The H3ac and H3no antibody were used and the protocol was followed as outlined in 2.2.8, using the Soniprep MSE method (2.2.12.2a) and the NaCl cleanup method (2.2.12.5a). Samples were treated with 12 sonication pulses and protein A agarose beads. The experiment produced no DNA as measured by qPCR analysis.

The failure of the initial ChIP run necessitated the need for further optimisation. The sonication step was again investigated to establish its reproducibility. Sonication was repeated a number of times to asses the reproducibility of the sonicator. This was found to be low, therefore, alternative means of sonication were investigated. A Bioruptor was subsequently used for sonication. Again, however, the amount of sonication required to produce the desired DNA-chromatin fragment size was unknown. The Bioruptor instruction manual suggested that 12 pulses of 30 seconds at medium power was suitable for mammalian tissue. These settings were used as a basis for optimisation. Pulses of 30 seconds on, followed by 30 seconds off, at medium power was kept constant and the number of pulse was varied. Figure 4.2 shows that 15 pulses produced optimally sized fragments. In contrast to the previous sonicator, the Bioruptor demonstrated high reproducibility.

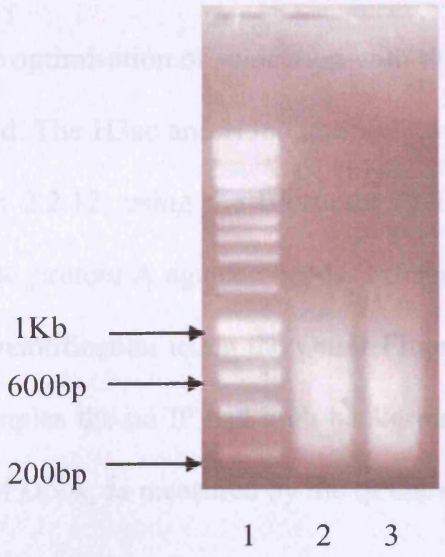

Figure 4.2: Gel showing DNA which has been pulsed 15 times in the Bioruptor. Lane 1 is 3µl of hyperladder I, lane 2 is DNA from plants treated in high R:FR and lane 3 is DNA from plants treated in low R:FR. Both samples of DNA were sonicated as outlined in 2.2.12.2b.

Figure 4.1 shows some of the initial attempts at sonicating tissue using the Soniprep. The 0 sample displayed a clear, high-molecular-weight band, presumably representing genomic DNA. The 3,6, 9 and 12 pulses produced a progressive decline in molecular weight and a concomitant formation of a tighter, brighter band in the region of 700bp, demonstrating that the Soniprep was functioning. However, the failure to obtain reproducibility using the soniprep (which could be accounted for by the fact that a number of the instruments dials were broken and it was impossible to determine the power setting being used) led to the adoption of the Bioruptor. Figure 4.2 is an example of the sonication conditions used for all the ChIP results. A band in the region of 200 – 1000 bp can clearly be seen. High reproducibility was routinely obtained using the Bioruptor.

Following the optimisation of sonication with the Bioruptor the complete ChIP protocol was performed. The H3ac and H3no antibody were used and the protocol was followed as outlined in 2.2.12, using the Bioruptor (2.2.12.2b) and the NaCl cleanup method (2.2.12.5a) and protein A agarose beads. Fifteen sonication pulses using the Bioruptor were used. Quantification using the Qubit Fluorometer suggested that relative to H3ac and H3no samples the no IP had high background levels; furthermore, there were was no recovery of DNA, as measured by the qPCR machine.

4.1.4.2 Optimisation of pre-clearing

One possible reason for the lack of DNA recovery was considered to be the excessive background binding of which could prevent specific binding. Taking this into consideration, the protocol was repeated using more washes and longer pre-clearing.

Increased pre-clearing of samples was performed. Instead of the standard 1 hour, 2 hours and 4 hours of pre-clearing were tried. Increased washing was also performed. With the number of washing steps doubled. This increase in pre-clearing time and number of washes had no effect and still no DNA was recovered as measured by the qPCR machine.

4.1.4.3 Optimisation of beads

A number of different protocols were analysed in an attempt to determine alternative methodologies which could be used. The type of beads used in ChIP experiments is a common variable with material of the beads: agarose and magnetic; and the surface antigen type: A and G; being possible options. It was considered that both the material and the surface types could be important variables and could be affecting antibody binding. Agarose A beads from Upstate were run in parallel with magnetic A and G beads from Invitrogen and magnetic A beads from NEB.

The change in beads still produced no DNA as measured by the qPCR machine. The magnetic A beads from Invitrogen, however, produced the lowest level of background binding in the no IP sample and also because of the ease of use of the magnetic beads compared to the agarose beads, the magnetic A Invitrogen beads were used in all future ChIP experiments.

4.1.4.4 Optimisation of antibodies and DNA purification

The antibodies were considered a potential problem. Despite the two antibodies, H3ac and H3no, being shown to work with *Arabidopsis* immunoprecipitations by Perales and Mas (2007), it was possible that they were not working in our experiments. The H3no antibody is raised against an unmodified epitope of the first 20 amino acids of H3. It is possible that *in planta*, the histones in these regions are modified, previous research suggests that the majority of histones are modified at least once (Johnson *et al.*, 2004). A high degree of histone modification *in planta* may therefore contribute to the inefficiency of this antibody with plant samples. The H3ac antibody is raised against an epitope for the first 20 amino acids of H3 that is acetylated at H3K9 and H3K14. It is possible that just one of these marks is present on H3 proteins in our samples. Without both marks present, the efficiency of antibody histone binding would be greatly reduced. It could also be that, as both of these antibodies are polyclonal that these antibodies are from animals which haven't produced antibodies with good efficacy. Taking this into consideration, alternative antibodies were sought. A monoclonal antibody against H3K9ac, shown to work by Guo *et al* (2008), was considered a good antibody to use because it is monoclonal, thereby reducing problems regarding the lot of the antibody. Since the start of this project, the authors had additionally shown that H3K9ac marks are associated with light signalling in *Arabidopsis*.

Despite the use of these new antibodies there was still no recovery of DNA. An alternative purification method was therefore sought. Previously, a chelex method to recover DNA had been attempted; however, it had yielded no DNA. Due to the lack of success using the NaCl recovery method it was deemed that it was worth re-trying the

chelex method. Using the chelex method and the H3K9ac and H3ac antibodies DNA was successfully recovered and a signal was generated on the qPCR machine. The amount of DNA recovered was, however, still low.

A vital part of the entire procedure was considered the antibody-chromatin-bead interaction. The ratio and absolute amount of antibody and chromatin were considered important variables that could influence the recovery of DNA. The ratio of antibody to chromatin was varied as was the amount of chromatin and antibody. Work by Guo and colleagues (2008) used a specific ratio of antibody to beads and chromatin. These ratios were used for the H3K9ac antibody. This increase in antibody and hence and increase in antibody to chromatin ratio was found to increase the yield of DNA.

It was still felt that the recovery of DNA could be increased further. In pursuit of this, length of cross-linking was varied. Cross-linking of DNA to proteins has the effect of denaturing proteins and linking them to the DNA. Excessive cross linking could therefore theoretically denature the epitope regions to which the antibody binds, hence decreasing antibody binding. A range of cross-linking times were compared: 10 minutes (which had been used up until this point), 5 minutes and 3 minutes. Although no real difference was observed using the different cross-linking times it was felt that 3 minutes would involve the least denaturation and was used. Length of cross-linking could affect sonication efficiency; therefore, the sonication step was calibrated again. It was found that 15 cycles on the Bioruptor still produced the desired sonication.

Finally, the length of the time the antibody-chromatin complexes were incubated with the beads was varied. Previously, 1 hour incubation had been used and it was considered that this may not have been long enough to permit antibody-bead binding. A

2 hour incubation was therefore tried. This increase in incubation time resulted in an increase in recovery of DNA.

These combined alterations in the ChIP procedure further improved the recovery of the DNA and meant that DNA was recovered with the H3ac, H3K9ac and at very low levels with the H3K4me2 antibodies. Experiments with high and low R:FR-treated tissue were subsequently performed with antibodies raised against H3ac and H3K9ac.

4.1.5 ChIP primers

Following the results in section 3.1, two R:FR-regulated genes were focused upon in the ChIP study. These were *ATHB2* and *PIL1*. *XTH15* was also studied, but to a much lesser degree. Regions of the *ACTIN2* and *PIF3* gene were also studied as negative controls. The region of *PIF3* studied is shown in figure S1.3 and the region of *ACTIN2* studied is shown in figure S1.9.

The primers used in section 3.1 in the analysis of *ATHB2* and *PIL1* were also used to study ChIP modifications. Additional primers were also designed, so that the majority of these genes and their immediate upstream regions were covered. The DNA sequences these primers covered are shown in figures S1.7 and S1.8 and the relative positions of the primers used are shown in figures 4.3 and 4.4.

ATHB2

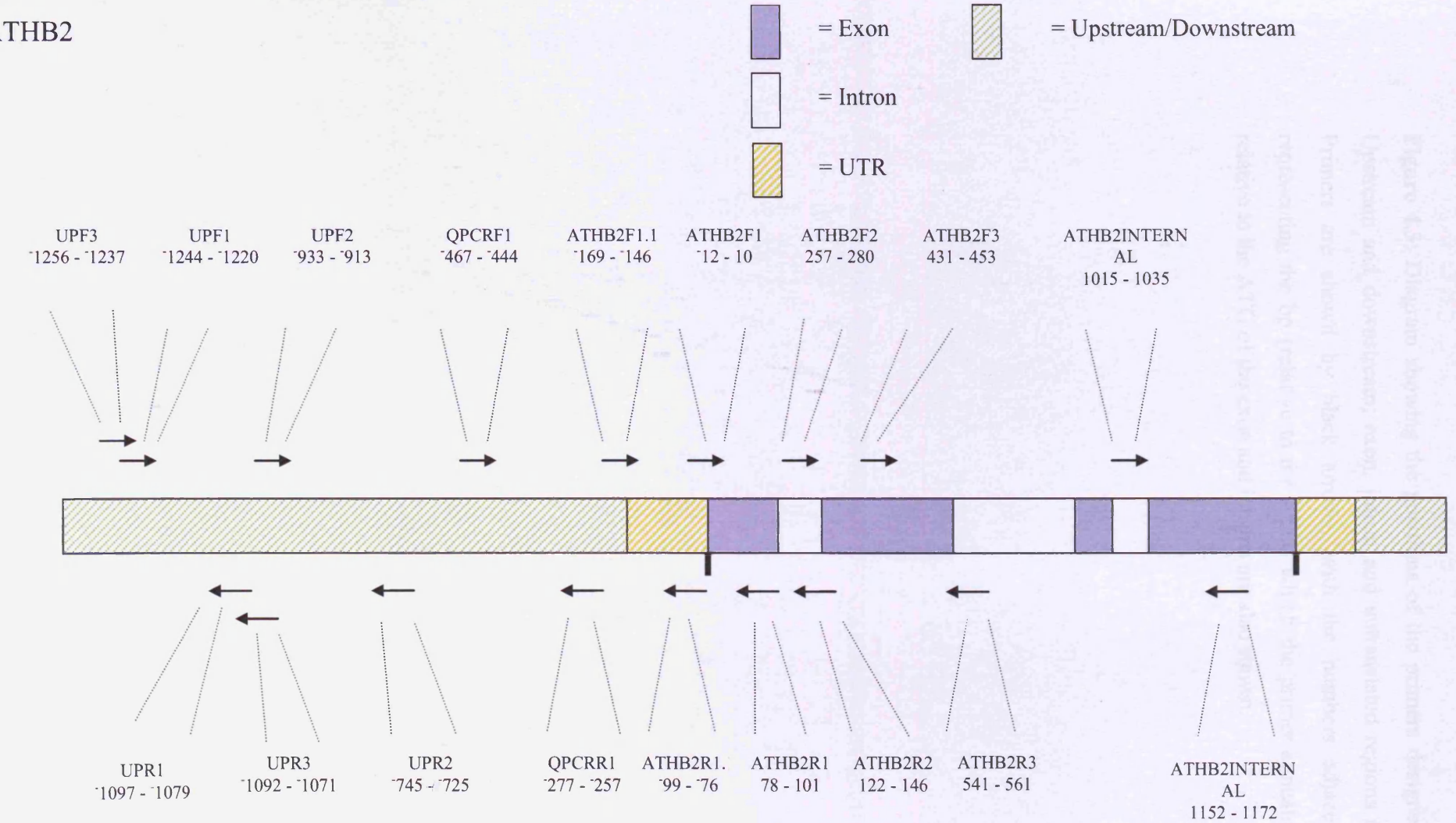

Exon/Intron Boundaries

Exon 1 = 0 – 160 Exon 2 = 263 – 562

Exon 3 = 830 – 910 Exon 4 = 938 – 1314

Figure 4.3: Diagram showing the positions of the primers designed against *ATHB2*. Upstream and downstream; exon, intron and untranslated regions (UTR) are shown. Primers are shown by black arrows, with the numbers adjacent to the arrows representing the bp (relative to the ATG) which the primer anneals to. The positions relative to the ATG of the exon and introns are also shown.

PIL1

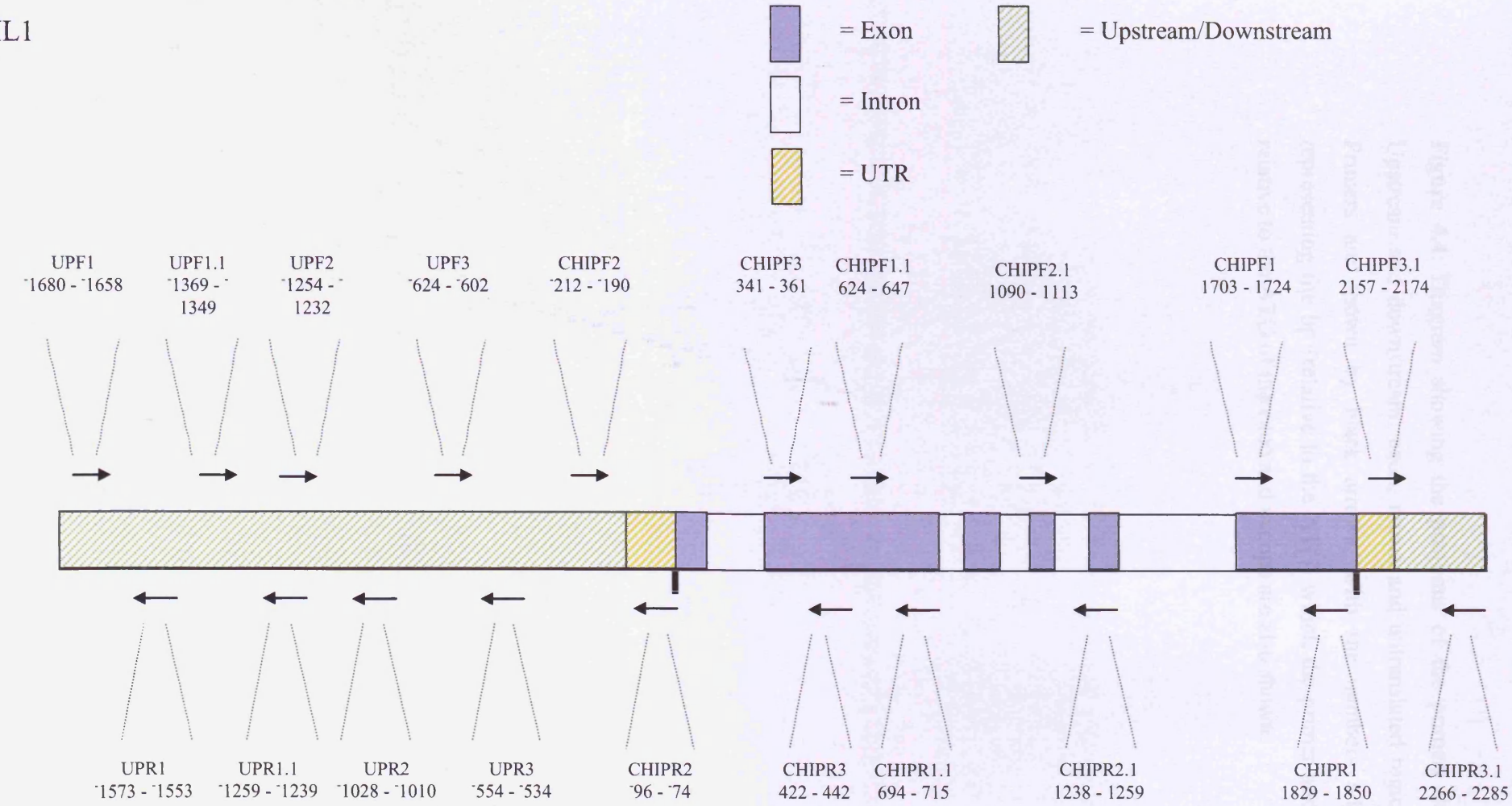

Exon/Intron Boundaries

Exon 1 = 0 – 74 Exon 2 = 249 - 783

Exon 3 = 865 – 972 Exon 4 = 1061 – 1126

Exon 5 = 1232 – 1297 Exon 6 = 1661 – 2062

Figure 4.4: Diagram showing the positions of the primers designed against *PIL1*. Upstream and downstream; exon, intron and untranslated regions (UTR) are shown. Primers are shown by black arrows, with the numbers adjacent to the arrows representing the bp (relative to the ATG) which the primer anneals to. The positions relative to the ATG of the exon and introns are also shown.

4.1.6 Confirming up-regulation of R:FR-regulated gene transcription

Before the ChIP experiments were conducted, a portion of the harvested tissue was removed and used to test the transcript levels of a number of R:FR-regulated genes. The purpose of this experiment was to confirm that the low R:FR treatment was resulting in a change in gene transcription of R:FR-regulated genes. If no change in transcript levels of these genes was observed, then a change in histone modifications would not be expected.

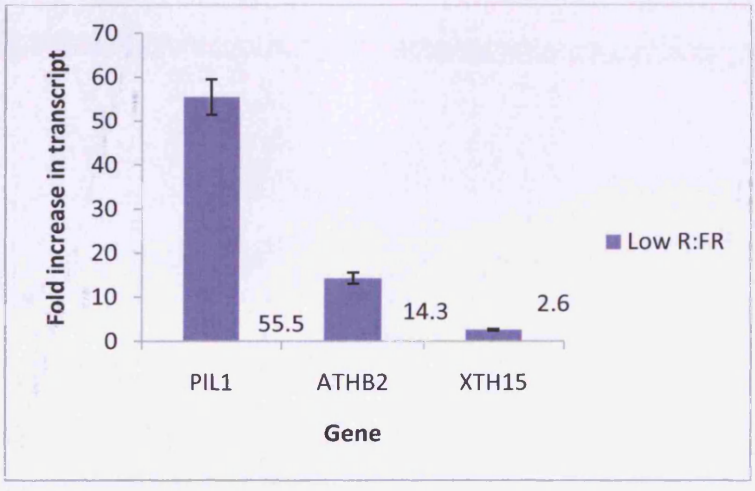

Figure 4.5: Fold increases in transcript abundance for *PIL1*, *ATHB2* and *XTH15* in response to a 4 h, low R:FR ratio treatment. Data are relative to high R:FR controls and are normalised to *ACTIN2*. Data represent mean values from three separate biological repeats. All plant tissue was grown in LD and harvested at 4 h after dawn.

Figure 4.5 shows that the low R:FR treatment resulted in an increase in transcription of the shade avoidance genes *PIL1*, *ATHB2* and *XTH15*. *PIL1* demonstrated the largest increase in transcript, followed by *ATHB2* and *XTH15*. This tissue was then used in ChIP experiments.

4.1.7 Data representation

Data from all the ChIP experiments was in the form of Ct values from the qPCR machine. Ct values represent the amount of template DNA present (3.1.1.2). The amount of DNA present in each precipitation is represented as a proportion of the DNA present in the respective input sample. This referred to as 'enrichment of input' on graphs .Data is shown for primer combinations which worked efficiently in ChIP experiments with good immunoprecipitation and DNA extraction.

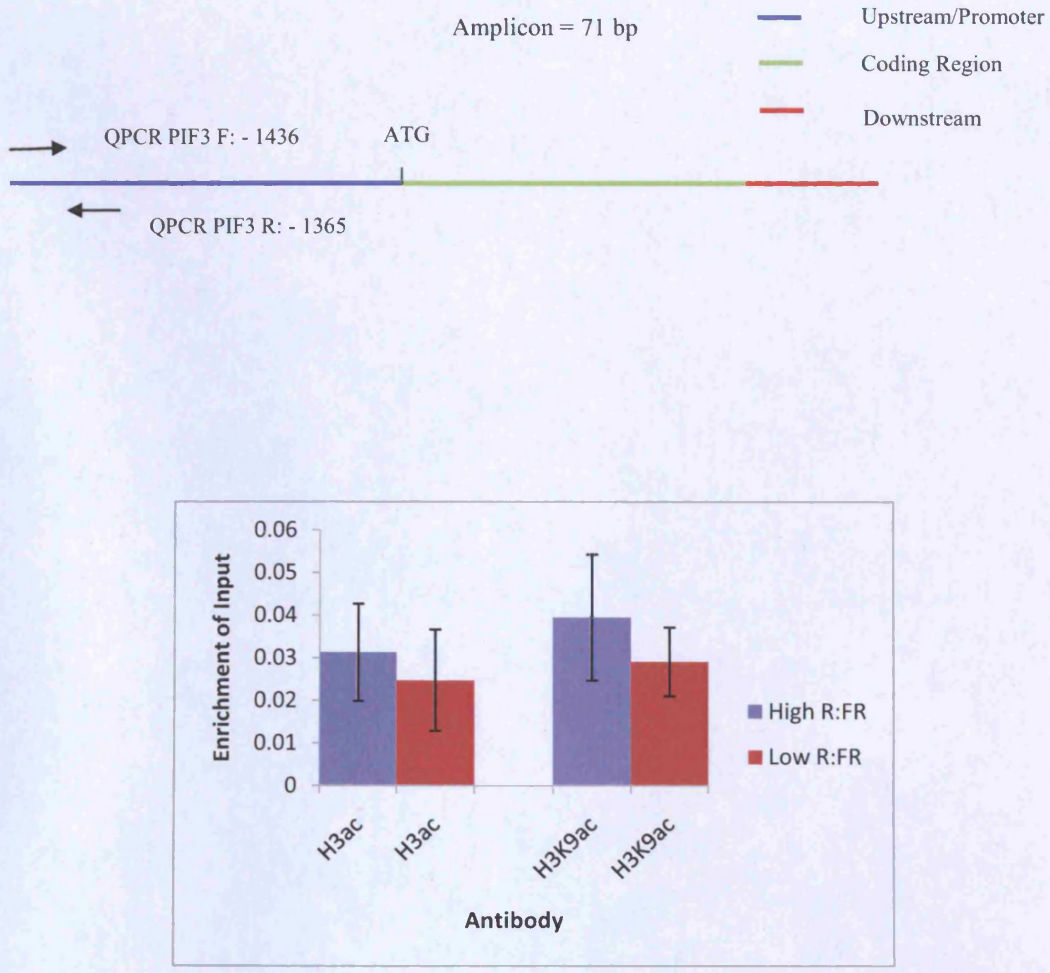

Figure 4.6: Fold enrichment of precipitated DNA using antibodies H3ac and H3K9ac and primers against *PIF3* (region shown in figure S1.3). Blue bars represent plants treated with high R:FR ratio and red bars represent plants treated with low R:FR ratio. The relative enrichment of each treatment is relative to input (input representing 1). Data are from three separate biological repeats. Each biological repeat consists of two or three qPCR repeats. Standard error bars are shown. Above the graph is a cartoon displaying the particulars of the primer set used.

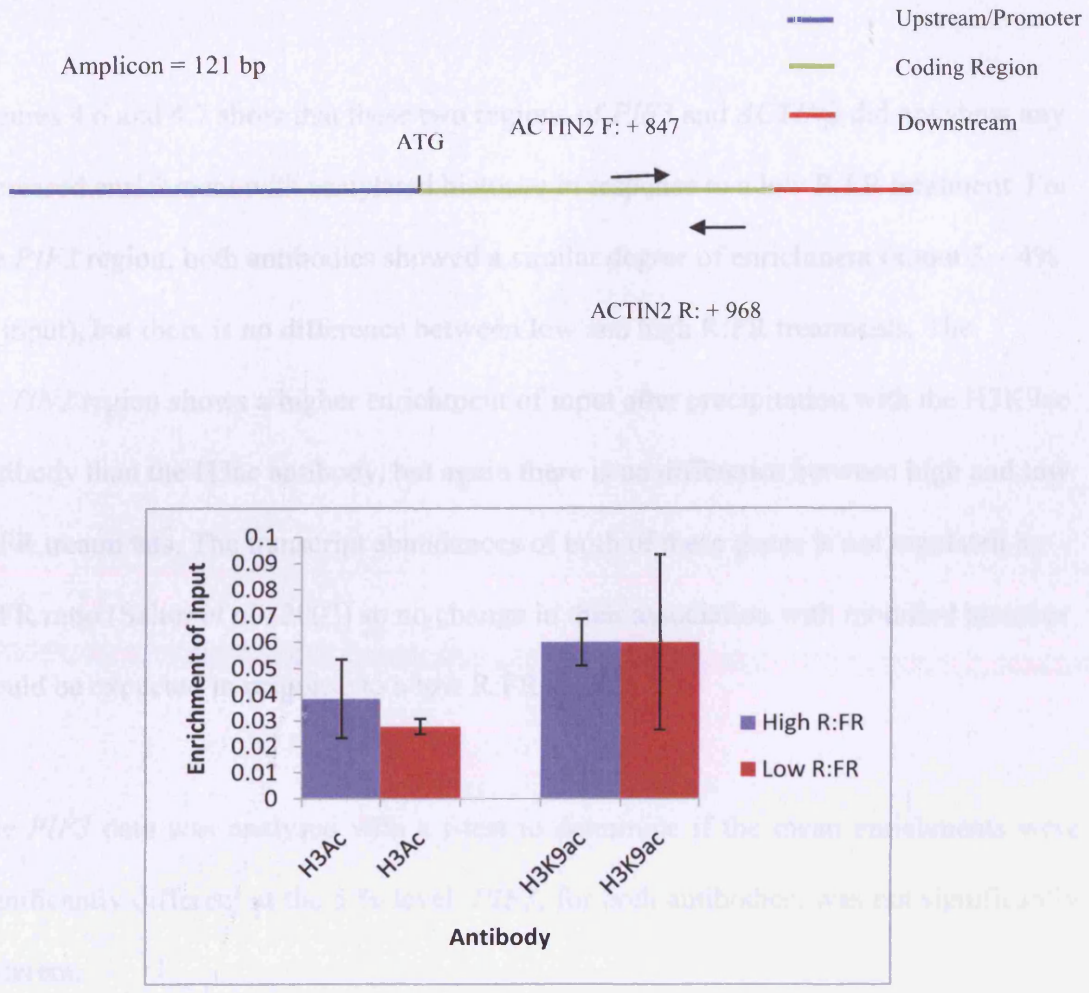

Figure 4.7: Fold enrichment of precipitated DNA using antibodies H3ac and H3K9ac and primers against *ACTIN2* (region shown in S1.9). Blue bars represent plants treated with high R:FR ratio and red bars represent plants treated with low R:FR ratio. The relative enrichment of each treatment is relative to input (input representing 1). Data are from two separate biological repeats. Each biological repeat consists of two or three qPCR repeats. Range bars are shown. Above the graph is a cartoon displaying the particulars of the primer set used.

4.1.8. *PIF3* and *ACTIN2* results

Figures 4.6 and 4.7 show that these two regions of *PIF3* and *ACTIN2* did not show any increased enrichment with acetylated histones in response to a low R:FR treatment. For the *PIF3* region, both antibodies showed a similar degree of enrichment (about 3 – 4% of input), but there is no difference between low and high R:FR treatments. The *ACTIN2* region shows a higher enrichment of input after precipitation with the H3K9ac antibody than the H3ac antibody, but again there is no difference between high and low R:FR treatments. The transcript abundances of both of these genes is not regulated by R:FR ratio (Salter *et al.,* 2003) so no change in their association with modified histones would be expected in response to a low R:FR signal.

The *PIF3* data was analysed with a t-test to determine if the mean enrichments were significantly different at the 5 % level. *PIF3*, for both antibodies, was not significantly different.

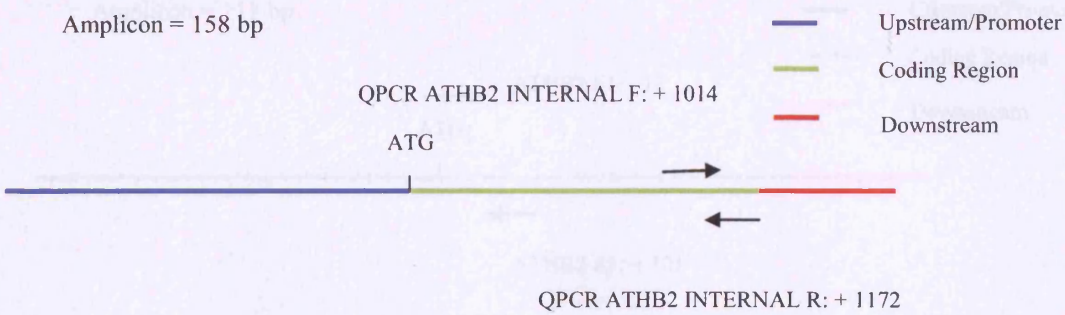

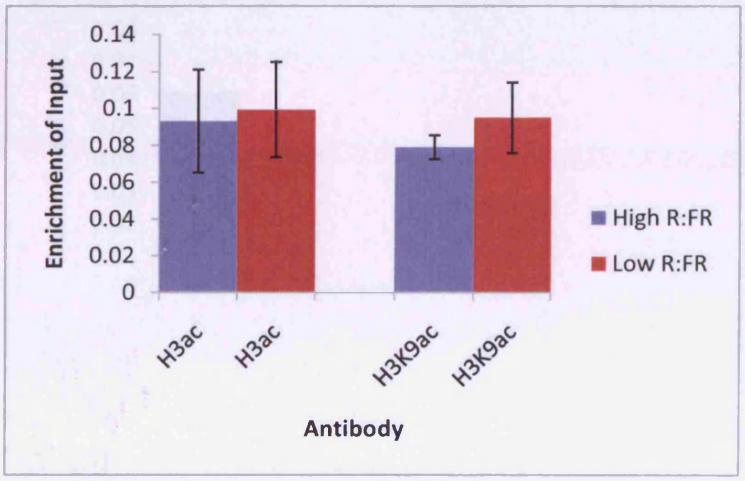

Figure 4.8: Fold enrichment of precipitated DNA using antibodies H3ac and H3K9ac and primers against *ATHB2* exon 4 (*ATHB2* internal). Blue bars represent plants treated with high R:FR ratio and red bars represent plants treated with low R:FR ratio. The relative enrichment of each treatment is relative to input (input representing 1). Data are from three separate biological repeats. Each biological repeat consists of two or three qPCR repeats. Standard error bars are shown. Above the graph is a cartoon displaying the particulars of the primer set used.

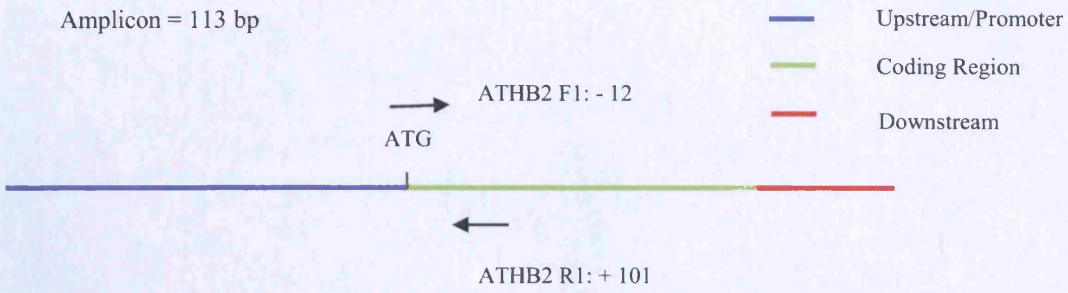

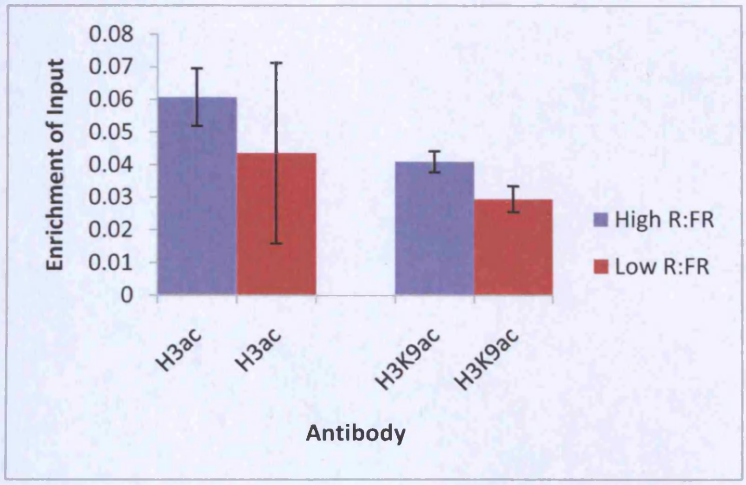

Figure 4.9: Fold enrichment of precipitated DNA using antibodies H3ac and H3K9ac and primers against *ATHB2* exon 1 (*ATHB2* F1/R1). Blue bars represent plants treated with high R:FR ratio and red bars represent plants treated with low R:FR ratio. The relative enrichment of each treatment is relative to input (input representing 1). Data are from two separate biological repeats. Each biological repeat consists of two or three qPCR repeats. Range bars are shown. Above the graph is a cartoon displaying the particulars of the primer set used.

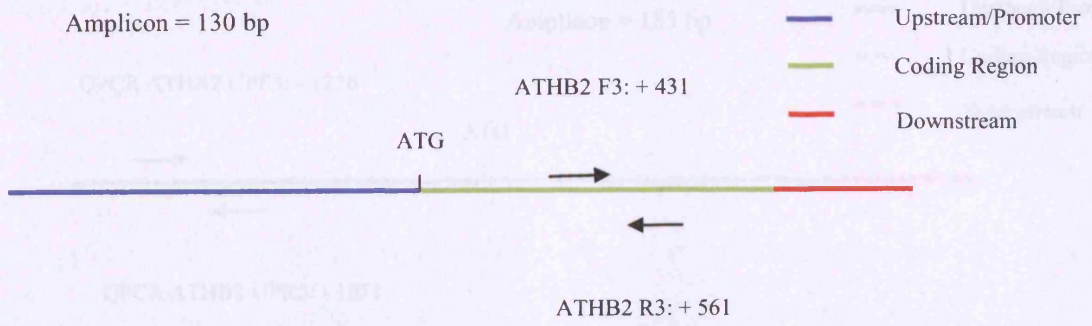

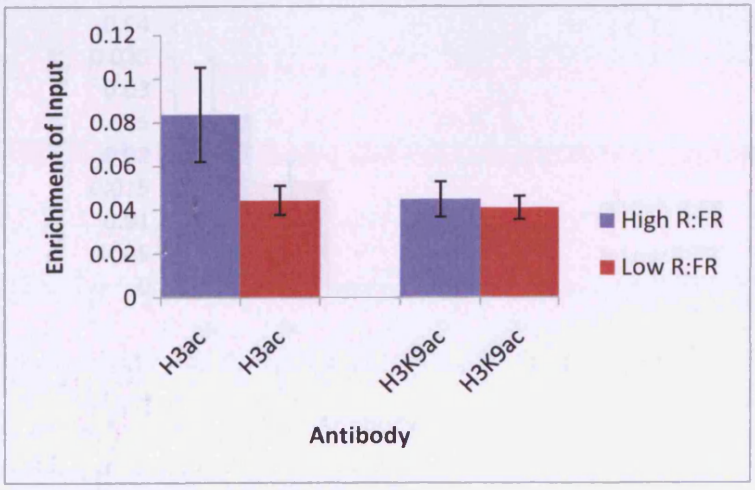

Figure 4.10: Fold enrichment of precipitated DNA using antibodies H3ac and H3K9ac and primers against *ATHB2* exon 2 (*ATHB2* F3/R3). Blue bars represent plants treated with high R:FR ratio and red bars represent plants treated with low R:FR ratio. The relative enrichment of each treatment is relative to input (input representing 1). Data are from three separate biological repeats. Each biological repeat consists of two or three qPCR repeats. Standard error bars are shown. Above the graph is a cartoon displaying the particulars of the primer set used.

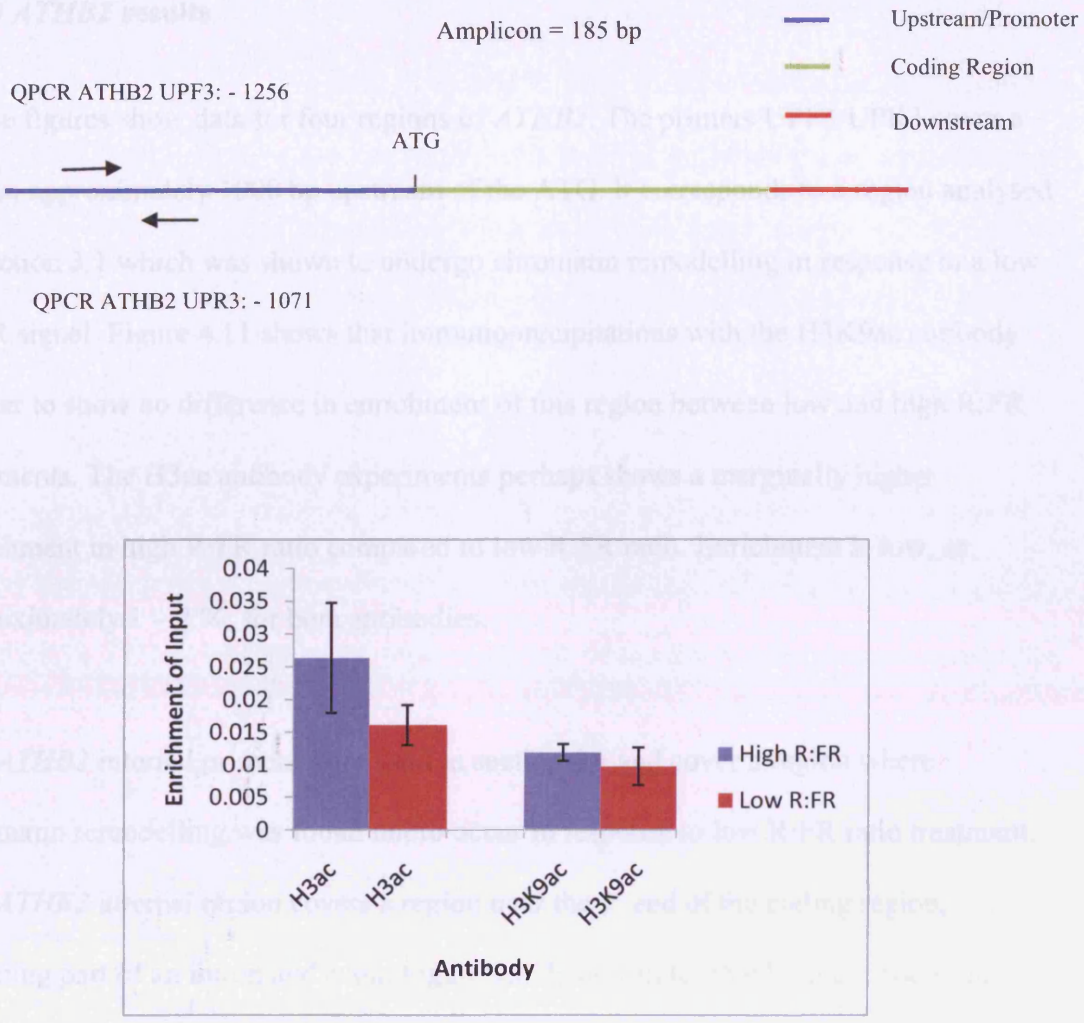

Figure 4.11: Fold enrichment of precipitated DNA using antibodies H3ac and H3K9ac and primers against an upstream region of the *ATHB2* promoter (ATHB2 UPF3/UPR3). Blue bars represent plants treated with high R:FR ratio and red bars represent plants treated with low R:FR ratio. The relative enrichment of each treatment is relative to input (input representing 1). Data are from three separate biological repeats. Each biological repeat consists of two or three qPCR repeats. Standard error bars are shown. Above the graph is a cartoon displaying the particulars of the primer set used.

4.1.9 *ATHB2* results

These figures show data for four regions of *ATHB2*. The primers UPF3/UPR3 cover a region approximately 1000 bp upstream of the ATG. It corresponds to a region analysed in section 3.1 which was shown to undergo chromatin remodelling in response to a low R:FR signal. Figure 4.11 shows that immunoprecipitations with the H3K9ac antibody appear to show no difference in enrichment of this region between low and high R:FR treatments. The H3ac antibody experiments perhaps shows a marginally higher enrichment in high R:FR ratio compared to low R:FR ratio. Enrichment is low, at approximately 1 – 2 %, for both antibodies.

The *ATHB2* internal primers were used in section 3.1 and cover a region where chromatin remodelling was found not to occur in response to low R:FR ratio treatment. The *ATHB2* internal region covers a region near the 3' end of the coding region, spanning part of an intron and exon. Figure 3.8 demonstrates that both antibodies have precipitated DNA to a similar extent, in the region of 8 – 10 % of input and show no difference in the amount of enrichment between low and high R:FR ratio treatments.

Figure 4.9 shows data for a primer set called ATHB2 F1/R1, which spans the start codon of *ATHB2* and extends into the first exon. Both antibodies show a similar amount of enrichment, approximately 3 – 6 %. The H3ac antibody does not appear to show any enrichment of this sequence in response to a low R:FR ratio treatment. The H3K9ac antibody shows a very slight increase in enrichment of this sequence in the high R:FR ratio treatment.

Figure 4.10 shows data for a primer set called ATHB2 F3/R3 which covers an exon in the middle of the gene and part of an intron. The H3K9ac antibody shows similar enrichment for this sequence in both high and low R:FR treatments, with an enrichment of input of about 4 %. The H3ac antibody shows an enrichment of about 4% in the low R:FR treatment but an enrichment of about 8 % in the high R:FR treatment. The error bars, are however, large.

Experiments with a minimum of 3 biological repeats were analysed with a students t-test to determine if the mean enrichments were significantly different at the 5 % level. None of the *ATHB2* regions, with either antibody, were significantly different using this analysis.

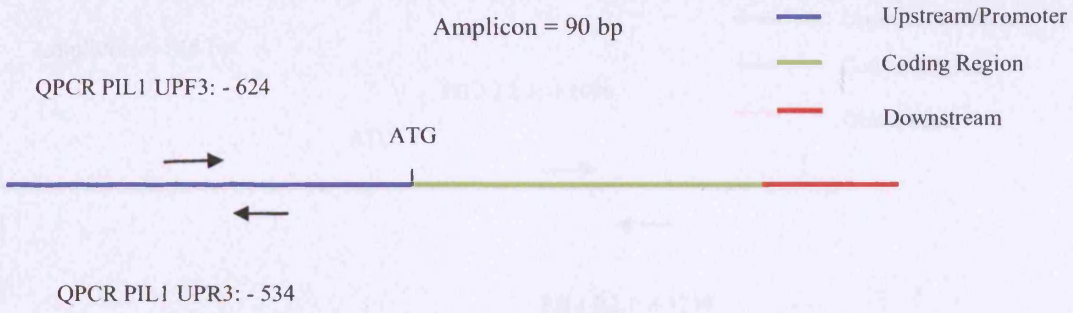

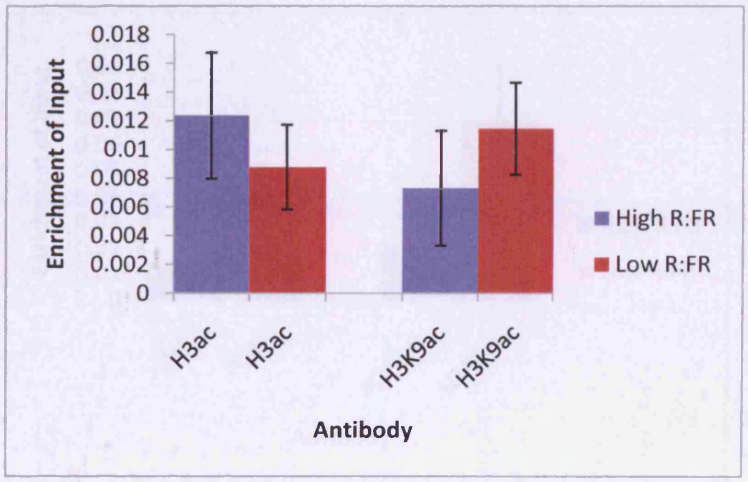

Figure 4.12: Fold enrichment of precipitated DNA using antibodies H3ac and H3K9ac and primers against a region of the *PIL1* promoter (PIL1 UPF3/UPR3). Blue bars represent plants treated with high R:FR ratio and red bars represent plants treated with low R:FR ratio. The relative enrichment of each treatment is relative to input (input representing 1). Data are from two separate biological repeats. Each biological repeat consists of two or three qPCR repeats. Range bars are shown. Above the graph is a cartoon displaying the particulars of the primer set used.

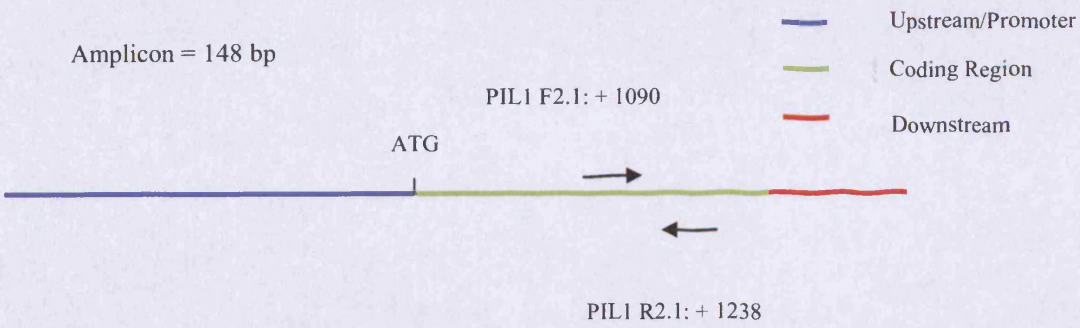

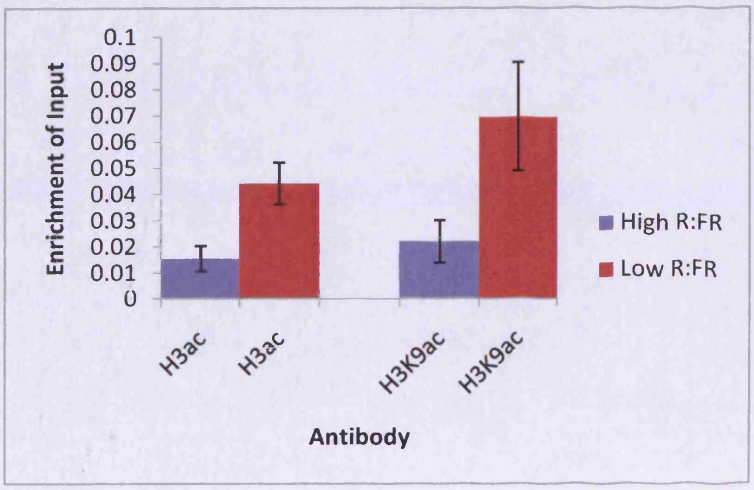

Figure 4.13: Fold enrichment of precipitated DNA using antibodies H3ac and H3K9ac and primers against a region containing *PIL1* exons 4 and 5 (PIL1 F2.1/R2.1). Blue bars represent plants treated with high R:FR ratio and red bars represent plants treated with low R:FR ratio. The relative enrichment of each treatment is relative to input (input representing 1). Data are from three separate biological repeats. Each biological repeat consists of two or three qPCR repeats. Standard error bars are shown. Above the graph is a cartoon displaying the particulars of the primer set used.

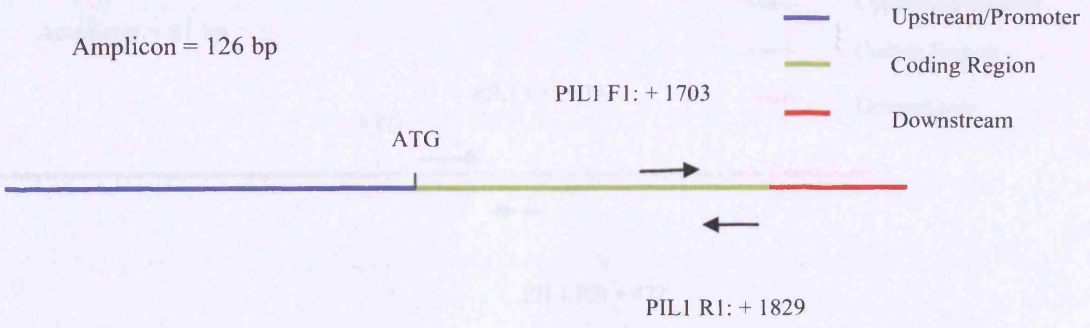

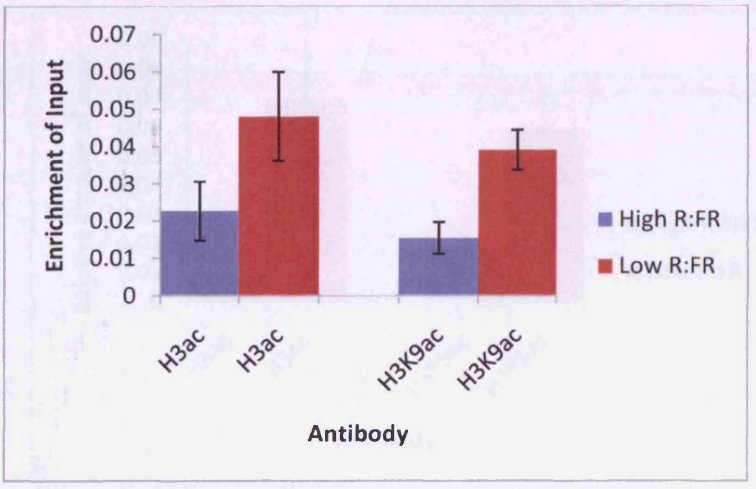

Figure 4.14: The fold enrichment of precipitated DNA using antibodies H3ac and H3K9ac and primers against a region of exon 6 of *PIL1* (PIL1 F1/R1). Blue bars represent plants treated with high R:FR ratio and red bars represent plants treated with low R:FR ratio. The relative enrichment of each treatment is relative to input (input representing 1). Data are from three separate biological repeats. Each biological repeat consists of two or three qPCR repeats. Standard error bars are shown. Above the graph is a cartoon displaying the particulars of the primer set used.

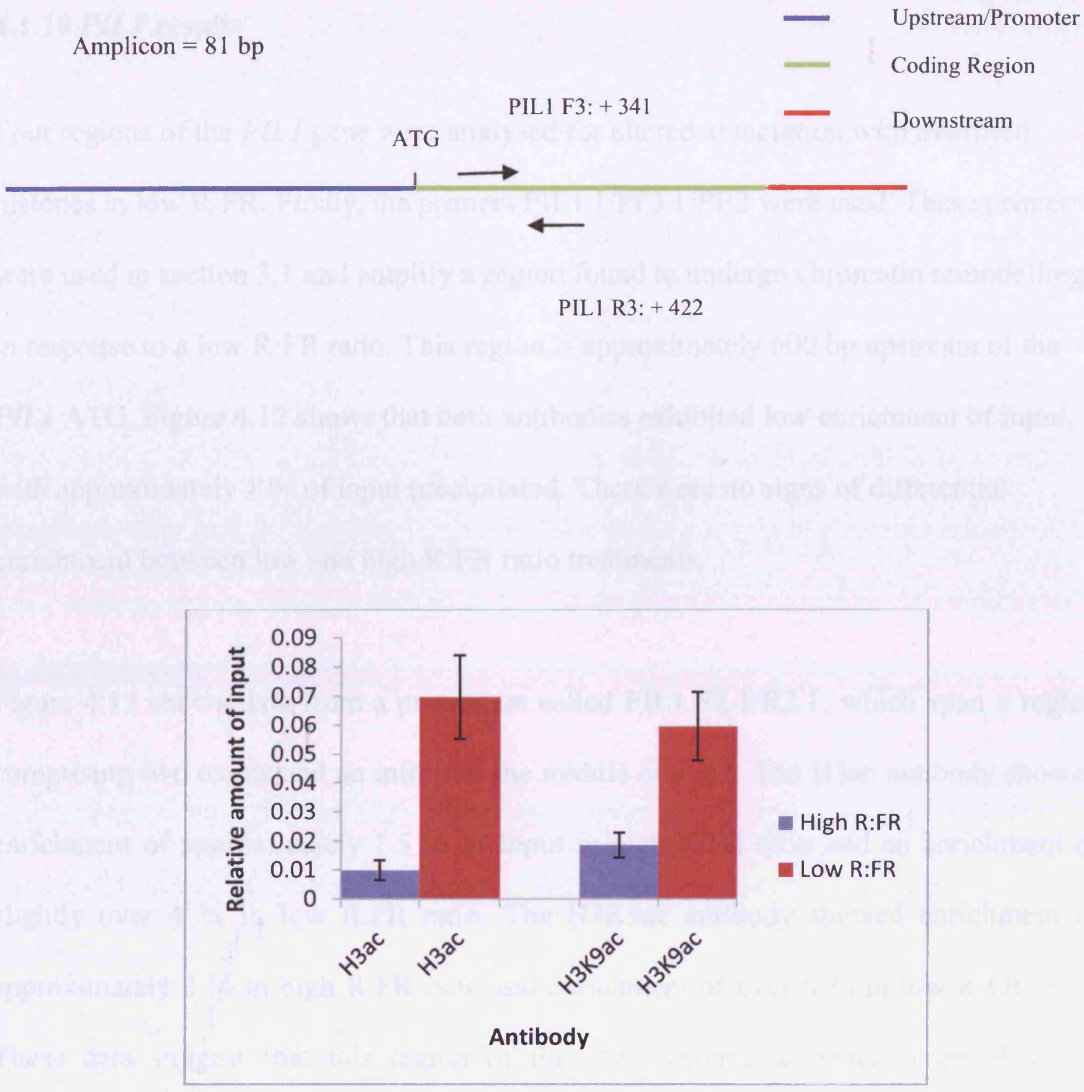

Figure 4.15: Fold enrichment of precipitated DNA using antibodies H3ac and H3K9ac and primers against a region of *PIL1* exon 2 (PIL1 F3/R3). Blue bars represent plants treated with high R:FR ratio and red bars represent plants treated with low R:FR ratio. The relative enrichment of each treatment is relative to input (input representing 1). Data are from three separate biological repeats. Each biological repeat consists of two or three qPCR repeats. Standard error bars are shown. Above the graph is a cartoon displaying the particulars of the primer set used.

4.1.10 *PIL1* results

Four regions of the *PIL1* gene were analysed for altered association with modified histones in low R:FR. Firstly, the primers PIL1 UPF3/UPR3 were used. These primers were used in section 3.1 and amplify a region found to undergo chromatin remodelling in response to a low R:FR ratio. This region is approximately 600 bp upstream of the *PIL1* ATG. Figure 4.12 shows that both antibodies exhibited low enrichment of input, with approximately 1 % of input precipitated. There were no signs of differential enrichment between low and high R:FR ratio treatments.

Figure 4.13 shows data from a primer set called PIL1 F2.1/R2.1, which span a region comprising two exons and an intron in the middle of *PIL1*. The H3ac antibody showed enrichment of approximately 1.5 % of input in high R:FR ratio and an enrichment of slightly over 4 % in low R:FR ratio. The H3K9ac antibody showed enrichment of approximately 2 % in high R:FR ratio and enrichment of over 6 % in low R:FR ratio. These data suggest that this region of the *PIL1* coding sequence is enriched for acetylated histone H3 at region K9 and possibly region K14 in response to a low R:FR treatment and that enrichment is about 3 fold of that observed in high R:FR ratio conditions.

Another region of the *PIL1* promoter was analysed, shown in figure 4.14. The primers used were PIL1 F1/R1 and they cover a region at the 3' end of the region, comprising the final exon. The H3ac antibody in high R:FR ratio showed enrichment of approximately 2 % and in low R:FR ratio, almost 5 %. The H3K9ac antibody shows enrichment in high R:FR ratio of slightly over 1 % and enrichment of almost 4 % in low

R:FR ratio. Therefore, both antibodies are in agreement that this region of the *PIL1* coding region is enriched for acetylation of histone H3, as for region PIL1 F2.1/R2.1.

A final region of *PIL1* was analysed. Primers PIL1 F3/R3 cover a region of the second exon in the 5' coding region. Figure 4.15 shows that H3ac antibody precipitated approximately 1 % of input in high R:FR ratio and in low R:FR ratio precipitated over 6 % of input. The H3K9ac antibody had levels of enrichment of almost 2 % of input in low R:FR ratio and almost 6 % of input in low R:FR ratio. This is another region of the *PIL1* coding region which is shown to be enriched for H3 acetylation in response to a low R:FR signal.

Experiments with a minimum of 3 biological repeats were analysed with a students t-test to determine if the mean enrichments were significantly different at the 5 % level. The regions PIL1 F2.1/R2.1 using H3ac, PIL1 F1/R1 using H3K9ac; and PIL1 F3/R3 using H3K9ac and H3ac were all significant. None of the other immunoprecipitations for *PIL1* were significant with this analysis.

4.2 TSA experiments

Perlaes and Mas (2007) investigated the effects of using histone deacetylase (HDAC) inhibitors on gene expression. Having shown that *TOC1* undergoes rhythmic association with acetylated and de-acetylated histones and that these associations are tightly coupled with changes in gene expression, they reasoned that HDAC inhibitors should be capable of disrupting this regulation. It was considered that a similar approach could be adopted here. If histone acetylation is important in the regulation of gene expression responses to low R:FR ratio, then inhibition of HDACs should modulate these.

The experiment involved transferring seedlings into Petri dishes containing either the HDAC inhibitor, Trichostatin A (TSA), in buffered Dimethyl sulfoxide (DMSO) or a control solution of DMSO. These were left to incubate for an hour before half were transferred to low R:FR ratio. At particular time-points, plants were removed, RNA extracted and gene expression assessed. The experimental procedure is detailed in 2.2.13. All data is normalised to the 0 time-point of the control high R:FR ratio treated seedlings.

4.2.1 Plant growth conditions

WT *Arabidopsis* Col plants were grown on soil for 14 days in LD at 22°C high R:FR. One hour after dawn on the 15th day (Zeitgeiber Time 1: ZT1), seedlings were treated with TSA before transfer to low R:FR at ZT2.

4.2.2 Primers used

Primers used are ATHB2 internal F and R and PIL1 F3 and R3, they are shown in 2.2.14.

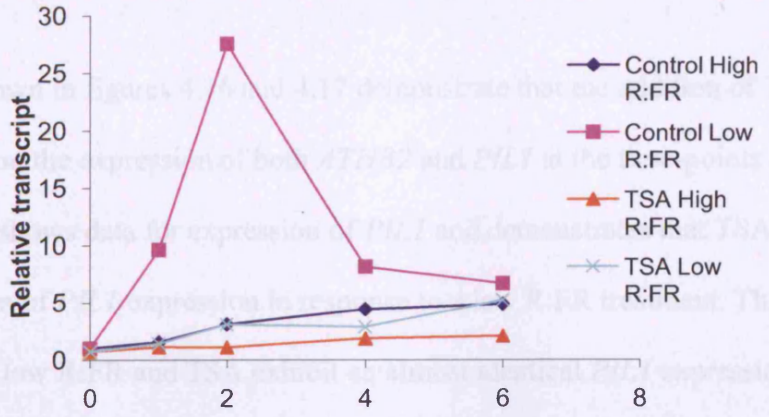

Figure 4.16: Relative transcript abundance of *PIL1* compared to control high R:FR ratio treated seedlings at time point 0. Seedlings were either treated with high or low R:FR ratio and with or without TSA (10 μM). Data is from one biological repeat and three technical qPCR repeats.

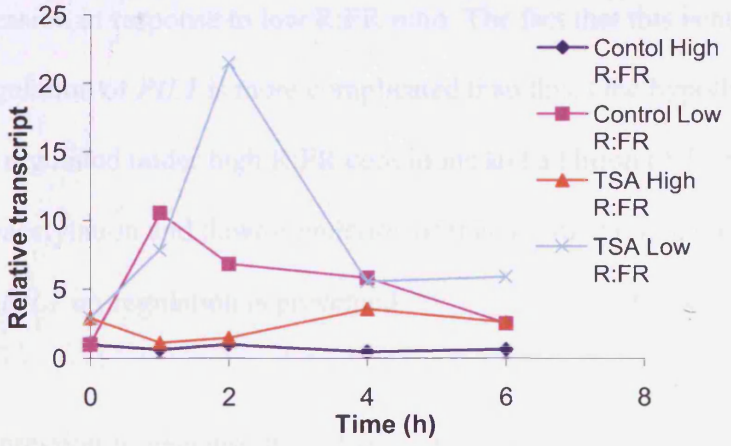

Figure 4.17: Relative transcript abundance of *ATHB2* compared to control high R:FR ratio treated seedlings at time point 0. Seedlings were either treated with high or low R:FR ratio and with or without TSA (10 μM). Data is from one biological repeat and three technical qPCR repeats.

4.2.3 TSA results

The data shown in figures 4.16 and 4.17 demonstrate that the addition of TSA has a clear effect on the expression of both *ATHB2* and *PIL1* at the time-points analysed. Figure 4.16 shows data for expression of *PIL1* and demonstrates that TSA abrogates the up-regulation of *PIL1* expression in response to a low R:FR treatment. The seedlings treated with low R:FR and TSA exhibit an almost identical *PIL1* expression profile to that of seedlings grown in high R:FR ratio. This suggests that preventing de-acetylation results in *PIL1* expression not being up-regulated in response to a low R:FR treatment. At first, this seems counter intuitive because the findings from the ChIP experiments suggest that *PIL1* is acetylated in response to a low R:FR ratio treatment and TSA, which inhibits de-acetylation, might be expected to result in heightened and prolonged acetylation of *PIL1* (as is seen in *TOC1* (Perales and Mas 2007)), resulting in increased *PIL1* expression in response to low R:FR ratio. The fact that this is not seen suggests that the regulation of *PIL1* is more complicated than this. One hypothesis is that *PIL1* is negatively regulated under high R:FR conditions and addition of TSA prevents the normal de-acetylation and down-regulation of this negative regulator in low R:FR ratio and hence *PIL1* up-regulation is prevented.

ATHB2 expression in response to a TSA treatment is somewhat different. In contrast to *PIL1*, figure 3.17 shows that *ATHB2* expression is increased in both magnitude and duration and is slightly phase shifted (as seen in *TOC1* (Perales and Mas 2007)) in response to TSA treatment and low R:FR ratio treatment. This seems to suggest a different mechanism of regulation of *ATHB2* compared to *PIL1*. The ChIP data for *ATHB2* suggests that the regions analysed are not acetylated at the residues studied.

This does not mean, however, that *ATHB2* is not acetylated at other regions. Another possibility is that *ATHB2* is not itself acetylated but TSA treatment promotes acetylation of a positive regulator. Until more is known about the regulation of *ATHB2* it is not possible to determine what is occurring. All that can be said is that it appears that acetylation is important in the regulation of *ATHB2*, either directly or indirectly. The enhanced expression of *ATHB2* with TSA treatment in low R:FR additionally gives confidence that the abrogation of *PIL1* signalling is biologically meaningful and not an artefact due to chemical toxicity.

4.3 Discussion

Following the results obtained in the DNaseI sensitivity experiments, an analysis of histone modifications in response to a low R:FR ratio treatment was undertaken. The results of the ChIP investigation show that low R:FR treatment results in an altered association of acetylated H3 with shade avoidance marker genes.

The levels of enrichment obtained were compared to other studies that had performed ChIP in *Arabidopsis*. Guo *et al* (2008) showed clearly that the level of enrichment relative to input can vary widely for different antibodies and their paper shows enrichment levels of input from 0.1 % to 15 %. The enrichment obtained here, is well within this range, with the lowest levels of enrichment of input being in the region of 0.5 % and the highest levels of enrichment of input around 10 %. Guo *et al* (2008) also found that in response to a particular treatment, enrichment can increase at a particular location for a specific modification by up to about 5 fold. Here, the highest enrichment in response to treatment is approximately 6 fold. The numbers obtained from this investigation are therefore similar to those of published results and this provides further confidence in the data.

The R:FR regulated genes *PIL1* and *ATHB2* and the control gene *PIF3* and *ACTIN2* were investigated for histone modifications in response to a low R:FR ratio signal. Figures 4.6 and 4.7 show the data for *PIF3* and *ACTIN2*, respectively. They demonstrate that the regions of these genes analysed do not show enrichment of H3 acetylation of residues K9 and K14 in response to a low R:FR ratio signal. One region of each of these control genes was studied. The region of the *PIF3* promoter analysed is

approximately 1500 bp upstream of the ATG. Previous work has suggested that the promoter regions of genes are modified (Bastow *et al.,* 2004). However, other work has suggested that it is the coding regions that exhibit the greatest enrichment of histone modifications (Pokholok *et al.* 2005). Given the conflicting data, a coding region of *ACTIN2* was analysed. The region of *ACTIN2* analysed is in exon 2, in the 3' coding region of the gene. Future experiments should involve the addition of controls with additional regions of *ACTIN2* and *PIF3*, being analysed.

Ideally in the ChIP investigation, the entire promoter and coding regions of *PIL1, ATHB2* and *XTH15* would have been covered with overlapping primers. This wasn't done for *XTH15* because of time constraints. The entire sequences of *ATHB2* and *PIL1* were not investigated as a number of the designed primer combinations failed to produce a product. Primer design programmes could be utilised to design primers with better efficacy. This should be performed to determine if there are regions of *ATHB2* which are modified in response to a low R:FR signal and also to accurately map the regions of *PIL1* which are modified. Other antibodies could also be tested as it might be the case that *ATHB2* associates with histones containing different modifications in low R:FR.

Four regions of *ATHB2* were analysed, shown in figures 4.8 – 4.11, comprising 3 coding and 1 promoter regions. Results demonstrate that none of these regions are enriched for acetylation on histone H3 at residues K9 or K14 in response to a low R:FR signal. Two regions of the *ATHB2* coding region, shown in figure 4.10 and 4.11, do show minor increases in enrichment in the high R:FR treatment, however, the difference is small and not significant using the t test method. It therefore appears that

the regions of *ATHB2* analysed do not undergo acetylation at H3K9 or H3K14 in response to low R:FR signal.

In total, four regions of *PIL1* were analysed. These data are shown in figures 4.12 – 4.15. Figure 4.12 shows data for a region of the *PIL1* promoter. This region is not modified on H3 at regions K9 or K14 in response to a low R:FR signal. This is in contrast to the three different coding regions shown in figures 4.13 – 4.15, which all show modifications of H3 at position K9 and possibly at position K14 (although they are not all significant at the 5 % level). From the data, it is only possible to conclude that H3K9ac association increases in response to a low R:FR signal at these regions. It is possible that H3K14ac association is also increasing as the H3ac antibody also recognises H3K14ac. With more time, this could be investigated through ChIP experiments using antibodies raised against H3K14.

Studies in yeast have suggested that in actively transcribed genes, H3K9ac acetylation is particularly prominent at the 5' end of the coding region with a slightly less prominent H3K9ac peak at the 3' end of the coding region (Pokholok *et al.,* 2005). Furthermore, regions of H3K9ac were found to strongly correlate with H3K14ac marks, except that the H3K14ac was not as prominent in the 3' coding region of genes. H4ac marks (the antibody used recognised acetylated K5, K8, K12 and K16 so it was not possible to tell which exact marks) and H3K4me3 also correlated with the presence of H3K9ac. This broadly agrees with the results found for a low R:FR treatment, with acetylation of *PIL1* found in the 5' and 3' coding regions This study also found that there was a strong correlation between transcription rates and enrichment of modifications. It was shown that highly expressed genes were frequently enriched for

H3K9ac and K3K14ac across the entire coding region; however, genes that were transcribing at lower levels were enriched at the 5' coding regions, but across the rest of the coding region enrichment was no higher than background (Pokholok *et al.,* 2005). Different levels of gene expression could potentially explain some of the differences observed between *PIL1* and *ATHB2* acetylation. From the data obtained, it is not directly possible to determine whether *PIL1* is expressed at a higher level that *ATHB2*. However, if assumptions are made then estimations can be made to the relative expression of *PIL1* and *ATHB2*. The mRNA raw data demonstrates that *PIL1* has a Ct value at least 3 - 4 cycles lower than *ATHB2* (data not shown) for the same low R:FR treated samples. Given that both sets of primers used to measure *PIL1* and *ATHB2* expression have a similarly high efficiency and if it can be assumed that *PIL1* and *ATHB2* have similar RNA stability/RNA extraction rates, then *PIL1* is transcribed somewhere in the region of 10 times (2^{3-4}) more than *ATHB2*. Pokholok *et al* (2005) have demonstrated, in yeast, that a 10 fold difference in transcription rates between two genes could be sufficient to produce a significantly different enrichment profile. They showed that a highly-expressed gene could exhibit a 4-fold H3K9ac/H3K14ac enrichment at the 5' of the coding region and approximately 2 - 3 fold enrichment across the rest of the coding region; whereas, a gene expressed 10 fold lower than this could exhibit a 1.5 fold H3K9ac/H3K14ac enrichment at the 5' coding region and no enrichment in the rest of the coding region. This could be exactly what is occurring here with *PIL1* and *ATHB2*. *PIL1* demonstrates enrichment of H3K9ac/H314ac in the range of 3 – 6 fold at a number of sites across its coding region. This is in contrast to *ATHB2*, which does not show an enrichment in response to a low R:FR treatment. An enrichment of 1.5 could well be below the resolution of the ChIP experiments performed here. If so, then *ATHB2* could be being enriched for these modifications, but

just at such a low level that it is not easily detected. The work by Pokholok *et al* (2005) also demonstrates the variability in enrichment exhibited across a gene. It could well be that *ATHB2* is enriched at precise regions and the primer sets used missed these regions. The data here shows that *PIL1* is strongly associated with H3K9ac (and possibly H3K14ac) in low R:FR but *ATHB2*, is not. The mRNA expression data suggest that both genes are strongly up-regulated in response to a low R:FR signal; however, only one time-point was analysed and therefore both genes may subtly exhibit different regulation. Perales and Mas (2007) found that *TOC1* expression was correlated with H3 acetylation and that H3 acetylation was slightly advanced of *TOC1* expression. It is also therefore possible that the histone acetylation profile of *ATHB2* is already beginning to be removed at the time of harvesting, despite high levels of gene expression. If histone modifications directly induce transcription then these would be expected to be relatively tightly coupled. One caveat, in this line of reasoning, is that the stability of mRNAs are regulated by a number of processes (Fabian *et al.,* 2010) and an abundance of mRNAs does not necessarily mean that they have been recently transcribed. It is possible that that the high levels of *ATHB2* mRNA observed in these experiments are from prior transcriptional events. Histone marks would have therefore been completely removed at the time of harvesting

Another complicating matter is the fact that *ATHB2* may regulate its own transcription. Previous work has suggested that ATHB2 acts as repressor (Steindler *et al.,* 1999). Furthermore, it has been demonstrated *in vitro* and intimated *in vivo* that *ATHB2* is capable of binding its own promoter (Ohgishi et al., 2001). If ATHB2 can bind its own promoter then its expression can be rapidly regulated in a small feedback loop. It is possible that *ATHB2* regulates its own promoter by recruiting deacetylases, thereby

reducing transcription. Rapid increases in expression of *ATHB2* mRNA (and hence protein) would therefore rapidly de-acetylate the *ATHB2* promoter.

A more simple explanation for the results observed is that *ATHB2* is not regulated by H3K9/H3K14ac. It is possible that other histone marks and/or histones are important and these modifications should be investigated. Alternatively, *ATHB2* mRNA expression could be regulated by means other than chromatin modifications, such as by microRNAs or recruitment of transcription factors. A low R:FR ratio treatment may result in down-regulation of a microRNA that is negatively regulating *ATHB2* mRNA stability, consequently resulting in an increase in *ATHB2* mRNA expression (Bartel, 2009). However, it seems more likely that *ATHB2* is regulated at the transcriptional level given the fact that changes in DNaseI sensitivity of the *ABTH2* promoter are observed in response to low R:FR treatment.

The exact purpose of the histone acetylation marks investigated in this study is unknown. One theory is that acetylation could result in a signal that enhances protein recruitment and binding (Dion *et al.*, 2005). Alternatively, acetylation could reduce the positive charge of histones which results in reduced affinity to negatively charged DNA (Hong *et al.*, 1993) and disruption of local and higher-order chromatin structures (Dion *et al.*, 2005). If this simple explanation were true it would presumably mean that regions that become acetylated also become more open in structure, translating into increases in DNaseI sensitivity. Unfortunately, none of the regions analysed in this study underwent both histone acetylation and increases in DNaseI sensitivity. The reason for this was that the DNaseI experiments were performed first and then the ChIP experiments were performed. Some of the regions shown to exhibit increased DNaseI

sensitivity were tested for changes in histone acetylation states but none were found. Conversely, none of the regions which exhibited changes in histone acetylation were analysed in the DNaseI sensitivity study. Given more time, the regions which demonstrated changes in acetylation would be studied for changes in DNaseI sensitivity as this would determine if histone acetylation of these regions is associated with DNaseI sensitivity, which would indicate an association between acetylation and unwrapping of nucleosome-DNA contacts.

A key question is how changes in histone acetylation and DNsaeI sensitivity relate to increased transcription. Studies in yeast have found that it is common feature for the DNA at promoter regions of genes to associate weakly with nucleosomes compared to other regions of the genome. This results in a relative paucity of nucleosomes at promoters and increased accessibility to transcription factors compared to regions with higher nucleosome density (Sekinger *et al.,* 2005). Promoter regions, where transcription factors bind, are therefore intrinsically more accessible than the rest of the genome. This may allow binding of transcription factors/activators to these regions of lower histone density and this in turn results in recruitment of co-activators in the form of histone remodelling factors and HATs. These co-activators may either directly move nucleosomes or result in modifications that open up the DNA further, thereby enhancing binding of the transcriptional apparatus. Histone modifications may also result in the recruitment of certain factors involved in transcription and may aid and stabilise their binding. Previous work, in yeast, has suggested that elements of the transcriptional machinery can bind in the absence of chromatin remodelling but for the binding of RNA pol II and TFIID and initiation of transcription, nucleosome displacement is required. This has led to suggestions that this mechanism could

function when converging signals are required. It is possible that one signal permits the recruitment of chromatin remodelers and RNA pol II and the other signal permits formation of the other factors involved in transcription (Zanton and Pugh, 2006). Conflictingly, another study, again in yeast, found that a number of elements of the transcriptional complex, including TFIID and RNA pol II are required for the proper binding of chromatin remodelling complexes, as opposed to the other way round, but are not required for binding of HAT proteins. This highlights the complexity of the situation and suggests that there is probably some degree of heterogeneity in recruitment of factors to different promoters (Sharma *et al.*, 2003; Li *et al.*, 2007).

The results here demonstrate that for *PIL1*, both histone acetylation and a more open chromatin structure, as determined by DNaseI sensitivity, are correlated with increases in transcription in response to a low R:FR treatment. In contrast, *ATHB2*, was found to adopt a more open chromatin structure in response to a R:FR induced increase in transcription but did not undergo the same histone modifications as *PIL1* at the regions analysed. This could represent a different regulation of *PIL1* and *ATHB2* or it could represent a failure to identify the modifications of *ATHB2*. Further experiments will have to be performed to determine which the case is.

Chapter 5: Results

SHL, GCN5 and HD1

5.1 SHL, GCN5 and HD1

Having identified chromatin remodelling processes to be associated with R:FR ratio signalling, an attempt was made to identify and characterise some of the factors involved. The aim of this part of the project was to over-express and knock-down/knock-out expression of genes which are either known to be, or suspected to be, involved in chromatin remodelling in *Arabidopsis* and investigate whether they are also involved in low R:FR signalling. The three genes to be investigated were: *SHORT LIFE (SHL), GENERAL CONTROL NON-REPRESSIBLE 5 (GCN5) and HISTONE DEACETYLASE 1 (HD1).*

Work by Mussig and Altman (2003) found that over-expression and antisense knockdown of *SHL* resulted in alteration of R:FR regulated genes. This combined with the fact that *SHL* contains a PHD and BAH domain, both of which are associated with proteins that associate with chromatin, means that *SHL* could play a role in chromatin remodelling and plant light signalling (Mussig *et al.,* 2000). A homolog of *SHL, EARLY BOLTING IN SHORT DAYS (EBS)*, also contains a PHD and BAH domain and is involved in regulating flowering time by repressing FLOWERING LOCUS T (FT), which is known to be regulated at the chromatin level (Pineiro *et al.,* 2003; Adrian *et al.,* 2010).

HD1 encodes a protein which has been shown to be involved in modifying histones (Tian *et al.*, 2003). In a number of light treatments *hd1* mutants exhibit shorter hypocotyls than WT controls (Benhamed *et al.*, 2006). Additionally, plants mutant for *hd1* have been shown to display aberrant histone modifications profiles in response to light signals (Guo *et al.*, 2008). Given this information, it was considered that HD1 might also be involved in histone modifications in response to low R:FR ratio.

Mutation of *GCN5*, which encodes a HAT, results in a host of phenotypic abnormalities and reduction in acetylation levels of H3 (Bertrand *et al.*, 2003; Vlachonasios *et al.*, 2003). GCN5 has also been found to interact with factors involved in acclimatising plants to cold temperature (Stockinger *et al.*, 2001). It has also been shown to be involved in light signalling, as *gcn5* mutant plants grown under a number of light conditions exhibited longer hypocotyls than WT. Interestingly, the *gcn5/hd1* double mutant displayed WT hypocotyl lengths when grown under a range of light conditions, suggesting that GCN5 and HD1 may function antagonistically (Benhamed *et al.*, 2006). GCN5 was therefore investigated to see if it was involved in regulating histone modifications in response to R:FR treatments.

5.2 Restriction enzyme cloning over-expression of *SHL, GCN5* and *HD1*

The aim was to over express *SHL*, *GCN5* and *HD1* coding regions in Col *Arabidopsis* plants. Briefly, this would entail making cDNA of these genes from mRNA and PCR amplifying the cDNA, which could then be ligated into a vector. The insert would then be transferred to a plant specific vector and transformed into *Arabidopsis* plants. Seedlings from transformed plants would be selected for to identify those containing the construct. The expression of the constructs would then be measured by qPCR and those with suitable expression would be propagated. Plants would then be selected for those which contained a single insert and those that were homozygous for the insert. If time permitted, these plants would then be analysed for a range of shade avoidance phenotypes.

5.2.1 Plant growth conditions

To obtain tissue for cDNA synthesis, WT *Arabidopsis* Col plants were grown in continuous W at 22°C in high R:FR ratio for 3 weeks. Whole shoots were harvested, transferred to liquid nitrogen and stored at - 80°C.

5.2.2 Primer design

Primers were designed against the region surrounding the start and stop codons. The *SHL*, *GCN5* and *HD1* coding regions are shown in figure S1.10, S1.13 and S1.14, respectively. These genes would be cloned into pDRIVE, shown in figure S1.12, and the transferred to the plant specific vector, pROK2, shown in figure S1.11.

The restriction sites which could be used were constrained by the fact that restriction sites needed to be present in the cloning site of pROK2 and yet absent from the sequences of the genes to be cloned. This meant that the only available motif available for *GCN5* was SmaI, which therefore had to be cloned on to both the 5' and 3' end. In the case of *HD1*, SmaI was used at the 5' end of the gene and KpnI was used at the 3' end. A KpnI site was incorporated into the primer designed against the start codon and a SacI site was incorporated into the primer designed against the stop codon of *SHL*.

Primers used are shown in 2.2.14 and are labelled SHL over F and SHL over R, for *SHL*; GCN5 over F and GCN5 over R, for *GCN5*; and HD1 over F and HD1 over R, for *HD1*.

5.2.3 Amplifying *SHL*

Cloning of *SHL* was performed first, to ensure that the procedure could be successfully performed. RNA was extracted from the harvested tissue as and cDNA made from the RNA, as described in 2.2.9. Using this cDNA and the primers described in 5.2.2 a PCR reaction was set up using Phusion polymerase as outlined in 2.2.8.2. The PCR reactions were run on a 1% agarose gel and the gel imaged as described in 2.2.8.3.

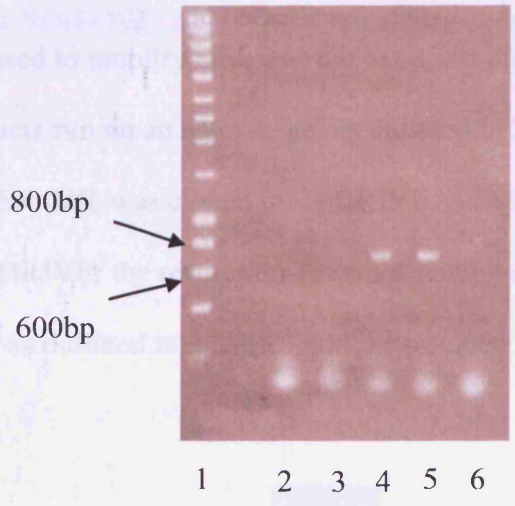

Figure 5.1: Five separate PCR reactions were performed with the *SHL* primers and cDNA. 5ul of each sample was run on the gel. Lanes 4 and 5 show a band of approximately 700bp. Lanes 2, 3 and 6 do not show any band. Lane 1 contains 3ul DNA hyperladder I.

5.2.4 Cloning *SHL* into pDRIVE

Lanes 4 and 5 of figure 5.1 show that the PCR reaction produced a band of approximately 700bp, which is the expected size of *SHL*. The band shown in lanes 4 and 5 were gel extracted as described in 2.2.8.4.1. The gel extracted DNA was incubated with pDRIVE as outlined in the pDRIVE handbook (http://www.qiagen.com). The pDRIVE vector map is shown in S1.12. The reaction was transformed into bacteria and plated as outlined in 2.2.3.1. Colonies were picked from the plate and the plasmids extracted as described in 2.2.8.4.2.

Using the primers used to amplify *SHL* and the extracted plasmids, PCR reactions were set up and the products run on an agarose gel as outlined in 2.2.8.2 and 2.2.8.3, with the aim of confirming that *SHL* was cloned into pDRIVE. As a further confirmation of *SHL* being cloned into pDRIVE, the restriction enzymes KpnI and SacI were used to restrict SHL from pDRIVE as outlined in 2.2.8.5.3 and the products run on a gel as described in 2.2.8.3.

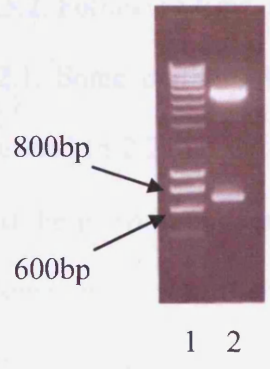

Figure 5.2: Lane 1 is 3µl of DNA hyperladder I. One of the purified plasmids from a positive colony was restricted with KpnI and SacI and this is shown in lane 2. A band of approximately 700bp is shown.

Figure 5.2 demonstrates that *SHL* had been successfully cloned into pDRIVE. PCR amplifications also confirmed that *SHL* was in PDRIVE (data not shown).

5.2.5 Cloning of *SHL* into pROK2

After confirming the presence of *SHL* in pDRIVE, the SHL-pDRIVE construct was sent off for sequencing as outlined in 2.1.7.

One of the constructs which contained *SHL*, without mutation, was then used as a template to remove *SHL* and incorporate it into pROK2. pROK2 and *SHL*-PDRIVE were incubated in a double digest reaction with the enzymes SacI and KpnI as outlined in 2.2.8.5.3. The *SHL*-pDRIVE reaction was run on a gel as described in 2.2.8.3 and the *SHL* -sized band was excised and extracted as outlined in 2.2.8.4.1. The pROK2 vector was incubated with SAP as outlined in 2.2.8.5.1. pROK2 and *SHL* were then ligated together as outlined in 2.2.8.5.2. Following ligation, the products were transformed into bacteria as outlined in 2.2.2.1. Some of the colonies were used for a template in a colony PCR reaction as described in 2.2.8.2. Of these, some which produced a *SHL* -sized band were cultured and the plasmid extracted as described in 2.2.8.4.2 (data not shown) These extracted plasmids were then used as a template in a restriction digest reaction as outlined in 2.2.8.5.3, shown in figure 5.3.

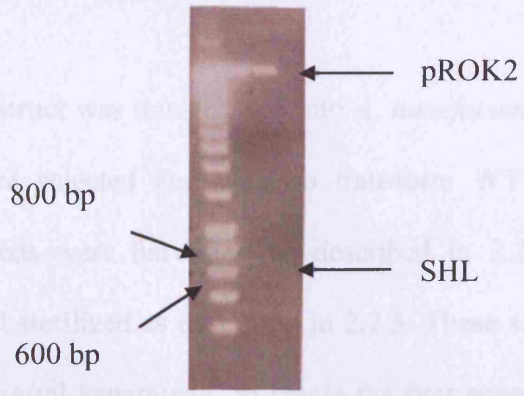

Figure 5.3: Putative *SHL*-pROK2 plasmids were extracted and restricted using KpnI and SacI and run on a gel. Both lanes show a faint band of approximately 700bp and a higher molecular weight band. The far left of the gel is 3ul of DNA hyperladder I

Figures 3.41 and 3.42 both show that *SHL* has been successfully cloned into pROK2. The band of approximately 700 bp in figure 3.36 is *SHL* and the higher molecular band is pROK2.

5.2.6 Plant transformation of the *SHL*-pROK2 construct

The *SHL*-pROK2 construct was transformed into *A. tumefaciens* as outlined in 2.2.3.3. Positive colonies were selected and used to transform WT *Arabidopsis* plants as outlined in 2.2.6. Seeds were harvested as described in 2.2.4 from these primary transformants (T_0) and sterilized as described in 2.2.5. These seeds were plated on LE media containing 40 μg/ml kanamycin, to create the first generation (T_1) of plants. A total of 8 seedlings survived and they were transferred to fresh plates. Tissue samples were taken from the surviving plants and RNA was extracted and cDNA was made from the RNA. This cDNA was then used in a qPCR reaction as described in 2.2.9, to determine the expression of *SHL* in individual plants. Seeds were then harvested as described in 2.2.4 from plants which displayed increased expression of *SHL*. The seeds from these plants were plated on LE media plates containing 40 μg/ml kanamycin, to create the second generation (T_2) of transformed plants. Those that produced seed with a 3:1 ratio of surviving seedlings to dying seedlings were assumed heterozygous with a single insertion. Seeds from these plants were plated onto LE media plates containing 40 μg/ml kanamycin and those that produced 100% of plants surviving were deemed to homozygous for the insert (T_3).

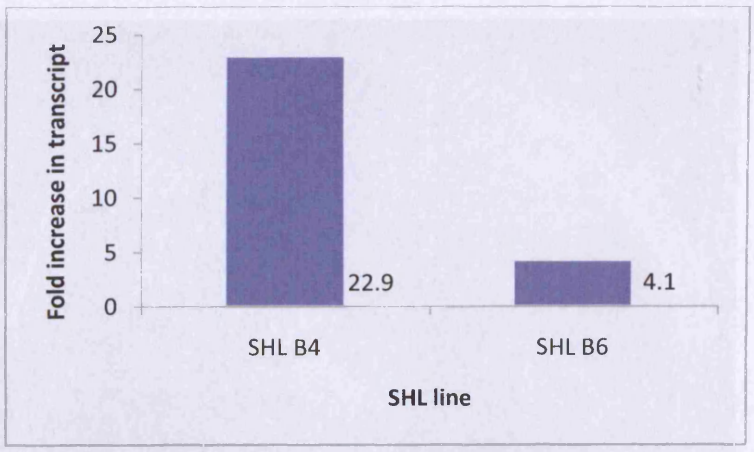

Figure 5.4: Two *SHL* over expressing lines tested for expression of *SHL* transcript relative to WT. Data is normalized to *ACTIN2*. Data is from three qPCR repeats.

Figure 5.4 shows *SHL* expression data from tissue harvested from two of the eight isolated T_1 lines. Both lines were later found to contain single insertions of the *SHL* plasmid and seeds were bulked. Both lines in figure 5.4 show an increase in *SHL* transcript.

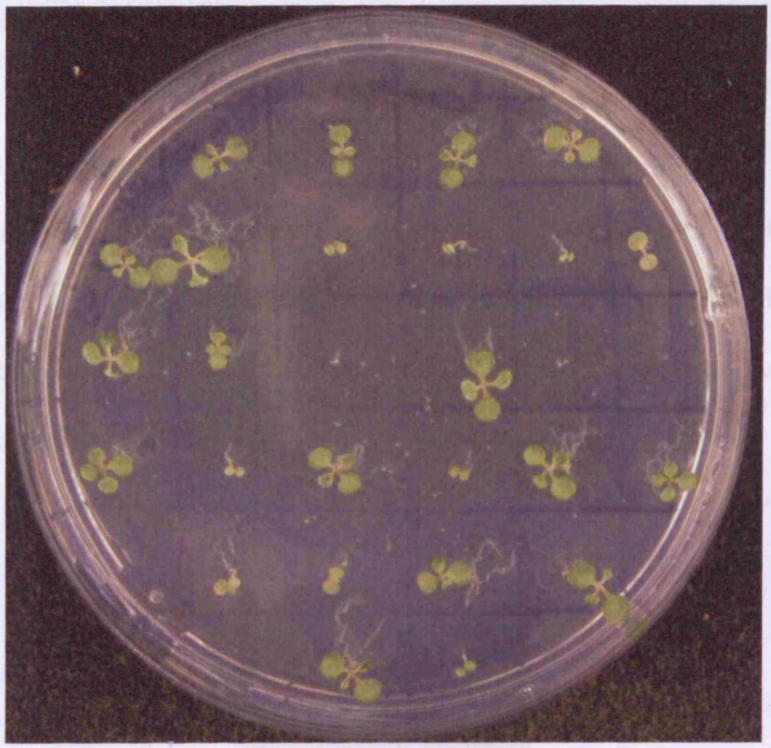

Figure 5.5: SHL line B4 plated at 2 weeks old. Plants are from the second generation of plants transformed with *SHL*-pROK2. The plate contains 40 µg/ml of kanamycin. The seedlings are segregating with a ratio of 3:1 in regards to resistant and non-resistant seedlings, respectively.

Figure 5.5 shows T_2 seedlings containing SHL-pROK2. Seedlings are segregating with ratio of 3:1 with regards to resistant and non-resistant seedlings, indicating that this line contains a single insertion of the SHL-pROK2 construct.

5.2.7 Amplifying *GCN5* and *HD1*

Once cloning of *SHL* had successfully been achieved, *GCN5* and *HD1* were cloned. The *HD1* and *GCN5* coding regions are shown in figures S1.13 and S1.14. RNA was extracted from the harvested tissue as described in 2.2.9.1. Using this cDNA and the primers described in 5.2.2, the PCR reactions were run a 1% agarose gel and the gel imaged as described in 2.2.8.3.

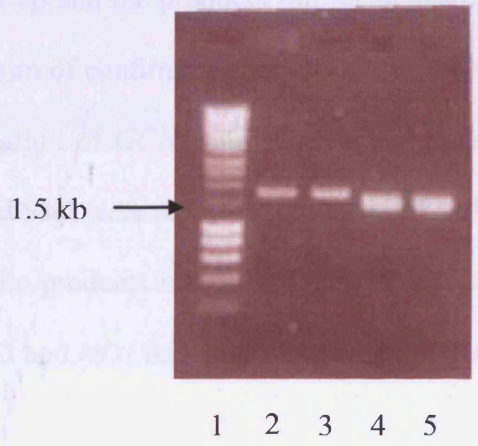

Figure 5.6: PCR amplification of *GCN5* and *HD1*. Lane 1 is 3µl of DNA hyperladder I. Lanes 2 and 3 are *GCN5* and lanes 4 and 5 are *HD1*. *GCN5* is approximately 1.5kb and *HD1* 1.7 kb.

Figure 5.6 shows that *GCN5* and *HD1* were successfully amplified. Lanes 2 and 3 show a band of approximately 1.5 kb, which corresponds to the expected size of *GCN5*. Lanes 4 and 5 show a band of approximately 1.7kb, which is the expected size of *HD1*.

5.2.7.1 Cloning *GCN5* and *HD1* into pDRIVE

The bands shown in figure 5.6 were gel extracted as described in 2.2.8.4.1. The gel extracted DNA was incubated with pDRIVE as outlined in the pDRIVE handbook. The reaction was transformed into bacteria and plated as outlined in 2.2.3.1. Colonies were picked from the plate and the plasmids extracted as described in 2.2.8.4.2.

Using the primers used to amplify *GCN5* and *HD1* and the extracted plasmids, PCR reactions were set up and the products run on an agarose gel as outlined in 2.2.8.2 and 2.2.8.3, with the aim of confirming that *GCN5* and *HD1* were cloned into pDRIVE. As a further confirmation of *GCN5* and *HD1* being cloned into pDRIVE, the restriction enzymes KpnI and SacI were used to restrict *GCN5* and *HD1* from pDRIVE as outlined in 2.2.8.5.3 and the products run on a gel as described in 2.2.8.3. Both of these tests showed that *GCN5* and *HD1* had been cloned into pDRIVE (data not shown).

5.2.7.2 Cloning of *GCN5* and *HD1* into pROK2

After confirming the presence of *GCN5* and *HD1* in pDRIVE, the constructs were sent off for sequencing as outlined in 2.1.7. One of the constructs which contained *GCN5* and one which contained *HD1*, without mutation, were then used as a template to remove *GCN5* and *HD1* and incorporate each into pROK2. pROK2 and *GCN5*-pDRIVE were incubated in a single digest reaction and *HD1*-pDRIVE and PROK2 were incubated in sequential single digest reactions as outlined in 2.2.8.5.3. The *GCN5*-pDRIVE and *HD1*-pDRIVE reactions were run on a gel as described in 2.2.8.3 and *GCN5* and *HD1* -sized bands were excised and extracted as outlined in 2.2.8.4.1. The pROK2 vector was incubated with SAP was outlined in 2.2.8.5.1. pROK2 and *GCN5*; and pROK2 and *HD1* were then ligated together as outlined in 2.2.8.5.2. Following ligation, the products were transformed into bacteria as outlined in 2.2.2.1. Very few colonies were produced and those that were small and similar to those produced on the negative control (these colonies only grew after several days in 37°C and did not represent genuine transformed bacteria). The cloning procedure was repeated multiple times but no positive colonies could be produced.

5.2.8 Results of restriction enzyme cloning

Transgenic plants over-expressing *SHL* were obtained using the pROK2 vector. These plants were checked to ensure they over-expressed *SHL* and were also checked to ensure that they contained single insertions.

It was attempted to generate *GCN5* and *HD1* over-expressing plants by a similar method. Both genes were successfully cloned into pDRIVE. Despite repeated attempts to clone *GCN5* and *HD1* into pROK2, this was not achieved. The reasons for unsuccessful cloning were unclear so an alternative was employed.

5.3 Gateway cloning

A traditional restriction enzyme based approach to over-express *GCN5* and *HD1* proved unsuccessful. An alternative method was sought using with Gateway cloning (Invitrogen). Gateway cloning uses a recombination approach instead of restriction enzymes to clone inserts into vectors. The Gateway approach entails using PCR to attach recombination sites to the inserts, which can then be used to recombine the insert into a vector with complimentary recombination sites. PCR products are recombined with a donor vector to form an entry vector. The entry vector is then used as donor vector which can be incubated with a variety of destination vectors, resulting in transfer of the insert from the donor to the destination vector. The destination vector can then be transformed into Agrobacterium which can be used to transform *Arabidopsis*.

The aim was to over express *GCN5, HD1* and *SHL* using the Gateway system. It was also decided that three SHL RNAi constructs would also be made in parallel to observe the effects of reducing the expression of *SHL*. Additional *SHL* over-expressing constructs were made so that they could be analysed in parallel with the *GCN5* and *HD1* constructs.

5.3.1 Plant growth conditions

To obtain tissue for cDNA synthesis, WT *Arabidopsis* Col plants were grown in continuous W at 22°C in high R:FR ratio for 3 weeks. Whole shoots were harvested, transferred to liquid nitrogen and stored at - 80°C.

5.3.2 Primer design

Primers were designed against regions of interest in each gene, with the addition of bacterial attachment (attB) sites. These allow the recombination of inserts into the donor vector. All PCR reactions used in the Gateway cloning approach required a two step cloning reaction. Gene specific primers were used initially and this was followed by a second PCR using generic Gateway linker primers. This was because the region to be added to the 5' and 3' end of each insert sequence was considered too long to do in one PCR reaction so, it was therefore achieved in two PCR reactions. These Gateway linker primers are called: GAT adaptor F and GAT adaptor R.

Three different sets of primers were designed to make 3 different RNAi constructs, one against the middle of *SHL* (*SHL* RNAi – primers used: GAT SHL RNAi central F and GAT SHL RNAi central R), one against the N terminal region of *SHL* (RNAi N – primers used: GAT SHL RNAi N F and GAT SHL RNAi N R) and a final one against the C terminal region of *SHL* (SHL C – primers used: GAT SHL RNAi C F and GAT SHL RNAi C R). Primers were also designed to make over expressing constructs: *HD1* – primers used: GAT HD1 OVER F and GAT HD1 OVER R; *GCN5* – primers used: GAT GCN5 OVER F and GAT GCN5 OVER R; and *SHL* – primers used: GAT SHL OVER F and GAT SHL OVER F. All primer sequences are shown in 2.2.14. The *SHL* RNAi regions are shown in S1.15.

5.3.3 Amplifying insert sequences and cloning into donor vector

RNA was extracted from the frozen tissue and cDNA made from RNA as outlined in 2.2.9.1 and 2.2.9.2. Following the Gateway cloning protocol described in 2.2.10, the inserts were PCR amplified and run on an agarose gel (figure 5.7), the bands of the relevant size were gel extracted and run again on an agarose gel (figure 5.8).

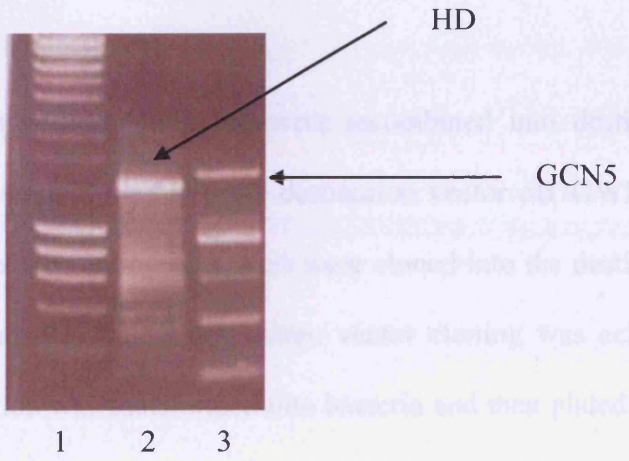

Figure 5.7: Agarose gel showing *HD1* and *GCN5* following PCR amplification. Lane 1 is 3 µl of hyperladder I, lane 2 is *HD1* and lane 3 is *GCN5*. *GCN5* and *HD1* are of the expected size.

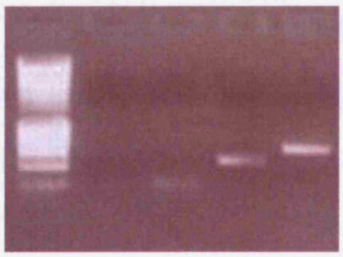

Figure 5.8: Gel purified PCR. Lane 1 is 3 µl of hyperladder I, lane 2 is RNAi C, lane 3 is RNAi central, lane 4 is RNAi N and lane 5 is SHL over. The SHL N and C are both about 550bp, the RNAi insert is about 200 bp and the SHL over insert in approximately 700bp. All inserts are of the correct size.

The PCR products were then recombined into pDONOR 221, shown in S1.16, using BP clonase II. An overnight reaction was set up and they were transformed into *E. coli*. In the Gateway system, the control of cell death B (ccbB) gene is situated between the recombination sites of both the entry and destination vector. This prevents growth of transformed bacteria unless the vector has had the insert recombined into it. Colonies were picked from the plate and grown overnight and plasmids extracted from them as described in 2.2.8.4.2. Plasmids were then sent for sequencing as described in 2.1.7.

Donor vectors carrying inserts without mutations were recombined into destination vectors. The RNAi constructs were cloned into the destination vector pB7GWIWG2, shown in figure S1.17. The over expressing constructs were cloned into the destination vector pBGW7, shown in figure S1.18. All destination vector cloning was achieved using LR clonase II. Each reaction was transformed into bacteria and then plated out as described in 2.2.3.1. Positive colonies were picked and plasmids extracted as described in 2.2.8.4.2. These were then purified and run on a gel as detailed in 2.2.8.3 to ensure inserts were in the destination vector. Again, due to the presence of the ccbB gene, colonies would only grow if they had been transformed with a plasmid that has had an insert recombined into it. All inserts were successfully cloned into the destination vector.

5.3.4 Transformation of destination vectors

The destination vectors with inserts were transformed into *A. tumefaciens* as outlined in 2.2.3.3. Positive colonies were selected and were used to transform WT *Arabidopsis* plants as outlined in 2.2.6. Seeds were harvested as described in 2.2.4 from the transformed (T_0) plants and sterilized as described in 2.2.5. These were plated on LE media containing 40 μg/ml kanamycin to create the T_1 generation of plants. Seedlings that survived were transferred to fresh plates. No seedlings survived for the *SHL* over expressing Gateway construct, the *SHL* RNAi N Gateway construct or the *GCN5* over expressing. Only a few, weak seedlings were present for the *SHL* RNAi central, *SHL* RNAi C and *HD1* over expressing Gateway constructs. Tissue samples were taken from the surviving plants and RNA was extracted as described in 2.2.9.1. cDNA was made from the RNA (2.2.9.2). This cDNA was then used in a qPCR reaction as described in 2.2.9.3, to determine the expression of the inserts or target genes to which the inserts were designed to knockdown. Unfortunately, transcript levels of *SHL* were not reduced and *HD1* was not over expressed in any of the plants tested (data not shown).

5.3.5 Gateway cloning results

All of the constructs: *SHL*-, *GCN5*- and *HD1*-over expressers and three RNAi knockdown constructs were successfully obtained in destination vectors. Attempts were made to transform the constructs into plants but unfortunately, none of the constructs were successful within the time-frame of this project.

5.4 Isolation of *shl*, *gcn5* and *hd1* SALK lines

The aim was to isolate *shl*, *gcn5* and *hd1* plants homozygous for T-DNA insertions. This would entail ordering the SALK lines and relevant primers, extracting DNA from individual plants and testing, using PCR, for the presence of T-DNA insertions. If plants homozygous for T-DNA insertions were not isolated, heterozygotes would be propagated until the next generation and tested again for plants with homozygous insertions. Homozygous plants would then be analysed for a range of R:FR-mediated responses.

5.4.1 Plant growth conditions

WT *Arabidopsis* Col plants were grown in parallel with SALK lines in either continuous W or LD at 22°C in high R:FR ratio for 3 weeks. Leaves were harvested, transferred to liquid nitrogen and stored at - 80°C.

5.4.2 Primer design

Primers were designed on the website: http://signal.salk.edu/tdnaprimers.2.html. The unique codes of the SALK lines to be investigated were entered on the website and 3 primer sequences were returned. Two of the sequences returned are called left primer (LP) and right primer (RP). These two primers are designed to span the region putatively containing the SALK insertion and should produce a product of approximately 900 – 1100 bp if the SALK insertion is absent. The third primer is designed to anneal to the left border (LB primer) of the SALK insert. The LB primer in combination with the RP should produce a band of approximately 700 bp, if the insert is present. Consequently, two PCR reaction need to be set up for each plant: one containing the LP and RP primers and one containing the RP and LB primers. A WT plant should produce a band in the LP + RP reaction; a heterozygote should produce two bands, one band in the LP + RP and one in the RP + LB reaction; and a plant homozygous for the SALK insertion should produce a band in the RP + LB reaction.

5.4.3 PCR SALK reactions

The following SALK lines were ordered:

SHL: 112541, 053996, 514363

HD1: 639443, 639445

GCN5: 606557, 526954

DNA was extracted from the frozen plant tissue as described in 2.2.8.1 and PCR reactions were performed as described in 2.2.8.2. These were run on a 1% agarose gel and the gel imaged as described in 2.2.8.3.

Despite repeated attempts to obtain *shl* homozygous lines, this could not be achieved. Heterozygous lines were obtained for all three SALK lines, however.

Repeated attempts to isolate *hd1* homozygous lines were also unsuccessful, with only heterozygotes obtained. However, a *hd1* homozgous line (639445) was later received as a kind gift from the Deng lab (Guo *et al.*, 2008).This was checked using the same SALK test and homozygosity was confirmed, suggesting that the test procedure itself was not the problem with previous attempts.

The *gcn5* SALK line 606557 was successfully obtained as a homozygote. Line, 526954, could only be obtained as a heterozygote.

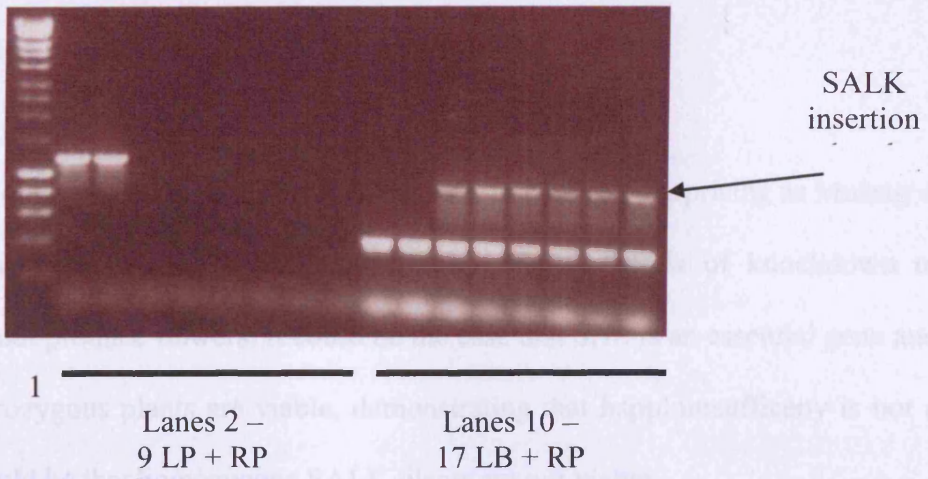

Figure 5.9: SALK test of *hd1* line 639445. The first lane, on the far left, is 3 µl of hyperladder I. The 8 lanes adjacent to this (2 – 9) comprise two WT plants (2 – 3) followed by 6 test plants (4 – 9). All of lanes 2 – 9 have been tested with primer LP and RP. Adjacent to this (lane 10 – 17) are the same samples, in the same order, tested with primers LB and RP.

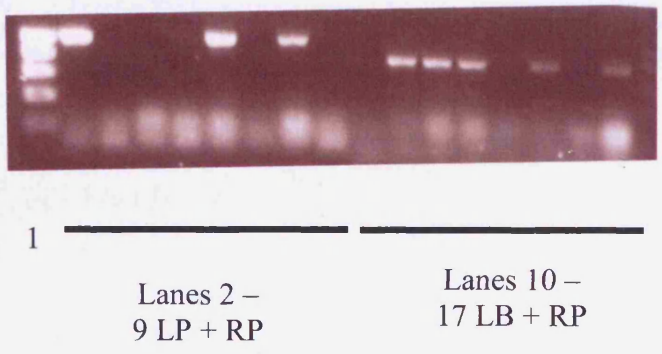

Figure 5.10: SALK test of *gcn5* line 606557. The first lane, on the far left, is 3 µl of hyperladder I. The 8 lanes adjacent to this (2 – 9) comprise one WT plants (2) followed by 7 test plants (4 – 9). All of lanes 2 – 9 have been tested with primer LP and RP. Adjacent to this (lane 10 – 17) are the same samples, in the same order, tested with primers LB and RP.

5.4.4 SALK line results

The failure to obtain homozygous *shl* SALK lines is not entirely surprising as Mussig *et al* (2000) found that *SHL* RNAi plants with the highest levels of knockdown of transcript did not produce flowers. It could be the case that *SHL* is an essential gene and although heterozygous plants are viable, demonstrating that haploinsufficeny is not a problem, it could be that homozygous SALK plants are not viable.

The failure to obtain *hd1* SALK lines and homozygous *gcn5* SALK line 526954 is surprising. It could be that the growth conditions being used were not particularly conducive to plants with these mutations. Consequently, mutant plants may have had a higher chance of not germinating or died during propagation.

hd1 and *gcn5* SALK lines were eventually obtained. These lines will be analysed in the future.

5.5 SHL, GCN5 and HD1 discussion

The aim of this part of the project was to generate transgenic plants for three genes: *GCN5*, *HD1* and *SHL*, that were suspected, or known to be involved, in chromatin regulation and considered possible factors involved in chromatin regulation in response to low R:FR treatment. A number of constructs were generated; however, there was insufficient time to analyse them. Given more time, a number of experiments would have been performed. Ideally, either each mutant would have been analysed by Southern blotting to ensure that only a single T-DNA insertion event was present in the genome. Alternatively, two knockout lines for each gene would have been obtained and verified against one another. All lines would have, initially, been investigated for the effect of a R:FR treatment on their hypocotyl and cotyledon growth. Lines would be grown in high R:FR ratio conditions for 3 days and then either maintained in high R:FR ratio or transferred to low R:FR ratio for 4 days. Hypocotyl length and cotyledon area would then have been compared to WT controls. This would have provided a quick experiment to determine if *SHL, GCN5* or *HD1* are involved in seedling shade avoidance. High R:FR controls would be analysed in parallel to ensure that any phenotypes observed were due to the low R:FR ratio treatment and not constitutive differences. Adults plants would also have been analysed for petiole length, leaf area, chlorophyll content and flowering times (the number of rosette leaves present at bolting) in both high and low R:FR. If these experiments generated any data indicating that these genes were involved in responses to low R:FR ratio then gene expression time courses of shade avoidance marker gene (e.g. *PIL1, ATHB2* and *XTH15*) would be performed in mutant and transgenic plants. Chromatin experiments could additionally be performed (discussed in chapter 6).

Chapter 6

General Discussion

6.1 General Discussion

The primary aim of this project was to determine if low R:FR treatment can elicit changes in chromatin structure in *Arabidopsis*. The results clearly demonstrate that there is chromatin regulation around shade avoidance genes in response to a low R:FR treatment. Treatment with low R:FR resulted in gross changes in chromatin, as shown by changes in DNaseI sensitivity, and changes in histone modifications, as shown by increased histone acetylation.

Three shade avoidance genes, *ATHB2, PIL1* and *XTH15*, all known to R:FR regulated, were investigated. All three genes were shown to undergo gross changes in chromatin structure in their promoter regions in response to a low R:FR treatment. Two of these genes, *ATHB2* and *PIL1*, were investigated for association with acetylated histones in response to a R:FR treatment, using ChIP. The coding region of *PIL1* was found to display enhanced association with histones acetylated at residues H3K9 and possibly at H3K14 in response to low R:FR treatment. The ChIP experiments were all performed with plants grown in LD cycles, with the R:FR treatment beginning at dawn and plants being harvested at ZT4, the point of maximal gene expression (Salter *et al.*, 2003). The DNaseI experiment used plants treated in an identical manner, additionally, however, separate DNaseI experiments were performed in which plants were grown in continuous light and treated with a 24 hour low R:FR treatment. Interestingly, there

were no changes in DNaseI sensitivity in these plants grown in continuous light and the increases in gene expression were less. These results are the first evidence that chromatin structure is important in the regulation of shade avoidance genes, both in regards to gross changes in chromatin structure and histone modifications.

One explanation for the different responses to light treatments observed in the DNaseI sensitivity experiments is that the transcriptional drivers of PIL1, ATHB2 and XTH15 could be differentially expressed between the two light treatments. PIF4 and PIF5 have both been shown to be involved in regulating shade avoidance genes and to be negatively regulated by Pfr (Lorrain *et al.,* 2008). Furthermore, PIF4 and PIF5 are both known to be circadian regulated (Nozue *et al.,* 2007). It could be that in constant light conditions, the disruption of the circadian clock and/or the increase in Pfr (due to no dark period) could result in down-regulation of PIF4 and PIF5, which results in reduced transcription of PIL1, ATHB2 and XTH15. This reduced transcription of these three genes could then account for the differences in chromatin structure, rather than chromatin structure being responsible for the differences in transcriptional profiles between the two light treatments.

An alternative explanation for the data from the DNaseI sensitivity experiments is that there could be a circadian component, in addition to a low R:FR component, in the regulation of chromatin structure and gene expression of these shade avoidance genes. The work here also suggests that chromatin modifications are co-incident with changes in gene expression. Previous work has shown that the expression of shade avoidance genes in response to a low R:FR ratio treatment are gated by the circadian clock (Salter *et al.,* 2003). Circadian gating is where the response to the same stimuli elicits a

differential response which is dependent on the circadian clock. Gene expression responses to other environmental stimuli, such as temperature, have also been shown to be gated by the circadian clock, for example those of the *CRT/DRE* Binding Factor (CBF) family, which are involved in cold acclimation (Fowler *et al.,* 2005). Furthermore, low R:FR ratio can induce the expression of the *CBFs*, but again, this response is gated by the circadian clock at the same temporal window as that for temperature (Franklin and Whitelam, 2007). The fact that it has been shown here that gene expression is associated with changes in chromatin structure and genes which respond to multiple environmental signals are circadian gated in the same manner, suggests that there could be an underlying, co-ordinated mechanism at play. Given the results found here, there is a possibility that this underlying mechanism involves changes to chromatin structure.

The results generated here provide a suitable set of tools to investigate the effect of circadian gating on chromatin structure. The DNaseI sensitivity data and the histone acetylation data can both be used as markers to assess how gross changes in chromatin structure and histone modifications are affected by the circadian clock. Experiments could be performed where plants are grown in LD conditions for 3 weeks and then transferred to continuous light conditions at ZT0 of the 22nd day, therefore recapitulating the experimental conditions used previously. Beginning at ZT0 of the 22nd day, plants would be transferred to low R:FR ratio and then harvested 4 hours later. This process would be repeated every 4 hours for 3 days. Plant would be harvested and used for gene expression, DNaseI sensitivity and ChIP experiments. The *PIL1* histone acetylation modifications and the *PIL1* and *ATHB2* DNaseI sensitivity regions previously identified, could be used as positive control regions and could be examined

to see how they vary over the time-course. These experiments will hopefully provide answers to a number of questions. Firstly, they should address the question as to whether low R:FR induced changes in gene expression are indeed correlated with changes in histone acetylation and changes in gross chromatin structure across multiple time-points. Additionally, they should address whether these changes in chromatin structure and histone modifications are circadian gated. These experiments will not answer more detailed questions about whether gross changes in chromatin structure or histone modifications come first or about the precise kinetics of the chromatin changes in relation to the changes in gene expression. These questions could, however, be addressed if a time-course with smaller intervals was used. The same tissue samples could also be used to investigate whether low R:FR treatment also results in chromatin changes around CBF genes. Furthermore, plants could be treated in an identical time-course with the exception that they are exposed to cold temperature treatments instead of low R:FR treatments and the changes in chromatin structure and histone modifications examined. This would provide an opportunity to examine whether responses to multiple environmental stimuli: temperature and light quality; are regulated by a conserved, chromatin mechanism.

Ancillary to the investigation of chromatin changes in response to low R:FR, a number of constructs were made to investigate three genes thought to be involved in regulating chromatin. These three genes were *SHL, GCN5* and *HD1*. Over-expression constructs of all three constructs were made. RNAi knockdown constructs of *SHL* were made in addition to obtaining knockout lines of *GCN5* and *HD1*. Two different cloning methods were utilised. One used a traditional, restriction enzyme based approach and the other used the Gateway cloning system, which uses a recombination approach. *SHL* was

successfully cloned using the restriction enzyme based approach. Three separate *SHL* RNAi constructs were cloned using the Gateway approach in addition to *SHL, GCN5* and *HD1* over-expression constructs. Of all of these constructs, only the *SHL* over-expression construct, generated using a traditional restriction enzyme based approach, was successfully transformed into plants. One *GCN5* SALK line and one *HD1* SALK line were additionally isolated.

Future aims would be to transform the rest of the constructs and analyse the transgenic plants. Shade avoidance phenotypes of the transgenic plants would be examined. These would include, amongst others, the measurement of hypocotyls, cotyledons and flowering times. Additionally, gene expression changes in response to changes in low R:FR ratio would be examined. The identification of aberrant molecular and phenotypic profiles in transgenic lines would suggest that these chromatin remodelling factors are involved in R:FR signalling. Transgenic plants could then be analysed with ChIP and DNaseI sensitivity assays to determine if there was aberrant chromatin regulation. Using the regions identified as undergoing chromatin remodelling and histone modifications, abnormal chromatin regulation in response to low R:FR could be examined in these transgenic plants. If chromatin structure was abnormal then antibodies could be purchased or raised (depending on whether antibodies are available) against SHL, GCN5 and HD1. Alternatively, tagged constructs could be made and transformed into plants. Tagged constructs would benefit from the fact that they would be easier to generate (if antibodies are unavailable), however would suffer from the fact that the tag may interfere with the protein and therefore may not faithfully recapitulate the behaviour of the native protein. ChIP could be used with these tagged constructs, or antibodies, to determine if these proteins do actually bind to shade avoidance genes and

this would provide further validation for their role in regulating chromatin structure. Further down the line, if these proteins are identified as being involved in regulating and binding shade avoidance genes, then the interacting partners of these proteins could be identified. Initially, pull-down assay could be used to determine whether chromatin remodelling proteins complex with the known shade avoidance regulators, PIF4 and PIF5 (Lorrain *et al.,* 2008; Hornitschek *et al.,* 2009) Co-immunoprecipitations could then be performed to determine whether other proteins interact with these chromatin remodelling proteins. This approach would have the potential to identify the transcription factors involved in regulating the expression of shade avoidance genes and in co-ordinately recruiting chromatin remodelling and modifying proteins. Together, the above experiments would provide a more complete picture of how signalling pathways operate to transduce changes in low R:FR ratio into changes in gene expression.

Appendix

5′

cttgttcatggtaacttactaatttatatgctttattagttgcagatagtgatatata
tcgaaaaatgaaagatctaattccaataattgtcaaagaggatttctaaatttctgtt
tgactaggtcatatattctcacgactcaacgatctaaccaatcacctacaacagaaaa
tttggttgaaataaaacgaaaagtgataagtccaaatgtttaaaacaaaaaaaaagta
aacaaaaggcaaaataagataactacgattagattttgttctcgccttatgaatatcc
taaaaattatctattagtgatagtttgataatcatctttgactgagaaaattgatgtc
acataaacattaatatagtatcaacattaatcattaatgatgcgactataattattat
tttatcacaatttcttagatttgataatttgtttaggtttgagagagttatatagagg
gggacaaagaagcaaagtttgtgattataaaattatttccattgaactaaagttttca
atagtttattcttgactttaataataataactattttgcccccagctagtcacatact
catgattgcaaaatctctctctctctctgcctctctatatattaacctttcttcttcc
tttactttctcatcttctatctctcaaaagaaaagcagacaactttatttgcaaaaac
agagtttttttttcttatcttgagaaagttcaacagaagATGTTCGAGAAAGACGATC
TGGGTCTAAGCTTAGGCTTGAATTTTCCAAAGAAACAGATCAATCTCAAATCAAATCC
ATCTGTTTCTGTTACTCCTTCTTCTTCTTCTTTTGGATTATTCAGAAGATCTTCATGG
AACGAGAGTTTTACTTCTTCAGGTACTTCATCGCTTTCTTCGTTCCTCTGTTTTTTTT
TATTTTTCCCCGGAAAAAACCTTAAAGGTCTCACCTTTTACTCTACTTTTCAATCTTA
TGCATGCAGTTCCAAACTCAGATTCGTCACAAAAAGAAACAAGAACTTTCATCCGAGG
AATCGACGTGAACAGACCACCGTCTACAGCGGAATACGGCGACGAAGACGCTGGAGTA
TCTTCACCTAACAGTACAGTCTCAAGCTCTACAGGGAAAAGAAGCGAGAGAGAAGAAG
ACACAGATCCACAAGGCTCAAGAGGAATCAGTGACGATGAAGATGGTGATAACTCCAG
GAAAAAGCTTAGACTTTCCAAAGATCAATCTGCTATTCTTGAAGAGACCTTCAAAGAT
CACAGTACTCTCAATCCGGTAATTTTTTTCTTCTTTTACTTATTGTTTCACCCGAGAA
AGTTTGGTTTTACTGGGAAAATTAATGGCTATGATAAATTGTGGAAACGAAAAAAGAA
CGCGTTAATGAAATATTCACATTAAAATGACTATTGTTACATGTTGACCAAAGAAAAA
ACATTACTACTACTATTTGTTTCGGTCTCTCATAAATGCAGATATTAATTTATAAATG
GCATTTTGGTAAATGTAGACTGATATCAAGGTTTTTTTCAACTTTTTTTCACAGAAGC
AGAAGCAAGCATTGGCTAAACAATTAGGGTTACGAGCAAGACAAGTGGAAGTTTGGTT
TCAGAACAGACGAGCAAGGTAAATAAAACACACACAAACAAAAGATCTCTCTATTTGC
CTGATTTATCTATTTTCTTATAAGGGTATTTTGGTAAATGTTTAACAGAACAAAGCTG
AAGCAAACGGAGGTAGACTGCGAGTTCTTACGGAGATGCTGCGAGAATCTAACGGAAG
AGAACCGTCGGCTACAAAAAGAAGTAACGGAATTGAGAGCACTTAAGCTCTCTCCTCA
GTTCTACATGCACATGAGCCCACCCACTACTTTGACCATGTGCC

Figure S1.1: Part of the coding and promoter region of *ATHB2*. Lower case type represents the *ATHB2* promoter region and upper case type represents *ATHB2* coding region. In black bold and underlined is the start codon of the coding region of *ATHB2*. The orange sequence which is not underlined is the *ATHB2* promoter probe F primer and the orange underlined sequence is the *ATHB2* promoter probe R primer. These two primers produce a product of 783 bp that is referred to as the *ATHB2* promoter probe. The red sequence which is not underlined is the *ATHB2* coding probe F primer and the red underlined sequence is the *ATHB2* coding probe R primer. These two primers produce a product of 654 bp that is referred to as the *ATHB2* coding probe. This was used in the Southern blot approach to DNaseI sensitivity assays.

5′

tggaatgatgtattattagcttttctatcctcactctaaaaacaatactatagtgagt
taaataatttgatcatttcaatgtagattaaaatttttattaaaagaagaaaaatttaa
aagcctataacaaaataaaaaaggaggctcgaggtatgatgggtgtagcagaagagct
ggcaacagctatcgactgagtgattacgaactcagtactcagtgttctcagctcacac
actctttttttgttctctttctttttggacagctttcattttctcttttctttttttcta
ttttgtttcaaaattccatccatattaaaataggcctgatcatgagaataaaggaaat
actaatgatgagtttctcaataatgcaataagatgcaattattatgagctatttacta
ttgaaaatgagcaaataaatgtcaaaacacaatctggttaagttagagcaactccatt
gtataggattcatgtagtttctaagaaaacaaaatgtattaatattttacttttacat
ccaaaaaaccaacttatatgagtaatagaaacgatcctaatattaggaattttagaga
ttttctctcatctgtttcttaacttttcaatatttttatttttttaaaattgtatgagt
ttctactaagaaactactgctggagttggtcttagcttcccaatgcttctccacctat
atatatgcatatctccttcttaaaactcatctcacaccaaaacacaaagctctcatct
tcttttagtttccaaactcacccccacaactttcatttctatcaaccaaacccaa**ATG**
GGTCCAAGTTCGAGCCTCACCACCATCGTGGCGACTGTTCTTCTTGTGACATTGTTCG
GTTCGGCCTACGCAAGCAACTTCTTCGACGAGTTTGACCTCACTTGGGGTGACCACAG
AGGCAAAATCTTCAACGGAGGAAATATGCTGTCTTTGTCGCTGGACCAGGTTTCCGGG
TCAGGTTTCAAATCCAAAAAAGAGTATTTGTTCGGTCGGATCGATATGCAGCTCAAAC
TTGTCGCCGGAAACTCGGCCGGCACCGTCACTGCTTACTACGTAGCGTTTTCAAACTC
ACACTCACTCATAATGTTGCTAAAACTGAAGAGACTCTTTTCTAAATTTGTTTGAACG
TACATGTTTGCAGTTGTCTTCACAAGGAGCAACACATGACGAGATAGACTTTGAGTTT
CTAGGTAACGAGACAGGGAAGCCTTATGTTCTTCACACCAATGTCTTTGCTCAAGGGA
AAGGAGACAGAGAGCAACAGTTTTATCTCTGGTTCGACCCAACCAAGAACTTCCACAC
TTACTCCATTGTCTGGAGACCCCAACACATCATGTAAACATCCATCGATCTATTTTCT
CTAACAATAAGTGAAAGACGTAGATCTTGACTCTCTTGTTCTTGTCTCTGCAGATTCT
TGGTGGACAATTTACCCATTAGAGTGTTCAACAATGCAGAGAAGCTCGGCGTTCCTTT
CCCAAAGAGTCAACCCATGAGGATCTACTCTAGCCTGTGGAATGCAGACGATTGGGCC
ACGAGAGGTGGTCTAGTCAAGACTGACTGGTCCAAGGCTCCTTTCACAGCTTACTACA
GAGGATTCAACGCTGCGGCTTGCACAGCCTCTTCAGGATGTGACCCTAAATTCAAGAG
TTCTTTTGGTGATGGTAAATTGCAAGTGGCAACCGAGCTCAATGCTTATGGCAGGAGG
AGACTCAGATGGGTTCAGAAATACTTCATGATC

Figure S1.2: Part of the coding and promoter region of *XTH15*. Lower case type represents the *XTH15* promoter region and upper case type represents *XTH15* coding region. In black bold and underlined is the start codon of the coding region of *XTH15*. The orange sequence which is not underlined is the *XTH15* promoter probe F primer and the orange and red underlined sequence in the middle of the figure is the *XTH15* promoter probe R primer. These two primers produce a product of 714 bp that is referred to as the *XTH15* promoter probe. The red sequence which is partially underlined is in the middle of the figure is the *XTH15* coding probe F primer and the red underlined sequence is the *XTH15* coding probe R primer. These two primers produce a product of 766 bp that is referred to as the *XTH15* coding probe. This was used in the Southern blot approach to DNaseI sensitivity assays.

5'

ttaaattattcatagacacaccatgaattaattgtaataatgcgaaggacctgtatca
tgt**aacagagacagacgaagtgtgcag**aggtcggtgagaagcaatttggt**caccatgc**
tccaactctcttctctaggtccctttgctttaattttctcgtttaataacaatatct
tatgaaagcagttaccatatcaattgaaggattgtataataccgtaatttatttatat
atagtacatctaattaaacattaattatttctactaatagcctaaaaccactactaat
acaacaactagtacttgtttacgataattattaaacttgtctcgatacctacaacatg
cccaaaaaagtaatcaatactttgtttaatcacaaagatctcagtgagatggttctat
agatagtatttctgatttgttagtatattagagaattgaccatctattaaaataagag
aatgaacactatttgataaaacaatacatacgcaattatcattgtctttaatttttat
caaagtaatcatacgatcgactatttgtatgcaaaaattcatcattttatttgcaaaa
aaaaacaaacaaacatggtagaattgtatttggtgtgtgttttaacaaattgttgcaa
tgtttagtgcaacatatataatccactatatataatcattgacataattaatatttga
ttatatgaagcaatttctctttaattatgtgtttataaatatagggagaaaagaaaaa
tagagagaaaggtaaagagtagagctaatgattcgggcgacgctaaaaggttgaatgt
tcgagagaaacggagtctcagagactgtgaaaacaaaaaatcaaaatcctcagttaca
gacgatttggtcccctctcttctctctctgcgtccgtcttgtgcgtcgatttgtctcc
atctccttctctctccgcctactttctcaggactactccaattcgccgacttttttctc
ctctgttctctgcatttggattgatgccactttaatactttgaggttctcactctctc
tttctctcttcgctgacttcgattgcttcagtacccttttttctcaggtcagctacgat
gatagctttattcagacaagaagatcaaagttttgatctttttgttttggttttctta
agagatggttaattaggtcttgagtgcgctgttttgaatcgttcttcagtgtgattaa
acaattggttttgatttgactaatcatgttgccattaaactaagtgaaaatctctgct
ttttttatattgcatattgatgattgagacattgatttcttttctatttctttatttc
ccagtttctaatttgggaactgaaaagttttctaatttaagcattacaaagtgtacaa
ttttttgtttctggcaagtttttcttggcctaattcgtctatttttatgaattcaccttt
ttaggatcaagacttcgtaaaagattgtttctgtaaaacgcaacacc CCTCTGTT
TGAGCTTTTCA

Figure S1.3: The coding region and part of the promoter region of *PIF3*. Lower case type represents the *PIF3* promoter region and upper case type represents the *PIF3* coding region. In black bold and underlined is the start codon (ATG) of *PIF3*. Highlighted in red are the sequences of the *PIF3* primers used in the qPCR approach for the DNaseI sensitivity assay. Red underlined sequences indicate forward primers and red not underlined indicate reverse primers, they are called QPCR PIF3 F and QPCR PIF3 R, respectively.

5’

acttatggtatatgatgatactctctcaacatcctcattaacatcatcactattaagt
taacaaaaagaaaaagaaaacatcattataagttattaataagtttaaatagtagtat
tttatattctggtacaatgtactgtttttggtcattaagtggttcaacgacaaaagta
aaactcatgcggtcgaccatgcgttagaagaagaaaatctgaaaagaagtttgaatt
ctttaatttttcataaaaagaagtttgaattcaattcaaccgttttgtttagttct
tctttaattaactttatcactaatgtttaaaagtaaaaggtttttaaagtgtgcaaca
agcgtgactctttggcctttagagtcatcaagaagggtaatcatttttttactcttt
ctcgacaatagcaatcaaattatcattcccacttttaataatctcataaaataaagtc
aatcatagttaaaatttgataaattccatggaaatgataaaaatttgattttactatt
gttggatgtgcaattgttcatggtaacttactaatttatatgctttattagttgcaga
tagtgatatatatcgaaaaatgaaagatctaattccaataattgtcaaagaggatttc
taaatttctgtttgactaggtcatatattctcacgactcaacgatctaaccaatcacc
tacaacagaaaatttggttgaaataaaacgaaaagtgataagtccaaatgtttaaaac
aaaaaaaaagtaaacaaaaggcaaaataagataactacgattagattttgttctcgcc
ttatgaatatcctaaaaattatctattagtgatagtttgataatcatctttgactgag
aaaattgatgtcacataaacattaatatagtatcaacattaatcattaatgatgcgac
tataattattatttatcacaatttcttagatttgataatttgtttaggtttgagaga
gttatatagaggggacaaagaagcaaagtttgtgattataaaattatttccattgaa
ctaaagttttcaatagtttattcttgactttaataataataactattttgcccccagc
tagtcacatactcatgattgcaaaatctctctctctctctgcctctctatatattaac
ctttcttcttcctttacttttctcatcttctatctctcaaaagaaaagcagacaacttt
atttgcaaaaacagagtttttttttcttatcttgagaaagttcaacagaagATGATGT
TCGAGAAAGACGATCTGGGTCTAAGCTTAGGCTTGAATTTTCCAAAGAAACAGATCAA
TCTCAAATCAAATCCATCTGTTTCTGTACTCCTTCTTCTTCTTCTTTTGGATTATTCA
GAAGATCTTCATGGAACGAGAGTTTTACTTCTTCAGGTACTTCATCGCTTTCTTCGTT
CCTCTGTTTTTTTTTATTTTTCCCCGGAAAAAACCTTAAAGGTCTCACCTTTTACTCT
ACTTTTCAATCTTATGCATGCAGTTCCAAACTCAGATTCGTCACAAAAAGAAACAAGA
ACTTTCATCCGAGGAATCGACGTGAACAGACCACCGTCTACAGCGGAATACGGCGACG
AAGACGCTGGAGTATCTTCACCTAACAGTACAGTCTCAAGCTCTACAGGGAAAAGAAG
CGAGAGAGAAGAAGACACAGATCCACAAGGCTCAAGAGGAATCAGTGACGATGAAGAT
GGTGATAACTCCAGGAAAAAGCTTAGACTTTCCAAAGATCAATCTGCTATTCTTGAAG
AGACCTTCAAAGATCACAGTACTCTCAATCCGGTAATTTTTTTCTTCTTTTACTTATT
GTTTCACCCGAGAAAGTTTGGTTTTACTGGGAAAATTAATGGCTATGATAAATTGTGG
AAACGAAAAAAGAACGCGTTAATGAAATATTCACATTAAAATGACTATTGTTACATGT
TGACCAAAGAAAAAACATTACTACTACTATTTGTTTCGGTCTCTCATAAATGCAGATA
TTAATTTATAAATGGCATTTTGGTAAATGTAGACTGATATCAAGGTTTTTTTCAACTT
TTTTTCACAGAAGCAGAAGCAAGCATTGGCTAAACAATTAGGGTTACGAGCAAGACAA
GTGGAAGTTTGGTTTCAGAACAGACGAGCAAGGTAAATAAAACACACACAAACAAAAG
ATCTCTCTATTTGCCTGATTTATCTATTTTCTTATAAGGGTATTTTGGTAAATGTTTA
ACAGAACAAAGCTGAAGCAAACGGAGGTAGACTGCGAGTTCTTACGGAGATGCTGCGA
GAATCTAACGGAAGAGAACCGTCGGCTACAAAAAGAAGTAACGGAATTGAGAGCACTT
AAGCTCTCTCCTCAGTTCTACATGCACATGAGCCCACCCACTACTTTGACCATGTGCC
CTTCATGTGAACACGTGTCGGTCCCGCCACCACAACCTCAGGCTGCTACGTCAGCGCA
CCACCGGTCGTTGCCGGTCAATGCGTGGGCTCCTGCGACGAGGATATCTCACGGCTTG
ACTTTTGACGCTCTTCGTCCTAGGTCCTAA

Figure S1.4: The coding region and part of the promoter region of *ATHB2*. Lower case type represents the *ATHB2* promoter region and upper case type represents the *ATHB2* coding region. In black bold and underlined are the start codon (ATG) and the stop codon (TAA) of the coding region of *ATHB2*. Highlighted in red are the sequences of the *ATHB2* primers used in the qPCR approach for the DNaseI sensitivity assay. Red underlined sequences indicate forward primers and red not underlined indicate reverse primers. From 5' to 3' the first pair of forward and reverse primers are QPCR ATHB2 UPF1 and QPCR ATHB2 UPR1 respectively. The second pair of forward and reverse primers are QPCR ATHB2 UPF2 and QPCR ATHB2 UPR2 respectively. The final set of forward and reverse primers, which lie in the coding region, are QPCR ATHB2 INTERNAL F and QPCR ATHB2 INTERNAL R respectively. Highlighted in yellow are an additional pair of primers, the most 5' of the two highlighted yellow primers is QPCR ATHB2 UPF3 and the most 3' one is QPCR ATHB2 UPR3.

5′

ataaatattagtaacccttatgatttctcgttttgtcctgcaaactattattatatacagaa
caatatggatttgattggtttcaatagacgatccttgtatattacatagaatagttttctagtt
ccattacaatttccaaatgatttgttacaaagctacaagattattcgaaataggatttcatcca
taagagagaatggtgtggtcgacgctacaatgttgatttattggttgtggtttgcatcttgggg
atgtcaaatcctaagtttcaagttcttgtaaaaacgttttcaggtttctttaatatattttaat
attaatgtaaaaagaaaagatatagcttttgtacaaaaaaatttgtttaatcactatgtaggag
gatgcgatcaaattcatggaatgatgtattattagcttttctatcctcactctaaaaacaatac
tatagtgagttaaataatttgatcatttcaatgtagattaaaattttattaaaagaagaaaaat
ttaaaagcctataacaaaataaaaaaggaggctcgaggtatgatgggtgtagcagaagagctgg
caacagctatcgactgagtgattacgaactcagtactcagtgttctcagctcacacactctttt
tttgttctctttctttggacagctttcattttctcttttctttttctattttgtttcaaaat
tccatccatattaaaataggcctgatcatgagaataaaggaaatactaatgatgagtttctcaa
taatgcaataagatgcaattattatgagctatttactattgaaaatgagcaaataaatgtcaaa
acacaatctggttaagttagagcaactccattgtataggattcatgtagtttctaagaaaacaa
aatgtattaatattttacttttacatccaaaaaaccaacttatatgagtaatagaaacgatcct
aatattaggaattttagagattttctctcatctgtttcttaacttttcaatatttttatttttt
aaaattgtatgagtttctactaagaaactactgctggagttggtcttagcttcccaatgcttct
ccacctatatatatgcatatctccttcttaaaactcatctcacaccaaaacacaaagctctcat
cttcttttagtttccaaactcacccccacaactttcatttctatcaaccaaaacccaaATGGGTC
CAAGTTCGAGCCTCACCACCATCGTGGCGACTGTTCTTCTTGTGACATTGTTCGGTTCGGCCTA
CGCAAGCAACTTCTTCGACG

Figure S1.5: Part of the coding region and promoter region of *XTH15*. Lower case type represents the *XTH15* promoter region and upper case type represents *XTH15* coding region. In black bold and underlined is the start codon (ATG). Highlighted in red are the sequences of the primers used in the qPCR approach for the DNase I sensitivity assay. The red underlined sequence is the QPCR XTH15 UPF1 primer and the red sequence which is not underlined is the QPCR XTH15 UPR1 primer.

5'

cggtcggtaaaagaatttagaatgtgtcgagagggtaaaaatggagaagacgacaaga
tagtagcagtcgttagaaacaaacaagaaagaagggagggagacaaaataacacaaag
gggtggatgaatcacgcggcattcacgtgaagtgcacgtgaacttggccaaaaaaagc
ctaattgtgggtcccatttaaagagaaaactaaagcctttaagaaagggcccatccat
atatgtcttaataatggcgtgaaggttctttccgctcacgtgggccttttgtgcccgt
ctctctcgcatgtcactcactacagttttactagtgttttgttttatttttgataaca
acattattgatttttttcggtctacctaagttttgacctttctttttaattgtgaa
caattgaacatgcgtattacttattgataatacttttatcttcaataaaaaaaataac
acacgaacataatatagaaatagtgtgttccaatactggagattatttagtaagttca
gttggacgctttgtcattgcatagtttggaatttattcctaaactttctaagaacacg
ttcttataggaatttgcatgacgaaaaaatcaatactagttgcattattgttggagca
tcatcgggagtgatttttttgtgttttcctatttactacattgtgttttcctgacct
tttaaataaaaaggaaatacacaaaaccatatataaatatatgtatatatatatctga
ctgtgctcaagtaaaattcacggatcagacgttaaaaaaatgatcatgcttaatattt
tctcattttagatgaagacaaaaaaaaaaaaaaggaattgcaatcgtagatttgactt
tatttttatttaatttttctattctttttccgaaagcagagaaaaatggagcggtgga
gagtagagaagtcggtcataagaatgtctctctctctatttctttgtctttcactatc
gcccatacattatcttgcttctttcatttattccatcaatatttttgttttaaaatga
aagatttacacattaacatgaatacttatactactctttatcgcgtatatatagtata
gtctatgttattatgaatttatgattatatttttttctataaaacgtgcgaaaactcat
ttcacatatacaaacaaatatatacgttttgtattaaaaaaaagcaactgtaaatttt
ataaatctgaaatgtaacatttgaagtcgaccaaagtttgtaaggtaataatttgtac
taattctccatactgtgtcataatcacgattcaaggataaatatatgagttgtggacc
aaaacaaatcctccatatcaatcaatcataaatgaaataagcgaatatacatatatac
aaccgactatatatatatatatatgctgctcttcattaaccccaagaaagaaaaccaa
agtgtgaagtccgaatctctctgattctacaattcacaaaaaccggaaaaaaaaaaag
acaagtaaagaaagctttgttcagtttacttcaATGGAAGCAAAACCCTTAGCAT
CATCATCATCTGAACCAAACATGATTTCTCCATCATCAAACATTAAACCAAA
gtaagtttattatggtttcatctacacttttgcgacttctataaacata

Figure S1.6: Part of the coding region and promoter region of *PIL1*. Lower case type represents the *PIL1* promoter region and upper case type represents *PIL1* coding region. In black bold and underlined is the start codon (ATG). Highlighted in red are the sequences of the primers used in the qPCR approach for the DNase I sensitivity assay. The red underlined sequence is the QPCR PIL1 UPF3 primer and the red sequence which is not underlined is the QPCR PIL1 UPR3 primer.


5’

Forward

ATHB2 UPF1 – tcaacatcctcattaacatcatca
ATHB2 UPF2 – aagtgtgcaacaagcgtgac
ATHB2 UPF3 – gatgatactctctcaacat
ATHB2 F1 – tgttctcgccttatgaatatcct
CHIPATHB2F1 – gttcaacagaagATGATGTTCG
CHIPATHB2F2 – atgcagTTCCAAACTCAGATTCG
CHIPATHB2F3 – CAGATCCACAAGGCTCAAGAGG
ATHB2InternalF1 – CGGAGGTAGACTGCGAGTTC
CHIPATHB2F1.1 – gctagtcacatactcatgattgc

Reverse

ATHB2 UPR1 – TCGACCGCATGAGTTTTA RC – taaaactcatgcggtcga
ATHB2 UPR2 –CATGAACAATTGCACATCCA RC – tggatgtgcaattgttcatg
ATHB2 UPR3 – CGCATGGGTCGACCGCATGAG RC – ctcatgcggtcgacccatgcg
ATHB2 R1 –TGCTTCTTTGTCCCCCTCTA RC – tagaggggacaaagaagca
CHIPATHB2R1 –GAAGGAGTAACAGAAACAGATGG RC –
CCATCTGTTTCTGTTACTCCTTC
CHIPATHB2R2 CTCTCGTTCCATGAAGATCTTCTG RC –
CAGAAGATCTTCATGGAACGAGAG
CHIPATHB2R3 – GGATTGAGAGTACTGTGATC RC –GATCACAGTACTCTCAATCC
ATHB2InternalF2 – GAAGGGCACATGGTCAAAGT RC –
ACTTTGACCATGTGCCCTTC
CHIPATHB2R1.1 – GATAGAAGATGAGAAAGTAAAGG RC –
cctttactttctcatcttctatc

Figure S1.7: The primers designed against *ATHB2* (AT4G16780) for use in ChIP. Primers are colour coded to help identification of their location. The start and stop codons are highlighted in blue. Ignoring the highlighted primer sequences, lower case black type indicate upstream/downstream regions; lower case red type indicates UTR regions; upper case yellow type represents exons, lower case purple type represents introns. Reverse primers are written first with their 5' orientation and then their reverse complement (RC).


5’

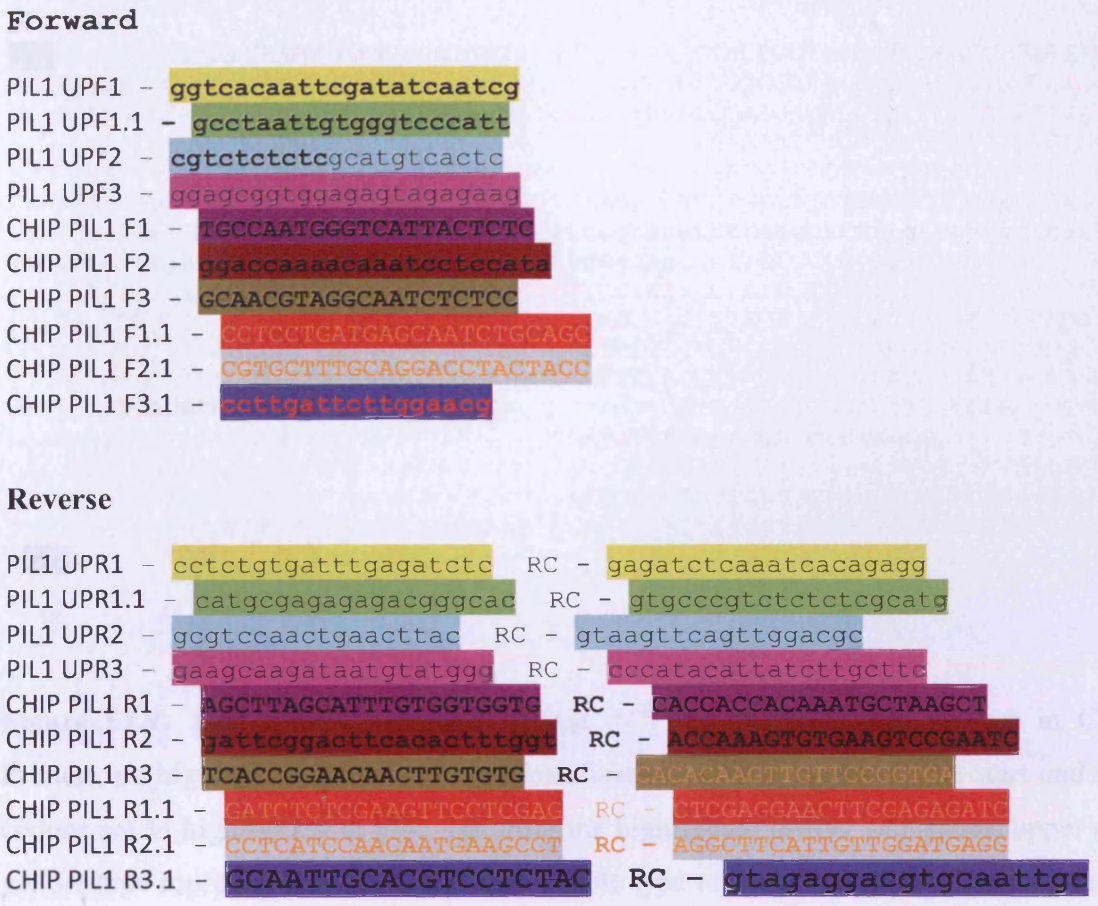

Figure S1.8: The primers designed against *PIL1* (AT2G46970) for use in ChIP. Primers are colour coded to help identification of their location. The start and stop codons are in highlighted in blue. Ignoring the highlighted primer sequences, lower case black type indicate upstream/downstream regions; lower case red type indicates UTR regions; upper case yellow type represents exons, lower case purple type represents introns.

5'

ATGGCTGAGGCTGATGATATTCAACCAATCGTGTGTGACAATGGTACCGGTATGGTGAAGGCTGGATTTG
CAGGAGATGATGCTCCCAGGGCTGTTTTTCCCAGTGTTGTTGGTAGGCCAAGACATCATGGTGTCATGGT
TGGGATGAACCAGAAGGATGCATATGTTGGTGATGAAGCACAATCCAAGAGAGGTATTCTTACCTTGAAG
TATCCTATTGAGCATGGTGTTGTTAGCAACTGGGATGATATGGAAAAGATCTGGCATCACACTTTCTACA
ATGAGCTTCGTATTGCTCCTGAAGAGCACCCTGTTCTTCTTACCGAGGCTCCTCTTAACCCAAAGGCCAA
CAGAGAGAAGATGACTCAAATCATGTTTGAGACCTTTAACTCTCCCGCTATGTATGTCGCCATCCAAGCT
GTTCTCTCCTTGTACGCCAGTGGTCGTACAACCGgttagtacattttaggcttttgtttatactcattg
atcattatttgaactgagctctgattatcttccattgaacagGTATTGTGCTGGATTCTGGTGATGGTGT
GTCTCACACTGTGCCAATCTACGAGGGTTTCTCTCTTCCTCATGCCATCCTCCGTCTTGACCTTGCTGGA
CGTGACCTTACTGATTACCTCATGAAGATCCTTACAGAGAGAGGTTACATGTTCACCACAACAGCAGAGC
GGGAAATTGTAAGAGACATCAAGGAGAAGCTCTCCTTTGTTGCTGTTGACTACGAGCAGGAGATGGAAAC
CTCAAAGACCAGCTCTTCCATCGAGAAGAACTATGAATTACCCGATGGGCAAGTCATCACGATTGGTGCT
GAGAGATTCAGATGCCCAGAAGTCTTGTTCCAGCCCTCGTTTGTGGGAATGGAAGCTGCTGGAATCCACG
AGACAACCTATAACTCAATCATGAAGTGTGATGTGGATATCAGGAAGGATCTGTACGGTAACATTGTGCT
CAGTGGTGGAACCACTATGTTCTCAGGTATCGCTGACCGTATGAGCAAAGAAATCACAGCACTTGCACCA
AGCAGCATGAAGATTAAGGTCGTTGCACCACCTGAAAGGAAGTACAGTGTCTGGATCGGTGGTTCCATTC
TTGCTTCCCTCAGCACATTCCAGCAGGTAAAAATTGATCAGATTTTGTTTCGAATTCTCTTACATGCAAA
TTGA

Figure S1.9: The primers designed against *ACTIN2* (AT3G18780) for use in ChIP. Primers are highlighted in red to help identification of their location. The start and stop codons are in highlighted in blue. Ignoring the highlighted primer sequences, upper case yellow type represents exons, lower case purple type represents introns. The primers are called ACTIN2 F and ACTIN2 R.

5'

ATGCCCAAGCAAAAAGCTCCAAGGAAGCAGCTCAAGTCCTATAAACTCAAACACATCA
ACAAGAGTATTCAAGAGGGAGATGCTGTGTTGATGCGGTCGTCGGAGCCTGGAAAACC
GTCGTACGTAGCGAGGGTAGAGGCGATCGAGACGGACGCGCGTGGATCGCACGCGAAA
GTTCGTGTGAGGTGGTATTATCGCCCTGAGGAATCTATCGGAGGGAGGAGACAATTCC
ATGGAGCCAAGGAGGTTTTTCTCTCTGACCACTTCGATTTTCAAAGCGCCGATACGAT
TGAAGGAAAGTGTAAGGTTCACAGTTTCAGTAGCTACACCAAACTTGACTCTGTTGGA
AACGACGACTTCTTCTGTCGTTTCGAGTACAATTCCACTACCGGCGCGTTTGATCCTG
ACAGAGTCACCGTGTTCTGCAAGTGTGAGATGCCGTATAACCCAGATGACTTGATGGT
GCAATGCGAGGAGTGTTCTGAGTGGTTTCATCCTTCTTGTATAGGAACAACAATAGAG
GAAGCTAAAAAGCCAGATAACTTCTACTGCGAAGAGTGTTCCCCACAACAGCAGAATT
TGCACAACTCTAATTCAACTTCCAATAACAGAGATGCTAAGGTGAATGGAAAGCGCAG
CCTGGAGGTAACTAAATCGAAGAACAAACACACTAAGCGACCAGGT**TAA**

Figure S1.10: *SHL* coding region. Highlighted in bold and underlined are the start and stop codons. The *SHL* coding region is 687 bp.

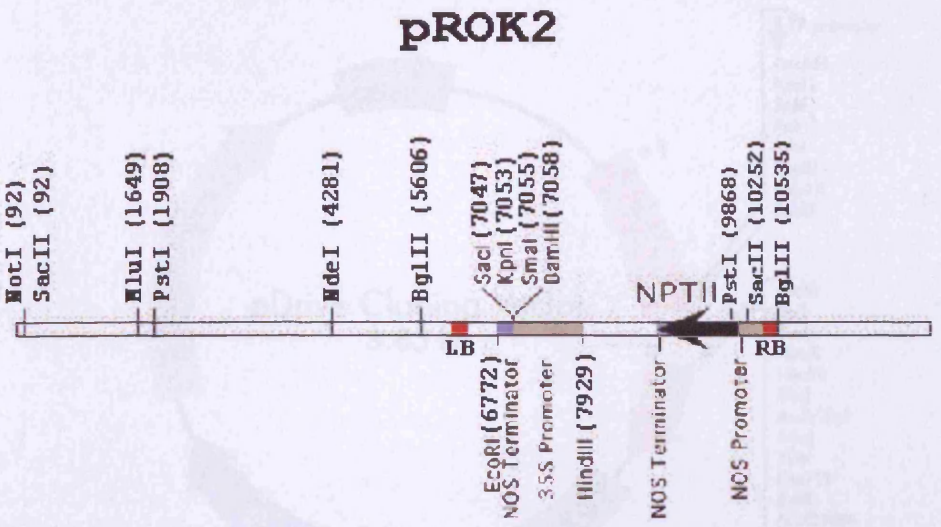

Figure S1.11: pROK2 plasmid. NPTII represents a kanamycin resistance gene. SacI, KpnI, SmaI and BamHI sites are all labeled in the cloning site.

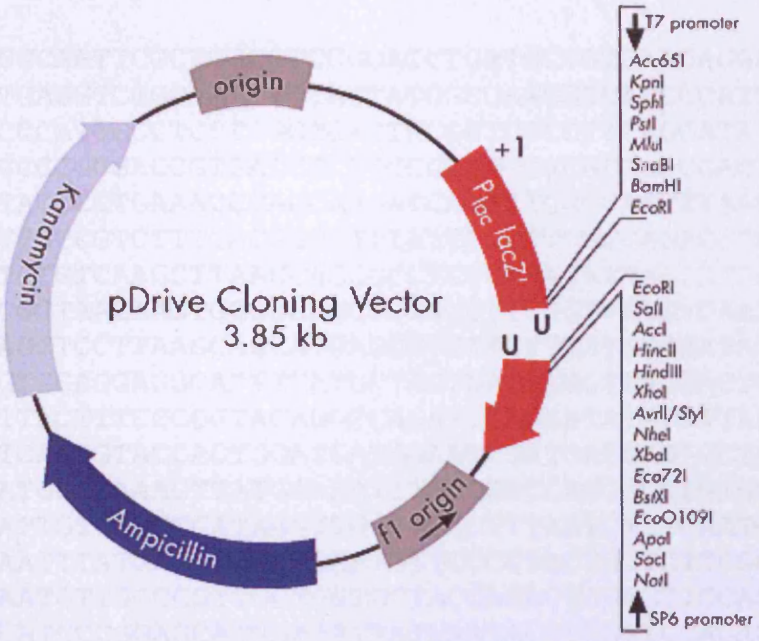

Figure S1.12: pDRIVE cloning vector. Kanamycin and Ampicillin resistance genes are shown as is the U overhang site where inserts are cloned.

5’

ATGGATACTGGCGGCAATTCGCTGGCGTCCGGACCTGATGGTGTGAAGAGGAAAGTTTGTTA
TTTCTATGACCCTGAGGTCGGCAATTACTACTATGGCCAAGGTCATCCCATGAAGCCCCATC
GCATCCGCATGACCCATGCCCTCCTCGCTCACTACGGTCTCCTTCAGCATATGCAGGTTCTC
AAGCCCTTCCCTGCCCGCGACCGTGATCTCTGCCGCTTCCACGCCGACGACTATGTCTCTTT
TCTCCGCAGCATTACCCCTGAAACCCAGCAAGATCAGATTCGCCAACTTAAGCGCTTCAATG
TTGGTGAAGACTGTCCCGTCTTTGACGGCCTTTATTCCTTTTGCCAGACCTATGCTGGAGGA
TCTGTTGGTGGCTCTGTCAAGCTTAACCACGGCCTCTGCGATATTGCCATCAACTGGGCTGG
TGGTCTCCATCACGCTAAGAAGTGCGAGGCCTCTGGCTTCTGTTACGTCAATGATATCGTCT
TAGCTATCCTAGAGCTCCTTAAGCAGCATGAGCGTGTTCTTTATGTCGATATTGATATCCAC
CACGGGGATGGAGTGGAGGAGGCATTTTATGCTACTGACAGGGTTATGACTGTCTCGTTTCA
TAAATTTGGTGATTACTTTCCCGGTACAGGTCACATTCAGGATATAGGTTATGGTAGCGGAA
AGTACTATTCTCTCAATGTACCACTGGATGATGGAATCGATGATGAGAGCTATCATCTGTTA
TTCAAGCCCATCATGGGGAAAGTTATGGAAATTTTCCGACCAGGGGCTGTGGTATTGCAATG
TGGTGCTGATTCATTGTCTGGTGATAGGTTGGGGTGCTTTAATCTTTCAATCAAAGGTCATG
CTGAGTGCGTCAAATTTATGAGATCGTTCAATGTTCCCCTACTGCTCTTGGGTGGTGGTGGT
TACACTATCCGCAATGTTGCCCGTTGCTGGTGCTACGAGACTGGAGTTGCACTTGGAGTTGA
AGTTGAAGACAAGATGCCGGAGCATGAATATTATGAATACTTTGGTCCAGACTATACACTTC
ACGTTGCTCCAAGTAACATGGAAAATAAGAATTCTCGTCAGATGCTTGAAGAGATTCGCAAT
GACCTTCTCCACAATCTCTCTAAGCTTCAGCATGCTCCAAGTGTACCATTTCAGGAAAGACC
ACCTGATACAGAGACTCCCGAGGTTGATGAAGACCAAGAAGATGGGGATAAAAGATGGGATC
CGGATTCAGACATGGATGTTGATGATGACCGTAAACCTATACCAAGCAGAGTAAAAAGAGAA
GCTGTTGAACCAGATACAAAGGACAAGGATGGACTGAAAGGAATTATGGAGCGTGGAAAAGG
TTGTGAGGTGGAGGTGGATGAGAGTGGAAGCACTAAGGTTACAGGAGTAAACCCAGTGGGAG
TGGAGGAAGCAAGTGTGAAAATGGAAGAGGAAGGAACAAACAAGGGTGGGGCGGAGCAGGCG
TTTCCTCCTAAAACA**TAA**

Figure S1.13: *HD1* coding region. Highlighted in bold and underlined are the start and stop codons. The *HD1* coding region is 1506 bp.

5’

ATGGACTCTCACTCTTCCCACCTCAACGCCGCCAATCGTTCCCGCAGTTCTCAGACTCCTTC
TCCTTCTCATTCCGCCTCCGCCTCCGTCACTTCTTCTCTCCACAAACGCAAACTCGCCGCCA
CCACGGCAGCGAATGCAGCCGCTTCTGAAGATCACGCCCCTCCTTCTTCCTCTTTCCCTCCT
TCCTCCTTCTCTGCCGATACTCGCGACGGCGCTTTAACCTCCAACGATGAACTCGAGAGCAT
CTCCGCTCGCGGCGCCGATACAGATTCAGATCCTGATGAATCAGAGGATATAGTCGTGGATG
ATGACGAGGACGAATTTGCTCCTGAACAGGACCAGGACTCTTCTATCCGCACATTCACCGCC
GCTCGACTCGATTCCAGCTCTGGAGTCAACGGTTCGAGTCGCAACACTAAACTTAAGACGGA
AAGCTCCACGGTGAAGCTTGAGAGCTCTGATGGTGGAAAAGATGGTGGATCATCTGTGGTTG
GGACTGGTGTGAGTGGCACTGTTGGAGGAAGCTCAATCTCAGGGCTCGTGCCAAAGGATGAG
TCTGTTAAGGTATTGGCTGAGAATTTCCAGACTAGCGGAGCTTACATTGCCAGAGAAGAGGC
TTTGAAAAGAGAGGAGCAAGCAGGACGACTCAAATTTGTTTGTTACTCAAATGATTCCATTG
ATGAGCATATGATGTGCTTGATTGGGTTGAAGAACATTTTTGCAAGACAGTTACCTAATATG
CCCAAGGAGTACATTGTTCGTCTTCTGATGGATAGGAAACATAAGTCTGTTATGGTACTAAG
AGGGAATCTAGTTGTAGGTGGTATCACGTATCGTCCATATCACAGTCAGAAGTTTGGGGAAA
TAGCATTTTGTGCAATCACAGCAGATGAACAAGTAAAAGGTTACGGTACCAGATTGATGAAC
CACTTGAAACAACATGCACGTGATGTTGATGGATTGACGCATTTTCTTACTTATGCTGACAA
CAATGCTGTTGGTTACTTCGTCAAGCAGGGTTTTACTAAAGAGATTTACTTGGAGAAAGATG
TATGGCATGGGTTCATTAAAGACTATGATGGTGGTCTCCTTATGGAATGCAAAATTGATCCA
AAGCTGCCATATACGGATTTGTCAAGCATGATACGCCAGCAAAGAAAGGCAATTGATGAAAG
GATAAGAGAGTTATCAAACTGTCAGAATGTGTATCCAAAAATTGAGTTTCTAAAGAATGAAG
CTGGAATTCCTAGAAAGATTATCAAAGTTGAGGAAATACGTGGCTTAAGGGAAGCTGGTTGG
ACCCCAGATCAGTGGGGGCACACTCGTTTCAAATTATTCAATGGTTCTGCTGATATGGTGAC
AAATCAAAAACAGTTGAATGCACTCATGCGTGCGCTTTTAAAGACAATGCAAGACCATGCTG
ATGCTTGGCCTTTCAAAGAACCAGTGGATTCTCGCGATGTCCCTGATTACTATGACATCATT
AAGGATCCCATTGATCTGAAGGTAATTGCAAAGAGGGTAGAGTCGGAACAGTATTACGTGAC
ATTGGATATGTTTGTTGCGGATGCGAGACGGATGTTTAACAATTGTAGAACTTACAACTCCC
CCGATACCATTTATTACAAATGTGCAACCAGGTTGGAAACACACTTCCATAGCAAAGTACAA
GCAGGTCTCCAATCTGGTGCTAAATCTCAA**TAG**

Figure S1.14: *GCN5* coding region. Highlighted in bold and underlined are the start and stop codons. The *GCN5* coding region is 1707 bp.

5′
ATGCCCAAGCAAAAAGCTCCAAGGAAGCAGCTCAAGTCCTATAAACTCAAACACATCA
ACAAGAGTATTCAAGAGGGAGATGCTGTGTTGATGCGGTCGTCGGAGCCTGGAAAACC
GTCGTACGTAGCGAGGGTAGAGGCGATCGAGACGGACGCGCGTGGATCGCACGCGAAA
GTTCGTGTGAGGTGGTATTATCGCCCTGAGGAATCTATCGGAGGGAGGAGACAATTCC
ATGGAGCCAAGGAGGTTTTTCTCTCTGACCACTTCGATTTTCAAAGCGCCGATACGAT
TGAAGGAAAGTGTAAGGTTCACAGTTTCAGTAGCTACACCAAACTTGACTCTGTTGGA
AACGACGACTTCTTCTGTCGTTTCGAGTACAATTCCACTACCGGCGCGTTTGATCCTG
ACAGAGTCACCGTGTTCTGCAAGTGTGAGATGCCGTATAACCCAGATGACTTGATGGT
GCAATGCGAGGAGTGTTCTGAGTGGTTTCATCCTTCTTGTATAGGAACAACAATAGAG
GAAGCTAAAAAGCCAGATAACTTCTACTGCGAAGAGTGTTCCCCACAACAGCAGAATT
TGCACAACTCTAATTCAACTTCCAATAACAGAGATGCTAAGGTGAATGGAAAGCGCAG
CCTGGAGGTAACTAAATCGAAGAACAAACACACTAAGCGACCAGGTTAA

Figure S1.15: *SHL* coding region showing the regions to which RNAi knockdown constructs were designed. Highlighted in red is the RNAi N region, highlighted in yellow is the RNAi central region and underlined is the RNAi C region.

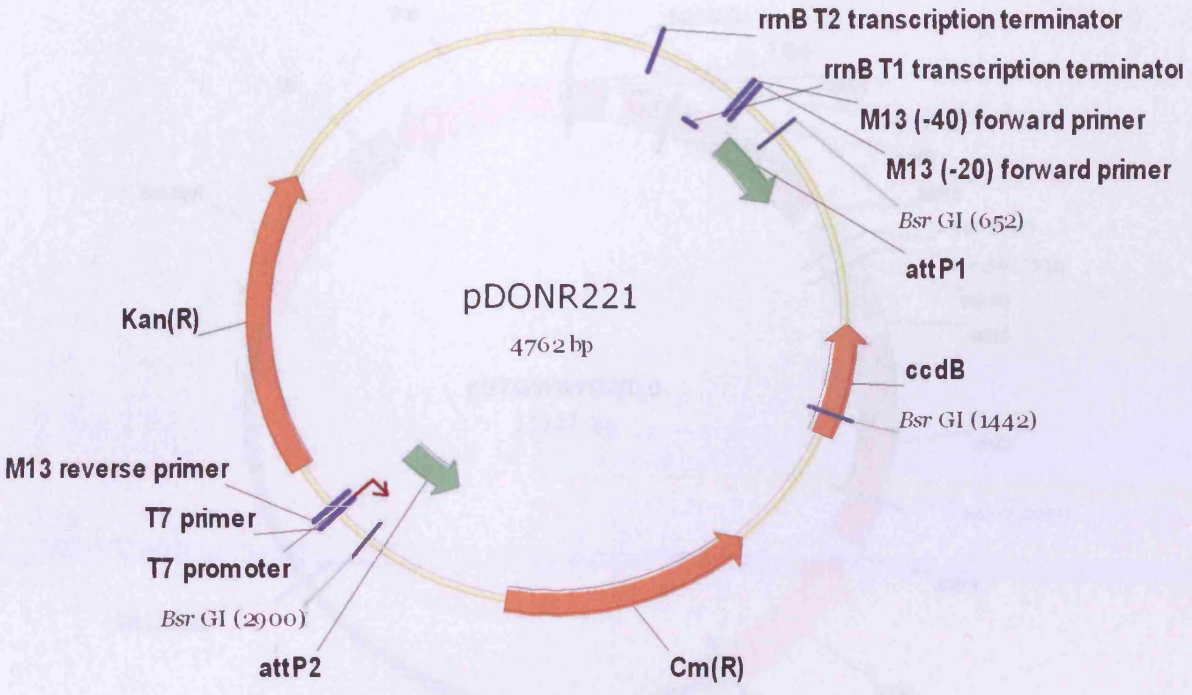

Figure S1.16: pDONOR221. The *ccdB* gene is shown and is flanked by attP1 and attP2 sites, indicating the positions where the insert will recombine.

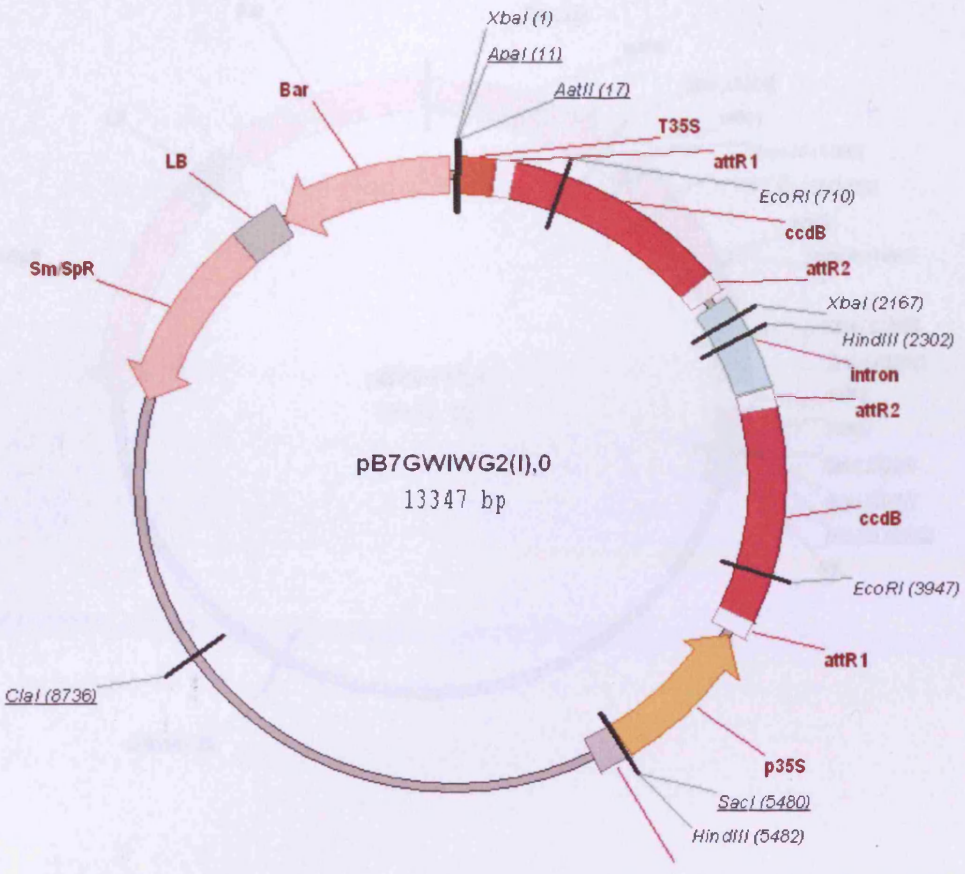

Figure S1.17: pB7GWIWG2. The *ccdB* gene is shown and is flanked by attR1 and attR2 sites, indicating the positions where the insert will recombine. This destination vector is used for generating hairpin constructs, hence the presence of two regions for the insert to be cloned into.

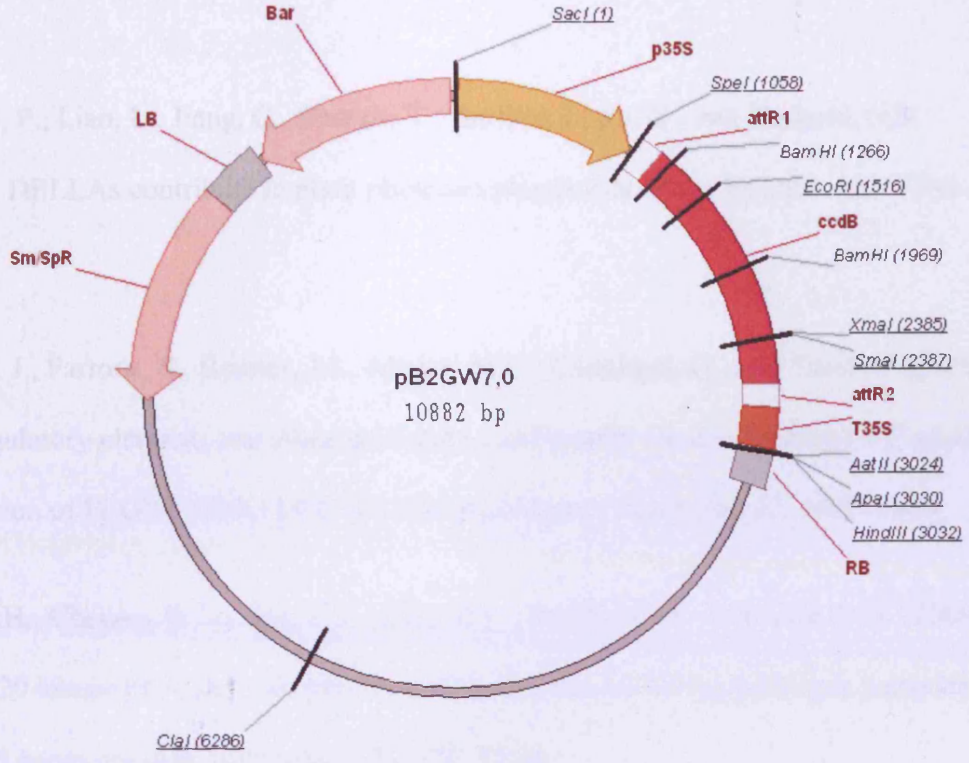

Figure S1.18: pB2GW7. The *ccdB* gene is shown and is flanked by attR1 and attR2 sites, indicating the positions where the insert will recombine. This destination vector is used over-expressing constructs.

Reference

Achard, P., Liao, L., Jiang, C., Desnos, T., Bartlett, J., Fu, X., and Harberd, N.P. (2007). DELLAs contribute to plant photomorphogenesis. Plant Physiol. *143,* 1163-1172.

Adrian, J., Farrona, S., Reimer, J.J., Albani, M.C., Coupland, G., and Turck, F. (2010). cis-Regulatory elements and chromatin state coordinately control temporal and spatial expression of FLOWERING LOCUS T in *Arabidopsis*. Plant Cell *22,* 1425-1440.

Ahn, S.H., Cheung, W.L., Hsu, J.Y., Diaz, R.L., Smith, M.M., and Allis, C.D. (2005). Sterile 20 kinase phosphorylates histone H2B at serine 10 during hydrogen peroxide-induced apoptosis in S. cerevisiae. Cell *120,* 25-36.

Alabadi, D., Oyama, T., Yanovsky, M.J., Harmon, F.G., Mas, P., and Kay, S.A. (2001). Reciprocal regulation between TOC1 and LHY/CCA1 within the *Arabidopsis* circadian clock. Science *293,* 880-883.

Allan, J., Harborne, N., Rau, D.C., and Gould, H. (1982). Participation of core histone "tails" in the stabilization of the chromatin solenoid. J. Cell Biol. *93,* 285-297.

ALLFREY, V.G., FAULKNER, R., and MIRSKY, A.E. (1964). Acetylation and Methylation of Histones and their Possible Role in the Regulation of Rna Synthesis. Proc. Natl. Acad. Sci. U. S. A. *51,* 786-794.

Al-Sady, B., Ni, W., Kircher, S., Schafer, E., and Quail, P.H. (2006). Photoactivated phytochrome induces rapid PIF3 phosphorylation prior to proteasome-mediated degradation. Mol. Cell *23,* 439-446.

Ang, L.H., Chattopadhyay, S., Wei, N., Oyama, T., Okada, K., Batschauer, A., and Deng, X.W. (1998). Molecular interaction between COP1 and HY5 defines a regulatory switch for light control of *Arabidopsis* development. Mol. Cell *1,* 213-222.

Angelov, D., Charra, M., Seve, M., Cote, J., Khochbin, S., and Dimitrov, S. (2000). Differential remodeling of the HIV-1 nucleosome upon transcription activators and SWI/SNF complex binding. J. Mol. Biol. *302,* 315-326.

Aukerman, M.J., Hirschfeld, M., Wester, L., Weaver, M., Clack, T., Amasino, R.M., and Sharrock, R.A. (1997). A deletion in the PHYD gene of the *Arabidopsis* Wassilewskija ecotype defines a role for phytochrome D in red/far-red light sensing. Plant Cell *9,* 1317-1326.

Bartel, D.P. (2009). MicroRNAs: target recognition and regulatory functions. Cell *136,* 215-233.

Bastow, R., Mylne, J.S., Lister, C., Lippman, Z., Martienssen, R.A., and Dean, C. (2004). Vernalization requires epigenetic silencing of FLC by histone methylation. Nature *427,* 164-167.

Baulcombe, D. C., Saunders, G., R., Bevan, M., W., Mayo, M., A., and Harrison B., D. (1986). Expression of biologically active viral satellite RNAfrom the nuclear genome of transformed plants. Nature *321,* 446-449.

Bauer, D., Viczian, A., Kircher, S., Nobis, T., Nitschke, R., Kunkel, T., Panigrahi, K.C., Adam, E., Fejes, E., Schafer, E., and Nagy, F. (2004). Constitutive photomorphogenesis 1 and multiple photoreceptors control degradation of phytochrome interacting factor 3, a transcription factor required for light signaling in *Arabidopsis*. Plant Cell *16,* 1433-1445.

Beggs, C.J., Holmes, M.G., Jabben, M., and Schafer, E. (1980). Action Spectra for the Inhibition of Hypocotyl Growth by Continuous Irradiation in Light and Dark-Grown Sinapis alba L. Seedlings. Plant Physiol. *66,* 615-618.

Benhamed, M., Bertrand, C., Servet, C., and Zhou, D.X. (2006). *Arabidopsis* GCN5, HD1, and TAF1/HAF2 interact to regulate histone acetylation required for light-responsive gene expression. Plant Cell *18,* 2893-2903.

Benvenuto, G., Formiggini, F., Laflamme, P., Malakhov, M., and Bowler, C. (2002). The photomorphogenesis regulator DET1 binds the amino-terminal tail of histone H2B in a nucleosome context. Curr. Biol. *12,* 1529-1534.

Berger, S.L. (2002). Histone modifications in transcriptional regulation. Curr. Opin. Genet. Dev. *12,* 142-148.

Bertrand, C., Bergounioux, C., Domenichini, S., Delarue, M., and Zhou, D.X. (2003). *Arabidopsis* histone acetyltransferase AtGCN5 regulates the floral meristem activity through the WUSCHEL/AGAMOUS pathway. J. Biol. Chem. *278,* 28246-28251.

Bordoli, L., Husser, S., Luthi, U., Netsch, M., Osmani, H., and Eckner, R. (2001). Functional analysis of the p300 acetyltransferase domain: the PHD finger of p300 but not of CBP is dispensable for enzymatic activity. Nucleic Acids Res. *29,* 4462-4471.

Boylan, M.T., and Quail, P.H. (1989). Oat Phytochrome Is Biologically Active in Transgenic Tomatoes. Plant Cell *1,* 765-773.

Boylan, M.T., and Quail, P.H. (1989). Oat Phytochrome Is Biologically Active in Transgenic Tomatoes. Plant Cell *1,* 765-773.

Briggs, W.R., Beck, C.F., Cashmore, A.R., Christie, J.M., Hughes, J., Jarillo, J.A., Kagawa, T., Kanegae, H., Liscum, E., Nagatani, A., *et al.* (2001). The phototropin family of photoreceptors. Plant Cell *13,* 993-997.

Butler, W.L., Norris, K.H., Siegelman, H.W., and Hendricks, S.B. (1959). Detection, Assay, and Preliminary Purification of the Pigment Controlling Photoresponsive Development of Plants. Proc. Natl. Acad. Sci. U. S. A. *45,* 1703-1708.

Carabelli, M., Morelli, G., Whitelam, G., and Ruberti, I. (1996). Twilight-zone and canopy shade induction of the Athb-2 homeobox gene in green plants. Proc. Natl. Acad. Sci. U. S. A. *93,* 3530-3535.

Carabelli, M., Sessa, G., Baima, S., Morelli, G., and Ruberti, I. (1993). The *Arabidopsis* Athb-2 and -4 genes are strongly induced by far-red-rich light. Plant J. *4,* 469-479.

Casal, J.J., Yanovsky, M.J., and Luppi, J.P. (2000). Two photobiological pathways of phytochrome A activity, only one of which shows dominant negative suppression by phytochrome B. Photochem. Photobiol. *71,* 481-486.

Cashmore, A.R., Jarillo, J.A., Wu, Y.J., and Liu, D. (1999). Cryptochromes: blue light receptors for plants and animals. Science *284,* 760-765.

Charron, J.B., He, H., Elling, A.A., and Deng, X.W. (2009). Dynamic landscapes of four histone modifications during deetiolation in *Arabidopsis*. Plant Cell *21,* 3732-3748.

Chen, M., Chory, J., and Fankhauser, C. (2004). Light signal transduction in higher plants. Annu. Rev. Genet. *38,* 87-117.

Choi, G., Yi, H., Lee, J., Kwon, Y.K., Soh, M.S., Shin, B., Luka, Z., Hahn, T.R., and Song, P.S. (1999). Phytochrome signalling is mediated through nucleoside diphosphate kinase 2. Nature *401,* 610-613.

Christie, J.M. (2007). Phototropin blue-light receptors. Annu. Rev. Plant. Biol. *58,* 21-45.

Christie, J.M., Reymond, P., Powell, G.K., Bernasconi, P., Raibekas, A.A., Liscum, E., and Briggs, W.R. (1998). *Arabidopsis* NPH1: a flavoprotein with the properties of a photoreceptor for phototropism. Science *282,* 1698-1701.

Chua, Y.L., Brown, A.P., and Gray, J.C. (2001). Targeted histone acetylation and altered nuclease accessibility over short regions of the pea plastocyanin gene. Plant Cell *13,* 599-612.

Clack, T., Mathews, S., and Sharrock, R.A. (1994). The phytochrome apoprotein family in *Arabidopsis* is encoded by five genes: the sequences and expression of PHYD and PHYE. Plant Mol. Biol. *25,* 413-427.

Clack, T., Shokry, A., Moffet, M., Liu, P., Faul, M., and Sharrock, R.A. (2009). Obligate heterodimerization of *Arabidopsis* phytochromes C and E and interaction with the PIF3 basic helix-loop-helix transcription factor. Plant Cell *21,* 786-799.

Crosio, C., Cermakian, N., Allis, C.D., and Sassone-Corsi, P. (2000). Light induces chromatin modification in cells of the mammalian circadian clock. Nat. Neurosci. *3,* 1241-1247.

Curtis, A.M., Seo, S.B., Westgate, E.J., Rudic, R.D., Smyth, E.M., Chakravarti, D., FitzGerald, G.A., and McNamara, P. (2004). Histone acetyltransferase-dependent chromatin remodeling and the vascular clock. J. Biol. Chem. *279,* 7091-7097.

de Lucas, M., Daviere, J.M., Rodriguez-Falcon, M., Pontin, M., Iglesias-Pedraz, J.M., Lorrain, S., Fankhauser, C., Blazquez, M.A., Titarenko, E., and Prat, S. (2008). A molecular framework for light and gibberellin control of cell elongation. Nature *451,* 480-484.

Deforce, L., Tomizawa, K., Ito, N., Farrens, D., Song, P.S., and Furuya, M. (1991). In vitro assembly of apophytochrome and apophytochrome deletion mutants expressed in yeast with phycocyanobilin. Proc. Natl. Acad. Sci. U. S. A. *88,* 10392-10396.

Devlin, P.F., and Kay, S.A. (2000). Cryptochromes are required for phytochrome signaling to the circadian clock but not for rhythmicity. Plant Cell *12,* 2499-2510.

Devlin, P.F., Patel, S.R., and Whitelam, G.C. (1998). Phytochrome E influences internode elongation and flowering time in *Arabidopsis*. Plant Cell *10,* 1479-1487.

Devlin, P.F., Yanovsky, M.J., and Kay, S.A. (2003). A genomic analysis of the shade avoidance response in *Arabidopsis*. Plant Physiol. *133,* 1617-1629.

Dion, M.F., Altschuler, S.J., Wu, L.F., and Rando, O.J. (2005). Genomic characterization reveals a simple histone H4 acetylation code. Proc. Natl. Acad. Sci. U. S. A. *102,* 5501-5506.

Djakovic-Petrovic, T., de Wit, M., Voesenek, L.A., and Pierik, R. (2007). DELLA protein function in growth responses to canopy signals. Plant J. *51,* 117-126.

Doi, M., Hirayama, J., and Sassone-Corsi, P. (2006). Circadian regulator CLOCK is a histone acetyltransferase. Cell *125,* 497-508.

Dowson-Day, M.J., and Millar, A.J. (1999). Circadian dysfunction causes aberrant hypocotyl elongation patterns in *Arabidopsis*. Plant J. *17,* 63-71.

Eberharter, A., and Becker, P.B. (2002). Histone acetylation: a switch between repressive and permissive chromatin. Second in review series on chromatin dynamics. EMBO Rep. *3,* 224-229.

Eickbush, T.H., and Moudrianakis, E.N. (1978). The histone core complex: an octamer assembled by two sets of protein-protein interactions. Biochemistry *17,* 4955-4964.

Eshed, Y., Baum, S.F., and Bowman, J.L. (1999). Distinct mechanisms promote polarity establishment in carpels of *Arabidopsis*. Cell *99,* 199-209.

Fabian, M.R., Sonenberg, N., and Filipowicz, W. (2010). Regulation of mRNA translation and stability by microRNAs. Annu. Rev. Biochem. *79,* 351-379.

Fairchild, C.D., Schumaker, M.A., and Quail, P.H. (2000). HFR1 encodes an atypical bHLH protein that acts in phytochrome A signal transduction. Genes Dev. *14,* 2377-2391.

Fankhauser, C., Yeh, K.C., Lagarias, J.C., Zhang, H., Elich, T.D., and Chory, J. (1999). PKS1, a substrate phosphorylated by phytochrome that modulates light signaling in *Arabidopsis*. Science *284,* 1539-1541.

Feng, S., Martinez, C., Gusmaroli, G., Wang, Y., Zhou, J., Wang, F., Chen, L., Yu, L., Iglesias-Pedraz, J.M., Kircher, S., *et al.* (2008). Coordinated regulation of *Arabidopsis thaliana* development by light and gibberellins. Nature *451,* 475-479.

Fowler, S.G., Cook, D., and Thomashow, M.F. (2005). Low temperature induction of *Arabidopsis* CBF1, 2, and 3 is gated by the circadian clock. Plant Physiol. *137,* 961-968.

Franklin, K.A., Allen, T., and Whitelam, G.C. (2007). Phytochrome A is an irradiance-dependent red light sensor. Plant J. *50,* 108-117.

Franklin, K.A., Davis, S.J., Stoddart, W.M., Vierstra, R.D., and Whitelam, G.C. (2003). Mutant analyses define multiple roles for phytochrome C in *Arabidopsis* photomorphogenesis. Plant Cell *15,* 1981-1989.

Franklin, K.A., and Quail, P.H. (2010). Phytochrome functions in *Arabidopsis* development. J. Exp. Bot. *61,* 11-24.

Franklin, K.A., and Whitelam, G.C. (2007). Light-quality regulation of freezing tolerance in *Arabidopsis thaliana.* Nat. Genet. *39,* 1410-1413.

Franklin, K.A., and Whitelam, G.C. (2005). Phytochromes and shade-avoidance responses in plants. Ann. Bot. (Lond) *96,* 169-175.

Fujimori, T., Yamashino, T., Kato, T., and Mizuno, T. (2004). Circadian-controlled basic/helix-loop-helix factor, PIL6, implicated in light-signal transduction in *Arabidopsis thaliana.* Plant Cell Physiol. *45,* 1078-1086.

Fuks, F., Hurd, P.J., Deplus, R., and Kouzarides, T. (2003). The DNA methyltransferases associate with HP1 and the SUV39H1 histone methyltransferase. Nucleic Acids Res. *31,* 2305-2312.

Galburt, E.A., Grill, S.W., Wiedmann, A., Lubkowska, L., Choy, J., Nogales, E., Kashlev, M., and Bustamante, C. (2007). Backtracking determines the force sensitivity of RNAP II in a factor-dependent manner. Nature *446,* 820-823.

Garcia-Ramirez, M., Dong, F., and Ausio, J. (1992). Role of the histone "tails" in the folding of oligonucleosomes depleted of histone H1. J. Biol. Chem. *267,* 19587-19595.

Gil, P., Kircher, S., Adam, E., Bury, E., Kozma-Bognar, L., Schafer, E., and Nagy, F. (2000). Photocontrol of subcellular partitioning of phytochrome-B:GFP fusion protein in tobacco seedlings. Plant J. *22,* 135-145.

Grant, P.A., Duggan, L., Cote, J., Roberts, S.M., Brownell, J.E., Candau, R., Ohba, R., Owen-Hughes, T., Allis, C.D., Winston, F., Berger, S.L., and Workman, J.L. (1997). Yeast Gcn5 functions in two multisubunit complexes to acetylate nucleosomal histones: characterization of an Ada complex and the SAGA (Spt/Ada) complex. Genes Dev. *11,* 1640-1650.

Green, M.R. (2005). Eukaryotic transcription activation: right on target. Mol. Cell *18,* 399-402.

Grimaldi, B., Nakahata, Y., Kaluzova, M., Masubuchi, S., and Sassone-Corsi, P. (2009). Chromatin remodeling, metabolism and circadian clocks: the interplay of CLOCK and SIRT1. Int. J. Biochem. Cell Biol. *41,* 81-86.

Grunstein, M. (1997). Histone acetylation in chromatin structure and transcription. Nature *389,* 349-352.

Guo, H., Yang, H., Mockler, T.C., and Lin, C. (1998). Regulation of flowering time by *Arabidopsis* photoreceptors. Science *279,* 1360-1363.

Guo, L., Yin, B., Zhou, J., Li, X., and Deng, X.W. (2006). Development of rabbit monoclonal and polyclonal antibodies for detection of site-specific histone modifications and their application in analyzing overall modification levels. Cell Res. *16,* 519-527.

Guo, L., Zhou, J., Elling, A.A., Charron, J.B., and Deng, X.W. (2008). Histone modifications and expression of light-regulated genes in *Arabidopsis* are cooperatively influenced by changing light conditions. Plant Physiol. *147,* 2070-2083.

Hall, A., Kozma-Bognar, L., Toth, R., Nagy, F., and Millar, A.J. (2001). Conditional circadian regulation of PHYTOCHROME A gene expression. Plant Physiol. *127,* 1808-1818.

Hamiche, A., Sandaltzopoulos, R., Gdula, D.A., and Wu, C. (1999). ATP-dependent histone octamer sliding mediated by the chromatin remodeling complex NURF. Cell *97,* 833-842.

Harberd, N.P., Belfield, E., and Yasumura, Y. (2009). The angiosperm gibberellin-GID1-DELLA growth regulatory mechanism: how an "inhibitor of an inhibitor" enables flexible response to fluctuating environments. Plant Cell *21,* 1328-1339.

Hassan, A.H., Neely, K.E., and Workman, J.L. (2001). Histone acetyltransferase complexes stabilize swi/snf binding to promoter nucleosomes. Cell *104,* 817-827.

Havas, K., Flaus, A., Phelan, M., Kingston, R., Wade, P.A., Lilley, D.M., and Owen-Hughes, T. (2000). Generation of superhelical torsion by ATP-dependent chromatin remodeling activities. Cell *103,* 1133-1142.

Henderson, I.R., and Dean, C. (2004). Control of *Arabidopsis* flowering: the chill before the bloom. Development *131,* 3829-3838.

Hennig, L., Buche, C., Eichenberg, K., and Schafer, E. (1999). Dynamic properties of endogenous phytochrome A in *Arabidopsis* seedlings. Plant Physiol. *121,* 571-577.

Hennig, L., Stoddart, W.M., Dieterle, M., Whitelam, G.C., and Schafer, E. (2002). Phytochrome E controls light-induced germination of *Arabidopsis*. Plant Physiol. *128,* 194-200.

Hiltbrunner, A., Tscheuschler, A., Viczian, A., Kunkel, T., Kircher, S., and Schafer, E. (2006). FHY1 and FHL act together to mediate nuclear accumulation of the phytochrome A photoreceptor. Plant Cell Physiol. *47,* 1023-1034.

Hiltbrunner, A., Viczian, A., Bury, E., Tscheuschler, A., Kircher, S., Toth, R., Honsberger, A., Nagy, F., Fankhauser, C., and Schafer, E. (2005). Nuclear accumulation of the phytochrome A photoreceptor requires FHY1. Curr. Biol. *15,* 2125-2130.

Hodges, C., Bintu, L., Lubkowska, L., Kashlev, M., and Bustamante, C. (2009). Nucleosomal fluctuations govern the transcription dynamics of RNA polymerase II. Science *325,* 626-628.

Hong, L., Schroth, G.P., Matthews, H.R., Yau, P., and Bradbury, E.M. (1993). Studies of the DNA binding properties of histone H4 amino terminus. Thermal denaturation

studies reveal that acetylation markedly reduces the binding constant of the H4 "tail" to DNA. J. Biol. Chem. *268,* 305-314.

Hornitschek, P., Lorrain, S., Zoete, V., Michielin, O., and Fankhauser, C. (2009). Inhibition of the shade avoidance response by formation of non-DNA binding bHLH heterodimers. EMBO J. *28,* 3893-3902.

Hsu, J.Y., Sun, Z.W., Li, X., Reuben, M., Tatchell, K., Bishop, D.K., Grushcow, J.M., Brame, C.J., Caldwell, J.A., Hunt, D.F., *et al.* (2000). Mitotic phosphorylation of histone H3 is governed by Ipl1/aurora kinase and Glc7/PP1 phosphatase in budding yeast and nematodes. Cell *102,* 279-291.

Huq, E., Al-Sady, B., and Quail, P.H. (2003). Nuclear translocation of the photoreceptor phytochrome B is necessary for its biological function in seedling photomorphogenesis. Plant J. *35,* 660-664.

Huq, E., Kang, Y., Halliday, K.J., Qin, M., and Quail, P.H. (2000). SRL1: a new locus specific to the phyB-signaling pathway in *Arabidopsis*. Plant J. *23,* 461-470.

Huq, E., and Quail, P.H. (2002). PIF4, a phytochrome-interacting bHLH factor, functions as a negative regulator of phytochrome B signaling in *Arabidopsis*. EMBO J. *21,* 2441-2450.

Huq, E., Tepperman, J.M., and Quail, P.H. (2000). GIGANTEA is a nuclear protein involved in phytochrome signaling in *Arabidopsis*. Proc. Natl. Acad. Sci. U. S. A. *97,* 9789-9794.

Ito, T., Levenstein, M.E., Fyodorov, D.V., Kutach, A.K., Kobayashi, R., and Kadonaga, J.T. (1999). ACF consists of two subunits, Acf1 and ISWI, that function cooperatively in the ATP-dependent catalysis of chromatin assembly. Genes Dev. *13,* 1529-1539.

Jasencakova, Z., Meister, A., Walter, J., Turner, B.M., and Schubert, I. (2000). Histone H4 acetylation of euchromatin and heterochromatin is cell cycle dependent and correlated with replication rather than with transcription. Plant Cell *12,* 2087-2100.

Johnson, D.S., Mortazavi, A., Myers, R.M., and Wold, B. (2007). Genome-wide mapping of in vivo protein-DNA interactions. Science *316,* 1497-1502.

Johnson, E., Bradley, M., Harberd, N.P., and Whitelam, G.C. (1994). Photoresponses of Light-Grown phyA Mutants of *Arabidopsis* (Phytochrome A Is Required for the Perception of Daylength Extensions). Plant Physiol. *105,* 141-149.

Johnson, L., Mollah, S., Garcia, B.A., Muratore, T.L., Shabanowitz, J., Hunt, D.F., and Jacobsen, S.E. (2004). Mass spectrometry analysis of *Arabidopsis* histone H3 reveals distinct combinations of post-translational modifications. Nucleic Acids Res. *32,* 6511-6518.

Karimi, M., Inze, D., and Depicker, A. (2002). GATEWAY vectors for Agrobacterium-mediated plant transformation. Trends Plant Sci. *7,* 193-195.

Khanna, R., Huq, E., Kikis, E.A., Al-Sady, B., Lanzatella, C., and Quail, P.H. (2004). A novel molecular recognition motif necessary for targeting photoactivated phytochrome signaling to specific basic helix-loop-helix transcription factors. Plant Cell *16,* 3033-3044.

Kim, L., Kircher, S., Toth, R., Adam, E., Schafer, E., and Nagy, F. (2000). Light-induced nuclear import of phytochrome-A:GFP fusion proteins is differentially regulated in transgenic tobacco and *Arabidopsis*. Plant J. *22,* 125-133.

Kircher, S., Gil, P., Kozma-Bognar, L., Fejes, E., Speth, V., Husselstein-Muller, T., Bauer, D., Adam, E., Schafer, E., and Nagy, F. (2002). Nucleocytoplasmic partitioning of the plant photoreceptors phytochrome A, B, C, D, and E is regulated differentially by light and exhibits a diurnal rhythm. Plant Cell *14,* 1541-1555.

Kireeva, M.L., Hancock, B., Cremona, G.H., Walter, W., Studitsky, V.M., and Kashlev, M. (2005). Nature of the nucleosomal barrier to RNA polymerase II. Mol. Cell *18,* 97-108.

Knezetic, J.A., and Luse, D.S. (1986). The presence of nucleosomes on a DNA template prevents initiation by RNA polymerase II in vitro. Cell *45,* 95-104.

Kouzarides, T. (2007). Chromatin modifications and their function. Cell *128,* 693-705.

Kumar, S.V., and Wigge, P.A. (2010). H2A.Z-containing nucleosomes mediate the thermosensory response in *Arabidopsis*. Cell *140,* 136-147.

Lagarias, J.C., and Lagarias, D.M. (1989). Self-assembly of synthetic phytochrome holoprotein in vitro. Proc. Natl. Acad. Sci. U. S. A. *86,* 5778-5780.

Lee, D.Y., Hayes, J.J., Pruss, D., and Wolffe, A.P. (1993). A positive role for histone acetylation in transcription factor access to nucleosomal DNA. Cell *72,* 73-84.

Lee, J., He, K., Stolc, V., Lee, H., Figueroa, P., Gao, Y., Tongprasit, W., Zhao, H., Lee, I., and Deng, X.W. (2007). Analysis of transcription factor HY5 genomic binding sites revealed its hierarchical role in light regulation of development. Plant Cell *19,* 731-749.

Li, B., Carey, M., and Workman, J.L. (2007). The role of chromatin during transcription. Cell *128,* 707-719.

Lin, C., Yang, H., Guo, H., Mockler, T., Chen, J., and Cashmore, A.R. (1998). Enhancement of blue-light sensitivity of *Arabidopsis* seedlings by a blue light receptor cryptochrome 2. Proc. Natl. Acad. Sci. U. S. A. *95,* 2686-2690.

Liu, X.L., Covington, M.F., Fankhauser, C., Chory, J., and Wagner, D.R. (2001). ELF3 encodes a circadian clock-regulated nuclear protein that functions in an *Arabidopsis* PHYB signal transduction pathway. Plant Cell *13,* 1293-1304.

Loidl, P. (2004). A plant dialect of the histone language. Trends Plant Sci. *9,* 84-90.

Lorch, Y., LaPointe, J.W., and Kornberg, R.D. (1987). Nucleosomes inhibit the initiation of transcription but allow chain elongation with the displacement of histones. Cell *49,* 203-210.

Lorch, Y., Zhang, M., and Kornberg, R.D. (1999). Histone octamer transfer by a chromatin-remodeling complex. Cell *96,* 389-392.

Lorrain, S., Allen, T., Duek, P.D., Whitelam, G.C., and Fankhauser, C. (2008). Phytochrome-mediated inhibition of shade avoidance involves degradation of growth-promoting bHLH transcription factors. Plant J. *53,* 312-323.

Luger, K., Mader, A.W., Richmond, R.K., Sargent, D.F., and Richmond, T.J. (1997). Crystal structure of the nucleosome core particle at 2.8 A resolution. Nature *389,* 251-260.

Makino, S., Matsushika, A., Kojima, M., Yamashino, T., and Mizuno, T. (2002). The APRR1/TOC1 quintet implicated in circadian rhythms of *Arabidopsis thaliana*: I. Characterization with APRR1-overexpressing plants. Plant Cell Physiol. *43,* 58-69.

Martinez-Garcia, J.F., Huq, E., and Quail, P.H. (2000). Direct targeting of light signals to a promoter element-bound transcription factor. Science *288,* 859-863.

Mas, P., Alabadi, D., Yanovsky, M.J., Oyama, T., and Kay, S.A. (2003). Dual role of TOC1 in the control of circadian and photomorphogenic responses in *Arabidopsis*. Plant Cell *15,* 223-236.

Mathews, S. (2010). Evolutionary studies illuminate the structural-functional model of plant phytochromes. Plant Cell *22,* 4-16.

Matsushita, T., Mochizuki, N., and Nagatani, A. (2003). Dimers of the N-terminal domain of phytochrome B are functional in the nucleus. Nature *424,* 571-574.

Mazzella, M.A., Cerdan, P.D., Staneloni, R.J., and Casal, J.J. (2001). Hierarchical coupling of phytochromes and cryptochromes reconciles stability and light modulation of *Arabidopsis* development. Development *128,* 2291-2299.

Mizuguchi, G., Shen, X., Landry, J., Wu, W.H., Sen, S., and Wu, C. (2004). ATP-driven exchange of histone H2AZ variant catalyzed by SWR1 chromatin remodeling complex. Science *303,* 343-348.

Mockler, T.C., Guo, H., Yang, H., Duong, H., and Lin, C. (1999). Antagonistic actions of *Arabidopsis* cryptochromes and phytochrome B in the regulation of floral induction. Development *126,* 2073-2082.

Monte, E., Alonso, J.M., Ecker, J.R., Zhang, Y., Li, X., Young, J., Austin-Phillips, S., and Quail, P.H. (2003). Isolation and characterization of phyC mutants in *Arabidopsis* reveals complex crosstalk between phytochrome signaling pathways. Plant Cell *15,* 1962-1980.

Mussig, C., and Altmann, T. (2003). Changes in gene expression in response to altered SHL transcript levels. Plant Mol. Biol. *53,* 805-820.

Mussig, C., Kauschmann, A., Clouse, S.D., and Altmann, T. (2000). The *Arabidopsis* PHD-finger protein SHL is required for proper development and fertility. Mol. Gen. Genet. *264,* 363-370.

Nagatani, A., Reed, J.W., and Chory, J. (1993). Isolation and Initial Characterization of *Arabidopsis* Mutants That Are Deficient in Phytochrome A. Plant Physiol. *102,* 269-277.

Nagy, F., and Schafer, E. (2002). Phytochromes control photomorphogenesis by differentially regulated, interacting signaling pathways in higher plants. Annu. Rev. Plant. Biol. *53,* 329-355.

Ni, M., Tepperman, J.M., and Quail, P.H. (1999). Binding of phytochrome B to its nuclear signalling partner PIF3 is reversibly induced by light. Nature *400,* 781-784.

Ni, M., Tepperman, J.M., and Quail, P.H. (1998). PIF3, a phytochrome-interacting factor necessary for normal photoinduced signal transduction, is a novel basic helix-loop-helix protein. Cell *95,* 657-667.

Nishioka, K., Chuikov, S., Sarma, K., Erdjument-Bromage, H., Allis, C.D., Tempst, P., and Reinberg, D. (2002). Set9, a novel histone H3 methyltransferase that facilitates transcription by precluding histone tail modifications required for heterochromatin formation. Genes Dev. *16,* 479-489.

Nozue, K., Covington, M.F., Duek, P.D., Lorrain, S., Fankhauser, C., Harmer, S.L., and Maloof, J.N. (2007). Rhythmic growth explained by coincidence between internal and external cues. Nature *448,* 358-361.

Ohgishi, M., Oka, A., Morelli, G., Ruberti, I., and Aoyama, T. (2001). Negative autoregulation of the *Arabidopsis* homeobox gene ATHB-2. Plant J. *25,* 389-398.

Oliva, R., Bazett-Jones, D.P., Locklear, L., and Dixon, G.H. (1990). Histone hyperacetylation can induce unfolding of the nucleosome core particle. Nucleic Acids Res. *18,* 2739-2747.

Osterlund, M.T., Hardtke, C.S., Wei, N., and Deng, X.W. (2000). Targeted destabilization of HY5 during light-regulated development of *Arabidopsis*. Nature *405,* 462-466.

Oyama, T., Shimura, Y., and Okada, K. (1997). The *Arabidopsis* HY5 gene encodes a bZIP protein that regulates stimulus-induced development of root and hypocotyl. Genes Dev. *11,* 2983-2995.

Ozsolak, F., Song, J.S., Liu, X.S., and Fisher, D.E. (2007). High-throughput mapping of the chromatin structure of human promoters. Nat. Biotechnol. *25,* 244-248.

Parks, B.M., and Quail, P.H. (1993). hy8, a new class of *arabidopsis* long hypocotyl mutants deficient in functional phytochrome A. Plant Cell *5,* 39-48.

Perales, M., and Mas, P. (2007). A Functional Link between Rhythmic Changes in Chromatin Structure and the *Arabidopsis* Biological Clock. Plant Cell

Peterson, C.L., and Workman, J.L. (2000). Promoter targeting and chromatin remodeling by the SWI/SNF complex. Curr. Opin. Genet. Dev. *10,* 187-192.

Pineiro, M., Gomez-Mena, C., Schaffer, R., Martinez-Zapater, J.M., and Coupland, G. (2003). EARLY BOLTING IN SHORT DAYS is related to chromatin remodeling factors and regulates flowering in *Arabidopsis* by repressing FT. Plant Cell *15,* 1552-1562.

Pokholok, D.K., Harbison, C.T., Levine, S., Cole, M., Hannett, N.M., Lee, T.I., Bell, G.W., Walker, K., Rolfe, P.A., Herbolsheimer, E., *et al.* (2005). Genome-wide map of nucleosome acetylation and methylation in yeast. Cell *122,* 517-527.

Qian, C., Zhang, Q., Li, S., Zeng, L., Walsh, M.J., and Zhou, M.M. (2005). Structure and chromosomal DNA binding of the SWIRM domain. Nat. Struct. Mol. Biol. *12,* 1078-1085.

Rea, S., Eisenhaber, F., O'Carroll, D., Strahl, B.D., Sun, Z.W., Schmid, M., Opravil, S., Mechtler, K., Ponting, C.P., Allis, C.D., and Jenuwein, T. (2000). Regulation of chromatin structure by site-specific histone H3 methyltransferases. Nature *406,* 593-599.

Reed, J.W., Nagatani, A., Elich, T.D., Fagan, M., and Chory, J. (1994). Phytochrome A and Phytochrome B Have Overlapping but Distinct Functions in *Arabidopsis* Development. Plant Physiol. *104,* 1139-1149.

Ren, B., Robert, F., Wyrick, J.J., Aparicio, O., Jennings, E.G., Simon, I., Zeitlinger, J., Schreiber, J., Hannett, N., Kanin, E., *et al.* (2000). Genome-wide location and function of DNA binding proteins. Science *290,* 2306-2309.

Ripperger, J.A., and Schibler, U. (2006). Rhythmic CLOCK-BMAL1 binding to multiple E-box motifs drives circadian Dbp transcription and chromatin transitions. Nat. Genet. *38,* 369-374.

Roberts, S.M., and Winston, F. (1997). Essential functional interactions of SAGA, a Saccharomyces cerevisiae complex of Spt, Ada, and Gcn5 proteins, with the Snf/Swi and Srb/mediator complexes. Genetics *147,* 451-465.

Robson, P., Whitelam, G.C., and Smith, H. (1993). Selected Components of the Shade-Avoidance Syndrome Are Displayed in a Normal Manner in Mutants of *Arabidopsis thaliana* and Brassica rapa Deficient in Phytochrome B. Plant Physiol. *102,* 1179-1184.

Roeder, R.G. (2005). Transcriptional regulation and the role of diverse coactivators in animal cells. FEBS Lett. *579,* 909-915.

Rogakou, E.P., Pilch, D.R., Orr, A.H., Ivanova, V.S., and Bonner, W.M. (1998). DNA double-stranded breaks induce histone H2AX phosphorylation on serine 139. J. Biol. Chem. *273,* 5858-5868.

Ruberti, I., Sessa, G., Lucchetti, S., and Morelli, G. (1991). A novel class of plant proteins containing a homeodomain with a closely linked leucine zipper motif. EMBO J. *10,* 1787-1791.

Sakamoto, K., and Nagatani, A. (1996). Nuclear localization activity of phytochrome B. Plant J. *10,* 859-868.

Salter, M.G., Franklin, K.A., and Whitelam, G.C. (2003). Gating of the rapid shade-avoidance response by the circadian clock in plants. Nature *426,* 680-683.

Sarma, K., and Reinberg, D. (2005). Histone variants meet their match. Nat. Rev. Mol. Cell Biol. *6,* 139-149.

Schaffer, R., Ramsay, N., Samach, A., Corden, S., Putterill, J., Carre, I.A., and Coupland, G. (1998). The late elongated hypocotyl mutation of *Arabidopsis* disrupts circadian rhythms and the photoperiodic control of flowering. Cell *93,* 1219-1229.

Schena, M., and Davis, R.W. (1992). HD-Zip proteins: members of an *Arabidopsis* homeodomain protein superfamily. Proc. Natl. Acad. Sci. U. S. A. *89,* 3894-3898.

Schultz, D.C., Friedman, J.R., and Rauscher, F.J.,3rd. (2001). Targeting histone deacetylase complexes via KRAB-zinc finger proteins: the PHD and bromodomains of KAP-1 form a cooperative unit that recruits a novel isoform of the Mi-2alpha subunit of NuRD. Genes Dev. *15,* 428-443.

Sekinger, E.A., Moqtaderi, Z., and Struhl, K. (2005). Intrinsic histone-DNA interactions and low nucleosome density are important for preferential accessibility of promoter regions in yeast. Mol. Cell *18,* 735-748.

Sessa, G., Carabelli, M., Sassi, M., Ciolfi, A., Possenti, M., Mittempergher, F., Becker, J., Morelli, G., and Ruberti, I. (2005). A dynamic balance between gene activation and repression regulates the shade avoidance response in *Arabidopsis*. Genes Dev. *19,* 2811-2815.

Sharma, V.M., Li, B., and Reese, J.C. (2003). SWI/SNF-dependent chromatin remodeling of RNR3 requires TAF(II)s and the general transcription machinery. Genes Dev. *17,* 502-515.

Sharrock, R.A., and Clack, T. (2002). Patterns of expression and normalized levels of the five *Arabidopsis* phytochromes. Plant Physiol. *130,* 442-456.

Sharrock, R.A., and Quail, P.H. (1989). Novel phytochrome sequences in *Arabidopsis thaliana*: structure, evolution, and differential expression of a plant regulatory photoreceptor family. Genes Dev. *3,* 1745-1757.

Shen, X., Yu, L., Weir, J.W., and Gorovsky, M.A. (1995). Linker histones are not essential and affect chromatin condensation in vivo. Cell *82,* 47-56.

Shen, Y., Khanna, R., Carle, C.M., and Quail, P.H. (2007). Phytochrome induces rapid PIF5 phosphorylation and degradation in response to red-light activation. Plant Physiol. *145,* 1043-1051.

Shimizu-Sato, S., Huq, E., Tepperman, J.M., and Quail, P.H. (2002). A light-switchable gene promoter system. Nat. Biotechnol. *20,* 1041-1044.

Shinomura, T., Nagatani, A., Chory, J., and Furuya, M. (1994). The Induction of Seed Germination in *Arabidopsis thaliana* Is Regulated Principally by Phytochrome B and Secondarily by Phytochrome A. Plant Physiol. *104,* 363-371.

Shogren-Knaak, M., Ishii, H., Sun, J.M., Pazin, M.J., Davie, J.R., and Peterson, C.L. (2006). Histone H4-K16 acetylation controls chromatin structure and protein interactions. Science *311,* 844-847.

Simpson, R.T., and Whitlock, J.P. (1976). Mapping DNAase l-susceptible sites in nucleosomes labeled at the 5' ends. Cell *9,* 347-353.

Skowyra, D., Zeremski, M., Neznanov, N., Li, M., Choi, Y., Uesugi, M., Hauser, C.A., Gu, W., Gudkov, A.V., and Qin, J. (2001). Differential association of products of alternative transcripts of the candidate tumor suppressor ING1 with the mSin3/HDAC1 transcriptional corepressor complex. J. Biol. Chem. *276,* 8734-8739.

Smith, C.M., Gafken, P.R., Zhang, Z., Gottschling, D.E., Smith, J.B., and Smith, D.L. (2003). Mass spectrometric quantification of acetylation at specific lysines within the amino-terminal tail of histone H4. Anal. Biochem. *316,* 23-33.

Solomon, M.J., Larsen, P.L., and Varshavsky, A. (1988). Mapping protein-DNA interactions in vivo with formaldehyde: evidence that histone H4 is retained on a highly transcribed gene. Cell *53,* 937-947.

Somers, D.E., Devlin, P.F., and Kay, S.A. (1998). Phytochromes and cryptochromes in the entrainment of the *Arabidopsis* circadian clock. Science *282,* 1488-1490.

Somers, D.E., Sharrock, R.A., Tepperman, J.M., and Quail, P.H. (1991). The hy3 Long Hypocotyl Mutant of *Arabidopsis* Is Deficient in Phytochrome B. Plant Cell *3,* 1263-1274.

Somers, D.E., Webb, A.A., Pearson, M., and Kay, S.A. (1998). The short-period mutant, toc1-1, alters circadian clock regulation of multiple outputs throughout development in *Arabidopsis thaliana*. Development *125,* 485-494.

Steger, D.J., and Workman, J.L. (1997). Stable co-occupancy of transcription factors and histones at the HIV-1 enhancer. EMBO J. *16,* 2463-2472.

Steindler, C., Matteucci, A., Sessa, G., Weimar, T., Ohgishi, M., Aoyama, T., Morelli, G., and Ruberti, I. (1999). Shade avoidance responses are mediated by the ATHB-2 HD-zip protein, a negative regulator of gene expression. Development *126,* 4235-4245.

Sterner, R., Boffa, L.C., Chen, T.A., and Allfrey, V.G. (1987). Cell cycle-dependent changes in conformation and composition of nucleosomes containing human histone gene sequences. Nucleic Acids Res. *15,* 4375-4391.

Stockinger, E.J., Mao, Y., Regier, M.K., Triezenberg, S.J., and Thomashow, M.F. (2001). Transcriptional adaptor and histone acetyltransferase proteins in *Arabidopsis* and their interactions with CBF1, a transcriptional activator involved in cold-regulated gene expression. Nucleic Acids Res. *29,* 1524-1533.

Strahl, B.D., and Allis, C.D. (2000). The language of covalent histone modifications. Nature *403,* 41-45.

Strasser, B., Sanchez-Lamas, M., Yanovsky, M.J., Casal, J.J., and Cerdan, P.D. (2010). *Arabidopsis thaliana* life without phytochromes. Proc. Natl. Acad. Sci. U. S. A. *107,* 4776-4781.

Tagami, H., Ray-Gallet, D., Almouzni, G., and Nakatani, Y. (2004). Histone H3.1 and H3.3 complexes mediate nucleosome assembly pathways dependent or independent of DNA synthesis. Cell *116,* 51-61.

Tepperman, J.M., Zhu, T., Chang, H.S., Wang, X., and Quail, P.H. (2001). Multiple transcription-factor genes are early targets of phytochrome A signaling. Proc. Natl. Acad. Sci. U. S. A. *98,* 9437-9442.

Tessadori, F., Schulkes, R.K., van Driel, R., and Fransz, P. (2007). Light-regulated large-scale reorganization of chromatin during the floral transition in *Arabidopsis*. Plant J. *50,* 848-857.

Tessadori, F., van Zanten, M., Pavlova, P., Clifton, R., Pontvianne, F., Snoek, L.B., Millenaar, F.F., Schulkes, R.K., van Driel, R., Voesenek, L.A., *et al.* (2009). Phytochrome B and histone deacetylase 6 control light-induced chromatin compaction in *Arabidopsis thaliana*. PLoS Genet. *5,* e1000638.

Thomashow, M.F. (1999). PLANT COLD ACCLIMATION: Freezing Tolerance Genes and Regulatory Mechanisms. Annu. Rev. Plant Physiol. Plant Mol. Biol. *50,* 571-599.

Tian, L., and Chen, Z.J. (2001). Blocking histone deacetylation in *Arabidopsis* induces pleiotropic effects on plant gene regulation and development. Proc. Natl. Acad. Sci. U. S. A. *98,* 200-205.

Tian, L., Wang, J., Fong, M.P., Chen, M., Cao, H., Gelvin, S.B., and Chen, Z.J. (2003). Genetic control of developmental changes induced by disruption of *Arabidopsis* histone deacetylase 1 (AtHD1) expression. Genetics *165,* 399-409.

Toledo-Ortiz, G., Huq, E., and Quail, P.H. (2003). The *Arabidopsis* basic/helix-loop-helix transcription factor family. Plant Cell *15,* 1749-1770.

Toth, R., Kevei, E., Hall, A., Millar, A.J., Nagy, F., and Kozma-Bognar, L. (2001). Circadian clock-regulated expression of phytochrome and cryptochrome genes in *Arabidopsis*. Plant Physiol. *127,* 1607-1616.

Ura, K., Hayes, J.J., and Wolffe, A.P. (1995). A positive role for nucleosome mobility in the transcriptional activity of chromatin templates: restriction by linker histones. EMBO J. *14,* 3752-3765.

Utley, R.T., Ikeda, K., Grant, P.A., Cote, J., Steger, D.J., Eberharter, A., John, S., and Workman, J.L. (1998). Transcriptional activators direct histone acetyltransferase complexes to nucleosomes. Nature *394,* 498-502.

van Attikum, H., and Gasser, S.M. (2005). The histone code at DNA breaks: a guide to repair? Nat. Rev. Mol. Cell Biol. *6,* 757-765.

Vlachonasios, K.E., Thomashow, M.F., and Triezenberg, S.J. (2003). Disruption mutations of ADA2b and GCN5 transcriptional adaptor genes dramatically affect *Arabidopsis* growth, development, and gene expression. Plant Cell *15,* 626-638.

Wagner, D., Fairchild, C.D., Kuhn, R.M., and Quail, P.H. (1996). Chromophore-bearing NH2-terminal domains of phytochromes A and B determine their photosensory specificity and differential light lability. Proc. Natl. Acad. Sci. U. S. A. *93,* 4011-4015.

Wagner, D., Tepperman, J.M., and Quail, P.H. (1991). Overexpression of Phytochrome B Induces a Short Hypocotyl Phenotype in Transgenic *Arabidopsis*. Plant Cell *3,* 1275-1288.

Walker, J., Chen, T.A., Sterner, R., Berger, M., Winston, F., and Allfrey, V.G. (1990). Affinity chromatography of mammalian and yeast nucleosomes. Two modes of binding of transcriptionally active mammalian nucleosomes to organomercurial-agarose columns, and contrasting behavior of the active nucleosomes of yeast. J. Biol. Chem. *265,* 5736-5746.

Waterborg, J.H. (1992). Existence of two histone H3 variants in dicotyledonous plants and correlation between their acetylation and plant genome size. Plant Mol. Biol. *18,* 181-187.

Weintraub, H., and Groudine, M. (1976). Chromosomal subunits in active genes have an altered conformation. Science *193,* 848-856.

West, M.H., and Bonner, W.M. (1980). Histone 2A, a heteromorphous family of eight protein species. Biochemistry *19,* 3238-3245.

Whitelam, G.C., Johnson, E., Peng, J., Carol, P., Anderson, M.L., Cowl, J.S., and Harberd, N.P. (1993). Phytochrome A null mutants of *Arabidopsis* display a wild-type phenotype in white light. Plant Cell *5,* 757-768.

Wolffe, A.P., and Hayes, J.J. (1999). Chromatin disruption and modification. Nucleic Acids Res. *27,* 711-720.

Wysocka, J., Swigut, T., Milne, T.A., Dou, Y., Zhang, X., Burlingame, A.L., Roeder, R.G., Brivanlou, A.H., and Allis, C.D. (2005). WDR5 associates with histone H3 methylated at K4 and is essential for H3 K4 methylation and vertebrate development. Cell *121,* 859-872.

Xue, Y., Canman, J.C., Lee, C.S., Nie, Z., Yang, D., Moreno, G.T., Young, M.K., Salmon, E.D., and Wang, W. (2000). The human SWI/SNF-B chromatin-remodeling complex is related to yeast rsc and localizes at kinetochores of mitotic chromosomes. Proc. Natl. Acad. Sci. U. S. A. *97,* 13015-13020.

Yamaguchi, R., Nakamura, M., Mochizuki, N., Kay, S.A., and Nagatani, A. (1999). Light-dependent translocation of a phytochrome B-GFP fusion protein to the nucleus in transgenic *Arabidopsis*. J. Cell Biol. *145,* 437-445.

Yamashino, T., Matsushika, A., Fujimori, T., Sato, S., Kato, T., Tabata, S., and Mizuno, T. (2003). A Link between circadian-controlled bHLH factors and the APRR1/TOC1 quintet in *Arabidopsis thaliana*. Plant Cell Physiol. *44,* 619-629.

Zanton, S.J., and Pugh, B.F. (2006). Full and partial genome-wide assembly and disassembly of the yeast transcription machinery in response to heat shock. Genes Dev. *20,* 2250-2265.

Zegerman, P., Canas, B., Pappin, D., and Kouzarides, T. (2002). Histone H3 lysine 4 methylation disrupts binding of nucleosome remodeling and deacetylase (NuRD) repressor complex. J. Biol. Chem. *277,* 11621-11624.

Zeidler, M., Zhou, Q., Sarda, X., Yau, C.P., and Chua, N.H. (2004). The nuclear localization signal and the C-terminal region of FHY1 are required for transmission of phytochrome A signals. Plant J. *40,* 355-365.

Zhou, Q., Hare, P.D., Yang, S.W., Zeidler, M., Huang, L.F., and Chua, N.H. (2005). FHL is required for full phytochrome A signaling and shares overlapping functions with FHY1. Plant J. *43,* 356-370.

Zhu, Y., Tepperman, J.M., Fairchild, C.D., and Quail, P.H. (2000). Phytochrome B binds with greater apparent affinity than phytochrome A to the basic helix-loop-helix factor PIF3 in a reaction requiring the PAS domain of PIF3. Proc. Natl. Acad. Sci. U. S. A. *97,* 13419-13424.